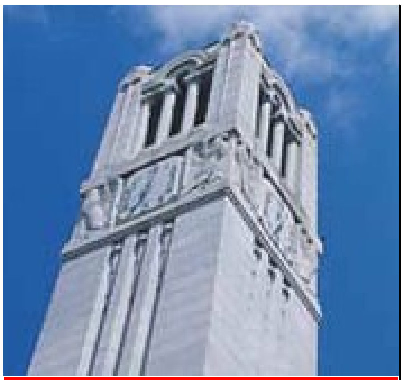

NC STATE UNIVERSITY

Constructed Facilities Laboratory
Department of Civil, Construction, and Environmental Engineering

Research Report
No. RD-06-06
FHWA/NC/2006-12

FULL SCALE TESTING OF OVERHANG FALSEWORK HANGERS ON NCDOT MODIFIED BULB TEE (MBT) GIRDERS

Prepared by:

Donlawit Ariyasajjakorn, ***Research Assistant***
Amir Mirmiran, Ph.D., P.E., ***(Florida International University)***
Emmett A. Sumner, Ph.D., P.E., ***Principle Investigator***

Prepared for:

North Carolina Department of Transportation
Research and Analysis Group
1 South Wilmington Street
Raleigh, North Carolina 27601

Constructed Facilities Laboratory
2414 Campus Shore Drive
North Carolina State University
Raleigh, NC 27695-7533
Tel: (919) 513-1733
Fax: (919) 513-1765
Email: cfl@ncsu.edu
Web Site: www.cfl.ncsu.edu

February 2006

Research Report

FULL SCALE TESTING OF OVERHANG FALSEWORK HANGERS ON NCDOT MODIFIED BULB TEE (MBT) GIRDERS

Prepared by

Donlawit Ariyasajjakorn
Research Assistant

Amir Mirmiran, Ph.D., P.E.
(*Florida International University*)

Emmett A. Sumner, Ph.D., P.E.
Principle Investigator

Submitted to

North Carolina Department of Transportation
Research and Analysis Group
1 South Wilmington Street
Raleigh, North Carolina 27601

NCSU-CFL Report No. RD-06-06
NCDOT Report No. FHWA/NC/2006-12

February 2006

Constructed Facilities Laboratory (CFL)
Department of Civil, Construction, and Environmental Engineering
North Carolina State University
Raleigh, NC 27695

Technical Report Documentation Page

1. Report No. FHWA/NC/2006-12	2. Government Accession No.	3. Recipient's Catalog No.
4. Title and Subtitle Full Scale Testing Of Overhang Falsework Hangers On NCDOT Modified Bulb Tee (MBT) Girders		5. Report Date February 15, 2006 6. Performing Organization Code
7. Author(s) Donlawit Ariyasajjakorn, Amir Mirmiran, Emmett A. Sumner		8. Performing Organization Report No.
9. Performing Organization Name and Address Department of Civil, Construction, and Environmental Engineering North Carolina State University Raleigh, North Carolina 27695		10. Work Unit No. (TRAIS) 11. Contract or Grant No.
12. Sponsoring Agency Name and Address North Carolina Department of Transportation Research and Analysis Group 1 South Wilmington Street Raleigh, North Carolina 27601		13. Type of Report and Period Covered Final Report July 1, 2004 - December 31, 2005 14. Sponsoring Agency Code 2005-18
Supplementary Notes:		

16. Abstract

Today's bridges are being constructed with longer spans and higher girder spacing. As a result, the use of precast prestressed concrete modified bulb tee (MBT) girders has significantly increased. The MBT girders have a wider and thinner top flange than other conventional precast concrete cross-sections. The strength of the thin top flange has been identified as a concern for the North Carolina Department of Transportation when edge of flange falsework hangers are used to support the overhang deck slab falsework system. In response to theses concerns, the NCDOT has funded research project number 2005-18 "Full Scale Testing of Overhang Falsework Hangers on NCDOT Modified Bulb Tee (MBT) Girders" to study the behavior of the edge of flange falsework hanger systems. This research includes full scale testing of standard falsework hangers manufactured by Dayton/Richmond and Meadow/Burke installed on an NCDOT MBT girder and an analytical investigation that utilized three dimensional finite element modeling. The effects of the girder shear reinforcement, interaction with adjacent loaded hangers, and the type of hanger were included in the experimental and analytical investigations. The finite element modeling was used to predict the response of the falsework hanger system.

It was concluded that the shear reinforcement, number of loaded hanger and the type of hanger affect the ultimate strength and behavior of hanger system. The observed ultimate strength of the Dayton/Richmond hangers was higher than the observed ultimate strength of the Meadow/Burke hangers. However, in all cases the observed ultimate loads were less than the manufacturer's specified ultimate strength. It was recommended that the safe working load of the Dayton/Richmond and Meadow/Burke falsework hanger embedded on the NCDOT modified bulb tee (MBT) girder be reduced, and that the use of different type of overhang hanger system such as through flange hanger appears to be necessary to support a 6,000 lb. safe working load (12,000 lb. ultimate).

17. Key Words Falsework, girders, girder bridges, tie rods, prestressed concrete bridges, formwork	18. Distribution Statement		
19. Security Classif. (of this report) Unclassified	20. Security Classif. (of this page) Unclassified	21. No. of Pages 245	22. Price

Form DOT F 1700.7 (8-72) **Reproduction of completed page authorized**

Disclaimer

The contents of this report reflect the views of the author(s) and not necessarily the views of the University. The author(s) are responsible for the facts and the accuracy of the data presented herein. The contents do not necessarily reflect the official views or policies of the North Carolina Department of Transportation or the Federal Highway Administration at the time of publication. This report does not constitute a standard, specification, or regulation.

Acknowledgments

Funding for this research was provided by the North Carolina Department of Transportation (project #2005-18). Appreciation is extended to Precast of the Carolinas, LLC for their donation of the test girder and to Meadow Burke and Dayton Superior for their donation of the falsework hangers and coil rods.

Executive Summary

Today's bridges are being constructed with longer spans and higher girder spacing. As a result, the use of precast prestressed concrete modified bulb tee (MBT) girders has significantly increased. The MBT girders have a wider and thinner top flange than other conventional precast concrete cross-sections. The strength of the thin top flange has been identified as a concern for the North Carolina Department of Transportation when edge of flange falsework hangers are used to support the overhang deck slab falsework system. In response to theses concerns, the NCDOT has funded research project number 2005-18 "Full Scale Testing of Overhang Falsework Hangers on NCDOT Modified Bulb Tee (MBT) Girders" to study the behavior of the edge of flange falsework hanger systems.

This research includes full scale testing of standard falsework hangers manufactured by Dayton/Richmond and Meadow/Burke installed on an NCDOT MBT girder and an analytical investigation that utilized three dimensional finite element modeling. The effects of the girder shear reinforcement, interaction with adjacent loaded hangers, and the type of hanger were included in the experimental and analytical investigations. The finite element modeling was used to predict the response of the falsework hanger system.

From the experimental results, the observed ultimate load of both hanger types, Dayton/Richmond and Meadow/Burke, were less than the ultimate strength specified by the manufacturers. The Dayton/Richmond and Meadow/Burke hanger systems failed at approximately 63% and 44% of the specified ultimate strengths, respectively.

The hanger system response predicted by the finite element models was similar to the experimentally observed response. The initial stiffness of the girder flange was higher than observed experimentally and the models were able to reasonably capture the observed failure modes.

It was concluded that the shear reinforcement, number of loaded hanger and the type of hanger affect the ultimate strength and behavior of hanger system. The observed ultimate strength of the Dayton/Richmond hangers was higher than the observed ultimate strength of the Meadow/Burke hangers. However, in all cases the observed ultimate loads were less than the manufacturer's specified ultimate strength. It was recommended that the safe working load of the Dayton/Richmond and Meadow/Burke falsework hanger embedded on the NCDOT modified bulb tee (MBT) girder be reduced, and that the use of different type of overhang hanger system such as through flange hanger appears to be necessary to support a 6,000 lb. safe working load (12,000 lb. ultimate).

Table of Contents

List of Tables

List of Figures

Full Scale Testing of Overhang Falsework Hangers on NCDOT Modified Bulb Tee (MBT) Girders

1.0 INTRODUCTION

1.1 Overview

As bridge technology has advanced, smaller and more slender girder cross-sections have been developed. To fulfill current economic and structural needs, girder cross-sections such as bulb tee girders, which have a wide top flange and a slender web, are being utilized. In North Carolina the standard bulb tee girder is commonly modified by increasing the top flange width. The revised cross-section is called a North Carolina Department of Transportation (NCDOT) modified bulb tee girder (MBT).

During construction of the deck slab overhang on NCDOT modified bulb tee (MBT) girder bridges construction loads must be supported by an overhang falsework system. These loads include concrete weight, screed load, machine load, live load and formwork weight. Within the falsework system, the loads are supported by the formwork and then transferred to the brackets and then to steel hangers embedded in the supporting girder flange. There are two types of falsework hanger details, edge of flange and through flange hanger, as shown in Figure 1.1. Because of easy installation, edge of flange falsework hanger systems are commonly used in NCDOT construction projects.

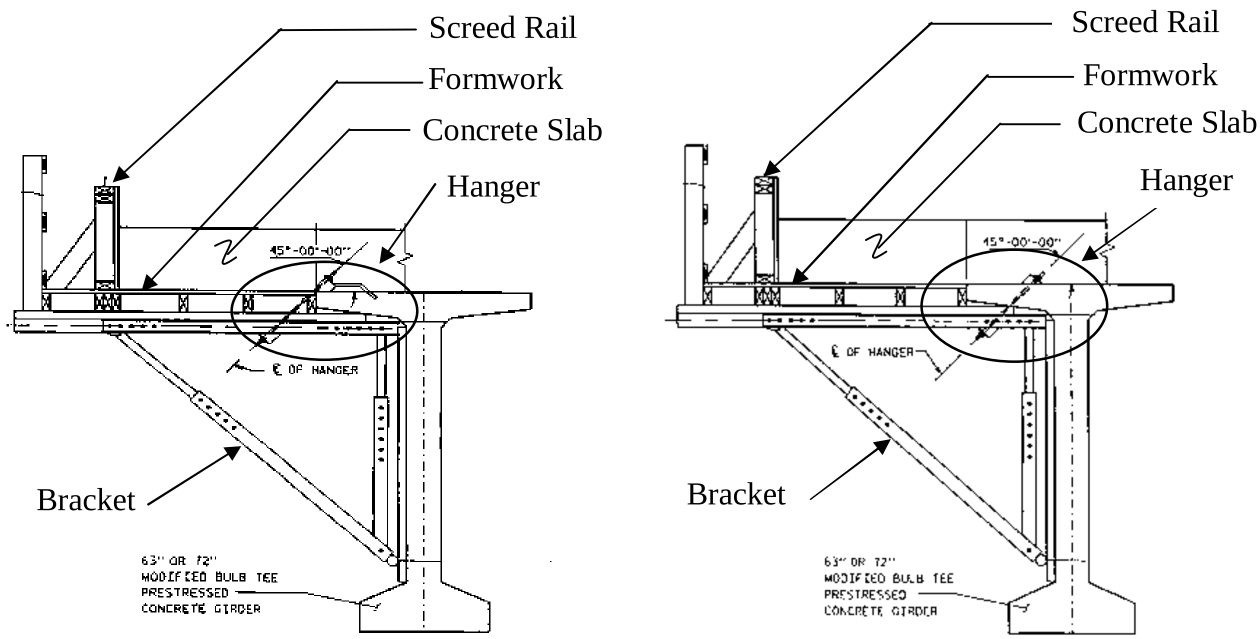

A) Edge of flange hanger

B) Through flange hanger

Figure 1.1 Common Overhang Falsework System Details

The hangers are installed at the edge of the top flange of the girder and connected to brackets by a coil rod. Typically hangers used for the overhang slab construction are 45-degree overhang hangers. The two types of edge of flange hangers commonly used in NCDOT construction projects are a C-24 type 4-APR from Dayton/Richmond and a HF-43 from Meadow/Burke Products, Inc. The manufacturer specified safe working load for both hangers is 6,000 lbs. The working load is based on 5,000 psi. concrete strength, 5 in. minimum concrete flange thickness and 2 to 1 safety factor.

The original bulb tee girder cross section was modified by increasing the width of the top flange. The Girder has 3½" flange thickness at the edge and increases to 5½" thickness at the web. The cross section of NCDOT modified bulb tee is shown in Figure 1.2. Because of the thin flange, the hanger load may cause bending failure of the top flange or punching shear failure in the concrete area under the hanger head. The construction loads applied to the girder will cause not only bending and shear but also torsion of the girder. Normally in the field, temporary lateral bracing is installed to prevent excessive torsional stresses in the girder. For the MBT girders which have a wide top flange, load from the hanger increases the applied torsion to the girder.

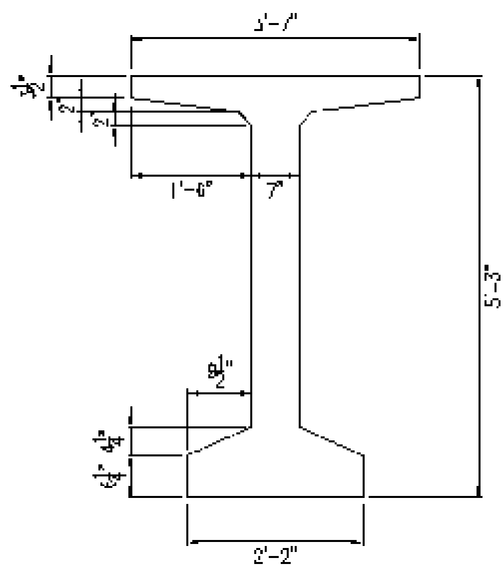

Figure 1.2 NCDOT modified bulb tee cross section

Because the NCDOT modified bulb tee has a thin flange thickness, which violates the manufacturer published requirements of the falsework hanger, the strength of the falsework hanger may need to be limited. The unknown falsework hanger strength could result in a failure during construction leading to delays and safety issues. To correct this problem NCDOT has funded this research (NCDOT project 2005-18) to study the behavior of the edge of flange falsework hanger system

1.2 Problem Statement

As mentioned above, the use of edge of flange falsework hangers requires a minimum 5 in. flange thickness while the NCDOT modified bulb tee girder provides only 3½ in. Therefore, the true behavior of the falsework hanger system on the NCDOT modified bulb tee girder is unknown.

There are several factors that can affect the behavior of the falsework hanger system: amount of shear reinforcement in the girder, effect of loaded adjacent hanger, and the hanger type. Experimental full scale test programs were created to investigate the behavior of the falsework hanger system, and finite element models were generated to predict the behavior of the hanger system.

1.3 Objective of Research

The primary objective of this research is to investigate the behavior of the falsework hanger on NCDOT MBT girders and to utilize analytical models to predict the behavior of the system.

This research consisted of two parts, experimental and analytical. The effects of the amount of shear reinforcement, the effect of loaded adjacent hangers and the type of hanger were investigated in the experimental investigation. The finite element models were generated to predict the behavior of the falsework system including the critical limit state, ultimate load, and the response of the system.

The results of this research will provide a reference to NCDOT for adjusting the safe working loads of the falsework hangers on the NCDOT modified bulb tee girder and also a guideline for thin flanged bridge girder construction.

1.4 Outline of Report

This report consists of 6 primary sections outlined as follows:

- Section 2 provides a background of the falsework hanger system and the experimental test results performed in the past by the manufacturer. The literature review of the related behavior is also included
- Section 3 provides details of the experimental test program performed for this research. The experimental results are presented and discussed.
- Section 4 briefly discusses the limit states within the falsework system, the finite element modeling and the analytical approach utilized to evaluate the behavior of the system.
- Section 5 contains a discussion and compares interesting parameters of the experimental test results. Comparisons between the finite element model and the experimental program are also made.
- Section 6 contains the recommendations for field application, primary conclusions, and the need for future research.
- Appendix A provides the details of experimental components such as the MBT girder and the lateral bracing.
- Appendices B-H contain summaries of the experimental tests. The summary consists of the basic parameters used in the test, the test layout, instrumentations, illustrations, and test results.
- Appendix I is the summary sheet of the finite element model. The finite element model summary sheets consist of the properties of materials, hanger model, crack pattern and the result from the program

- Appendix J is the summary sheet of the ACI design provisions related to the falsework system.

2.0 BACKGROUND AND LITERATURE REVIEW

2.1 Overview

In this section, any previous information that relates to the falsework hanger system, including the falsework system during the construction, past test results performed by the manufacturer, and a literature review, is discussed

The literature review of previous research related to the behavior of 45-degree overhang falsework hangers installed on the thin flange concrete girders is presented. Included are reviews of the bond strength between rebar and concrete, torsional behavior of concrete girder, punching shear strength of the concrete element and behavior of anchors in concrete.

2.2 Falsework System Construction

During casting of the girders, hangers are installed into the girder flange by dipping the hanger legs directly into the plastic concrete and positioning the hanger head on the edge of the flange. After the installation, the girder was cured and then transported to the construction site. Figure 2.1 shows a girder and the embedded hanger during the curing period.

During the bridge construction, the girders are set and brackets are attached to overhang hangers using a high strength threaded coil rod and nuts. Additional formwork panels are assembled, using the brackets as supports, to support the overhang slab and the deck screed. The hanger and falsework systems are installed to the bulb tee girder as shown in Figure 2.2. Hangers experienced ultimate loading when the concrete slab is cast and the screed is operated.

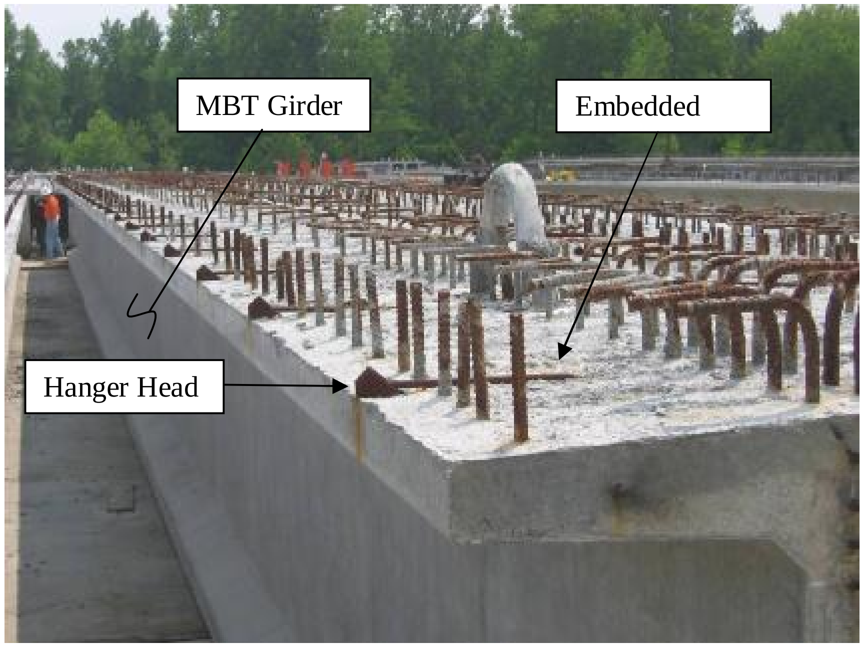

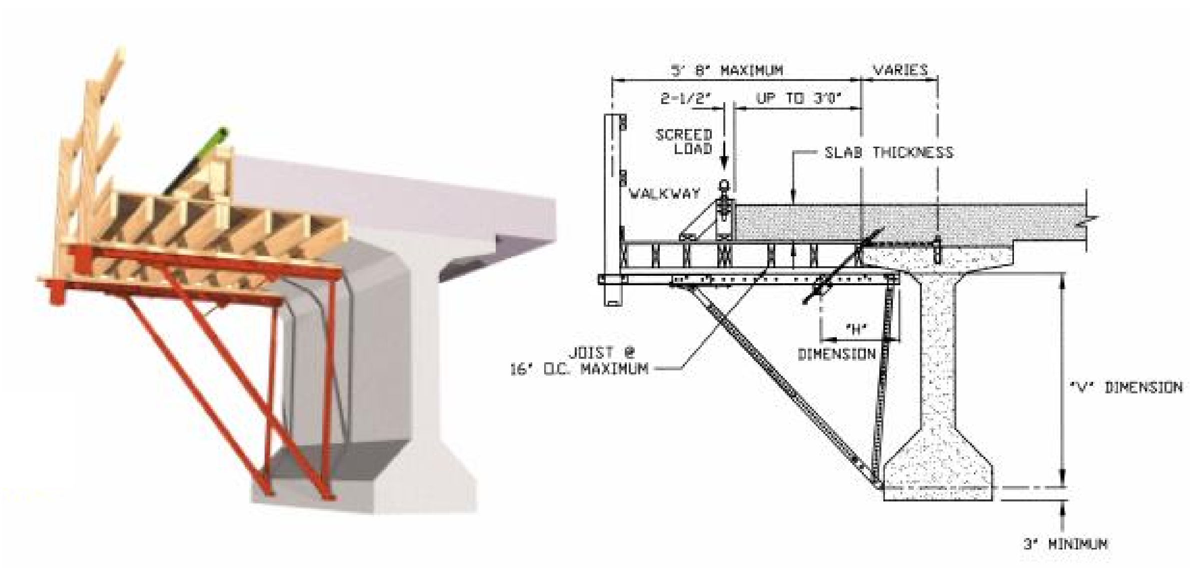

Figure 2.1 Bulb tee girder and hanger in precast yard

Figure 2.2 Typical falsework system installation (Meadow Burke, Forming hardware for bridge deck, 2003)

2.3 Manufacturer Test Results

Limited manufacturer testing information is available on the behavior of the hangers used in this study. A summary of the two available test reports is presented herein.

From a test report by Richmond Screw Anchor Co, the Dayton/Richmond 45 degree overhang hangers type HFR-HWA, which is similar to the C-24 hangers, was tested on July 23rd 1986. The hangers were clamped in a hanger test fixture. The fixture was set at a 45 degree angle and a ½” diameter coil rod was used. A lag-stud was installed using double nuts. The load was applied to the system by a 60,000 lb. Tinius Olsen testing machine. The tests were stopped after the load reached 15,000 lb. Some of the hanger tests failed by the excessive rotation of the hanger head at 12,000 lb.

On November 4th, 1998, Dayton/Richmond performed additional tests on 45 degree overhang hanger C-24 type 4-AP shown in Figure 2.3. Hangers were installed over the edge of a tested concrete girder. Load was applied at 45 degrees by a hydraulic cylinder. The cylinder was attached to a loading bracket which was bolted to the web of girder. The failure mode was 5-degree bending in the coil rod immediately above the top of the hanger’s coil nut. Based on a factor of safety 2 to 1, the test report mentioned that the safe working load of hanger, C-24 type 4-AP was 3300 lb.

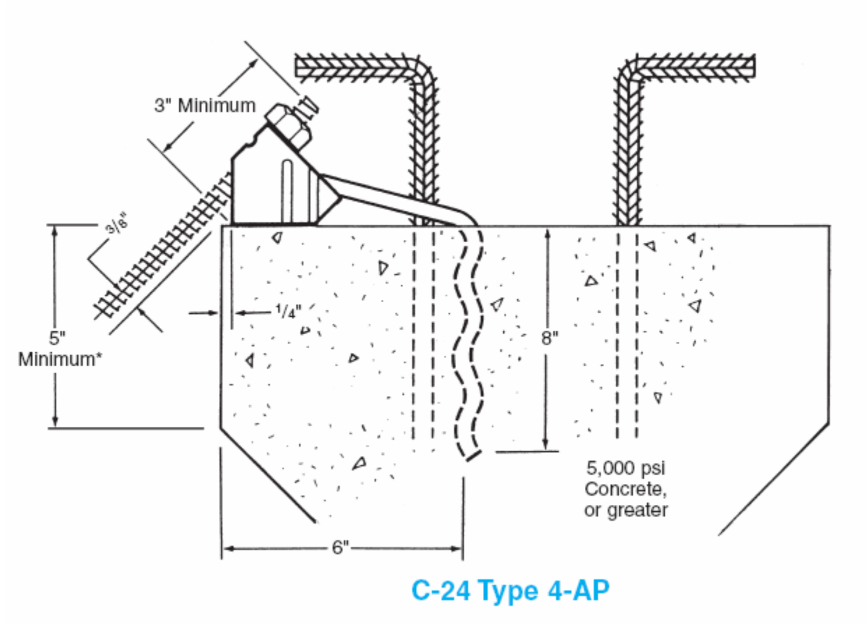

Figure2.3 Details of Dayton/Richmond C-24 type 4-AP (Dayton/Superior, Dayton/Richmond concrete accessory, 2005)

2.4 Related Behavior

There are many other types of structural behavior related to the hanger-girder flange system such as bond strength of concrete and steel hanger leg, torsional capacity of the girder, punching shear strength of the top flange and anchorage behavior.

Bond and Strength

Kemp (1986) developed design criteria for the bond between concrete and steel based on an extensive experimental research program that systematically studied the parameters thought to have a primary influence on bond behavior by using modified cantilever beams. For the beam with thin bottom cover, the cracks started initially right under the test bars and then wedge-shaped cracks developed before the eventual failure. For beams with a thicker clear bottom cover than the clear side cover and half the clear spacing between tow adjacent bars, the crack began horizontally at the same lever of test bars. Nominal stirrups improved ductility and ultimate bond strength. The ultimate strength equation for the bond stress was dependant on the effect of stirrups, auxiliary longitudinal reinforcement, clear concrete cover, concrete strength, and dowel force

Bazant et al. (1988) reported the results of reduced-scale tests of micro concrete specimens designed to examine the applicability of the size effect law and developed an approximate prediction formula. The test results on pullout of reinforcing bars from concrete confirmed that a size effect is present. The nominal shear bond stress at failure decreased as the specimen size increased. The larger specimens, with larger bars, tended to failed in a more brittle, splitting mode, while smaller specimens, with smaller bars, tended to fail in a less brittle or more plastic shear-pullout mode. This behavior follows the size effect law.

Donahey et al. (1985) presented the results of a study of the effects of the consolidation method and two-course construction on the bond strength of top-cast bars in bridge decks as a function of concrete slump and bleed, and slab depth. High-density consolidation and two-course construction were implemented to improve bridge deck quality. The use of low-slump concrete for the first course is recommended, since increased slump was detrimental to bond strength. Although the data was limited, deep slabs made with stiff, well-consolidated concrete could provide the same bond strengths as shallow slabs.

Clifton et al. (1983) compared the traditional pull-out test (cube concrete which had reinforced steel in the center) with the normal bond strength theory on the coated reinforcing bars. The creep properties of organic coated reinforcing bars should not be estimated solely on the basis of their bond strengths determined from pullout tests. The creep test appeared to be more discriminating than the pull out tests as judged by the wider range of creep ratios compared to pullout bond stress ratios.

Torsional behavior

Henry et al. (1974) studied the influence of shear on the behavior and strength of similar rectangular beams. They stated that prestressed concrete beams that are subjected to torsion, bending, and shear tend to fail in one of two modes of skewed bending. The bending mode of failure occurs for the proportion of torsion and moment, T/M, equal to or less than 0.22. The inclination of the controlling crack, θ, for the torsion mode failures was nearly constant. The value of θ did not increase with an increase in the value of T/M. The cracking torque was increased slightly with a small eccentricity and a small increase in the prestressing force. It was significantly affected by the value of T/M. The initial torsional stiffness of beams subjected to combined loads was only slightly less than the theoretical elastic torsional stiffness, the reduction being on the order of 5% to 15%. The initial torsional stiffness was nearly independent of the loading ratio, length of beam, and prestressing force. After cracking, the behavior depended primarily on the loading ratio. The strain in the stirrups generally reached yield for the torsion failure mode. In the presence of combined torsion, bending and shear, the ultimate torsional capacity of a beam could be increased up to 30% for a small amount of bending and shear. The bending capacity of a beam was not reduced substantially under combined loads until a torque equal to about 50% of the pure torque capacity was reached. Afterward, the bending capacity was reduced rapidly. The same criterion applied to shear.

Nukherjee et al. (1971) investigated the interaction of torsion, bending moment and flexural shear in prestressed concrete beams. They concluded that the torsional reinforcement, composed of rectangular ties and longitudinal bars at the corners, prevents a brittle type failure in prestressed beams. The torsional rotation capacity was substantially increased, accompanied by some increase in ultimate strength in pure torsion. An increase in prestress level caused a corresponding increase in ultimate strength, but reduced the torsional rotation capacity. The ultimate strength under pure torsion was not adversely affected by the eccentricity of prestress. A moderate amount of bending moment increases the ultimate torsional strength, and this increase may be substantial in beams with eccentric prestress. However, bending moments in excess of an optimum value cause rapid deterioration in torsional strength. For any combination of torsion and bending, the presence of flexural shear was detrimental to the torsional strength. The initial torsional stiffness was practically unaffected by the level of prestress, torque-moment ratio or flexural shear. The point of departure and the rate of deviation from the initial stiffness depended on the torque-moment ratio.

Wafa et al. (1995) studied the behavior of the high-strength concrete beam under torsion by changing the level of prestressing force, cross-section, and compressive strength of concrete. They concluded that the increase of tensile strength is not in direct proportion with the compressive strength. It was observed that the greater the concrete strength and prestressing level, the higher the observed cracking, ultimate torsional strength, and torsional stiffness. The space truss with softening of concrete was the best estimate of all.

Zararis et al. (1986) estimated the effects of the flange width in torsion and bending on the torsion capacity of reinforced concrete T-beams. They found out that there are two types of behavior for this study, full cracking and partial cracking of the beam Full cracking occurs when torsion prevails. Partial cracking occurs when the bending prevails. The experimental results showed that the effective overhanging flange width was greater than three times the flange thickness, as the CEB-FIB Model Code and ACI 318 recommend.

Punching Shear Strength

Ebeido et al. (1996) verified and substantiated the nonlinear finite-element model for use in estimating the punching strength of skew bridge decks. The punching-load capacity of deck slabs of skew composite steel-concrete bridges was affected by the following parameters: it increased with reduction of the girder spacing, decreased with increases in the angle of skew, improved with increases in the reinforcement ratio, it increased with increase in the size of longitudinal girders, was very sensitive to a change in the deck slab thickness and decreases at the panel adjacent to the obtuse corners, and increased when the load was adjacent to the end diaphragm

Azad et al. (1996) verified the accuracy and reliability of an analytical method for the computation of punching shear strength in a bridge deck slab. The failure of a deck slab in a girder slab bridge under a patch load was expected to produce punching-type failure with the top surface of the failed zone matching the loaded area. If the failure surface is approximated as an inclined slip plane, the angle of this plane is expected to lie within the range of 20 to 35 degrees with respect to the horizontal. The ACI formula was highly conservative in estimating the punching shear strength of the slab subjected to smaller patch loads. The Jiang and Shem Model appeared to hold true for a deck slab of low-to-moderate concrete strength.

Loo et al. (1997) studied a nonlinear finite element procedure for determining both the deflection and the punching shear strength at corner and edge column connections of reinforced concrete flat plates with or without spandrel beams. They discovered that good correlations are observed for the punching shear strengths, the collapse loads, and the load-deflection, as well as the crack patterns. The performance of the proposed method was satisfactory and consistent. For the computation of the punching shear strength, Loo and

Falamaki provided an accurate prediction for all results. Australia code gave good results from the models with torsion strips but overestimated for the model with spandrel beams. For the flat plate with free edges, both American code and British code overestimated the punching shear strength.

Ebeido et al. (1996) Verified and substantiated the modeling used in the nonlinear finite-element on the punching strength of skew bridge decks. The punching-load capacity of deck slabs of skew composite steel-concrete bridges was affected by the following parameters: it increased with reduction the girder spacing, decreased with increases in the angle of skew, improved with increase in the reinforcement ratio, increased with increase in the size of longitudinal girders sensitive to a change in the deck slab thickness and decreases at the panel adjacent to the obtuse corners, increased when the load was adjacent to the end diaphragm.

Anchorage Behavior

Dieter Lotze et al. (2001) studied the static behavior of anchors under combinations of tension and shear loading. The specimens were concrete blocks 39.5 in. wide, 24 in. deep and 87.5 in. long. There was a longitudinal bar placed in the middle of the concrete block. The specimens were load by actuator through the steel frame. The parameters that affected the behavior were concrete strength, anchor size, installation method, and loading direction, especially when shear dominated. For example low steel strength, small anchor diameters, and high strength concrete lead to small deformation capacities and ductile fractures. They also stated that the plasticity theory accurately predicts connection behavior and capacity for large eccentricity in shear test on two anchor connection. For low eccentricities, the strength was over predicted by the plasticity theory. The correction of the problem was done by assuming even distribution of shear to all anchors.

2.5 Need for Research

There are limited researches that partially relate to the behaviors of the falsework hanger system as mentioned in section 2.3. However, there is no literature that relates to the behavior of the falsework hanger embedded on the NCDOT modified bulb tee girder. The tests performed by Dayton/Richmond on November 4th, 1996 indicated that the hanger C-24 4-AP had a safe working load of only 3,300 lbs. while the hanger C-24 type 4-APR which is similar to the hanger C-24 type 4-AP has a safe working load of 6,000 lbs. Additionally, the manufacturer specifications require a bearing minimum concrete thickness of 5 in., but the NCDOT modified bulb tee top flange width is only 3½ in. thick. Therefore, this research is obviously needed for the understanding of the behaviors and to verify the ultimate strengths of the falsework hanger embedded on the NCDOT MBT girder.

The experimental and analytical programs were generated to investigate the behavior of the falsework hanger system. The details of the experimental and analytical investigations are discussed in the following sections.

3.0 EXPERIMENTAL INVESTIGATION

3.1 Overview

To investigate the behavior of edge of flange overhang falsework hangers installed in the top flange of modified bulb tee (MBT) girder seven full-scale tests were performed at the North Carolina State University Constructed Facilities Laboratory. Two types of hangers were used in the testing: Dayton C-24-APR and Meadow Burke HF-43. To fully understand the behavior, the effects of girder reinforcement and the interaction between adjacent hangers tested simultaneously was considered. The experimental test matrix is shown in Table 3.1.

Table 3.1 Experimental Test Matrix

Test ID	Hanger Type	Girder Shear Reinforcement	Hanger Spacing	Number of Loaded Hangers
DR-1-H	Dayton (C24-APR)	High	-	1
DR-1-L	Dayton (C24-APR)	Low	-	1
DR-2-L	Dayton (C24-APR)	Low	3'	2
MB-1-H	MB (HF43)	High	-	1
MB-1-L	MB (HF43)	Low	-	1
MB-2-L	MB (HF43)	Low	3'	2
MB-4-L	MB (HF43)	Low	3'	4

The test ID indicates the type of tested hanger, number of hangers tested simultaneously, and the amount of shear reinforcement within the girder at the test location. The first two letters indicate the type of hanger, DR for Dayton/Richmond hanger and MB for Meadow/Burke hanger. The number following the letters indicates the number of hangers tested. The last letter symbolizes the amount of girder shear reinforcement, H and L for high and low shear reinforcement, respectively. For example, test DR-1-H is a single Dayton/Richmond hanger test located in the high shear reinforcement area.

The single hanger tests simulated the load capacity that directly compared to the published manufacturer safe working load. Tests were performed in two different locations. One was at the end of the girder where there was high shear reinforcement and the other was at the middle of the girder where there was low shear reinforcement. Two and four hanger tests were performed to observe the interaction between adjacent hangers. Three foot spacing between adjacent hangers was used to simulate the typical field condition.

The load was applied to the hanger a 45 degree angle using a hydraulic cylinder. The girder was braced laterally at locations approximately three feet on either side of the test hanger location.

3.2 Test Specimens

3.2.1 Hangers

Two types of hangers were used in this test program. One was a single leg hanger manufactured by Dayton/Richmond, the other one was a double leg hanger manufactured by Meadow/Burke. The head of the Dayton/Richmond hanger was approximately 5/16 in. wide, 2 3/16 in. long and 1 15/16 in. tall and had 12 in. leg. The leg was embedded 3½ in. into concrete. The Meadow/Burke hanger had the same size hanger head and leg as Dayton/Richmond's. In an addition to the Dayton/Richmond hanger, Meadow/Burke had an extra front leg welded to the hanger head. The front leg was 2 1/8 in. long and embedded into an the concrete. There was an anchor at the end for hanger leg to provide extra resistance. Figures 3.1 and 3.2 illustrate the detail of the hangers. The hangers were installed along the edge of the MBT girder flange in accordance with the manufacturers' specifications. The hanger's leg embedded in the top of girder flange to generate the anchoring force to resist the horizontal forces applied to hanger. Figure 3.3 shows the Meadow/Burke hangers embedded on the MBT girder.

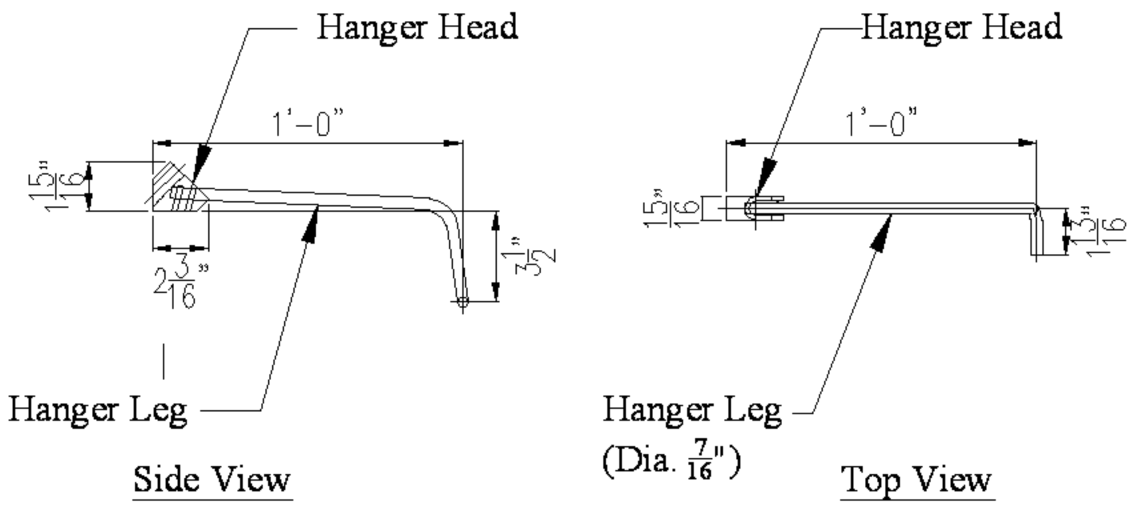

Figure 3.1 Dayton/Richmond Hanger Details

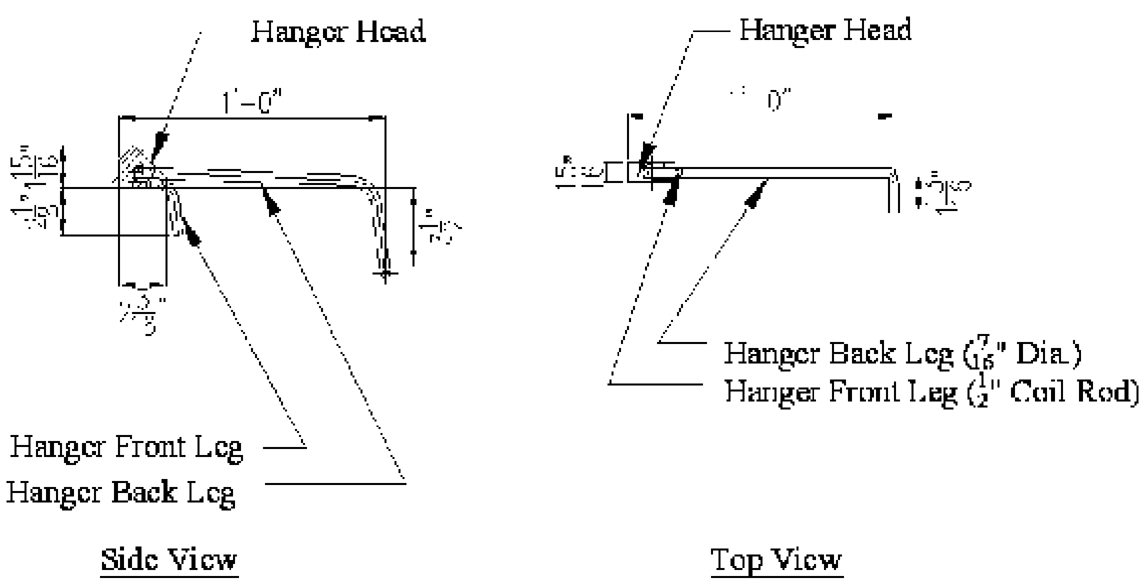

Figure 3.2 Meadow/Burke Hanger Details

Figure 3.3 Installed hangers

3.2.2 MBT Girder Details

A standard NCDOT 63” MBT girder was used in the test program. The girder was cast by Prestress of the Carolinas in Charlotte, NC on May 16th 2005. The Test Girder was 44 foot long with the two hanger types installed on separate sides of the girder. The MBT Section has a 43” wide top flange that is 3.5 in. thick at the edges. The complete cross-section dimensions are shown in Figure 3.4.

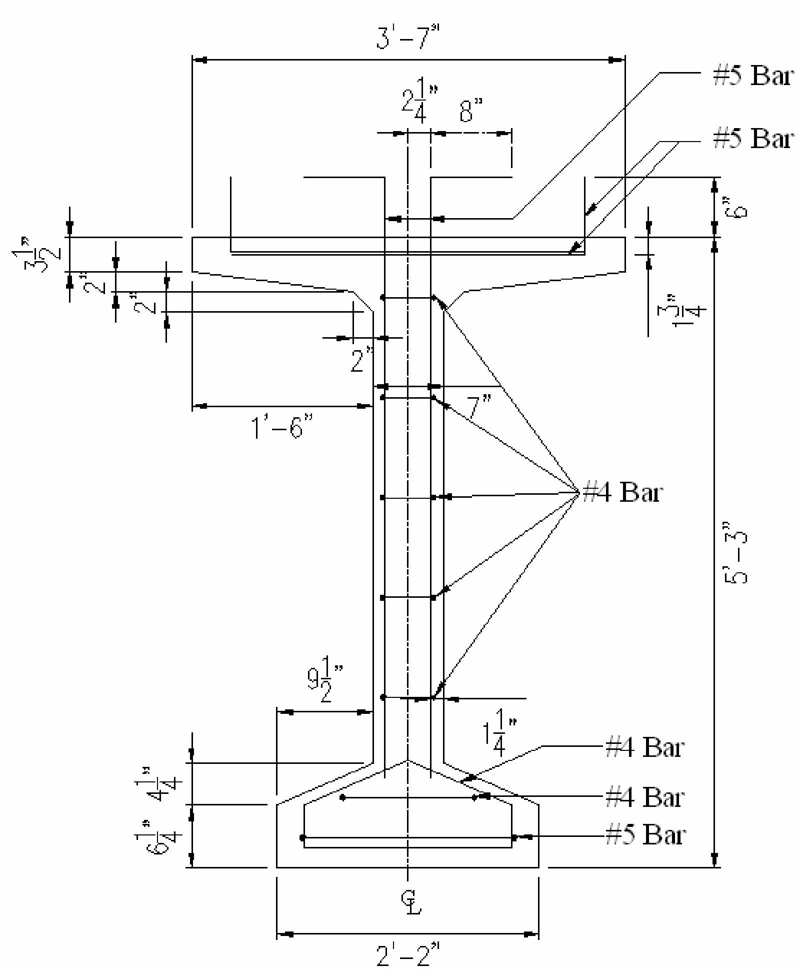

Figure 3.4 NCDOT MBT Girder details

The test girder reinforcement and prestressing forces were designed to emulate the stresses at the quarter point of an eighty foot span girder. Standard NCDOT reinforcement patterns were utilized. A detailed plan of the girder reinforcement is included in Appendix A. The girder prestressing consists of 32 strands. Two strands were within the top flange, six were within the web, and 24 were in the bottom flange. Ten strands were debonded to ensure a final prestressing stress of approximately 200 ksi. This stress was essentially constant throughout the length of the girder. Figure 3.5 shows the strands pattern at the end and mid-span of the girder.

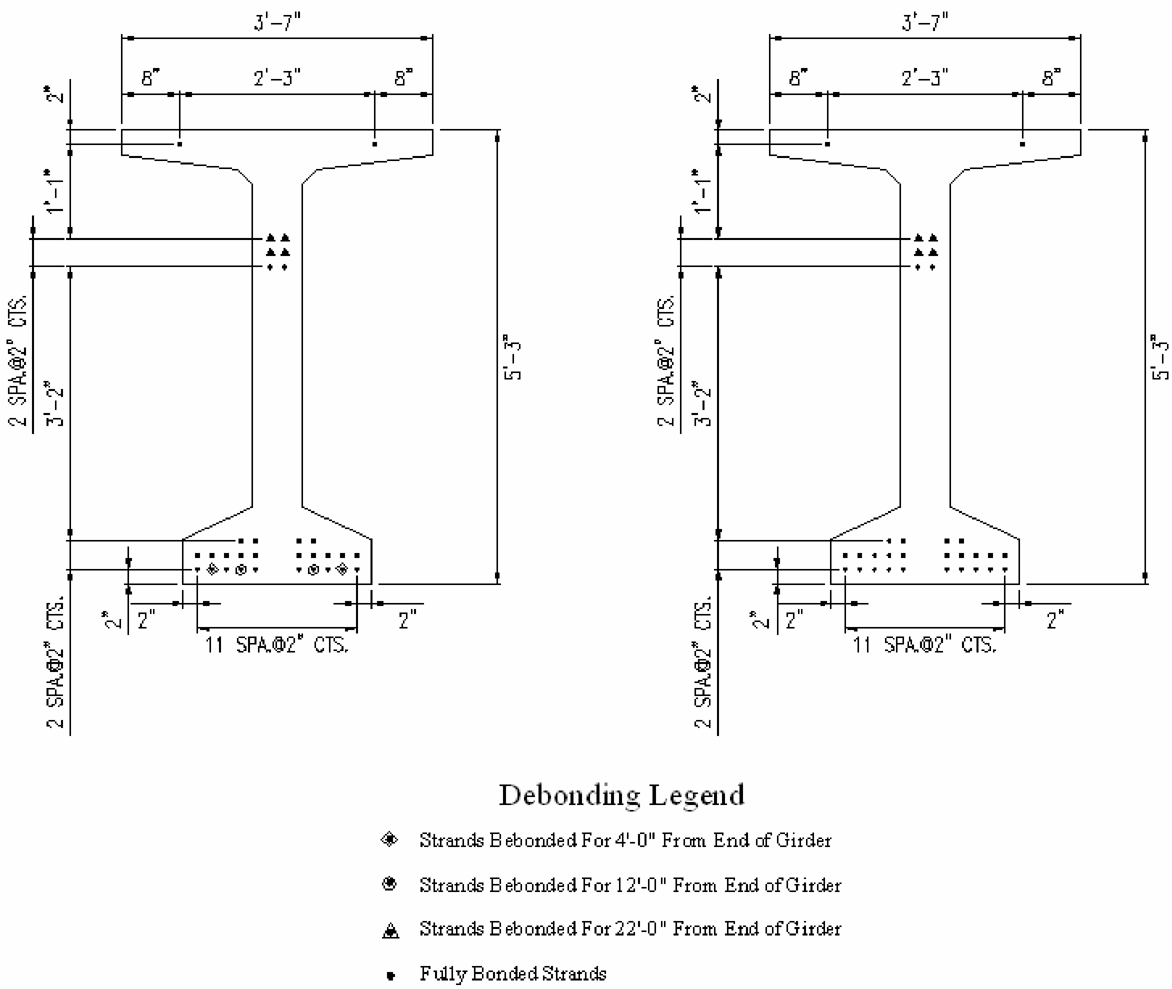

Figure 3.5 Prestressing strand detail

3.3 Test Setup

The test setup consisted of two major systems: loading and bracing/support systems. The loading system applied the load directly to the hanger at a 45-degree angle. The vertical component of applied load was resisted by a support system at both ends of the girder and the horizontal component was resisted by a bracing system at 3 feet away from a tested hanger as illustrated in Figure 3.6.

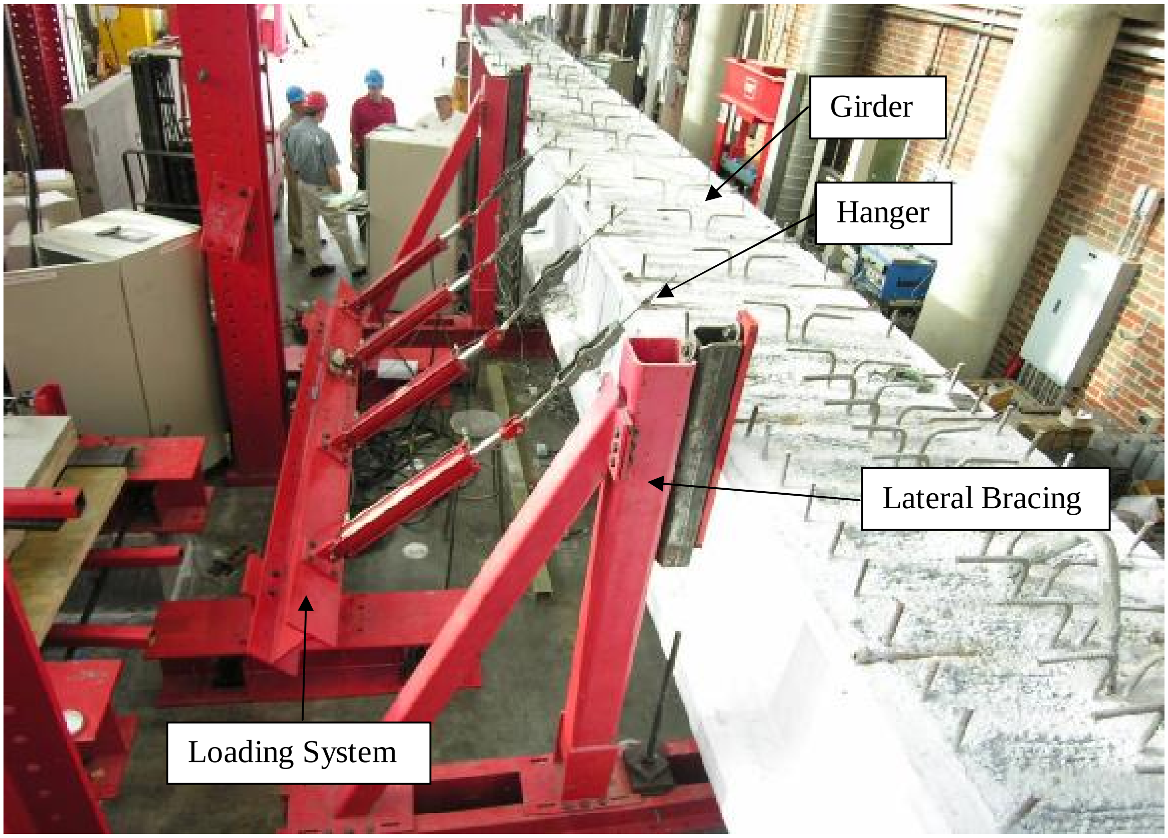

Figure 3.6 Test setup

3.3.1 Loading System

Tests were performed by applying load to one, two, or four hangers at the same time. A 45 degree load was applied using a hydraulic cylinder as shown Figure 3.7. To apply the load to the hanger, the load was transferred form the hydraulic cylinder to the eye-rod, clevises, coil rod and hanger, respectively. On the support side of the hydraulic cylinder, a reaction beam was connected to the laboratory reaction floor. The loading system was designed to resist the maximum load of 18 kips as controlled by the coil rod.

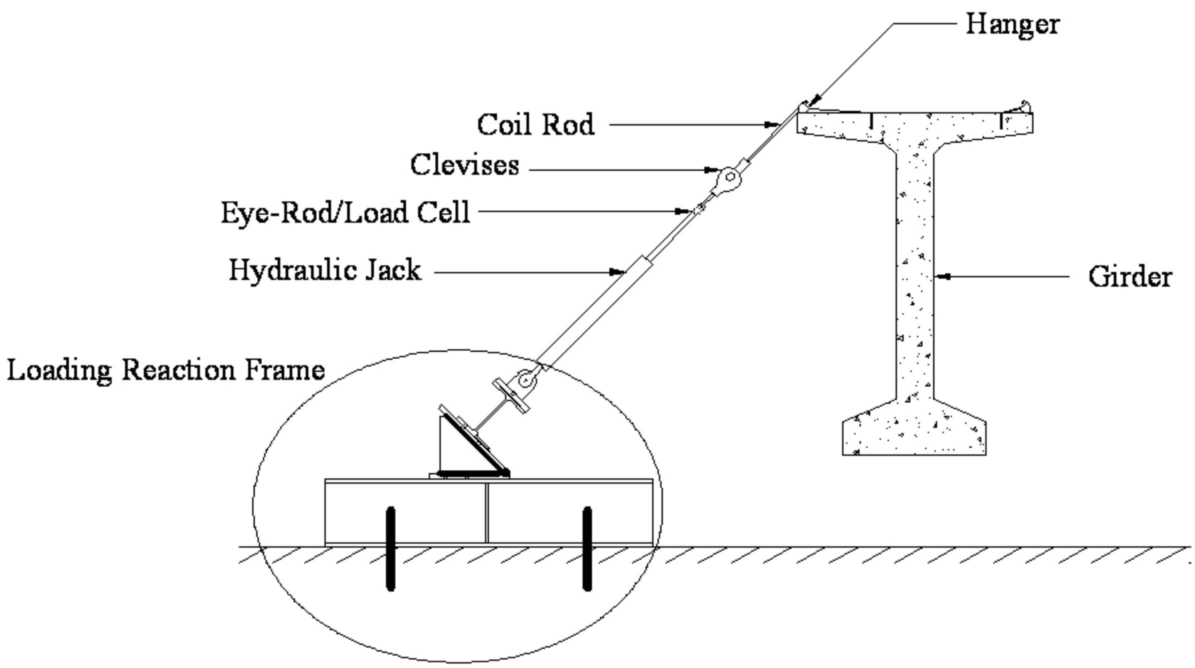

Figure 3.7 Loading system

Coil Rod

A standard ½ in. diameter coil rod was used to transfer the load from clevis to the hanger as shown in Figure 3.8. From manufacturer specifications, the coil rod was manufactured by high strength steel, had a minimum area of 0.1385 in^2, was based on a 2 to 1 safety factor, and had a manufacturer safe working load of 9,000 lbs.

Figure 3.8 Coil Rod (Dayton Superior, Dayton/Richmond concrete accessory, 2005)

Clevises

The clevises were manufactured by Cleveland City Forge. Two number 4 clevises were used to connect the coil rod and eye rod. According to the AISC manual, design strength of number 4 clevis is 52.5 kips. Clevises were connected to each other by a 1 in. diameter pin. After connected, one side was connected to an eye rod which had standard threads that fit with the clevis’ thread. The other end was connected to the coil rod by a coil nut. Figure 3.9 illustrates the clevises and connections.

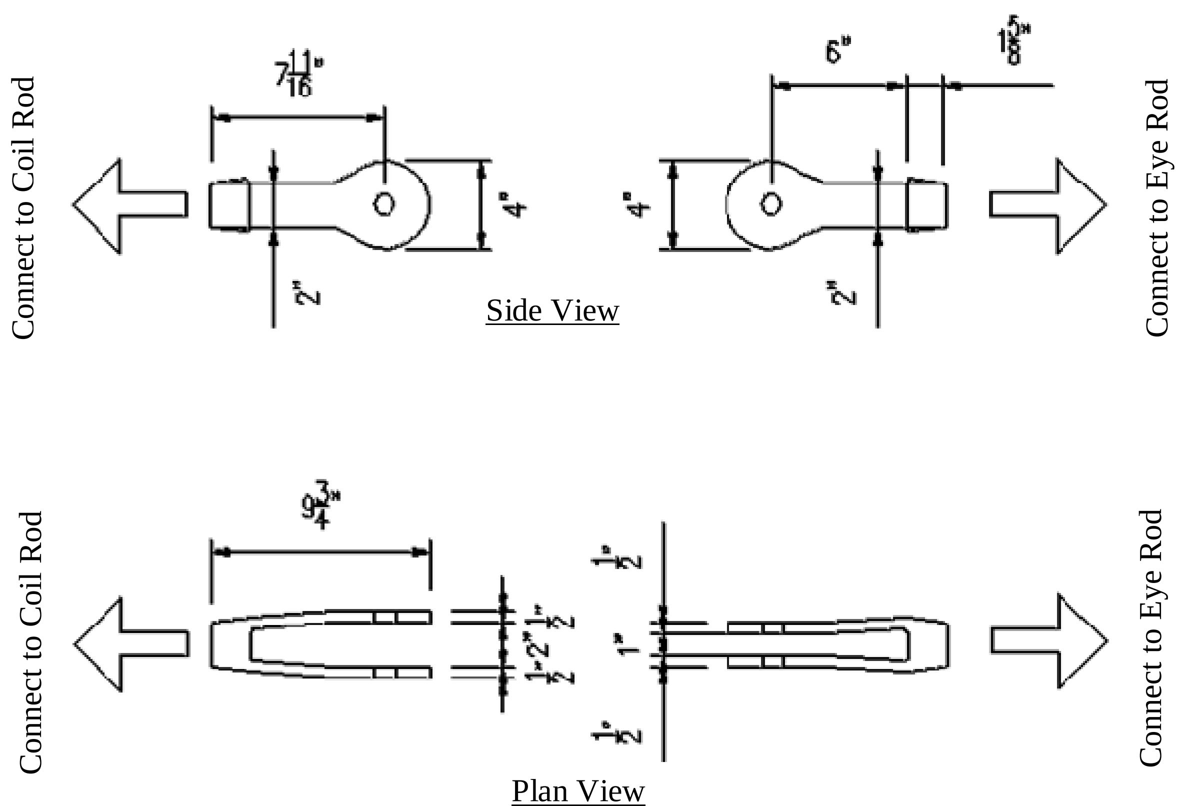

Figure 3.9 Clevis details

Eye Rod/Load Cell

An eye rod connected to the clevises with threads and a hydraulic cylinder connected by pin. The eye rod was 12 in. long with 4 in. of standard thread and had a 1 in. pin diameter. The inside and outside diameter of the eye was 1 in. and 2 in., respectively. From the manufacturer's specification, the eye rod is made of C-1035 carbon steel, and the yield load is 47,000 lbs. (Cleveland City Forge, 2005). Figure 3.10 shows the details of the eye rod.

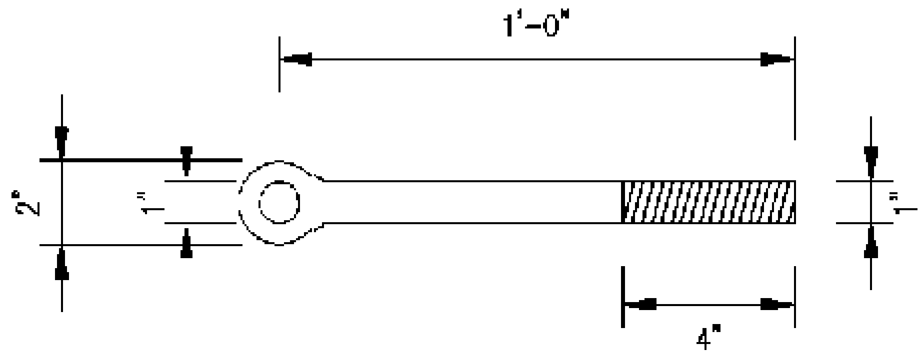

Figure 3.10 Eye rod detail

Hydraulic Cylinder

The hydraulic cylinder was a high-pressure tie-rod type double acting cylinder manufactured by Energy Manufacturing Company. The cylinder used in the test program had a 4 in. bore size, 2 in. rod diameter, and a 24 in. stroke as shown in Figure 3.11. Pins at both ends had 1.125 in. diameter. The maximum working pressure was 3,265 psi, which equates to a 30 kips working load. For each test, the cylinders started from 8 in. of stroke and retracted until hanger failure. The hydraulic cylinder applied load to the hanger through the eye rod, clevises and coil rod and was supported by the loading frame.

Figure 3.11 Hydraulic Cylinder

<u>Load reaction frame</u>

The Load reaction frame consisted of four components: cylinder bracket, loading supporting beam, loading bracket and supporting beam as shown in figure 3.12. The cylinder bracket was used to connect the hydraulic cylinder to the loading beam. A 1” half-circle end plate was welded to the square to form the cylinder bracket. Four 4-¾” diameter A325 bolts connected the cylinder bracket to the loading beam. A W10x70 was used as a 12 foot long loading beam. The loading beam was bolted to a loading bracket by 4-¾” diameter A325 bolts at both ends, generating a 45 degree load. Four 4-¾” diameter A325 bolts connected the loading bracket and the loading support beam together. The loading support beam was a

W14x95, 5 foot long and contained a full-stiffener at the midpoint. The loading support beam was prestressed to the floor by 1” diameter Dywidag bars. The prestressing force resisted the horizontal force by generating pressure between the loading support beam and the floor, creating high friction resistance. The loading frame is illustrated in Figure 3.12

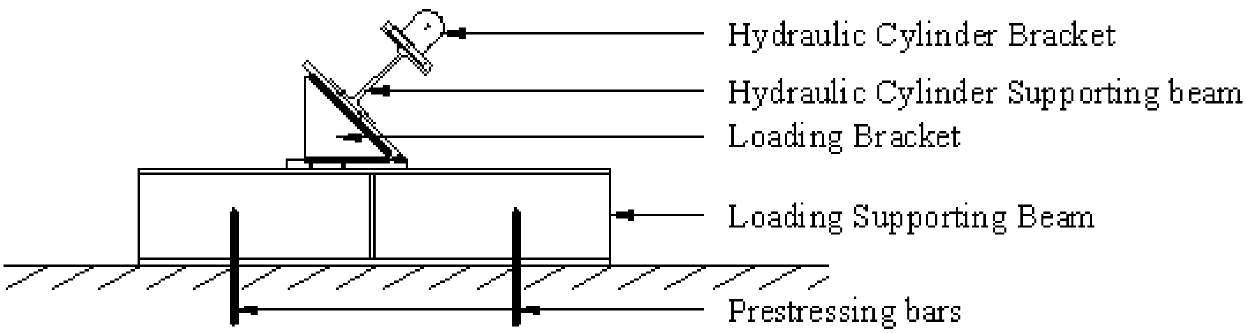

Figure 3.12 Load reaction frame

3.3.2 Lateral Bracing and Support System

The lateral bracing system was installed 3 feet on either side of the hanger. Lateral bracing consisted of an A-Frame bracing the top flange and a bracket to brace the bottom flange. Two types of lateral bracing systems were used in the test program: intermediate and end lateral bracing. The intermediate lateral bracing consisted of 2-C10x30 supports. The end lateral bracing used the same supports as the girder supports. Figure 3.13 and 3.14 shows the two types of lateral bracing systems used in the test program. A W14x145 was used as a girder supporting beam. An elastomeric bearing pad and steel plate were placed between the girder and supporting beam to generate pin-type connections and distribute the force to the supporting beam at both ends of the girder.

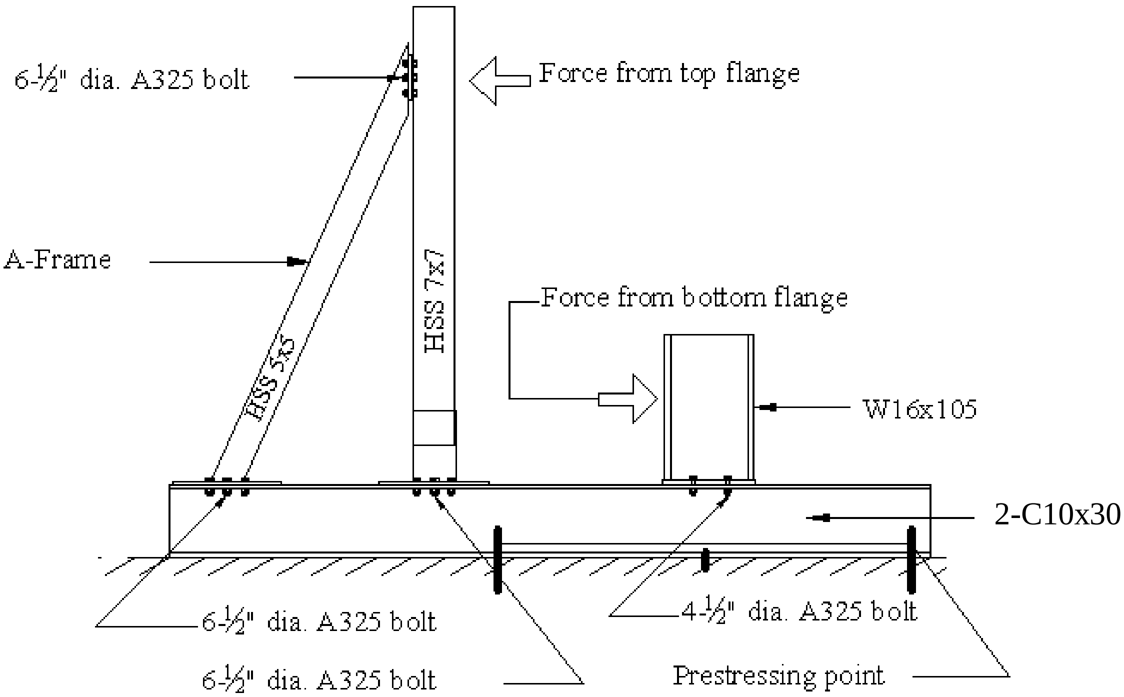

Figure 3.13 Intermediate lateral bracing system

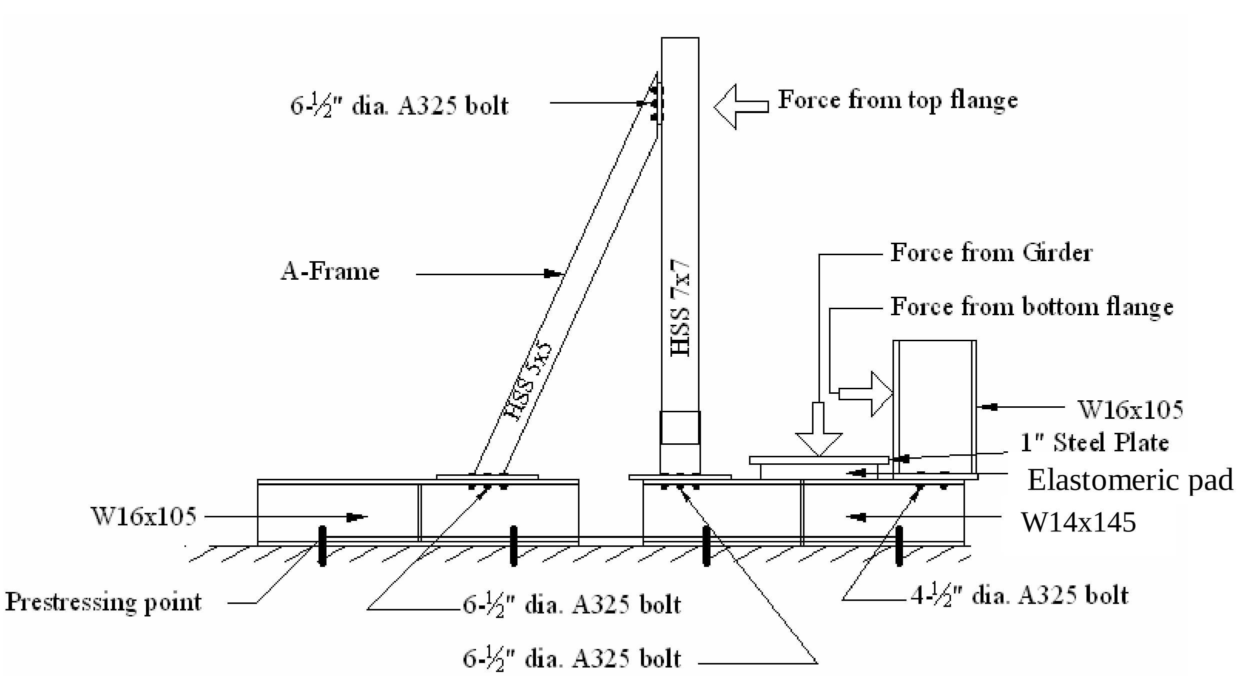

Figure 3.14 End Lateral Bracing and Supporting beam

3.4 Instrumentation

The test specimens were instrumented to capture the load, displacement and strain response. The instrumentation was connected to a PC-controlled data acquisition system and calibrated prior to use. Throughout the test, data points were recorded in intervals close enough to capture the specimen responses.

The eye rod mentioned in the loading system performed as a load cell by installing four uniaxial strain gages. The load cell was calibrated using an MTS load frame as shown in Figure 3.15.

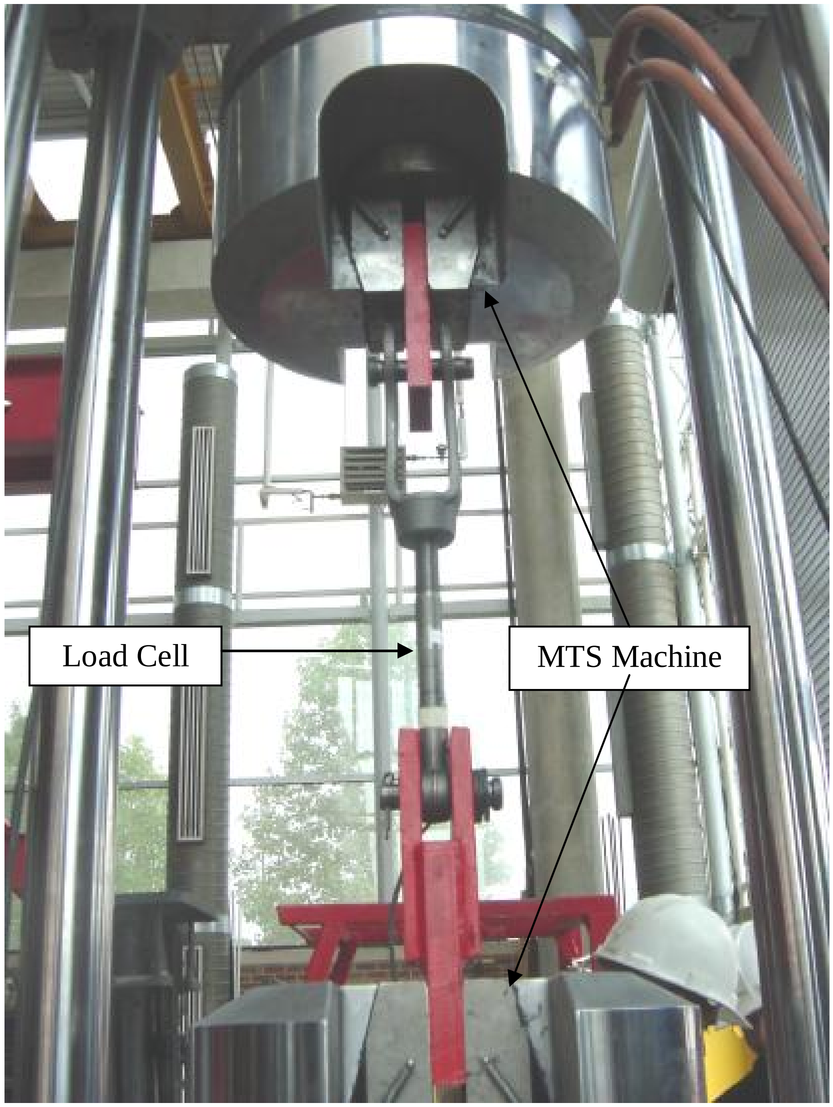

Figure 3.15 Load cell calibration

The displacement responses of the girder such as girder deflection, flange deflection, and girder rotation were captured by measuring the displacement in several points on the girder. To obtain the responses, linear and string potentiometers were used. Generally, flange deflections were captured using string potentiometers, and girder deflection and rotation were captured using linear potentiometers. Figure 3.16 shows the typical layout of the instrumentation. In appendix B to H, the location of the instrumentation used in each test is shown.

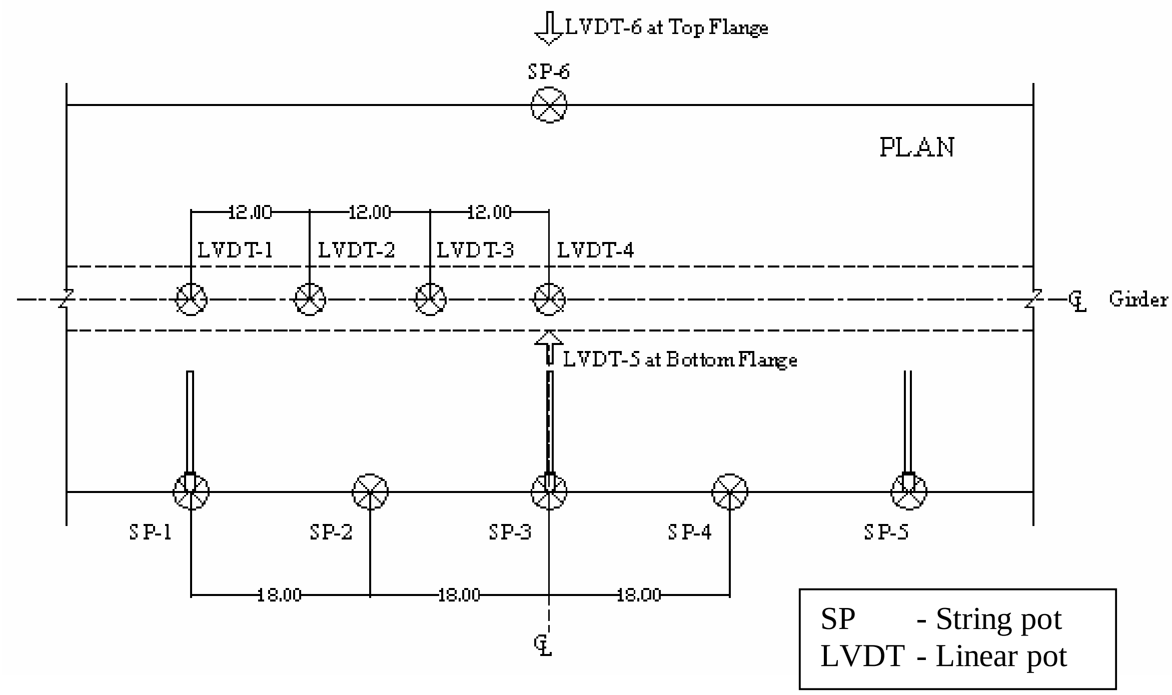

Figure 3.16 Typical instrumentation

Strain contour on the surface of the flange in the area around the hanger was monitored using PI-Gauges, an instrument measuring the displacement in one direction within gage lengths. The output of PI-Gauges was the total displacement within its two legs. The average strain within the gage length can be obtained by the following equation.

$$Strain = \frac{Displacement}{Gage\ length} \qquad \text{(Eqn. 3.1)}$$

The gage lengths that were used in instrumentation were 100 mm and 200 mm as illustrated in Figure 3.17. Figure 3.18 shows the PI-Gauge layout of the test DR-1-L. The details, gage length, direction and location, of the PI-gauges for each test are provided in appendices B to H.

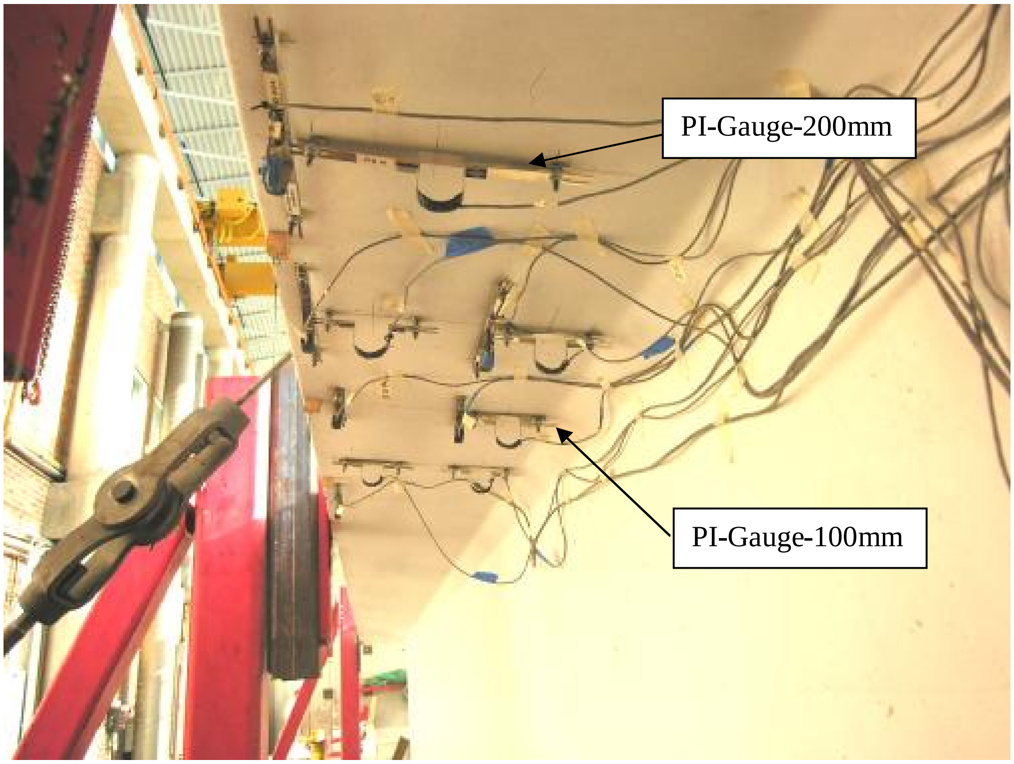

Figure 3.17 PI-gauges under the top flange for test DR-1-L

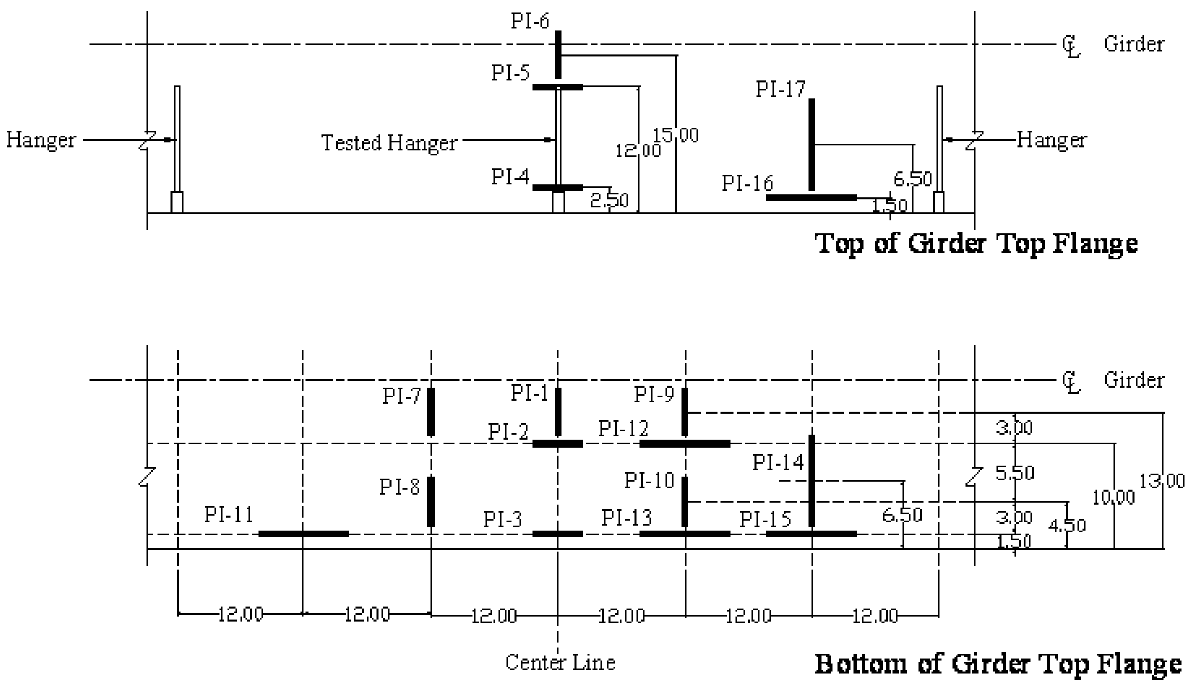

Figure 3.18 PI-gauges layout of test DR-1-L

3.5 Test Procedure

After the test specimens and supporting system were setup, the girder was cleaned and a white wash was applied to magnify cracking. The lateral bracing and loading system were then set up. For the intermediate lateral bracing system, spacers including a HSS5x5 and a ¼" thick soft pad were used as support for the lateral force. After all test specimens and test setup systems were put in place, the instruments were connected to the data acquisition system, calibrated and installed as shown in appendix B to H. Instruments were zeroed prior to application of the load.

A preload was applied to check the instrumentation. If the data from the preload period was satisfactory, the instruments were zeroed again, and load was applied to the hanger. The loading was divided into 3 steps, half of the manufacturer's working load, manufacturer's working load, and the ultimate load as illustrated in Figure 3.19. After reaching each load step, the hanger specimen was unloaded.

Testing was continued until one component of the connected system made up of the hanger, girder flange and loading system was disconnected from an adjacent component. Types of failure that were expected were coil rod rupture, hanger leg rupture, flange bending failure, punching shear failure and girder torsion failure. For the two and four hanger-testing program, testing was continued after failure of the first hanger by disconnecting the failed hanger and loading the remaining hangers until the last hanger failed. When the test was completed, data points for all sensors were reduced to a worksheet file. The test results will be discussed in the next sections.

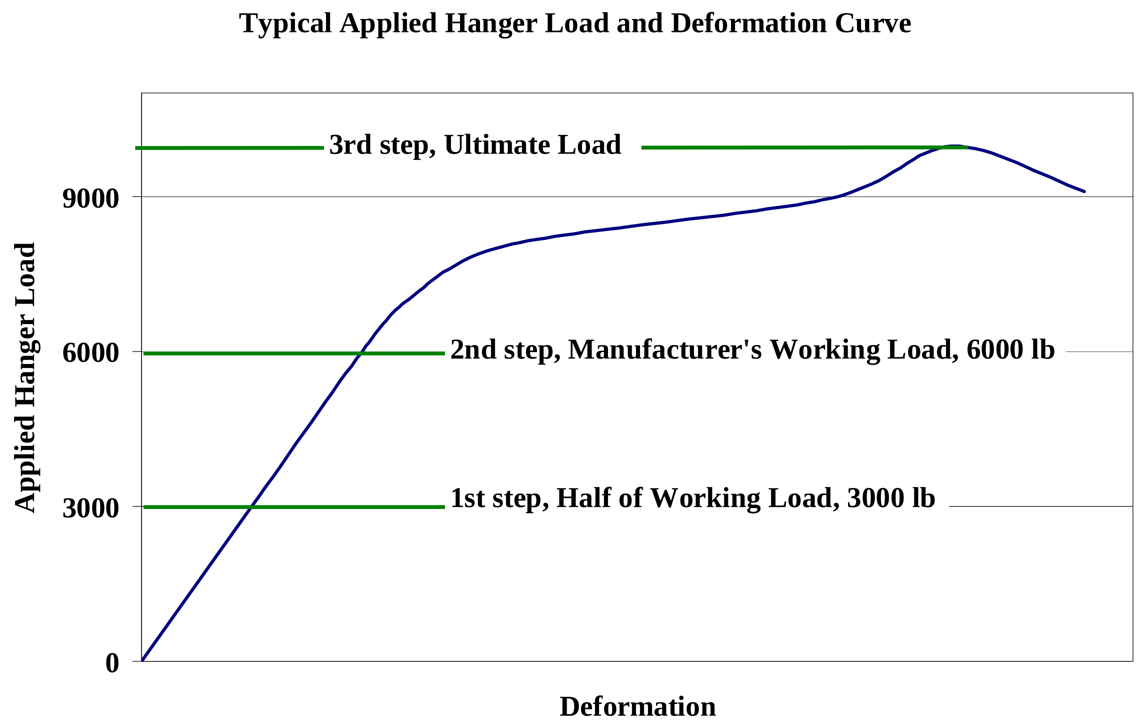

Figure 3.19 Load steps for each test

3.6 Test Results

The test summary reports for each test are available in Appendices B through H. Each report consists of the test specimen properties, test setup, photographs, typical experimental results and the failure type. The typical plots are the mid-span deflection at the center line of the test set up versus applied hanger load, relative deflection between mid-span and lateral support and the longitudinal strain at 1.5 inch from edge of flange versus applied hanger load. The summary of the ultimate load and the failure types of all seven full-scale hanger tests are shown in Table 3.2. One, two and four hanger results are discussed in the following sections.

Table 3.2 Summary of Results

Test ID	Test Name	Description	Ultimate Load	Manufacturer Ultimate Load	Failure Type
1	DR-1-H	Dayton/Richmond Hanger, one hanger pull, high reinforcement	9,200	12,000	Crush/ Spalling
2	DR-1-L	Dayton/Richmond Hanger, one hanger pull, low reinforcement	9,200	12,000	Crush/ Spalling
3	DR-2-L	Dayton/Richmond Hanger, two hanger pull, low reinforcement	10,200	12,000	Punch
4	MB-1-H	Meadow/Burke Hanger, one hanger pull, high reinforcement	8,500	12,000	Punch
5	MB-1-L	Meadow/Burke Hanger, one hanger pull, low reinforcement	6,500	12,000	Punch
6	MB-2-L	2 Meadow/Burke Hanger, two hanger pull, low reinforcement	6,700	12,000	Punch
7	MB-4-L	4 Meadow/Burke Hanger, four hanger pull, low reinforcement	5,800	12,000	Punch

3.6.1 One Hanger Test

Four single hanger tests were conducted, two Dayton/Richmond hangers and two Meadow/Burke hangers. Figure 3.20 and figure 3.21 show the edge of the flange vertical deflection and the applied hanger load from the Dayton Richmond hanger and the Meadow/Burke result, respectively.

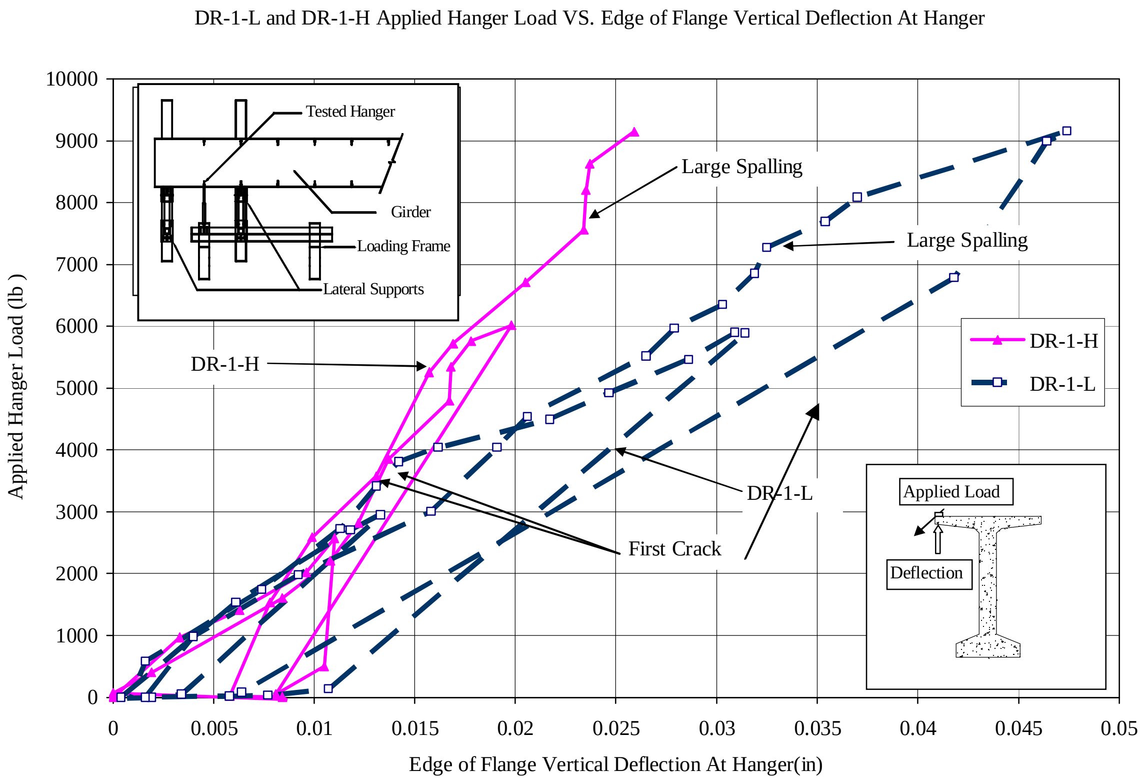

Figure 3.20 Dayton/Richmond hanger, edge of flange vertical deflection and applied hanger load

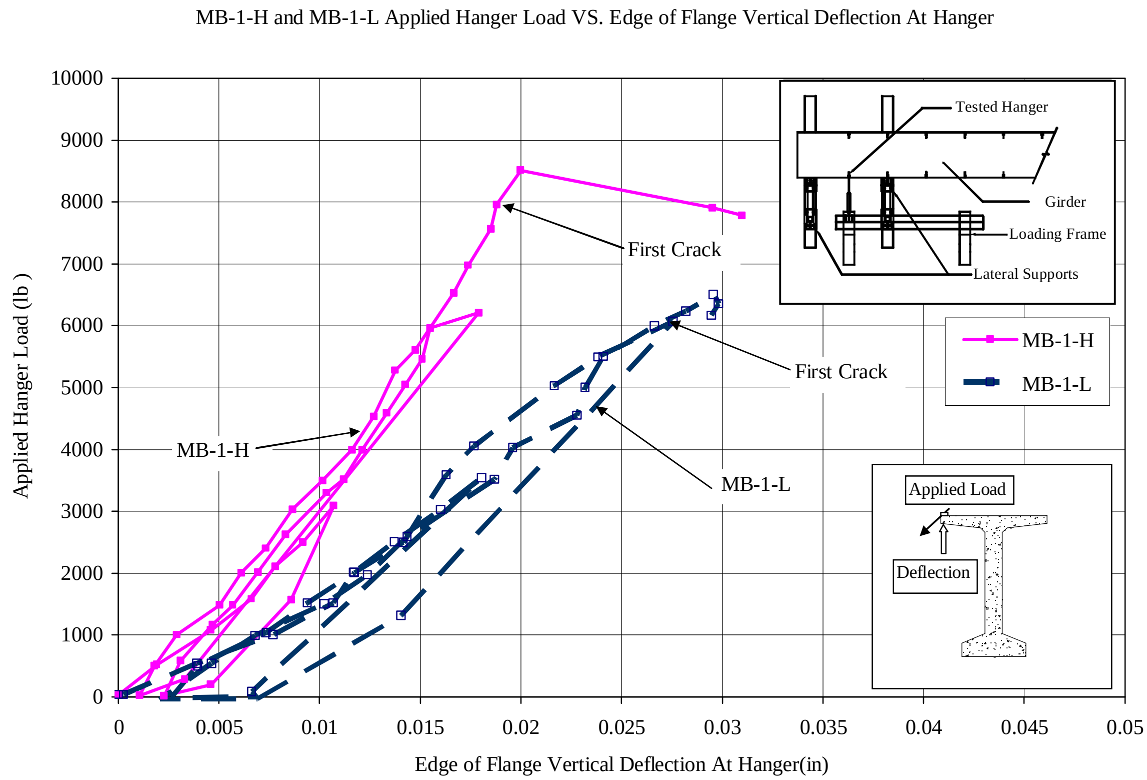

Figure 3.21 Meadow/burke hanger, edge of flange vertical deflection and applied hanger load

In the Dayton/Richmond hanger tests, the first crack was observed on the top flange at the back side of the hanger head at around 3,500 lb. for both tests. At this point, the back side of the hanger head started to lift up and the front side began to crush the concrete. As the load increased, the cracks propagated to the edge of the flange and the hanger head rotated (see Figure 3.22). Spalling of the concrete was found at 7,500 lbs. and 7,000 lbs. for test DR-1-H and DR-1-L, respectively (see Figure 3.23). After spalling of the concrete, the hanger head experienced large rotation. The hanger failed at 9,200 lbs. for test DR-1-H and DR-1-L as illustrated in Figure 3.24.

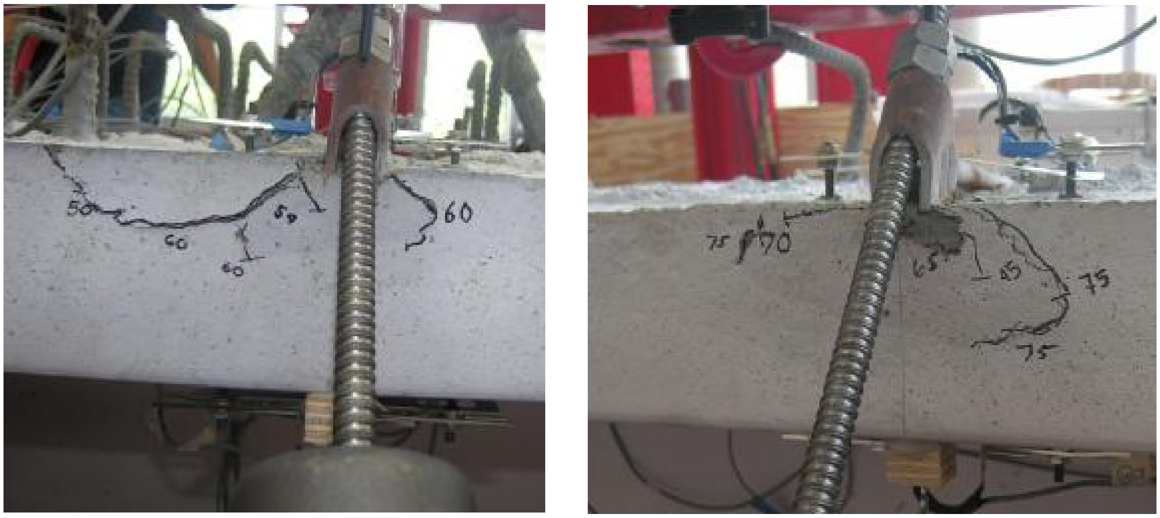

Test DR-1-H Test DR-1-L

Figure 3.22 Crack Propagations of test DR-1-H and DR-1-L

Test DR-1-H Test DR-1-L

Figure 3.23 Large spalling of concrete, test DR-1-H and DR-1-L

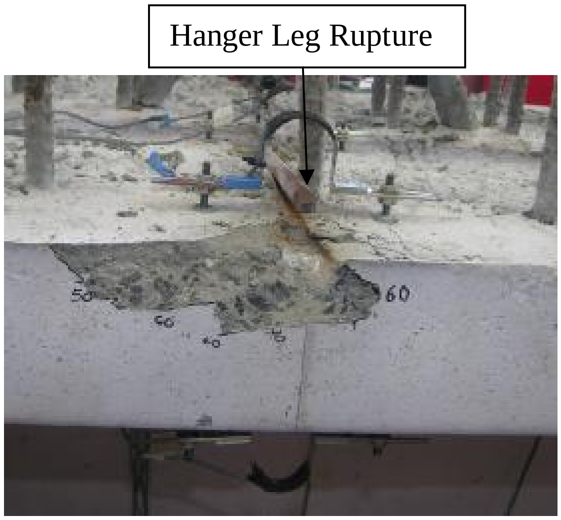

Test DR-1-H

Test DR-1-L

Figure 3.24 Failures of test DR-1-H and DR-1-L

For the Meadow/Burke hanger tests, no distress was observed during the low loads. For test MB-1-H, the first crack was observed at 8,000 lbs. around the back side of the front hanger leg. The cracks propagated while the applied load was sustained at 8,000 lbs. The punching shear failure occurred at 8,500 lbs. The first crack was observed at 6,000 lbs. in test MB-1-L. The crack propagated to the edge while the load was sustained similarly to test MB-1-H. The girder flange failed at 6,500 lbs. by punching shear failure. Figure 3.25 illustrates the failure modes of tests MB-1-H and MB-1-L.

Test MB-1-H

Test MB-1-L

Figure 3.25 Failures of test MB-1-H and MB-1-L

Strains captured by the PI-gauges were increase as the load was applied. High longitudinal tensile strain was developed at the bottom of the top concrete flange under the hanger head. The longitudinal strain decreased as the distance from the hanger head increased. Figure 3.26 illustrates the strain development for all the single hanger tests at 6000 lbs. The longitudinal tensile strains decreased while the distance form the edge of the girder flange along the center line increased. As see in Figure 3.27, the longitudinal tensile strain decreased in the same patterns for all of the single hanger tests. At 12 in. from the center line, transverse compressive strains under the girder flange increased as the distance form the edge of the girder flange increased, see Figure 3.28. The increasing in the compressive strain for the Dayton/Richmond hanger test was larger than the one from Meadow/Burke hanger tests.

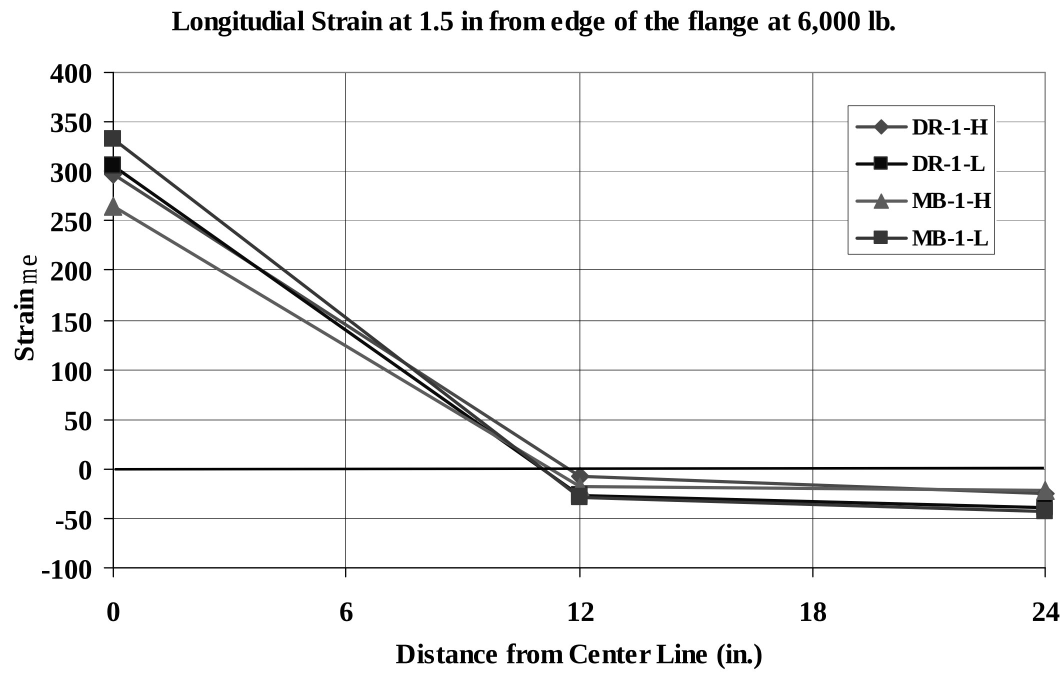

Figure 3.26 Strain developments along the girder flange for single hanger tests

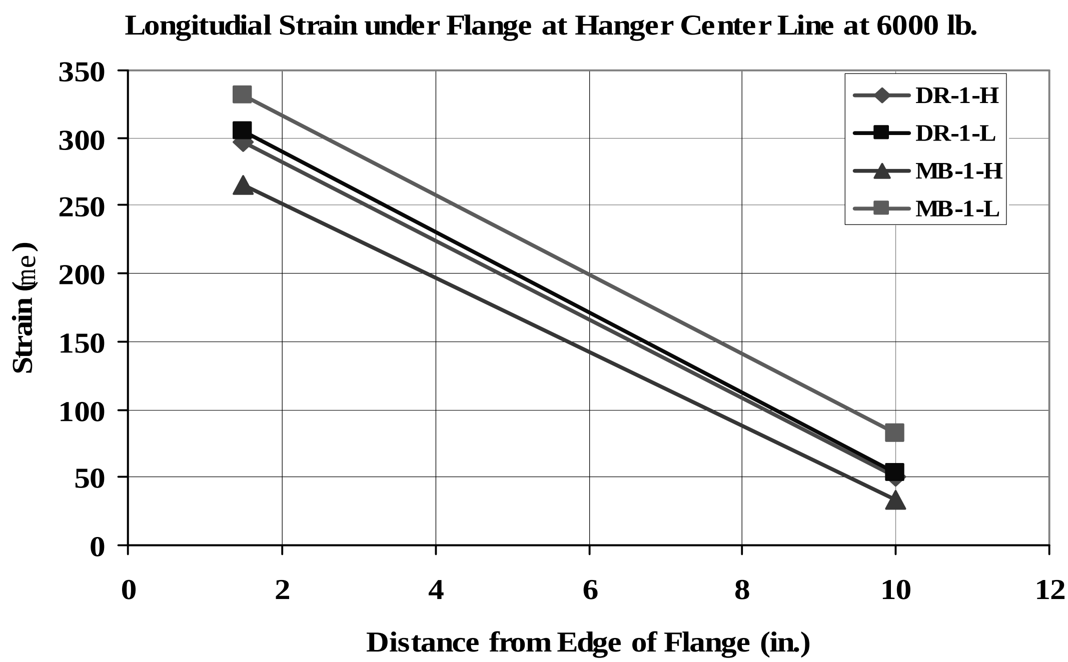

Figure 3.27 Strain developments along the center line for single hanger tests

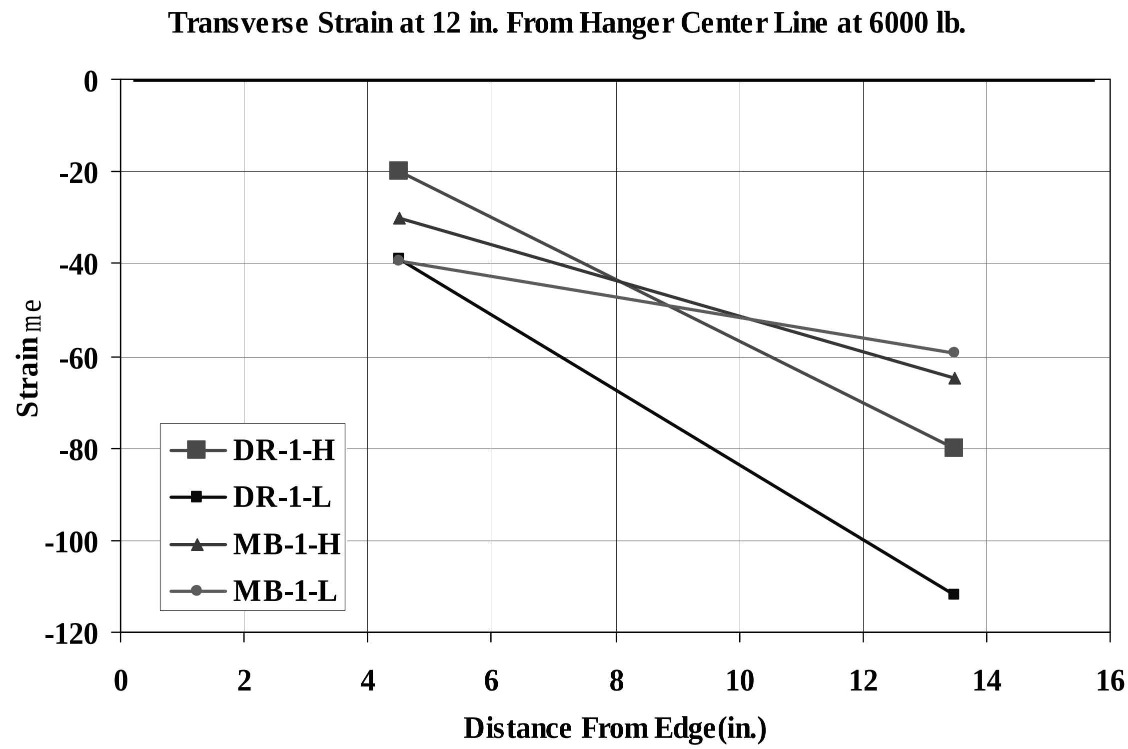

Figure 3.28 Strain developments at 12 in. form center line for single hanger tests

3.6.2 Two hanger test

Two hanger tests were conducted, one using Dayton/Richmond hangers and the other using Meadow/Burke hangers. Figure 3.29 and figure 3.30 show the edge of the flange vertical deflection and applied hanger load from the Dayton/Richmond hanger and Meadow/Burke hanger, respectively.

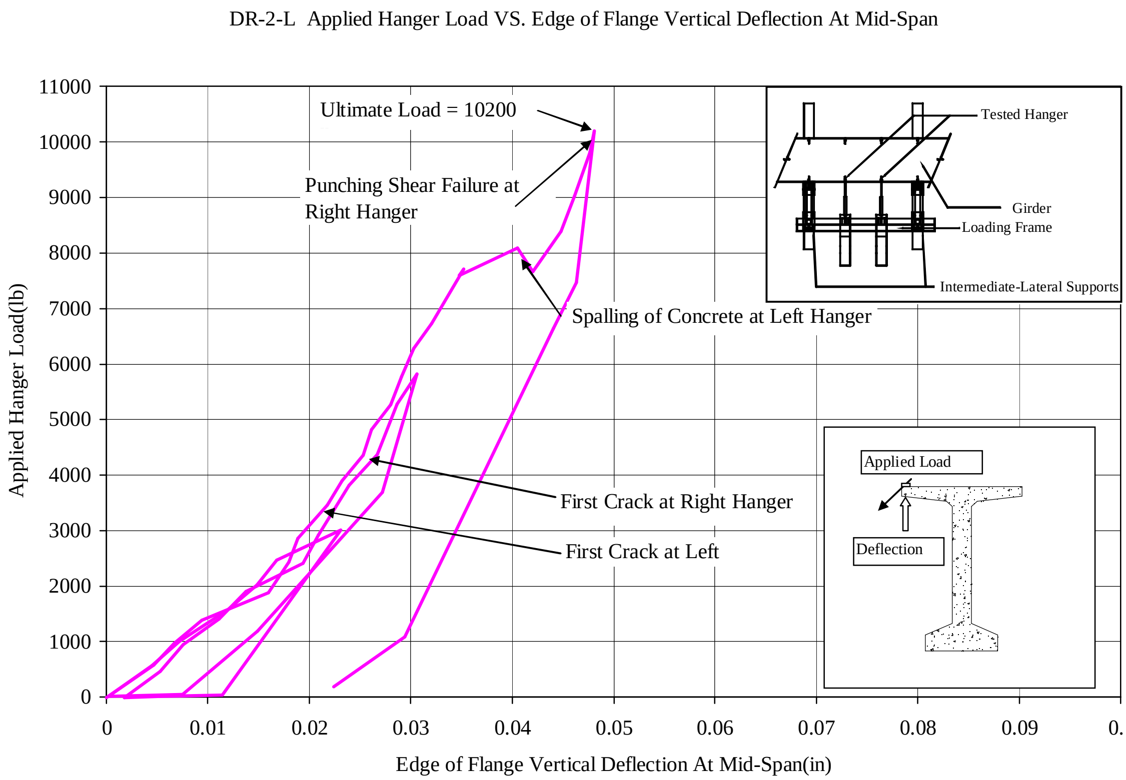

Figure 3.29 DR-2-L, edge of flange vertical deflection and applied hanger load

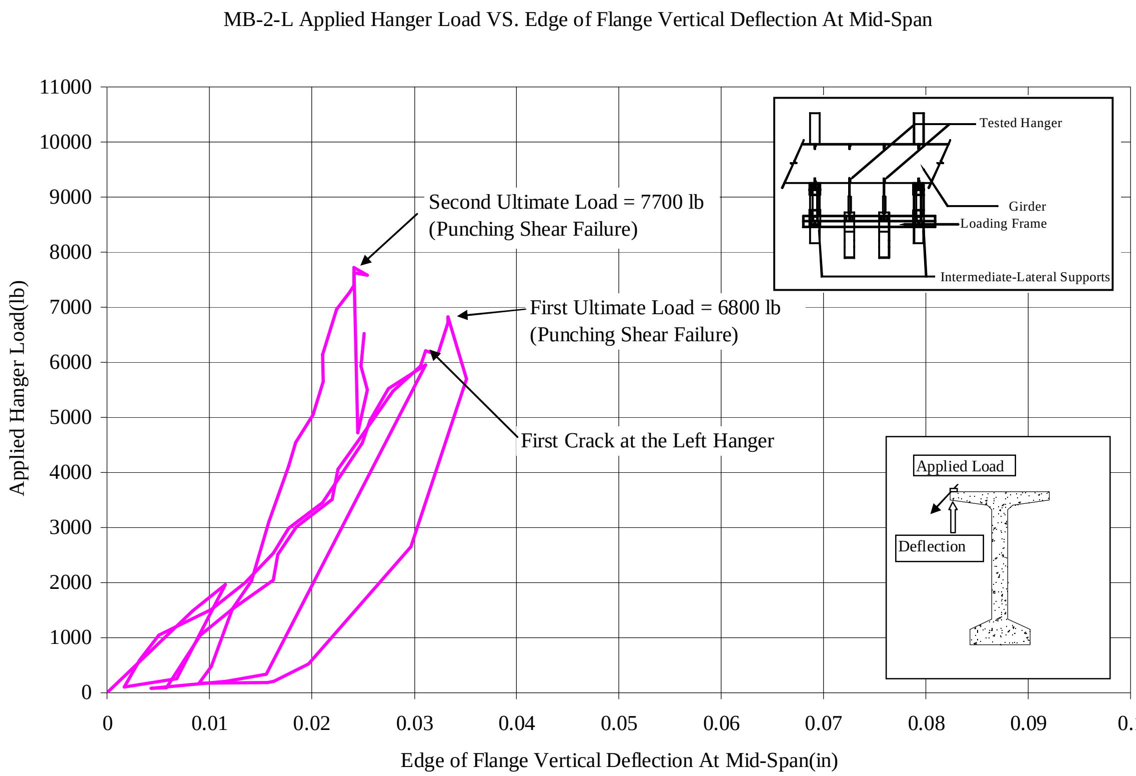

Figure 3.30 MB-2-L, edge of flange vertical deflection and applied hanger load

From figure 3.29, the first crack was observed at 3,500 lbs. for the left hanger and 4,500 lbs. for the right hanger. After the first crack was observed, both hangers started to rotate. The left hanger rotated more than the right one. At 8,000 lbs. large spalling of the concrete at the left hanger was noted as shown Figure 3.31. Testing was continuing after the first spalling. Large amounts of hanger rotation were noted. Punching shear failure occurred at the right hanger at 10,200 lbs. Figure 3.32 illustrates the left and right hanger conditions at failure.

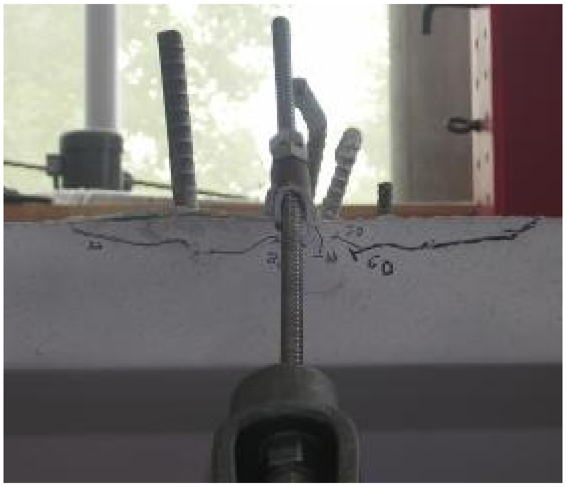

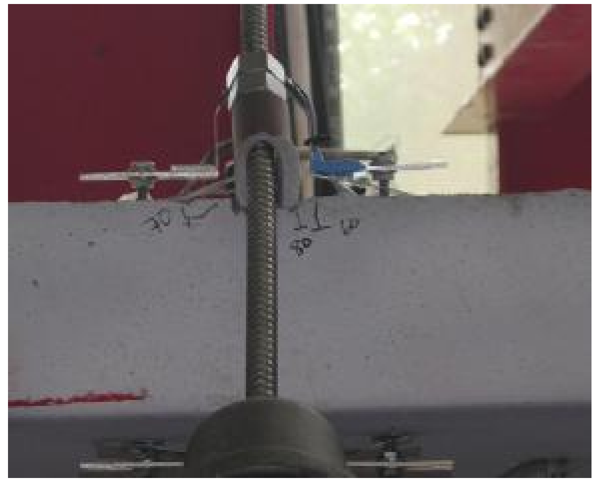

Left Hanger Right Hanger

Figure 3.31 Crack propagation of test DR-2-L

Left Hanger Right Hanger

Figure 3.32 Failures of test DR-2-L

For the Meadow/Burke hanger tests, no crack was observed during the early loads. The first crack was observed at 6,000 lbs. around the front hanger leg above the edge of the top flange. The crack propagated while the applied load was sustained as show in figure 3.33. The first failure occurred at 6,800 lbs. by punching failure. After the first failure on the left hanger, the right hanger was loaded alone. The second ultimate load for testing only the right hanger was 7,700 lbs. The failure types were punching failure as shown in Figure 3.34.

Left Hanger

Right Hanger

Figure 3.33 Test MB-2-L at 6500 lb.

a) Left Hanger

b) Right Hanger

Figure 3.34 Failures of test DR-2-L

The strain profiles were similar to the profiles from the single hanger tests. A high tensile strain was developed at the bottom of the girder flange under the hanger head. While the distance from the hanger head increased, the strain decreased to the compressive strain. Figure 3.35 shows the strain profile of the double hanger tests at the 6,000 lb. applied hanger load.

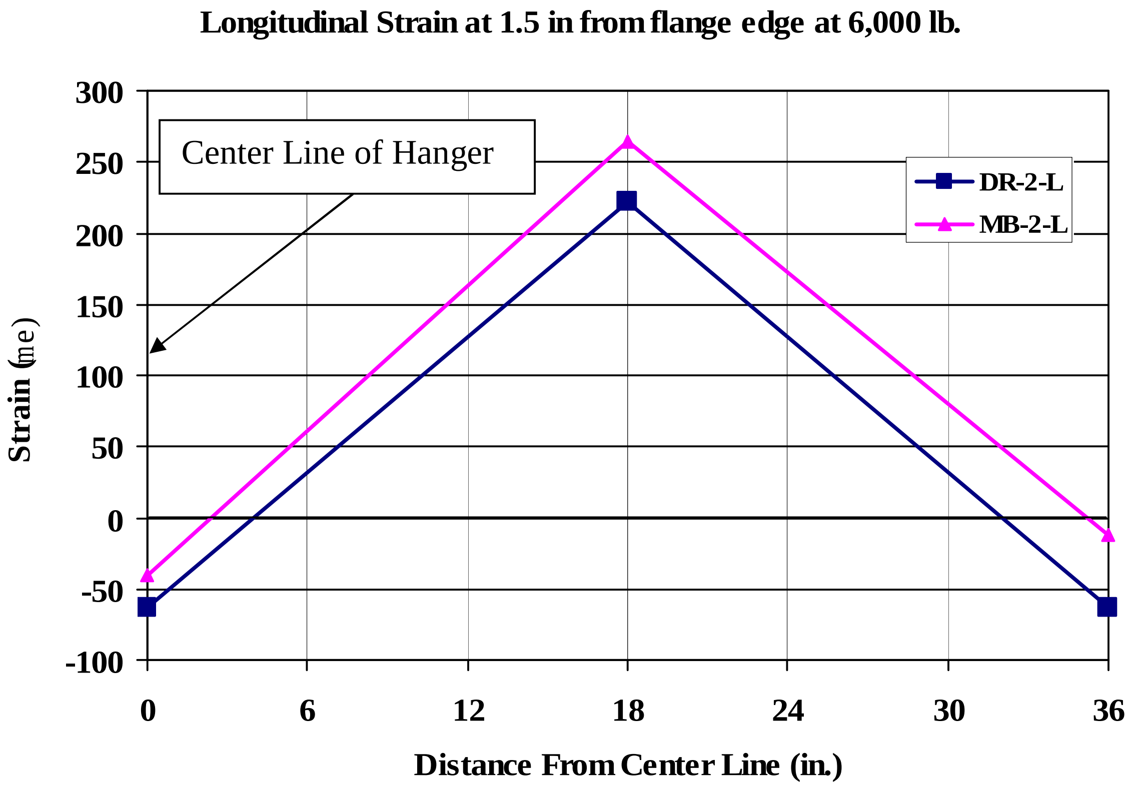

Figure 3.35 Strain developments for double hanger tests

3.6.3 Four hanger test

One test consisting of four Meadow/Burke hangers was conducted. Figure 3.36 shows the edge of flange vertical deflection versus the applied hanger load. After the first hanger failed, the test was continuing by loading the remaining hangers. This method was repeated until the last hanger failed.

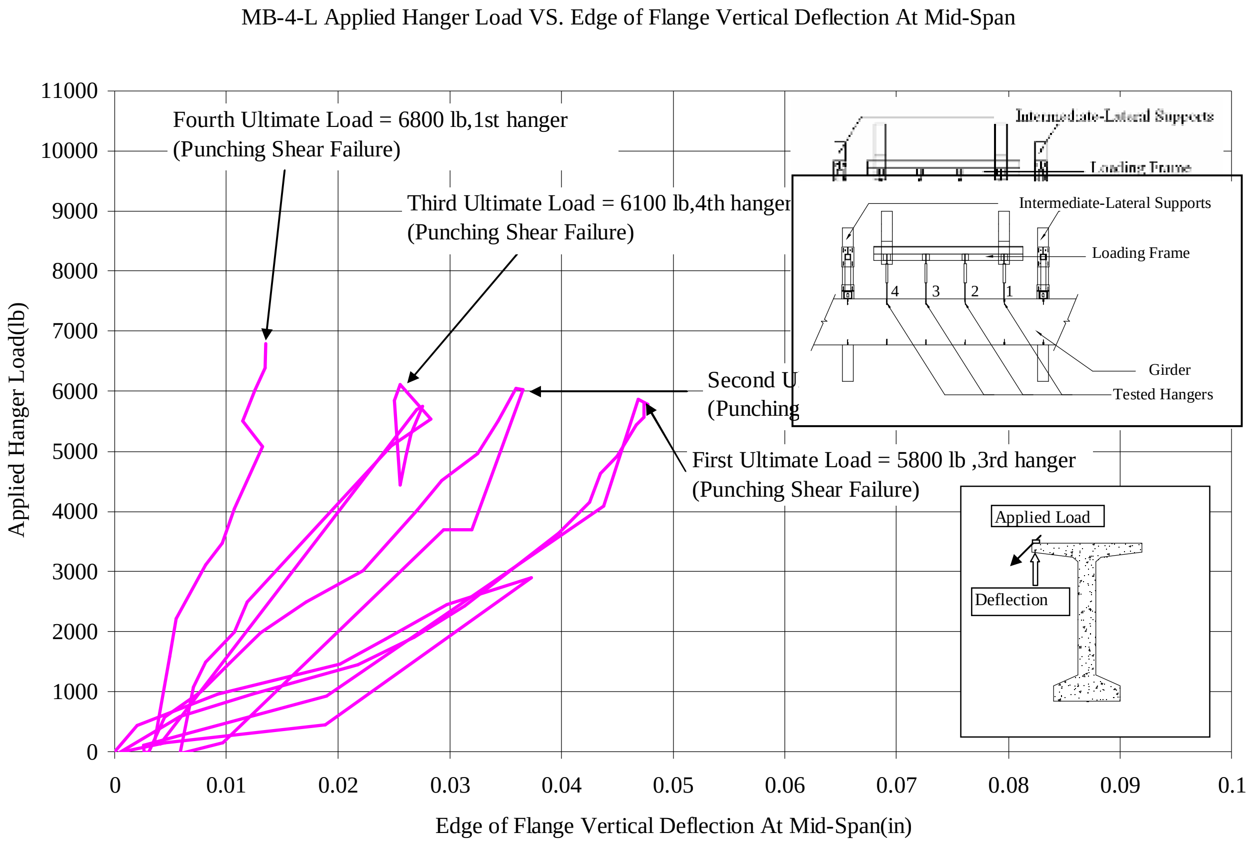

Figure 3.36 MB-4-L, edge of flange vertical deflection and applied hanger load

At 5,000 lbs., a crack was observed at the second and the third hangers. The crack started to propagate to the edge and bottom of the flange. For the third hanger, after the first crack was found at 5,000 lbs. applied hanger load, the crack propagated to the edge and bottom of the flange. The third hanger failed at 5,800 lbs. After the first failure occurred load was unloaded and reloaded again. At 6,000 lbs., the crack propagated to the edge and bottom of the flange at the second hanger and failed at 6,000 lbs. while load was sustained. After the second and third hanger failed, the first and fourth hangers were unloaded and reloaded again. The third failure occurred at the fourth hanger. For the fourth hanger, the first crack was observed at 5,500 lbs. and, like the second and the third, propagated to the edge and bottom at 6,000 lbs. The fourth hanger failed at 6,100 lbs. The first hanger was the last remaining hanger. The test proceeded accorded to the procedure. The first hanger started to crack at 6,000 lbs. and failed at 6,800 lbs. Figure 3.37 illustrates the failure of each hanger.

a) 1st Hanger

b) 2nd Hanger

c) 3rd Hanger

d) 4th Hanger

Figure 3.37 Failure of Test MB-4-L

The strain profile is illustrated in figure 3.38. High longitudinal tensile strains were observed at the bottom of the girder flange under each hanger head. Between the hanger heads, the longitudinal strains were decreased to compressive strain status.

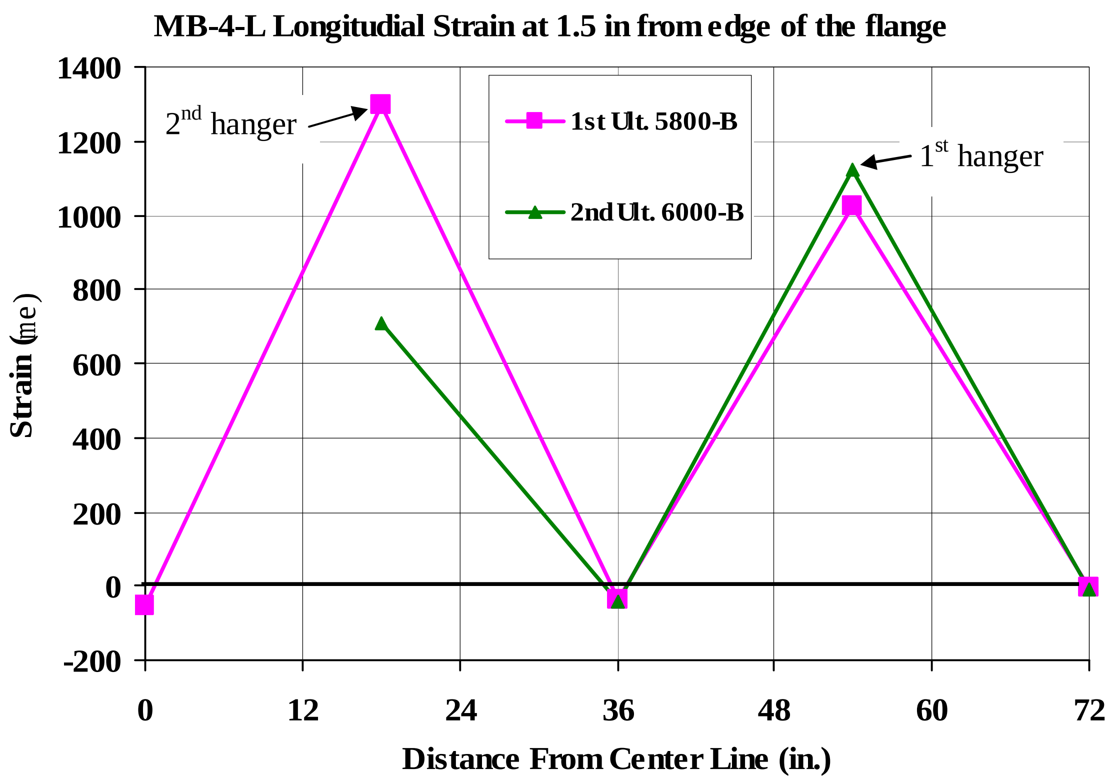

Figure 3.38 Strain developments for the four-hanger test

3.7 Summary

The experimental test program was designed to simulate the field conditions to observe the hanger assembles. There were three major parameters in the experimental test program; the shear reinforcement level, effect of adjacent loaded hanger and the type of hanger.

Due to the complex behavior of the falsework hanger system, some of the observed behavior cannot be predicted using simple hand calculations. To better understand the falsework hanger system behavior, an analytical investigation that includes a series of finite element models was conducted. The details of the analytical investigation are discussed in Section 4.

4.0 ANALYTICAL INVESTIGATION

This section will discuss the details of the analytical investigation used to predict the behavior of the falsework hanger system. The analytical investigation included the use of finite element models and the application of the ACI specification provisions. The finite element method was used to predict the complex behavior of the system. This included the prediction of the stress, strain, deflection, response, and the mode of failure. For the hanger system, the traditional design provisions of the ACI manual were also applied to predict the ultimate strength of the hanger system. To predict the behavior of the system correctly, each approach is used to predict the different type of failure modes as shown below.

4.1 Limit states/Failure modes

There are many types of limit states possible for the falsework hanger system. A list of the potential limit states is list below.

- Coil rod tension rupture
- Hanger failure (tension)
- Pullout of Hanger leg (tension)
- Bearing/ Rotation failure of hanger head
- Girder flange failure
    - Local Bearing/Crushing
    - Punching shear at hanger head
    - Flexural failure of flange
    - Shear failure of flange
- Torsional failure of girder

Some of the limit states such as coil rod tension rupture, hanger failure and pullout of the hanger leg were discussed in section 2. The other limit states were predicted by using the finite element and ACI approaches. Two types of the finite element models were generated to predict the complicated limit states, such as flange flexure and shear failure. The large finite element models were used to predict the global failures such as flexural and shear failure, and the small models were used to predict the local failure such as punching shear failure. There were three limit states that the ACI approach was used to predict the behaviors: the bearing failure, the punching shear failure of the girder flange, and the torsional failure of girder. Details of both analytical components are provided herein.

4.2 Finite Element Method

The finite element modeling program used to predict the behavior of the hanger system was ANACAP (ANATECH, 2004). This program consists of three modules. The first module is a preprocessor program called ANAGEN, which helps a user generate the model components including nodes, elements, boundary conditions, and material properties. The primary solver program is called ANACAP, which computes the response of the model generated by ANAGEN for each specified load step. After completing the calculations, ANACAP compiles the results in a text file format. The post processor called ANAPLOT was utilized to visualize the results for each particular load step. Common output of the post processor included the deformed shape of the model, stress and strain contours, crack patterns and a plot of the relationship between the load step and the parameter of interest.

A convergence study was performed to find the proper size of model and mesh sizes that were required. Because of the limitation in number of elements of the program, the advantage of symmetry of the structure was applied, and only one side of the top flange was modeled, see figure 4.1. A convergence study was made to investigate the length of the model required to allow the cracks to freely propagate. A trial and error approach was used to find the proper length needed in the model.

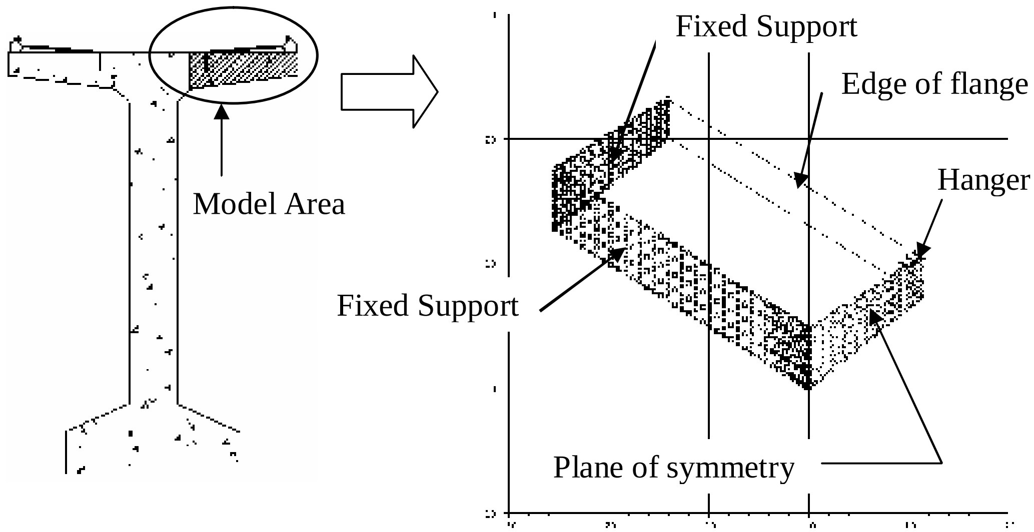

Figure 4.1 Detail of the modeled area

The finite element model study consisted of seven models, one for the convergence study, three for the Dayton/Richmond hanger and three for the Meadow/Burke hangers. For each type of hanger, models of one, two and four loaded hangers were generated. The analytical test matrix is shown in table 4.1

Table 4.1 Analysis Matrix

Test ID	# Loaded Hangers	Half Model Length
Convergent Study	1	40”
DR-1-L	1	40”
DR-2-L	2	58”
MB-1-L	1	40”
MB-2-L	2	58”
MB-4-L	4	94”
DR-Small	1	12”
MB-Small	1	12”

4.2.1 Material Modeling

Concrete modeling

The concrete material model that was used in this analysis was based on the Drucker-Prager modified J2 plasticity theory (ANATECH, 2004). This model concludes that tensile cracking occurs perpendicular to the direction of the largest tensile strains. When a crack occurs, the nominal stress is reduced and redistributed around the crack. When a crack is initiated, the stress normal to the crack surface is reduced to zero. A tension-stiffening model was applied when the crack became wide. The relationship between tensile stress and principal strain is shown in Figure 4.2

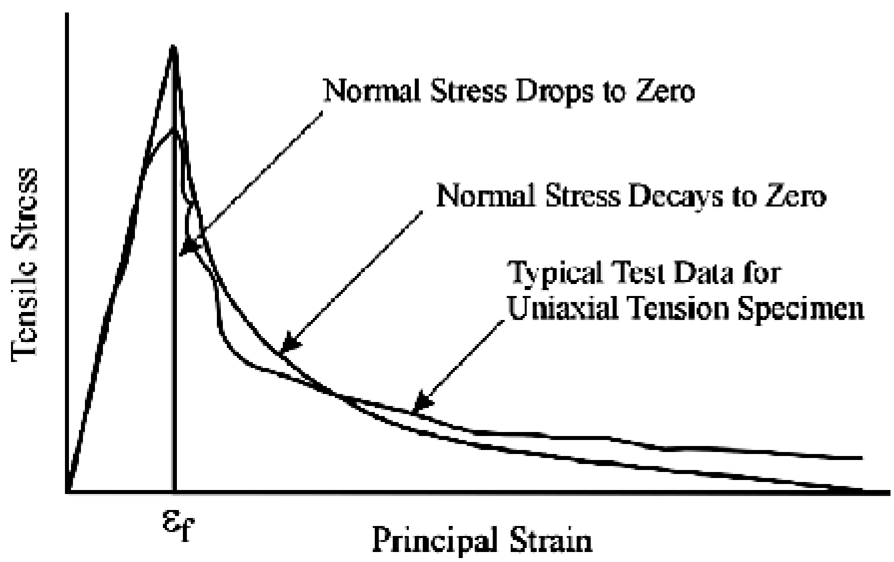

Figure 4.2 Reduction of the tensile stress after initial crack (ANATECH, 2004)

According to the ANACAP user's manual (ANATECH, 2004), a shear force applied along a crack causes tangential shear sliding, and deformation perpendicular to the crack. The sliding is resisted by a friction force from the aggregates. So, the smaller the crack width is, the greater the stiffness and strength. Figure 4.3 shows an example of shear stress capacity across the open crack.

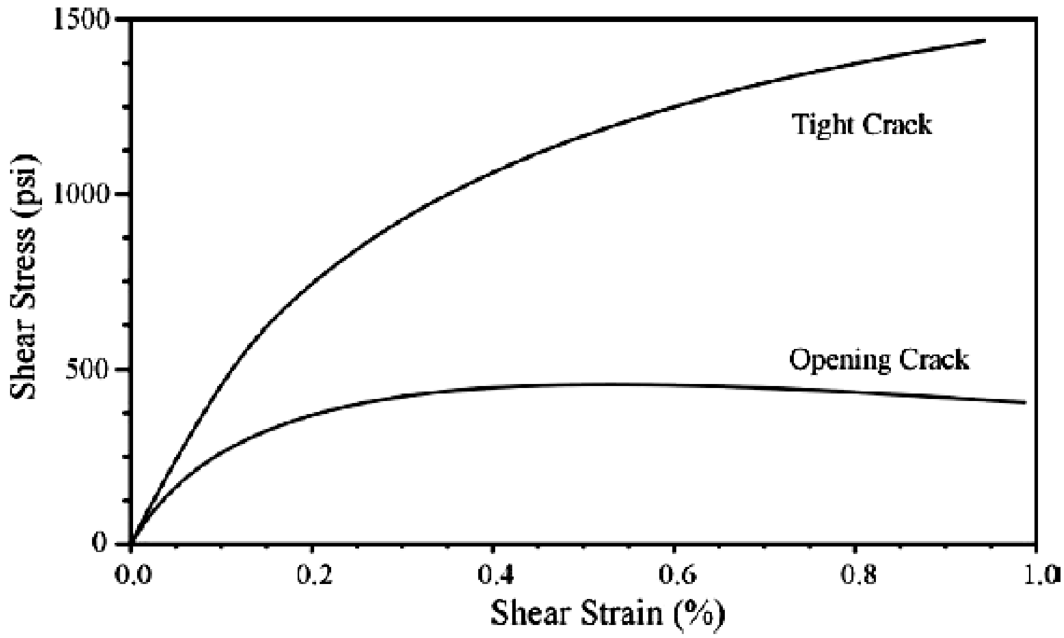

Figure 4.3 Example of shear stress capacity across open crack (ANATECH, 2004)

According to the ANACAP user's manual (ANATECH, 2004), the ANACAP model has built-in relations for the nominal compressive strength. These relations allow for linear behavior of compressive stresses below about half of the compressive strength.

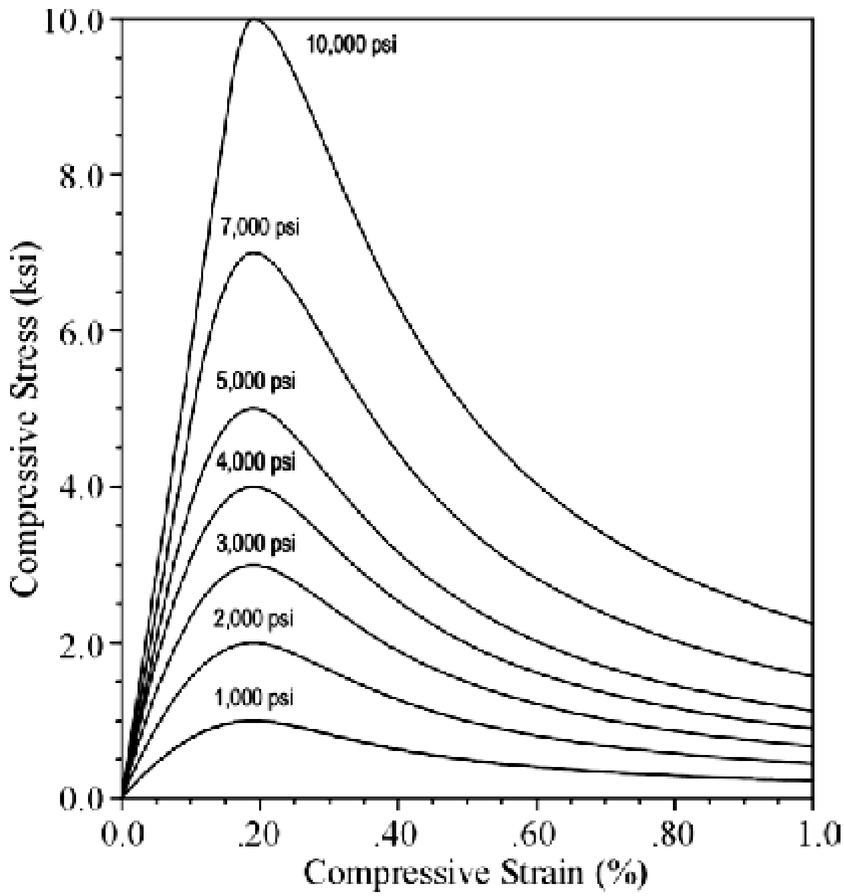

Figure 4.4 Behavior of concrete in uniaxial compression (ANATECH, 2004)

<u>Reinforcement model</u>

The reinforcement was modeled as individual sub-elements within the concrete elements. The stress and stiffness of the rebar sub-elements were superimposed on the concrete element in which the rebar resided (ANATEC, 2004). The rebar material behavior was handled with a separate constitutive model that treated the steel plasticity, strain hardening, and bond-slip behavior

For the reinforcement steel material model (ANATECH, 2004), yielding in the rebar material is treated using the classical J2 or Von Mises plasticity formulation with isotropic hardening. This formulation uses the effective stress and effective strain for defining increasing yield stress with plastic strain and assumes linear unloading. There are many types of failure modes for reinforcing steel. These modes include reaching the strain ductility limit in tension, buckling under compression, experiencing excessive shear stress, or due to bond slip and loss of anchorage with the concrete.

4.2.2 Girder Flange Model

The concrete girder flange was modeled in 3-dimensions with two fixed supports and one symmetry plane as shown in Figure 4.1. The details of the tested model parameters are discussed herein.

Element Type

Eight-node 3D continuum brick elements, B8, were used to generate the finite element model. This element consists of eight nodes, one at each corner of the element. The integration point was a 2x2x2-point with a single evaluation point to satisfy the material constitutive law. Because the B8 element uses a linear displacement interpolation to represent the displacement of the element, a shear-locking problem was encountered. The problem was eliminated by using a fine element mesh, discovered through a convergence study.

Material properties

The material properties used in the analytical program are as follows:

Concrete

Concrete strength	=	7,500	psi
Young’s modulus	=	4,770,000	psi
Mass Density	=	150	pcf

Poisson's ratio	=	0.167	

Rebar and Anchor

Yield Strength	=	60,000	psi
Young's modulus	=	29,000,000	psi
Poisson's ratio	=	0.3	

The prestressing reinforcement used in the model was modified from the true stress strain curve from PCI Handbook (PCI Handbook, 1999) as shown in Figure 4.5. Because the strand was prestressed before applying the hanger load, the prestressing reinforcement properties were entered using part of the full stress strain curve. Normally, in the field, the stress in the prestressing strand is around 150 ksi during construction. The prestressing reinforcement was modeled using the stress at construction as an origin point. The model utilizes prestressing reinforcement properties as follows:

Prestressing Strand

Grade	=	270,000	psi
Young's modulus	=	28,500,000	psi
Yield strength	=	100,000	psi
Ultimate strength	=	118,000	psi

Figure 4.5 shows the full stress strain curve of the 7-wire low relaxation strand grade 270 ksi and the part of the curve used to create the model. Figure 4.6 shows the prestressing reinforcement stress-strain curve used in the program.

Typical stress-srain diagram of 7-wire low relaxation prestressing strand

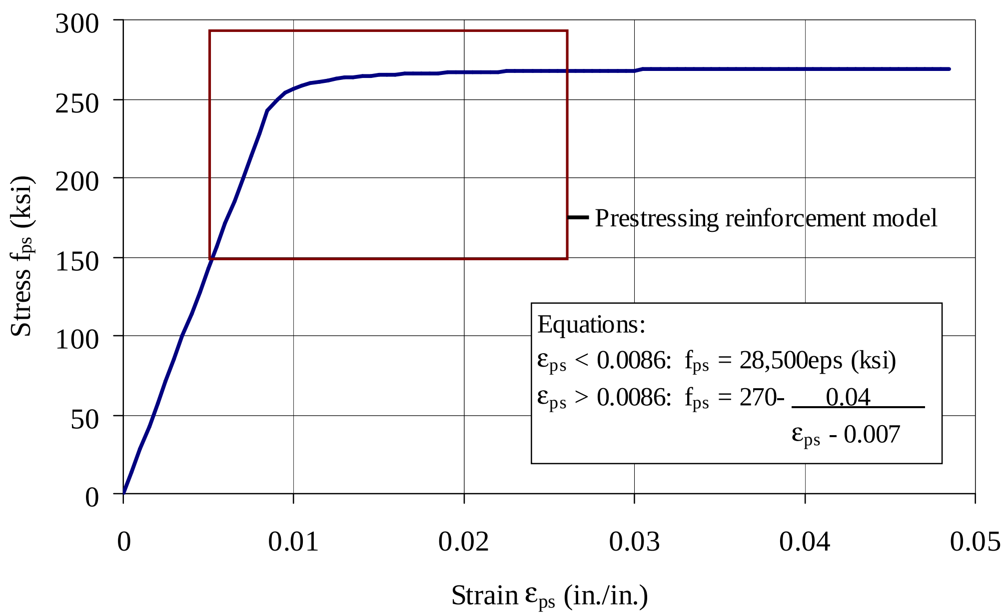

Figure 4.5 Stress-Strain curve of 7-wire low relaxation prestressing strand

Prestressing reinforcement stress strain curve model

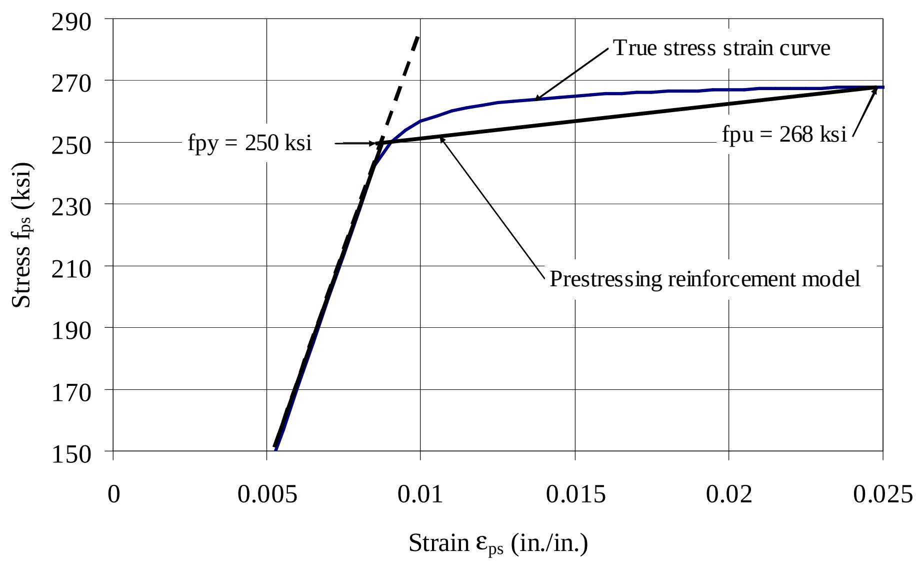

Figure 4.6 Prestressing reinforcement stress strain curve model

4.2.3 Hanger models

The Dayton/Richmond hanger model was generated by separating the load from the hanger into vertical and horizontal components as shown in Figure 4.7. The vertical component was the load from the hanger head applied directly to the concrete model. This load represented a bearing pressure applied at the tip of the edge of the flange. The other component was the horizontal force that transferred to the embedded hanger leg. The hanger leg was modeled as an anchor that embedded into the concrete flange. The horizontal load was applied directly to the anchor. Because of the 45 degree applied load and the assumption that the friction between hanger head and the concrete was negligible, the magnitude of the vertical force on the model applied by the hanger head and the horizontal force applied at the top of the anchor were equal. The Dayton/Richmond hanger model is shown in Figure 4.8.

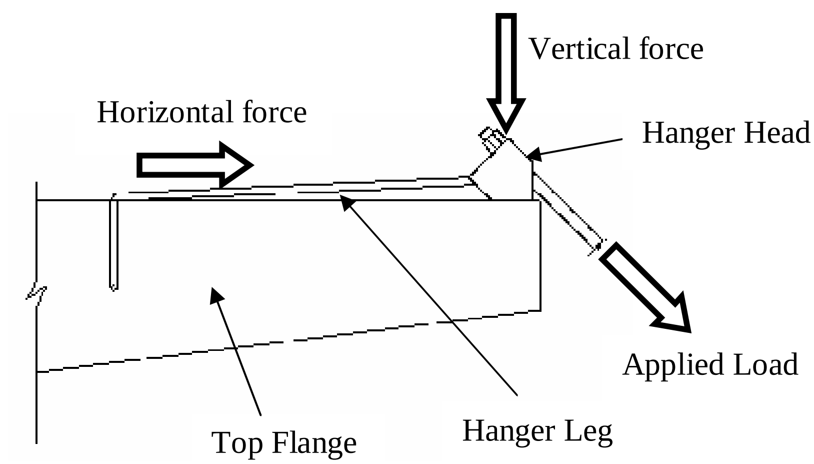

Figure 4.7 Load distributions from the Dayton/Richmond hanger to the flange

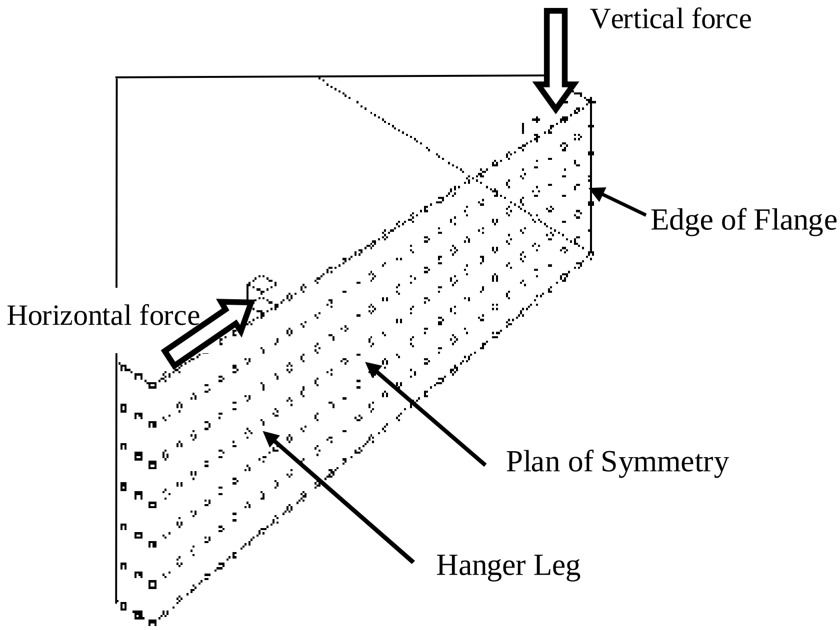

Figure 4.8 Details of the Dayton/Richmond hanger model

The Meadow/Burke hanger model was generated by separating the applied hanger load into three parts: hanger head, front hanger leg and back hanger leg as shown in Figure 4.9. Based on the zero horizontal friction assumption as in the Dayton/Richmond hanger model, only the hanger head applied vertical load to the model. The two hanger legs took the same magnitude horizontal force and the same amount of the vertical load applied by the hanger head. The Meadow/Burke hanger model is shown in figure 4.10.

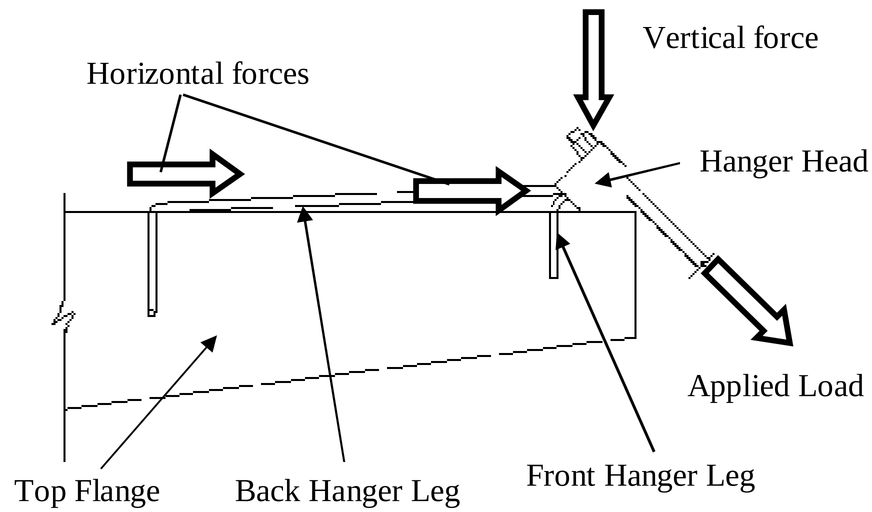

Figure 4.9 Load distributions from the Meadow/Burke hanger to the flange

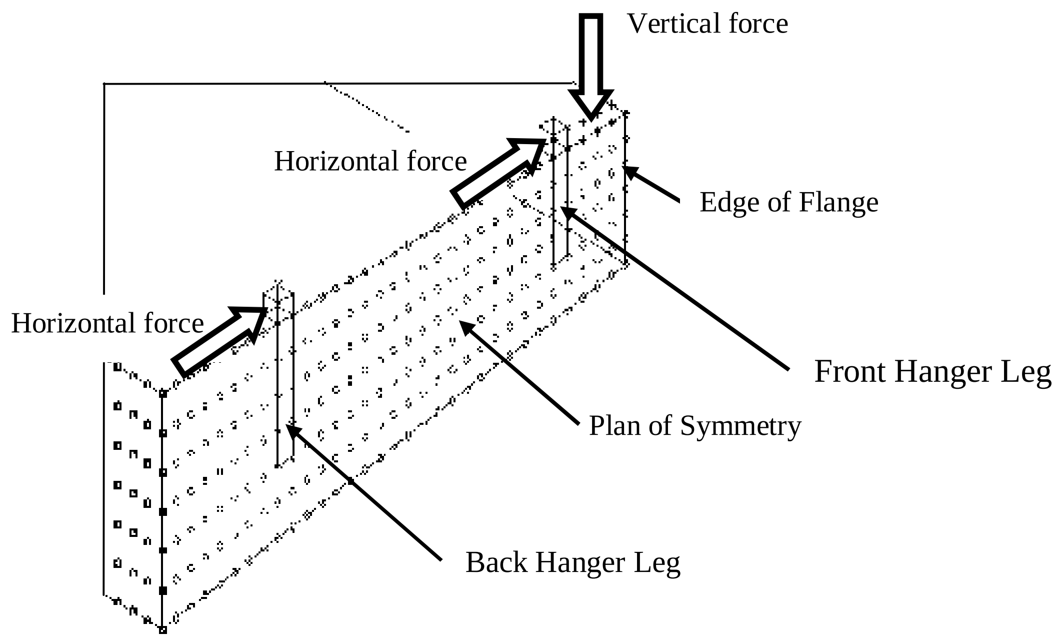

Figure 4.10 Details of the Meadow/Burke hanger model

4.2.4 Element and Model Size

A limitation of the element dimension was the aspect ratio between the short and the long sizes of an element. To encourage proper behavior of the element and to prevent the excessive distortion of an element, the aspect ratio was limited to less than three. The size of the elements used in the models was the result of a convergence study. The length of the model was also dependent on the number of simultaneously tested hangers. For the one, two and four hangers tests, the length of specimen was 40, 58 and 94 inches, respectively, to allow full crack propagation. The models of the one and two Dayton/Richmond hanger tests are shown in Figure 4.11 and Figure 4.12 and for the Meadow/Burke hanger tests in Figure 4.13, Figure 4.15 and Figure 4.15, respectively.

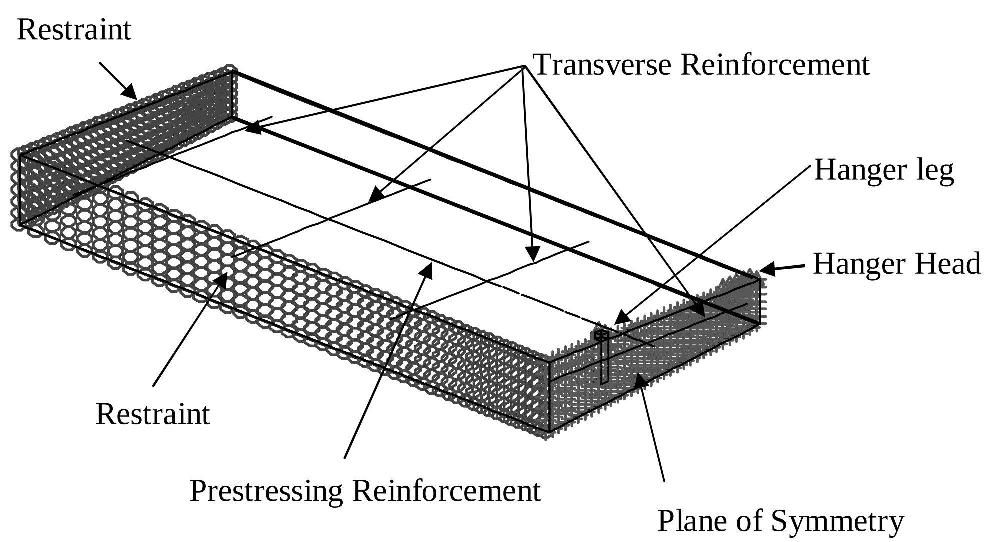

Figure 4.11 Dayton/Richmond single hanger model

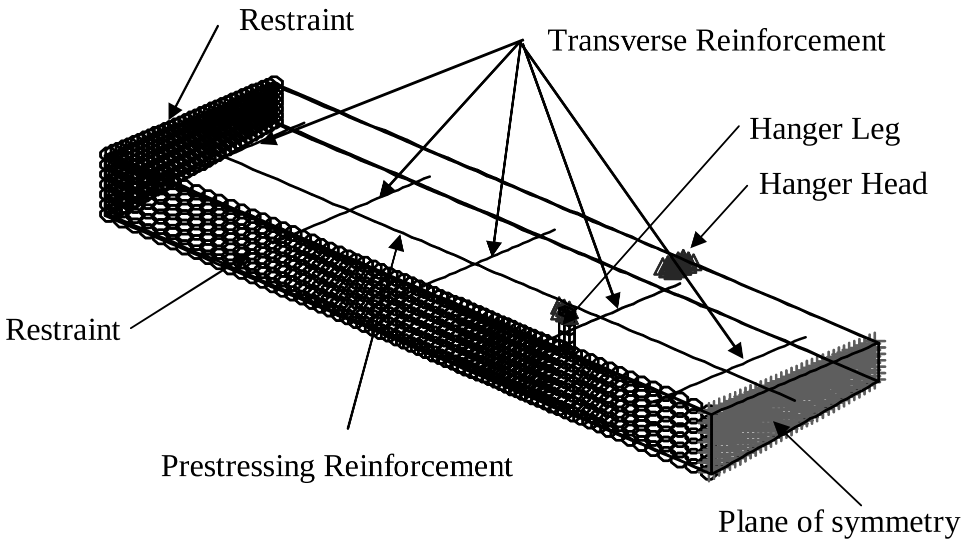

Figure 4.12 Dayton/Richmond double hanger model

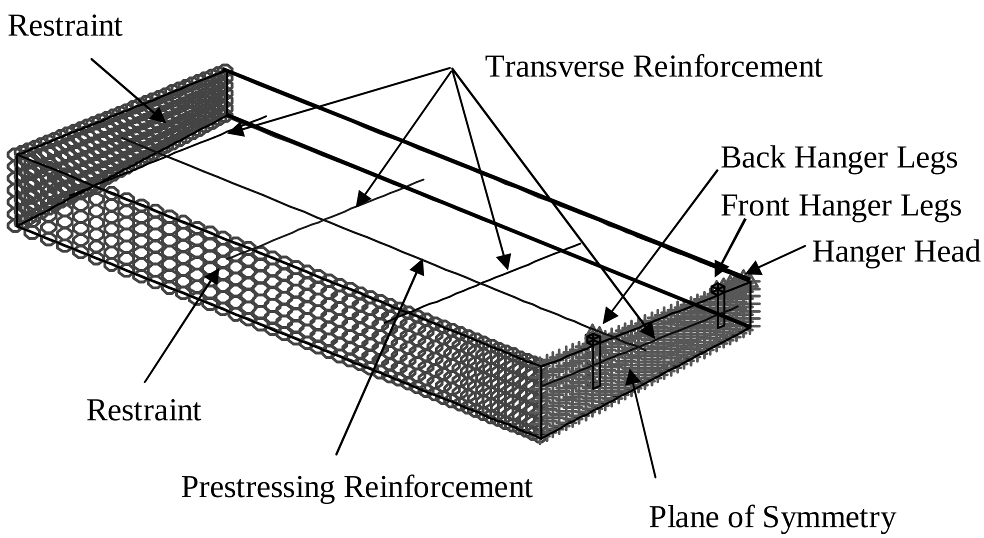

Figure 4.13 Meadow/Burke single hanger model

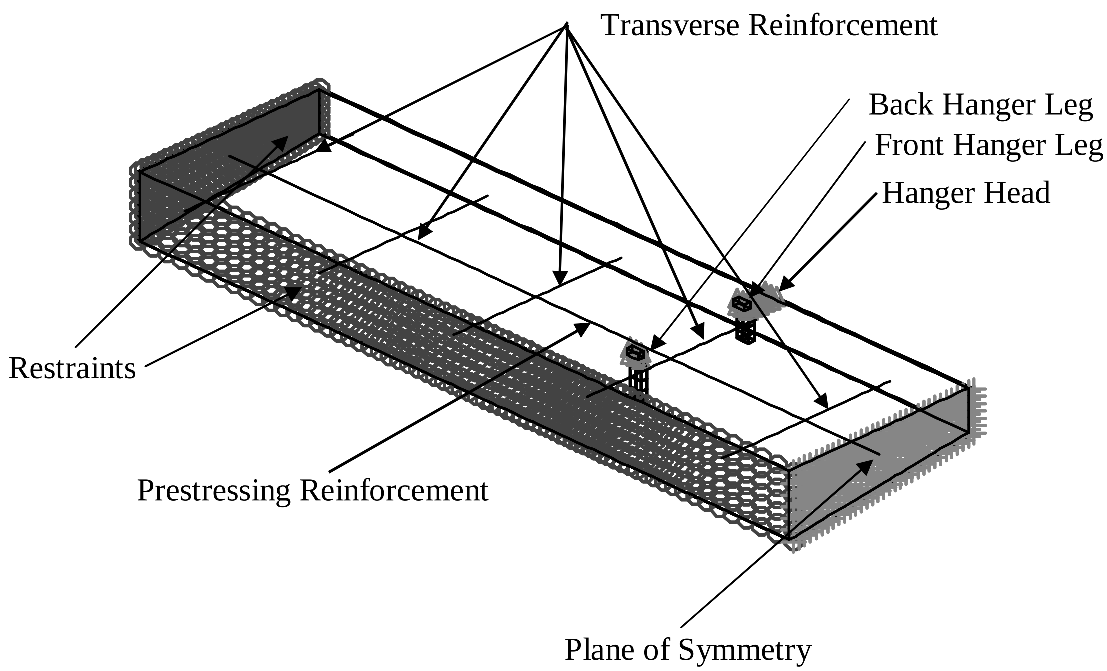

Figure 4.14 Meadow/Burke double hanger model

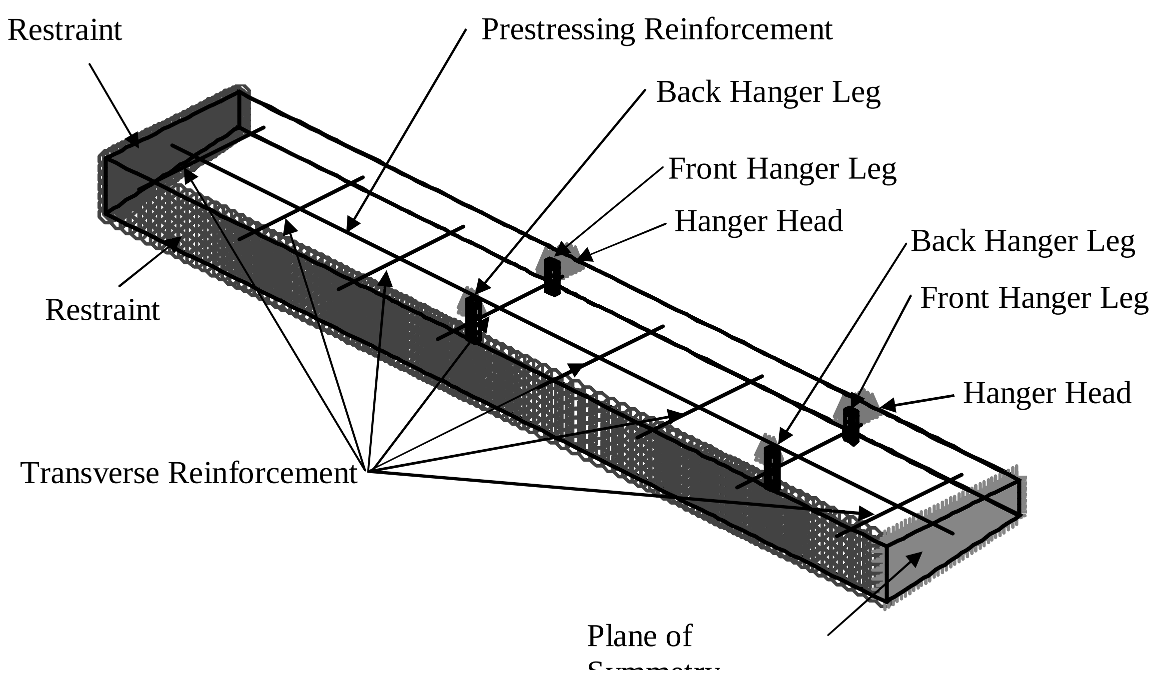

Figure 4.15 Four Meadow/Burke hanger model

There were two small flange models created to predict the localized type of failure such as the punching shear failure. The small models were generated by using a finer mesh size than the one of the original models. This allowed the model to capture the localized behavior and failure. The small finite element models were based on the single hanger Dayton/Richmond and Meadow/Burke hanger model. The length of the small model was decreased to 12” and the mesh size was refined by half. Figures 4.16 and 4.17 show the small Dayton/Richmond and Meadow/Burke single hanger models.

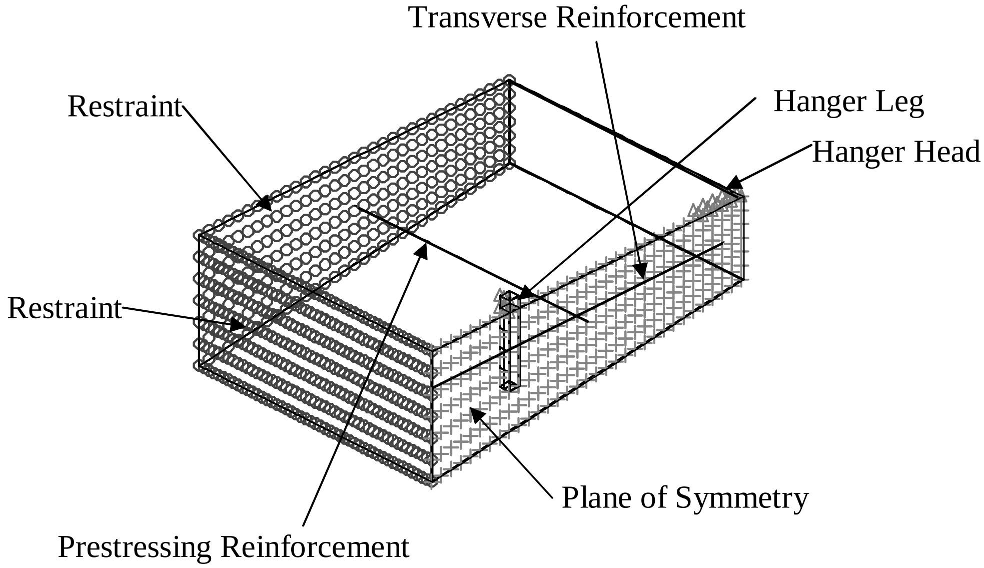

Figure 4.16 Small Dayton/Richmond hanger model

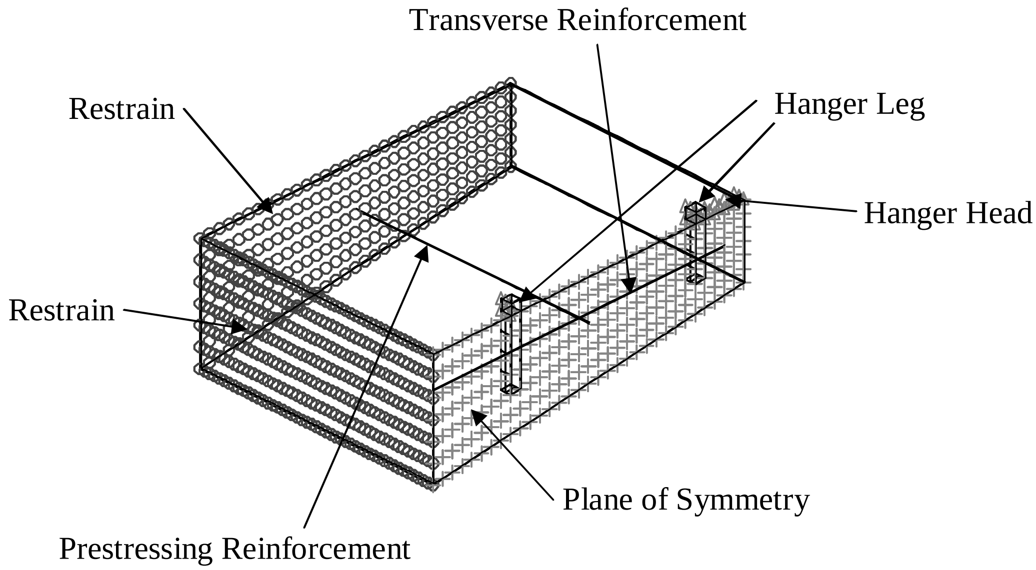

Figure 4.17 Small Meadow/Burke hanger model

The modifications of the small model to increase the strength of the hanger-flange system were performed by increasing the loaded area under the hanger head for the Dayton/Richmond hanger model and increasing the edge thickness of the Meadow/Burke hanger model to 5.5 in. and 6.5 in. The modified small Dayton/Richmond and Meadow/Burke hanger models are shown in Figure 4.18 and 4.19, respectively

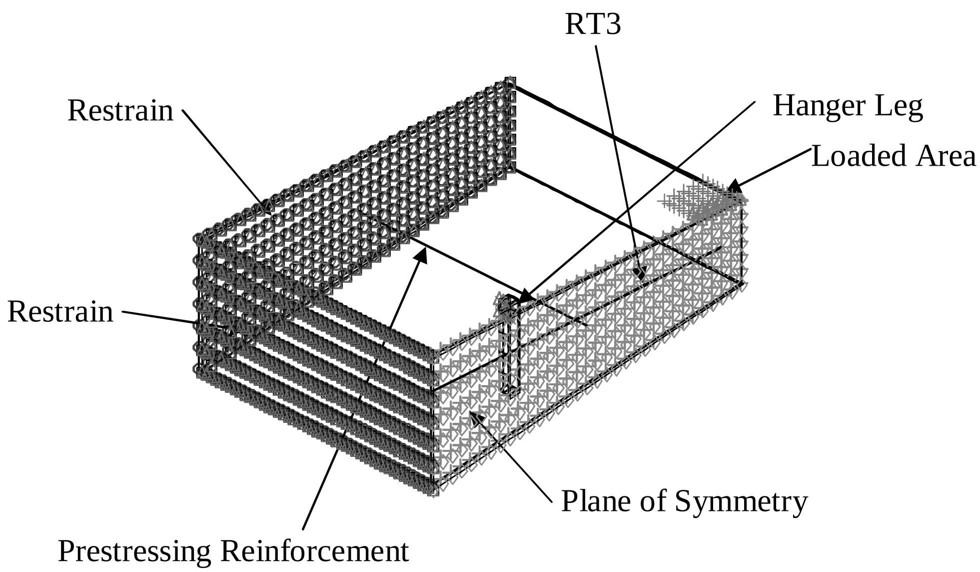

Figure 4.18 Modified DR-Small Finite element model

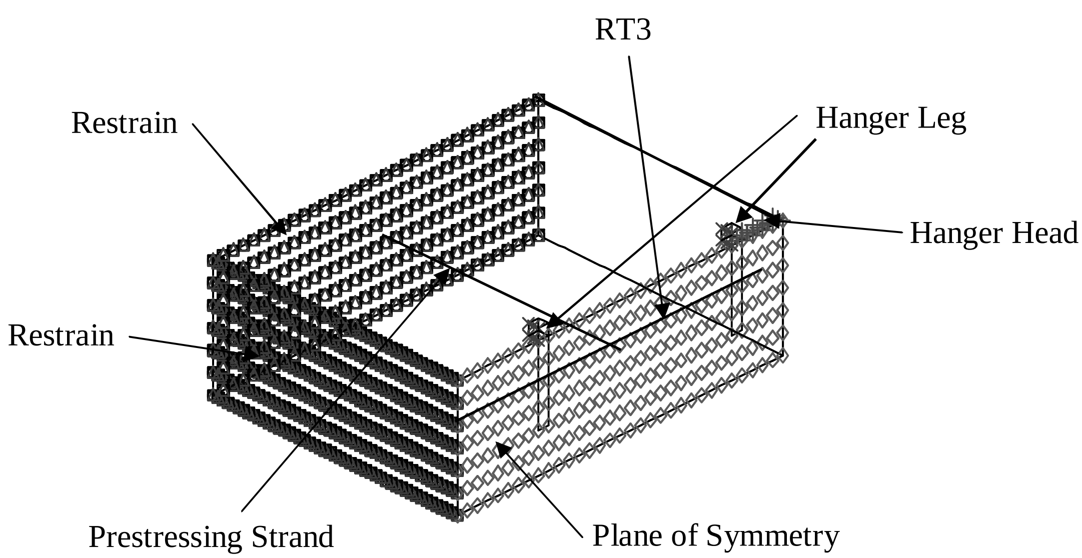

Figure 4.19 Modified MB-Small Finite element model

4.2.5 Finite Element Modeling Results

The results of the ANACAP analysis were loaded into the post-processing program, ANAPLOT. From the ANAPLOT program the crack pattern, stress contour, and relationship between the applied load and the interested parameter was reported for every 10 steps of the applied loading. The applied vertical and horizontal load shown in ANAPLOT was factored by the square root of two to match the applied hanger load from the experimental test program.

The results from the finite element modeling are summarized in Appendix I. The summary sheets include the corresponding experimental test ID, element properties, material properties, illustrations of the model, crack pattern and results for each finite element model. A summary of the convergence study and all results are discussed below.

<u>Convergence Study Results</u>

The flange model length was selected to be 40 in. This selection was made using a trial and error approach to determine the length of the flange model that would not affect the cracking pattern. In the convergence study, the models were analyzed using three different mesh sizes: coarse, medium and fine. The models had the same properties as described in section 4.2. The flange models were subjected to load using the Dayton/Richmond hanger. The load deformation responses for each mesh are shown in figure 4.20.

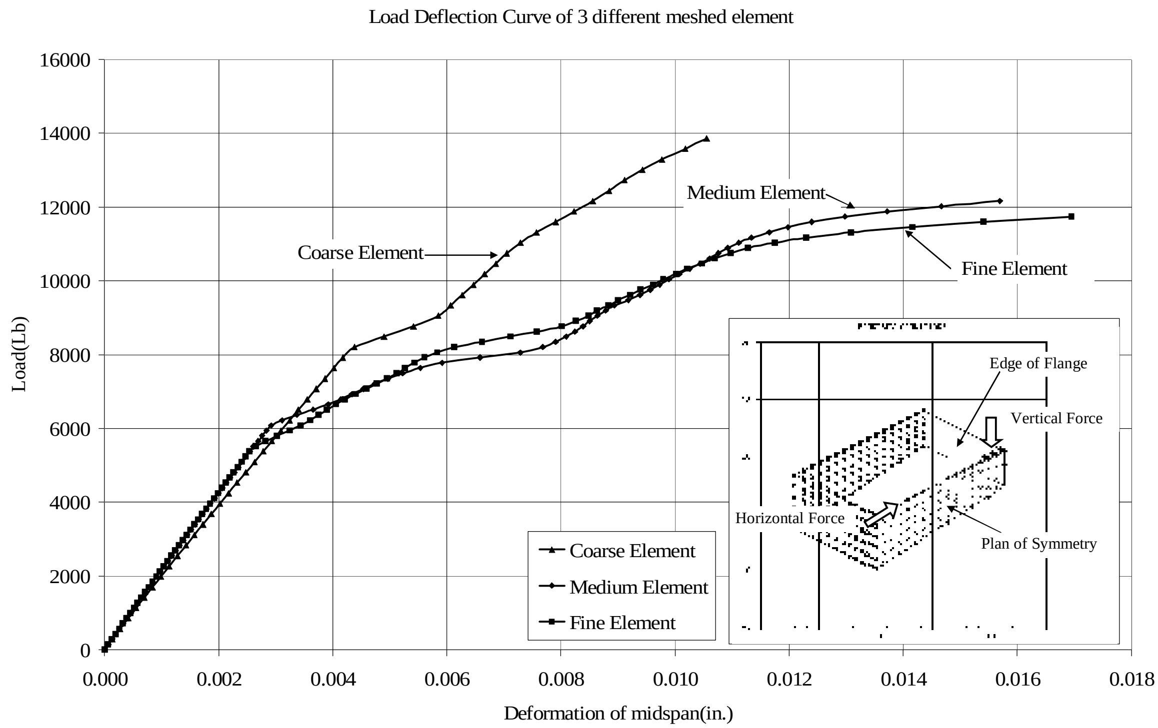

Figure 4.20 Load deflection curve for three different mesh sizes

As illustrated in Figure 4.20, the load-deflection response for the coarse, medium and fine meshes converge. Figures 4.21 and 4.22 show a comparison of the load and displacement at the yield and ultimate conditions for the three meshes. The results show decreasing changes in load and displacement, as the mesh is refined. The difference between the results from the medium and fine mesh sizes was less than 8%. Based on these results, the medium mesh size was selected for use in the finite element study.

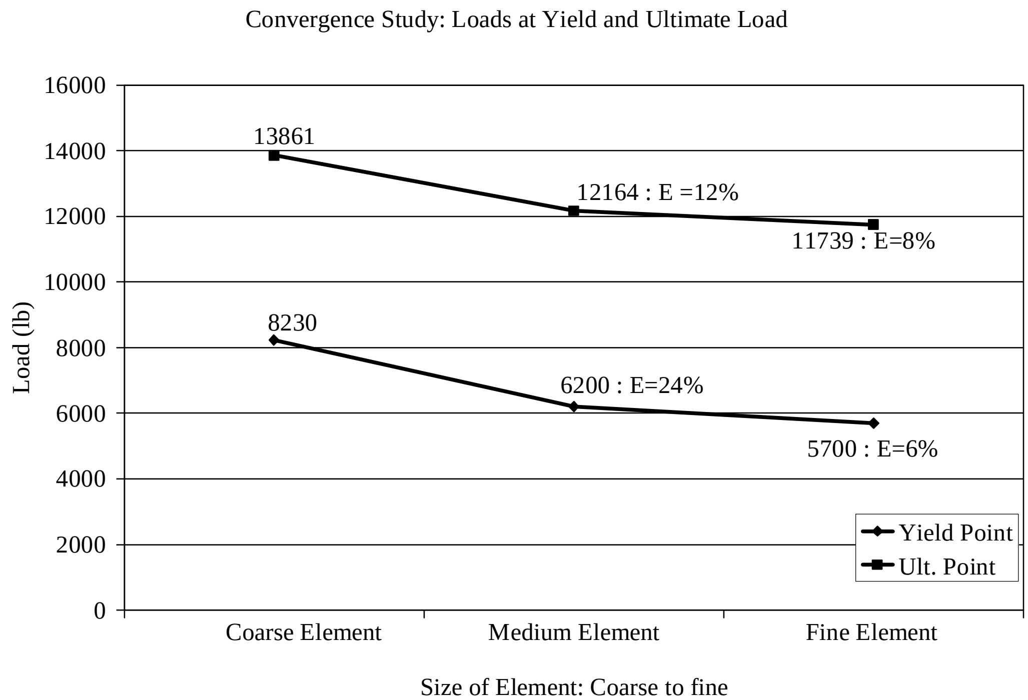

Figure 4.21 Comparison of yield and ultimate load for different mesh sizes

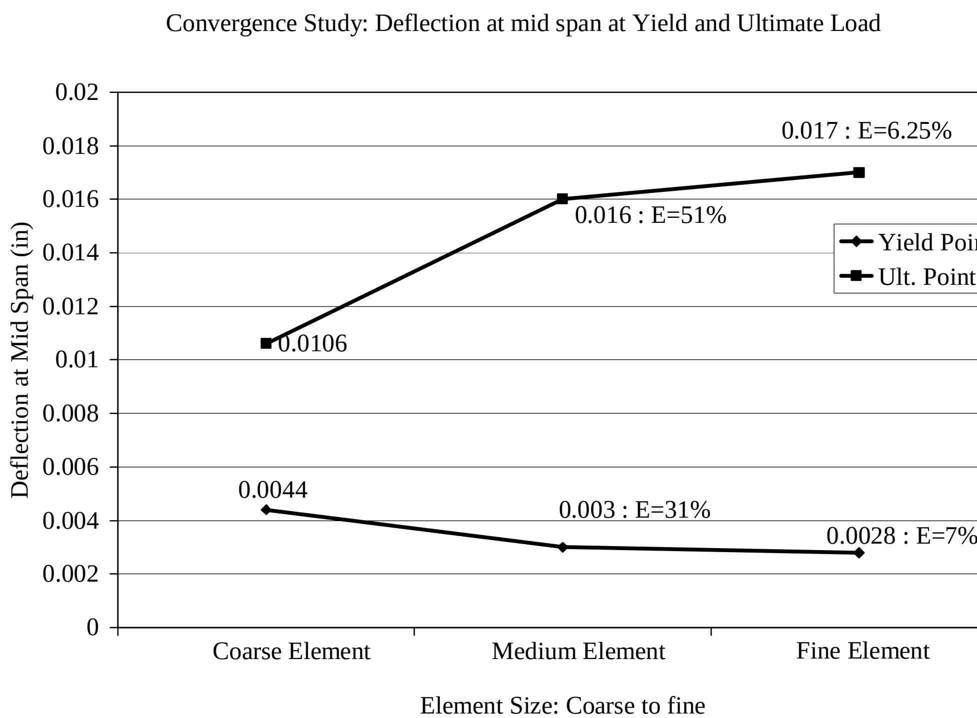

Figure 4.22 Comparison of deflection at yield and ultimate load for different mesh sizes

Dayton/Richmond model results

As discussed in the description of hanger models, the load from the Dayton/Richmond hanger was separated into horizontal and vertical components and applied at the embedded leg and flange tip, respectively. The results of the modeling indicated that cracks formed under the hanger head and at the top of the flange model around the embedded hanger leg. The crack propagated from the hanger leg to the edge. As the load was applied, the crack widths increased, and failure by combined, flexure and shear was observed. Figure 4.23 illustrates the crack propagation for the single hanger test.

For the two loaded hanger model results, the cracks originated from the backside of the hanger leg. The cracks propagated parallel to the edge of flange between the two hanger legs. Along the sides, the cracks propagated at approximately 45 degrees to the edge of flange, see Figure 4.24. The two hanger models failed by combined flexural and shear as shown in appendix I. Figure 4.25 shows the relationship of the applied hanger load and the mid-span deflection for the Dayton/Richmond hanger test.

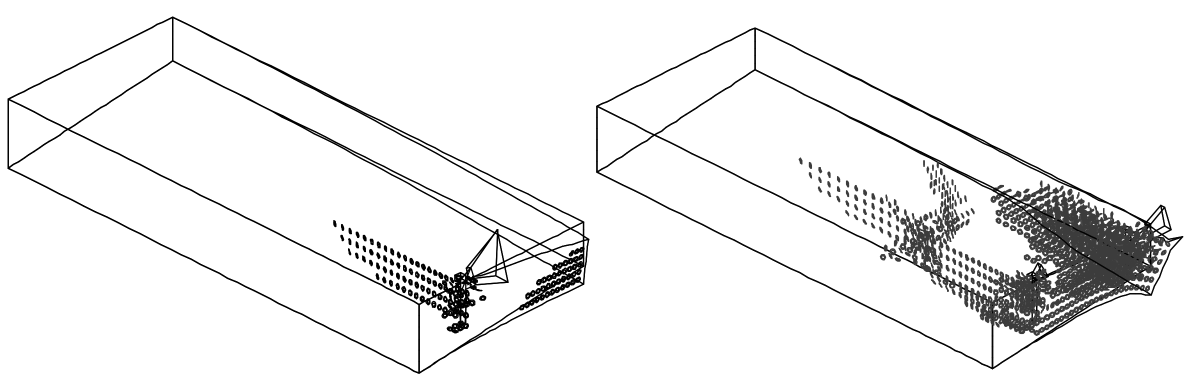

a) At 5,300 lb applied hanger load b) At 11,200 lb applied hanger load

Figure 4.23 Crack propagation of the single hanger test

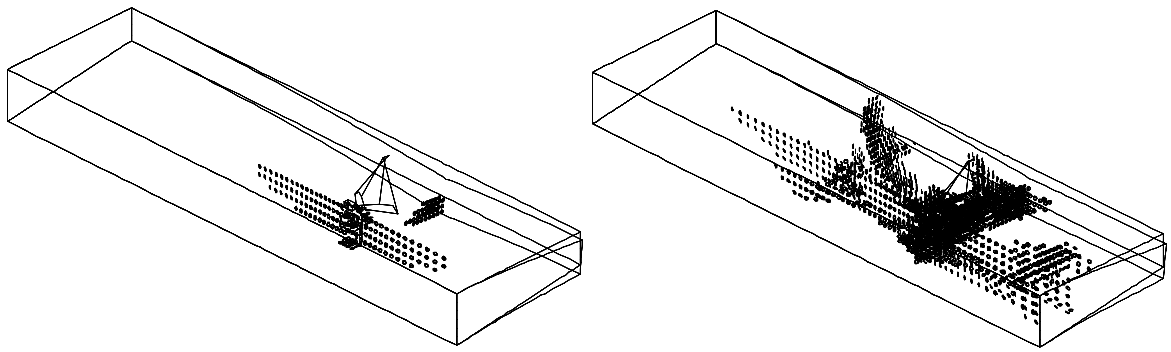

a) At 5,300 lb applied hanger load b) At 11,200 lb applied hanger load

Figure 4.24 Crack propagation of the two-hanger test

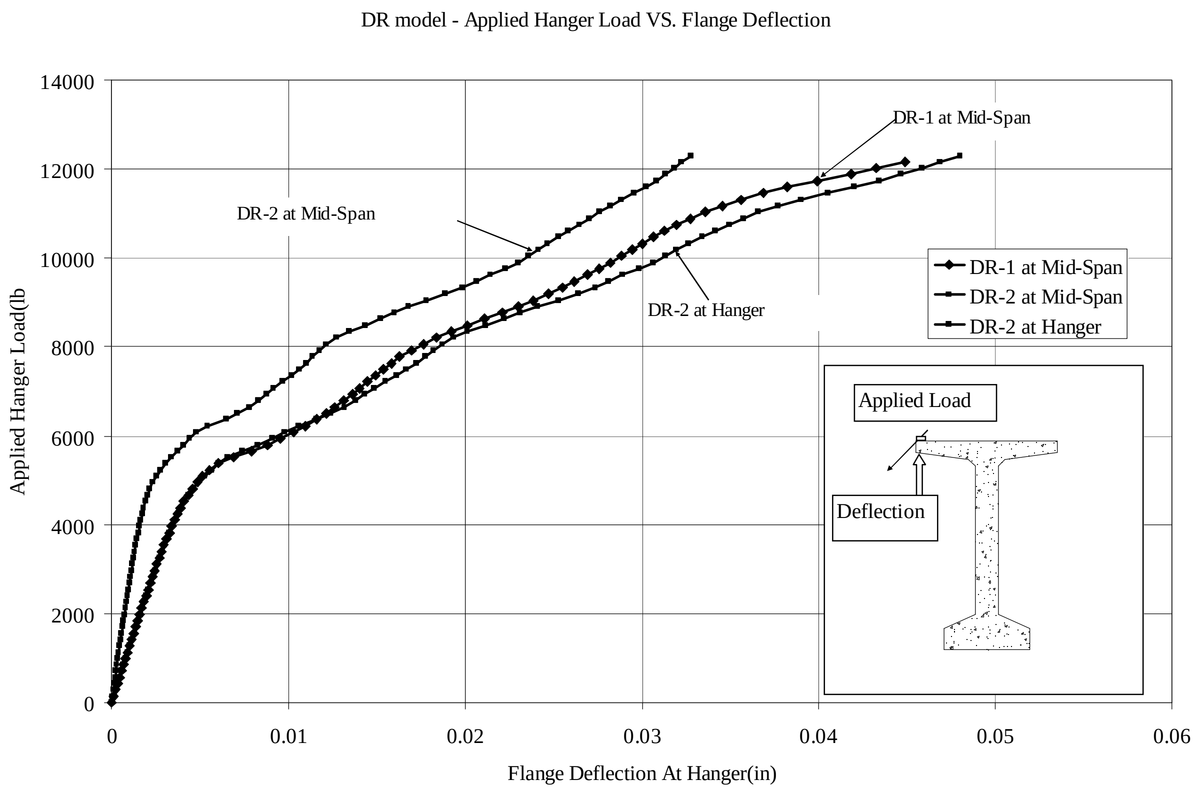

Figure4.25 Dayton/Richmond model results

Meadow/Burke model Results

For the Meadow/Burke models, the horizontal load was divided and applied to each embedded hanger leg. The results of the modeling indicate that the cracks form under the hanger head at the top of the flange and around the back hanger leg. The cracks propagated within the flange model and develop a shear cone as shown in Figure 4.26. As the loads are applied, the crack widths increase, and failure by punching shear is observed.

For the multiple hanger model, the general behavior was the same as the single hanger behavior. The cracks form at the tip of the flange under the hanger head for each loaded hanger. Between the back hanger legs, cracks propagated parallel to the edge of the flange model. Between hanger and support, cracks propagated 45 degrees to the edge of the model as in the Dayton/Richmond crack pattern; see Figure 4.27 and Figure 4.28. As the applied load is increased, cracks form under and around the hanger head and cause a punching shear failure. The results of the Meadow/Burke hanger modeling are shown in Figure 4.29.

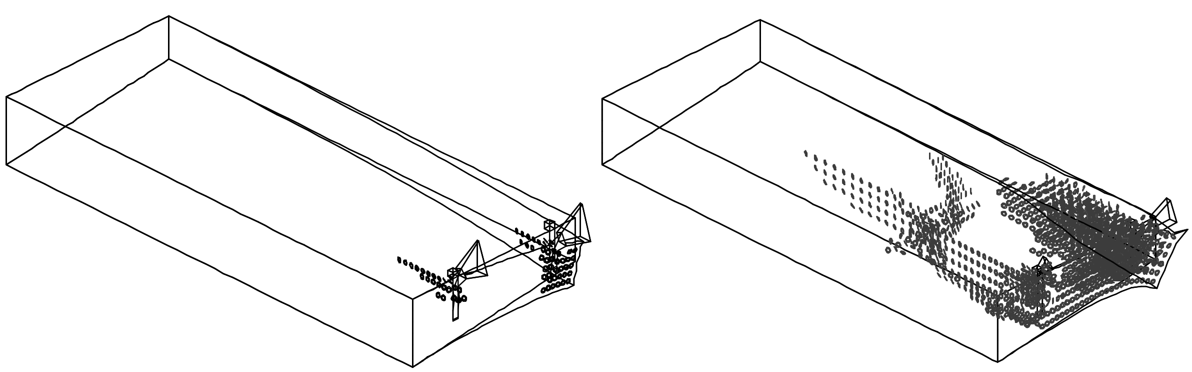

a) At 5,300 lb applied hanger load b) At 10,500 lb applied hanger load

Figure 4.26 Crack propagation of the single hanger test

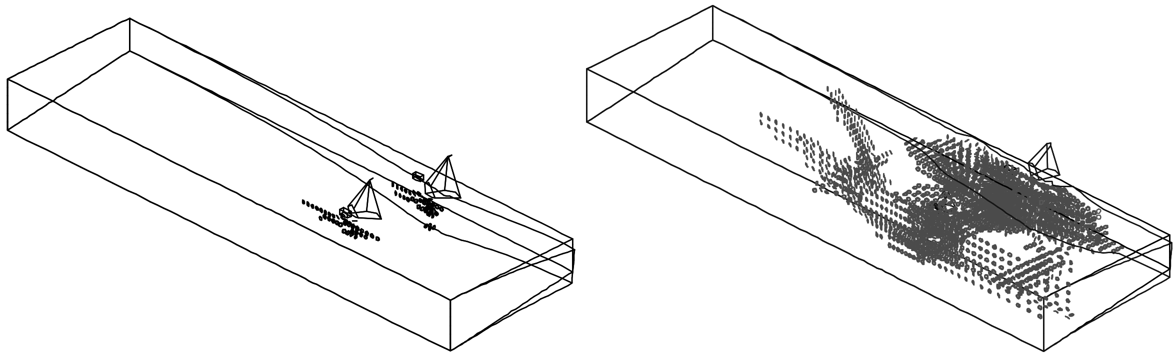

a) At 5,300 lb applied hanger load b) At 10,500 lb applied hanger load

Figure 4.27 Crack propagation of the double hanger test

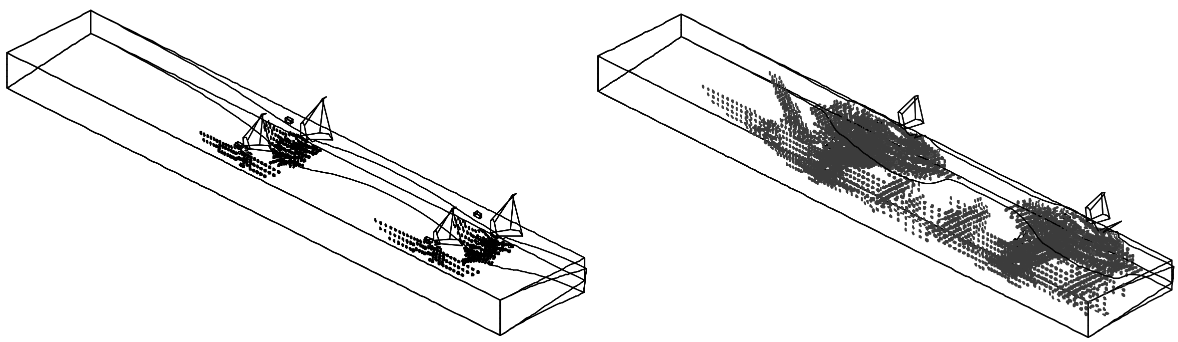

a) At 5,300 lb applied hanger load b) At 10,500 lb applied hanger load

Figure 4.28 Crack propagation of the double hanger test

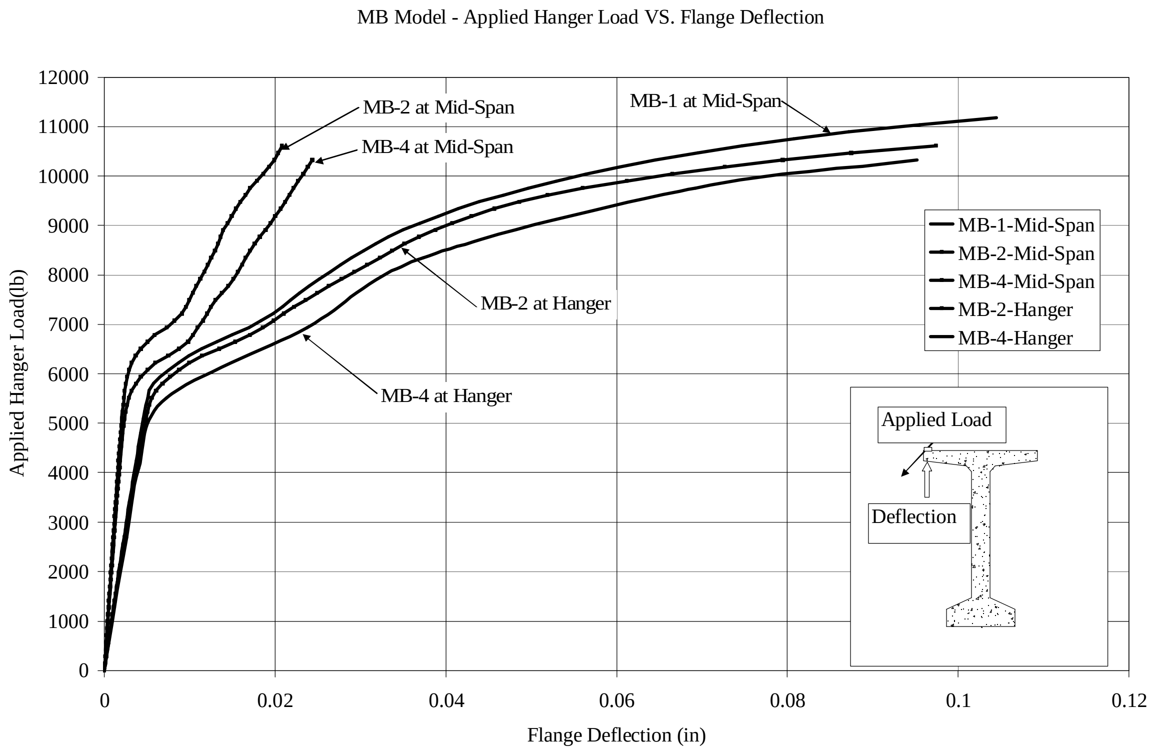

Figure 4.29 Meadow/Burke model results

Small finite element model Results

The small finite element model was designed to capture the localized failure. For the small Dayton/Richmond model, the applied hanger load versus the deflection at mid-span is shown in Figure 4.30. The cracks form at the flange around the embedded hanger leg and propagate to the edge and side supports as the load is applied, see Figure 4.31. The model fails by flexural failure at 12000 lbs., and the maximum deflection is 0.0124 in.

For the small Meadow/burke model, the cracks form at the flange under the hanger head and around the hanger leg. As the load is applied, the crack widths under the hanger head increase and the cracks propagate to the side support. The small Meadow/Burke model fails by a punching shear failure. The relationship between the applied hanger load and the deflection at mid-span is shown in Figure 4.30. At the failure, the ultimate load is 9500 lbs., and the maximum deflection is 0.0614 in. Figure 4.32 illustrates the crack propagation at two different load steps.

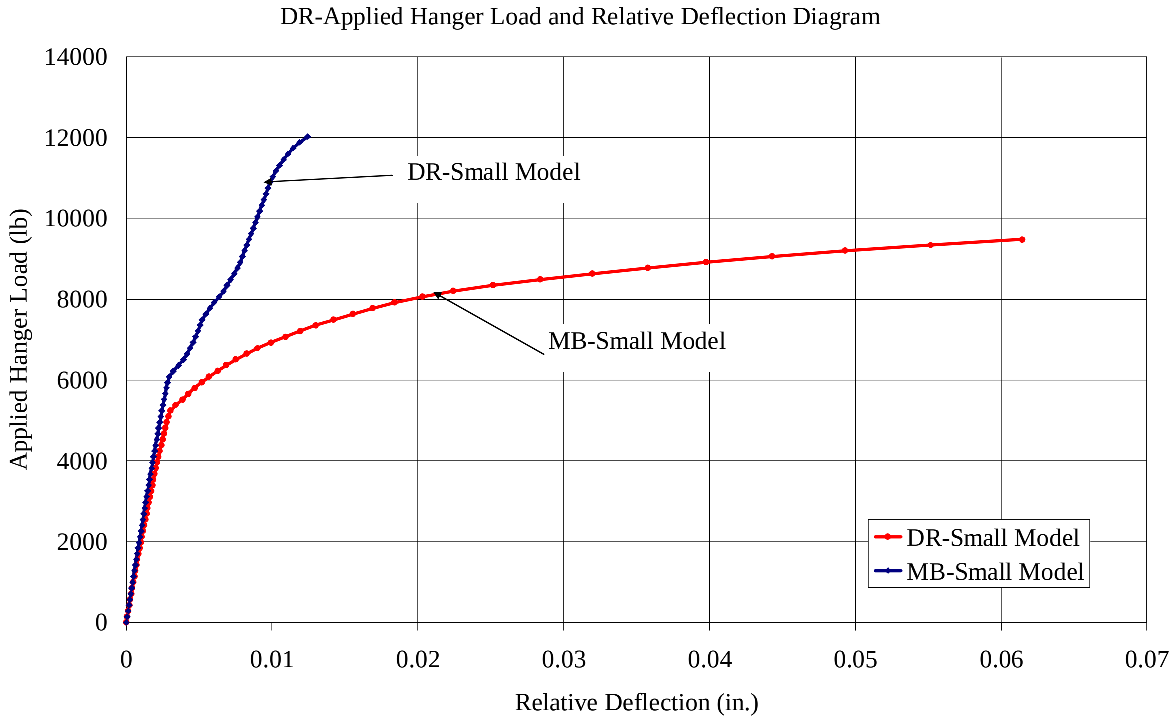

Figure 4.30 Small model results

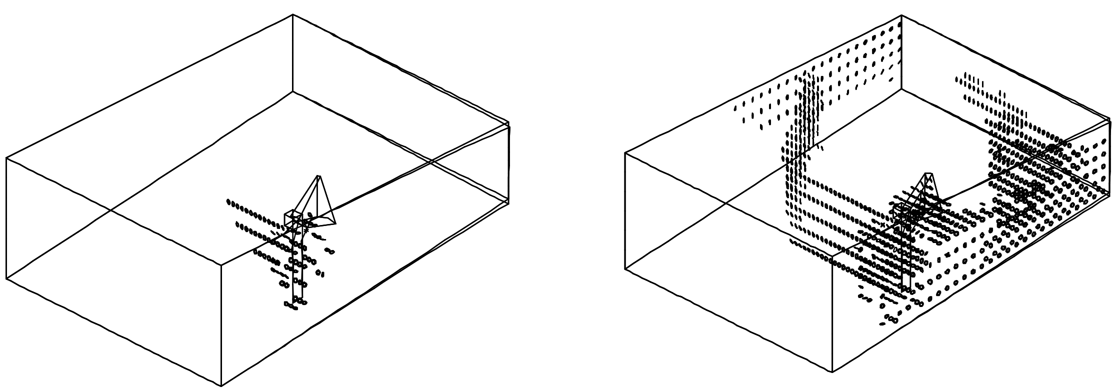

a) At 5,500 lb. applied hanger load

b) At 12,000 lb. applied hanger load

Figure 4.31 Dayton/Richmond small model's crack pattern

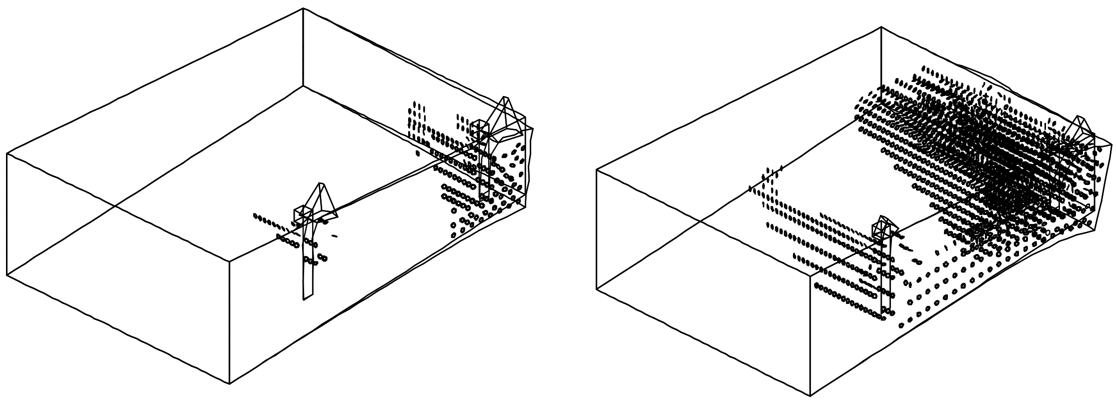

a) At 5,500 lb. applied hanger load b) At 9,000 lb. applied hanger load

Figure 4.32 Meadow/Burke small model's crack pattern

The strain profiles developed under the girder flange for the single hanger and small models are shown in Figure 4.33. A high tensile strain was observed at the centerline under the girder flange. The strain changed from a tensile strain to a compressive strain as the distance from the centerline increased. For the single hanger model, the compressive strain was close to zero and constant as the distance increased. For the small hanger model, the strain decreased approximately linearly as the distance from centerline increases.

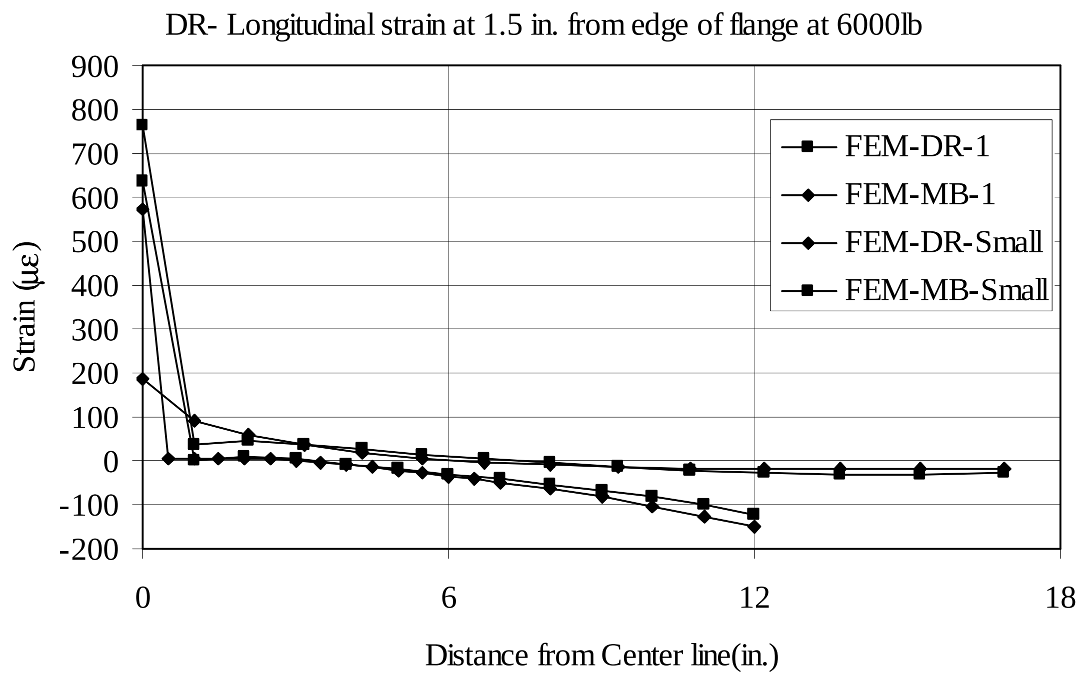

Figure 4.33 Strain profile at the 1.5 in. from the edge of flange of single and small model

Modified Small finite element model Results

The small models were modified to increase the overall strength of the system by increasing the loaded area under the hanger head for the Dayton/Richmond hanger and increasing the edge flange thickness of the girder flange model. The relationship between the applied hanger load and the relative deflection is shown in Figure 4.34.

The first cracks were observed at 5,000 lbs. for both models and had the same crack pattern at the ultimate load. Both Dayton/Richmond and Meadow/Burke hanger models failed at 12,000 lbs. by flexural-shear failure and punching shear failure, respectively.

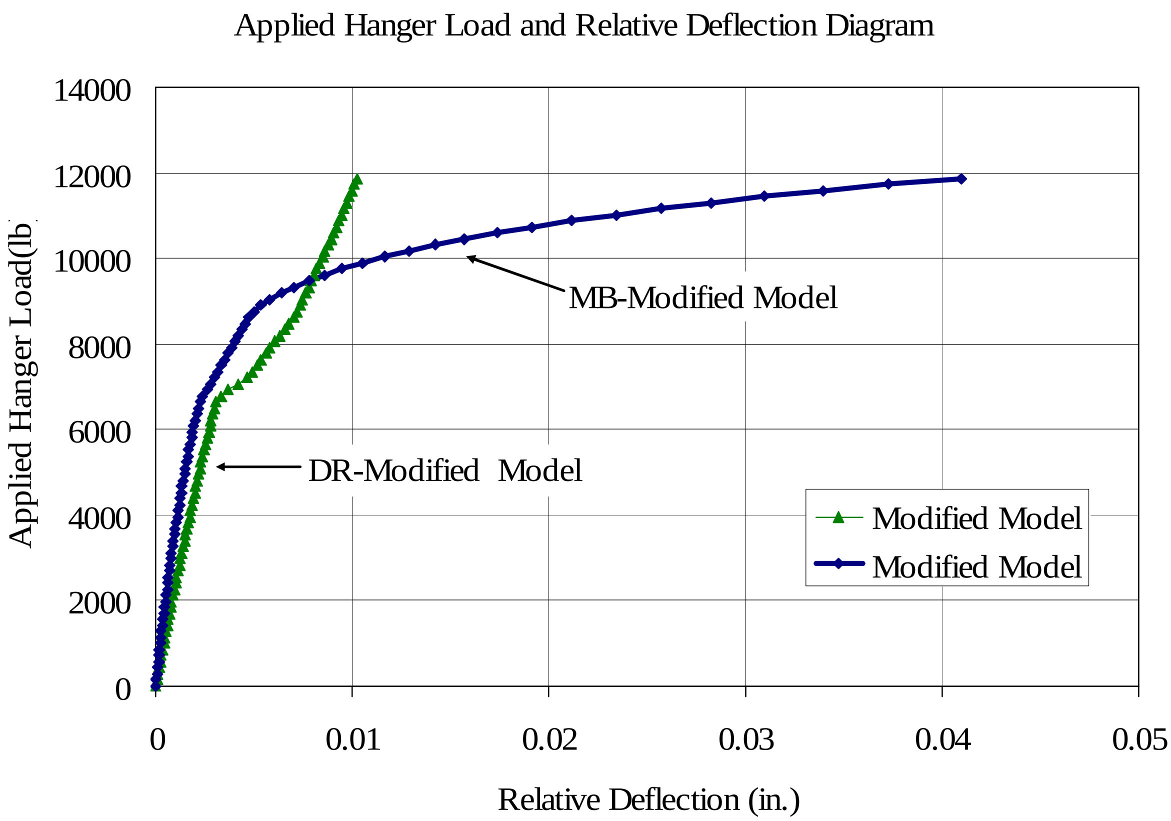

Figure 4.34 Modified small model results

The Dayton/Richmond and Meadow/Burke model results are summarized in table 4.2

Table 4.2 Summary of Analysis Result

Test ID	Ultimate Load (lb)	Maximum Vertical Displacement (in)	Mode of Failure
DR-1-L DR-2-L	12,200 12,300	0.0449 0.0480	Flexural Flexural
MB-1-L MB-2-L MB-4-L	11,200 10,600 10,300	0.1045 0.0976 0.0952	Punching Shear Punching Shear Punching Shear
DR-Small MB-Small	12,000 9,500	0.0124 0.0614	Flexural Punching Shear
DR-Modified	12,000	0.0104	Flexural
MB-Modified	12,000	0.0410	Punching Shear

4.3 Analytical/Design Method

From the limit states mentioned in section 4.1, the bearing failure, punching shear failure and the torsional strength was predicted by using the ACI318 specification provisions. The simple calculation for the bearing is provided in Appendix J. The punching shear failure was also predicted according to the ACI approach. The punching shear strength was a function of the vertical load applied to the flange model regardless of the horizontal load form the hanger leg. The torsional strength of the girder was calculated using the ACI approach.

4.3.1 Bearing Strength

The concentrated load applied on the concrete caused some crushing at the edge of the flange near a tested hanger before the hanger reached it's ultimate load. This failure could be calculated by following ACI318-02 Section 10.17. The actual contact area between the hanger head and the top of the flange model is shown in Figure 4.35.

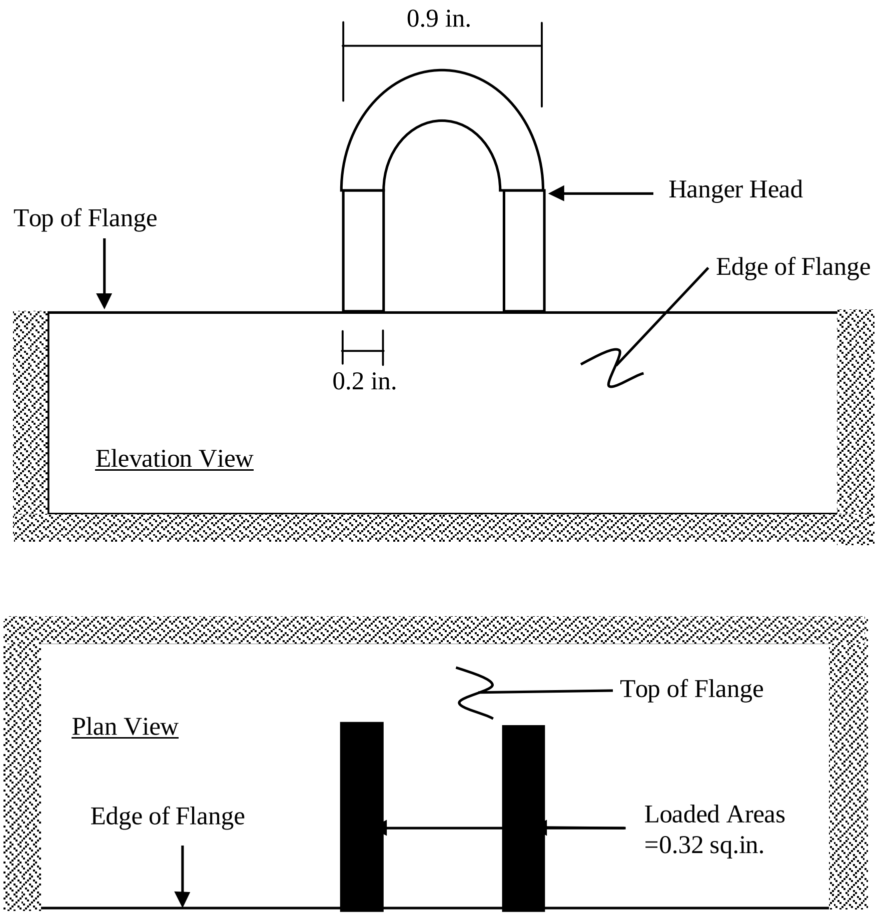

Figure 4.35 Actual loaded area of hanger head

The bearing strength equation was

$$F_{br} = 0.85 f_c^{'} A \tag{4.1}$$

Where F_{br} = Bearing strength, lb

$f_c^{'}$ = specified compressive strength of concrete, psi

A = loaded area, in^2

The details of the calculation are available in Appendix J. The calculated bearing strength is the vertical component of the applied hanger load. The modification factor of

1.414 was multiplied to the bearing strength to obtain the applied hanger load that causes a bearing failure. The calculated bearing strength was a 5800 lbs. applied hanger load.

4.3.2 Punching Shear Strength

According to ACI318-02 Chapter 11, the punching shear strength is developed based on the critical section. The critical section extends a distance of half the slab depth on each edge of the perimeter of the load as shown in Figure 4.36.

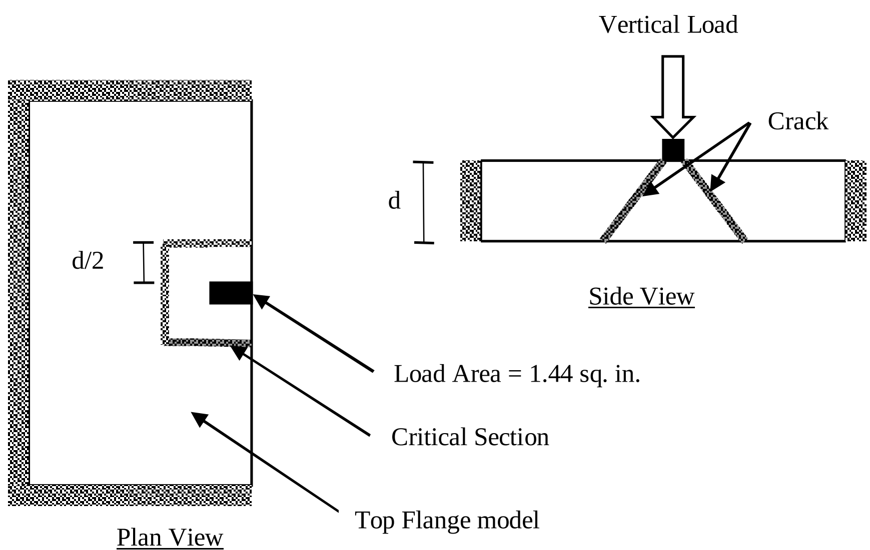

Figure 4.36 Critical section of punching shear failure

The Punching Shear Strength was the smallest of the following equations.

$$V_c = \left(2 + \frac{4}{b_c}\right)\sqrt{f_c^{'}}\, b_0 d \tag{4.2}$$

$$V_c = \left(\frac{a_s d}{b_0} + 2\right)\sqrt{f_c^{'}}\, b_0 d \tag{4.3}$$

$$V_c = 4\sqrt{f_c^{'}}\, b_0 d \tag{4.4}$$

Where: V_c = nominal shear strength provided by concrete, lb

$f_c^{'}$ = specified compressive strength of concrete, psi

b_0 = perimeter of critical section for slabs, in.

d = thickness of slab, in

a_s = constant used to compute V_c for edge column

b_c = ratio of long side to short side of concentrated load

Equations 4.2 to 4.4 give results of 15,000 lbs., 38,560 lbs., and 13,500 lbs., respectively. The details of the calculations are given in Appendix J. The nominal shear strength for concrete slabs is taken as 13,500 lbs. After modifying the punching shear strength by the modification factor, the calculated punching shear strength is a 19,100 lb. applied hanger load.

As shown in appendix J, if the punching shear strength is calculated from the actual critical section, as shown in Figure 4.37, the punching strength is 11,300 lb. applied hanger load.

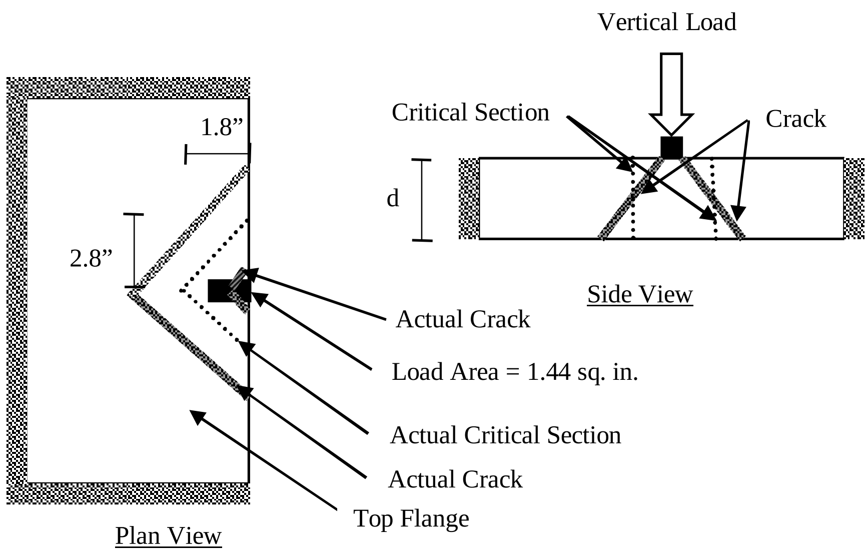

Figure 4.37 Critical section of punching shear failure

4.3.3 Torsional strength of girder

The purpose of this calculation was to check the torsional capacity of the girder to ensure no cracking of the girder would occur from the applied hanger load. The torque is created by the applied load being offset from the center of gravity of the girder as shown in Figure 4.38.

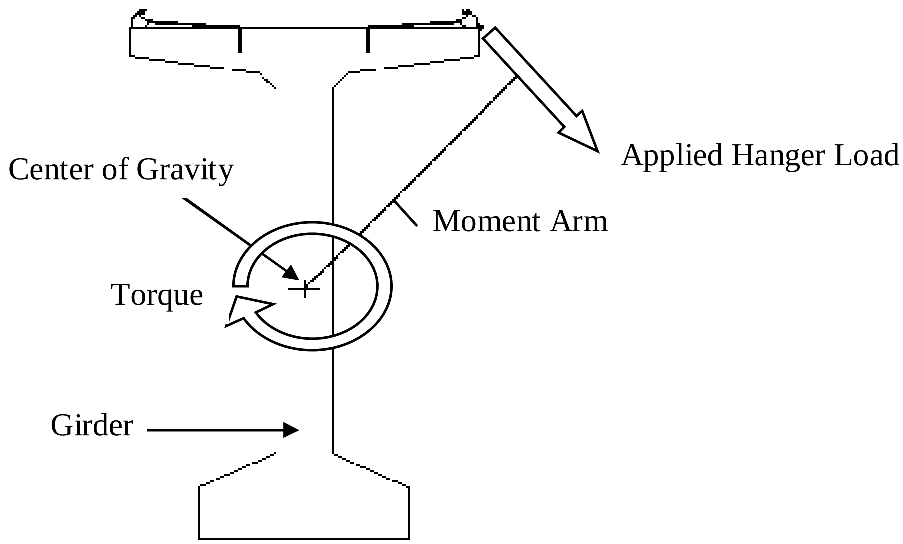

Figure 4.38 Torque on the Girder

From the geometry, the moment arm is 38-¼ in. The torque at each applied hanger, based on Section 3, is 459 kips-in. The maximum torsion that was applied at the mid-span of the girder for the four-hanger test was 459 kips-in, see details of the calculation in appendix J.

The cracking torque equation was obtained from ACI318-02, Section 11.6. This equation is valid for a prestressed member. The torsional strength was calculated using the following equation.

$$T_{cr} = 4\sqrt{f_c^{'}}\left(\frac{A_{cp}^2}{P_{cp}}\right)\sqrt{1+\frac{f_{pc}}{4\sqrt{f_c^{'}}}} \qquad (4.5)$$

Where: T_{cr} = Cracking Torque, lb-in.

$f_c^{'}$ = Specified compressive strength of concrete, psi

A_{cp} = Area enclosed by outside perimeter of concrete cross-section, in.^{2}

P_{cp} = Outside perimeter of the concrete cross-section, in.

f_{pc} = Compressive stress in concrete at centroid of cross-section resisting externally applied loads, psi

The area of the section is 814 in.^{2} and the outside perimeter is 227 in. The f_{pc} was equal 12.5% of $f_c^{'}$ for the standard girder specification. The cracking torque was 1,946,000 lb-in. at the mid-span of the test set up. The torsional strength of the girder was strong enough to prevent the crack due to torsion.

4.4 Summary

The finite element model was able to capture the behavior and limit states including the punching shear failure. The small finite element model results provide a good prediction of the load deflection relationship. The bearing failure was predicted by using the ACI approach. The ACI approach could predict the modes of failure such as the bearing failure and torsional strength of the girder. The punching shear failure can also be calculated using the ACI approach but can not be applied for the complicated behavior of the Meadow/Burke hanger model, which had a horizontal force applied at the very tip of the flange that the ACI code would not take into account.

Comparisons and discussions of the experimental investigations and analytical investigations were performed to investigate the efficiency of the analytical model compared to the results from the experimental testing program. The details of the comparisons and discussions are discussed in Section 5.

5.0 DISCUSSION OF RESULTS AND COMPARISONS

The experimental test program was designed to study the behavior of the Dayton/Richmond and Meadow/Burke hangers for use in the overhang falsework system. The experimental results were predicted by two approaches, ACI methodology (ACI318-02) and finite element study. The crushing strength and punching shear strength at ultimate load were calculated according to the ACI318-02 specification provisions. The finite element models were created to capture the behavior of each hanger assembly in more detail and to understand the behavior of the system more thoroughly. This section discusses the experimental and analytical results mentioned in Section 3 and Section 4 respectively. Comparisons of the results are made to investigate and study the behaviors of falsework hanger systems.

The effect of the girder shear reinforcement was studied by comparing single hanger tests in two different locations along the girder where the shear reinforcement spacing varied. The effect of loaded adjacent hangers was investigated by the comparison of multiple hanger tests. Comparisons between the Dayton/Richmond and Meadow/Burke hanger system were made to investigate the effect of front hanger leg of the Meadow/Burke hanger. The analytical results were compared with the experimental testing results to determine the accuracy of the analytical models.

A summary table of experimental and finite element results is presented in Table 5.1 and Table 5.2, respectively. The experimental data presented in Table 5.1 is also presented on the test summary sheets in Appendix B to H. Each summary sheet contains the details of the specimen properties, test configuration, test photographs, observed failure mode and primary results. The analytical results presented in Table 5.2 are also presented in Appendix I.

Table 5.1 Summary of experimental results

Test ID	Ultimate Load (lb.)	Deflection at Mid-Span (in.)	Mode of Failure
DR-1-H	9,200	0.0259	Crushing/Hanger
DR-1-L	9,200	0.0474	Crushing/Hanger
DR-2-L	10,200	0.0645	Punching Shear
MB-1-H	8,500	0.0200	Punching Shear
MB-1-L	6,500	0.0296	Punching Shear
MB-2-L	6,800	0.0333	Punching Shear
MB-4-L	5,800	0.0477	Punching Shear

Table 5.2 Summary of finite element modeling results

Test ID	Ultimate Load (lb)	Maximum Vertical Displacement (in)	Mode of Failure
DR-1-L	12,200	0.0449	Flexural
DR-2-L	12,300	0.0480	Flexural
MB-1-L	11,200	0.1045	Punching Shear
MB-2-L	10,600	0.0976	Punching Shear
MB-4-L	10,300	0.0952	Punching Shear
DR-Small	12,000	0.0124	Flexural
MB-Small	9,500	0.0614	Punching Shear

Analysis of the experimental and analytical results was performed to investigate the effects of the girder shear reinforcement spacing, the interaction of adjacent hangers, and the comparative strength of the Dayton/Richmond and Meadow/Burke hangers.

5.1 Effect of Girder Shear Reinforcement

Single hanger tests were performed at two different locations for each hanger type. One location was the end of girder which was highly reinforced with vertical and transverse shear reinforcement and the other was toward middle of the girder which was reinforced with approximately one forth less steel than the end-zone. The spacing of the shear stirrups at the end hanger is 6 in. and increased at the middle hanger to 24 in. Tests DR-1-H and DR-1-L are compared to show the effect of shear reinforcement of Dayton/Richmond, and tests MB-1-H and MB-1-L are compared for Meadow/Burke hanger.

5.1.1 Dayton/Richmond single hanger test comparison

The observed ultimate load of both tests was 9,200 lbs. The load at which crushing of the concrete was first observed was 7,000 lbs. and 7,500 lbs. for tests DR-1-H and DR-1-L, respectively. The crushing of the concrete under the hanger head allowed the hanger head to cut through the concrete. As a result, the hanger head began to rotate. As more load was applied to the hanger, the rotation increased. Both of the single Dayton/Richmond hanger tests resulted in failure of the hanger. Test DR-1-H failed by hanger leg rupture and test DR-1-L failed by a weld failure between the hanger bar and hanger head. Both failures were caused by the rotation of the hanger head due to the applied load. This caused excessive bending and tensile stresses in the hanger leg and failure in the weld between the hanger leg and hanger head.

Initially, the response of both tests was similar. After a load of 3,000 lbs. was applied, test DR-1-H's response was stiffer than test DR-1-L's until the ultimate load was reached. The deflection at a 3,000 lb. applied hanger load was 0.0119 in. and 0.0131 in. for test DR-1-H and DR-1-L, respectively. The girder flange of test DR-1-H deflected 10% less than the flange in test DR-1-L. At a 9,000 lb. applied hanger load, deflections were 0.0251 in. and 0.0459 in. for test DR-1-H and DR-1-L, respectively. The difference of deflection at mid-span increases from 10% to 45%.

The behavior of the two Dayton/Richmond single hanger tests was similar. The first crack was observed at approximately 3,500 lbs. At this point, the back side of the hanger head began to lift up resulting in a concentrated load at the front side of hanger head. The crushing of the concrete was observed from 7,500 to 8,000 lbs. After spalling of concrete occurred under the hanger, a large degree of hanger rotation was observed causing failure in the hanger due to an enhanced force at the hanger leg and the connection of the hanger leg and hanger head.

Both single Dayton/Richmond test specimens failed at 9,200 lbs. by the same type of failure mode. The consistency of the results from both tests did not show any effects of shear reinforcement because the failures occurred locally at the hangers. The effect of the girder shear reinforcement was indicated in the relationship between applied hanger load and flange deflection mentioned in Section 3.

5.1.2 Meadow/Burke hanger single hanger test comparison

The ultimate strengths were 8,500 lbs. and 6,500 lbs. in tests MB-1-H and MB-1-L, respectively. Both of the test specimens failed due to the punching shear of the girder flange. The ultimate load at the high shear reinforcement testing location was 24% larger than the ultimate load at the light shear reinforcement.

According to the mid-flange deflection and applied hanger load relationship stated in Appendix E and F, the stiffness of test MB-1-H was higher than that of MB-1-L. At the same applied load, test MB-1-L exhibited approximately 40-50% larger flange displacement than MB-1-H. At 6,000 lbs., the mid-span deflection of test MB-1-H was 0.0155 in. and of test MB-1-L was 0.0280 in. Test MB-1-H deflected 45% less than test MB-1-L. At ultimate load, the maximum deflection was 0.0200 in. in test MB-1-H and 0.0296 in. in test MB-1-L.

In test MB-1-H, the effects of the girder shear reinforcement are apparent. As shown in Appendix E, the cracks propagated past the end of the rebar which indicates that the rebar spacing restricted the development of the crack. Because of the higher shear reinforcement, test MB-1-H's maximum deflection was less than that observed in test MB-1-L. In terms of deflection, the flange deflection in higher reinforcement area was less than the deflection in light reinforcement. The change in shear reinforcement spacing form 24 in. to 6 in. increased the stiffness of the system by 45%. Therefore, the shear reinforcement increased not only the ultimate load of the hanger but also the overall stiffness of the system.

5.2 Effects of Multiple Loaded Hangers

During construction, multiple falsework hangers would likely be loaded close to the safe working load at the same time. The interaction of adjacent hangers could cause the reduction in load capacity of the hanger. The comparison of the test with one, two and four loaded hangers is used to investigate the interaction effects in terms of strength and deflection. The tests chosen for comparison had low reinforcement to eliminate the shear reinforcement effect. For the Dayton/Richmond hanger, tests DR-1-L and DR-2-L were compared. Tests MB-1-L, MB-2-L and MB-4-L were compared to illustrate the effect of the adjacent hanger of Meadow/Burke hanger.

5.2.1 Dayton/Richmond multiple hanger comparison

The DR-1-L and DR-2-L tests had the same behavior before the ultimate load. The crushing and large spalling occurred at 7,500 lbs. and 8,000 lbs. for the single hanger test and the double hanger test, respectively. After crushing of the concrete occurred, large deflections were observed in the double hanger test. The ultimate load of the single hanger test was 9,200 lbs. and the double hanger test was 10,200 lbs. The double hanger test's ultimate load was 9.8% higher than the single hanger test. The failure mode of the single hanger test was hanger failure, as mentioned in the single hanger comparison. The double hanger test failed by a punching shear failure.

At 3,000 lbs. and 6,000 lbs. applied hanger load, the deflections of test DR-1-L were 0.0158 in. and 0.0279 in. and that of test DR-2-L were 0.0198 in. and 0.0297 in. The double hanger test deflected approximately 20% and 6% at 3000 lb. and 6000 lb., respectively.

Normally, the ultimate load for a double hanger test should be less than for a single hanger test's ultimate load. From the test results, the double hanger test showed higher ultimate load than single hanger test's ultimate load. However, the failure modes of the two tests were different. Therefore, comparisons in terms of ultimate loads were not able to be made. In terms of mid-span deflections, the double hanger test deflected approximately 6-20% more than the single hanger test.

5.2.2 Meadow/Burke hanger comparison

The failure modes for all Meadow/Burke hanger tests was punching shear of the girder flange. The first cracks were observed just prior to the failure of the flange. As shown in Table 5.1, the ultimate load was decreased when more hangers were loaded. Test MB-4-L had the lowest ultimate load of 5,900 lbs. As detailed in Appendix I, the first failure occurred at the third hanger which was located between transverse reinforcements. The influence from the adjacent second and fourth hangers was not significant. The ultimate load in test MB-4-L was 11% less than that of test MB-1-L. The ultimate load of test MB-2-L was 6800 lbs. which is approximately 5% more than that of test MB-1-L.

The deflection at the centerline of the test setup at a 5,000 lb. applied hanger load for Meadow/Burke hanger tests were 0.0217, 0.0257 and 0.0450 in. for tests MB-1-L, MB-2-L and MB-4-L, respectively. The deflection increased approximately 18% and 107% for two and four hanger tests, respectively, compared to single hanger test.

From the Meadow/Burke test results, more hangers tested simultaneously caused a reduction in ultimate loads and increased the deflection at the mid-span. A higher ultimate load was observer for test MB-2-L than test MB-1-L. However, the difference in ultimate loading of these two tests was only 3%. The difference can be neglected because it is so small. A reduction in strength was observed in the four-hanger test. The hanger capacity of test MB-4-L was approximately 11% less than the strength of test MB-1-L. Therefore, a ultimate load reduction effect from testing adjacent hanger was observed in the loading of more than two hangers at a time. The number of loaded hangers increases the deflection at mid-span.

5.3 Comparison of the Dayton/Richmond and Meadow/Burke hangers

The Dayton/Richmond and Meadow/Burke hangers investigated in this research have the same manufacturer's safe working load. The hanger configuration is similar except that the Meadow/Burke hanger has a front hanger leg to prevent the rotation of the hanger head at high applied hanger loads. Comparisons of the hanger performance are included herein.

5.3.1 Single hanger test comparison

From the single hanger result, two failure modes were observed: hanger failure for Dayton/Richmond hanger and punching shear failure for Meadow/Burke hanger. For the Dayton/Richmond tests, the first crack in the flange was observed at around 3,000 lbs. to 3,500 lbs. and the hanger head simultaneously started to rotate forward. Unlike the Dayton/Richmond hanger, the Meadow/Burke hanger's head did not rotate after the crack was observed. The front leg of the hanger stiffened the hanger and prevented the hanger head from rotating.

The Dayton/Richmond hanger's leg was embedded into the concrete at a location 12 in. back from the hanger head. Because of this long leg, there was little rotational restraint to prevent the rotation of hanger head. A rotational behavior allowed the hanger to crush the concrete at the edge of the flange. When the rotation of the hanger occurred, the stress distribution under the hanger head changed and resulted in a concentrated load at the edge of flange. For the Meadow/Burke hanger, the additional front leg gave the rotational resistance of the hanger head. There was no bearing failure for the Meadow/Burke hanger test because the front leg prevented it from rotating.

At the same load magnitudes, the deflections of the Dayton/Richmond and Meadow/Burke hangers varied by 5%. Therefore, the deflection of the flange was not affected by the location of the horizontal force. It was affected by the vertical load applied by the hanger head to the flange only.

5.3.2 Double hanger test comparison

As mentioned in the single hanger test comparison, the behavior before the ultimate load from the double hanger was similar to the single hanger test. At the ultimate load, the shapes of the shear cone for two hanger tests were different. For the Dayton/Richmond double hanger test, a shear cone developed 45 degrees diagonally from the edge of the hanger head at the top of the flange to the bottom of the concrete flange without interference with rebar. The Meadow/Burke hanger test's shear cone was wider than the one from the Dayton/Richmond hanger. The ultimate load of the double hanger test was 10,200 lbs. and

6,800 lbs. in test DR-2-L and MB-2-L, respectively. The ultimate load from test MB-2-L was 50% less than test DR-2-L.

The front leg not only prevented the Meadow/Burke hanger head from rotating, it also transferred the horizontal force from the hanger head area. Therefore, there was no crack due to bearing failure observed in the Meadow/Burke hanger test but the hanger failed by a punching shear failure at approximately 34% less ultimate load than the one of the Dayton/Richmond hanger test.

The expansion of the shear cone was a result of the horizontal force from the front leg. The horizontal force from the hydraulic cylinder was taken by the two legs of the Meadow/Burke hangers, the front leg and the back leg. The front leg was short, so it takes more force than the back leg which had a longer length. The horizontal force from the front leg of the Meadow/Burke hanger reduced the punching shear strength and induced the formation of the cracks by putting more tension at the edge of the concrete flange. As see in Appendices E to I, the failure of the Meadow/Burke hanger tests began just behind the front leg and propagated to the edge.

5.4 Manufacturer Safe Working Load and Experimental Result

The Dayton/Richmond and Meadow/Burke hangers had published safe working load of 6,000 lb (Meadow Burke, 2003) (Dayton Superior, 2005). The safe working load was based on 2 to 1 safety factor, 5 degree rotation of coil rod as a failure condition, 45 degrees single hanger loading, concrete strength of 5,000 psi and 5 in. minimum concrete thickness for embedment and bearing (Meadow Burke, 2003) (Dayton Superior, 2005). Based on the assumptions above, the ultimate loads of Dayton/Richmond and Meadow/Burke hanger were calculated to be 12,000 lb.

The measured concrete compressive strength of the girder was 7,500 psi. To compare the hanger strength with the manufacturer's hanger strength, the ultimate load of each test result needed to be scaled down. For the failure modes of the single hanger tests, the bearing and punching shear strengths were taken into account. According to the ACI design approach mentioned in Section 4, the bearing and punching shear strength were functions of the square root of the concrete strength. Therefore, the applied hanger load for each test was scaled down by a factor of 0.82 to be comparable with the manufacturer's ultimate load. The summary of test results after the scale down is shown in Table 5.3.

Table 5.3 Summary of scaled single hanger tests

Test ID	Ultimate Load (lb.)	Max. Deflection (in.)	Mode of Failure
DR-1-H	7,500	0.0259	Crushing/Hanger
DR-1-L	7,500	0.0474	Crushing/Hanger
DR-2-L	8,400	0.0645	Punching Shear
MB-1-H	7,000	0.0200	Punching Shear
MB-1-L	5,300	0.0296	Punching Shear
MB-2-L	5,600	0.0333	Punching Shear
MB-4-L	4,800	0.0477	Punching Shear

No single test reached the manufacturer's ultimate load of 12,000 lb. The maximum scaled down ultimate loads were 8,400 lbs. and 7,000 lbs. from tests DR-2-L and MB-1-H, respectively. All ultimate loads from the Dayton/Richmond hanger tests were larger than the Meadow/Burke hanger tests. To directly compare the manufacturer ultimate load and indicate the common location of the hanger in the field, the single hanger tests at the light reinforcement zone were evaluated. Test DR-1-L's and MB-1-L's ultimate loads of 7,500 lbs. and 5,300 lbs. equals to 63% and 44% of the ultimate load of the manufacturer.

5.5 Experimental and Analytical Results Comparisons

To predict the behavior from the experimental test program, a series of finite element models were created as mentioned in Section 4. The purpose of the finite element models was to capture the response of the system and to predict the behavior of the girder flange. The modification of the finite element model is discussed at the end of this section.

5.5.1 Single hanger model

The experimental results chosen to compare with the finite element results were the tests performed in the light shear reinforcement zone. Because half of the top flange was modeled, results form finite element models indicated the deflection of the top flange by flexure, excluding girder rotation and displacement. To compare with the finite element model results, the differences between the vertical displacements at the centerline of the test set up and the lateral supports were used as relative deflections. The relative deflections from the full scale testing and finite element modeling results were compared. The single hanger tests of Dayton/Richmond and Meadow/Burke hangers test as shown in Figure 5.1 and Figure 5.2, respectively.

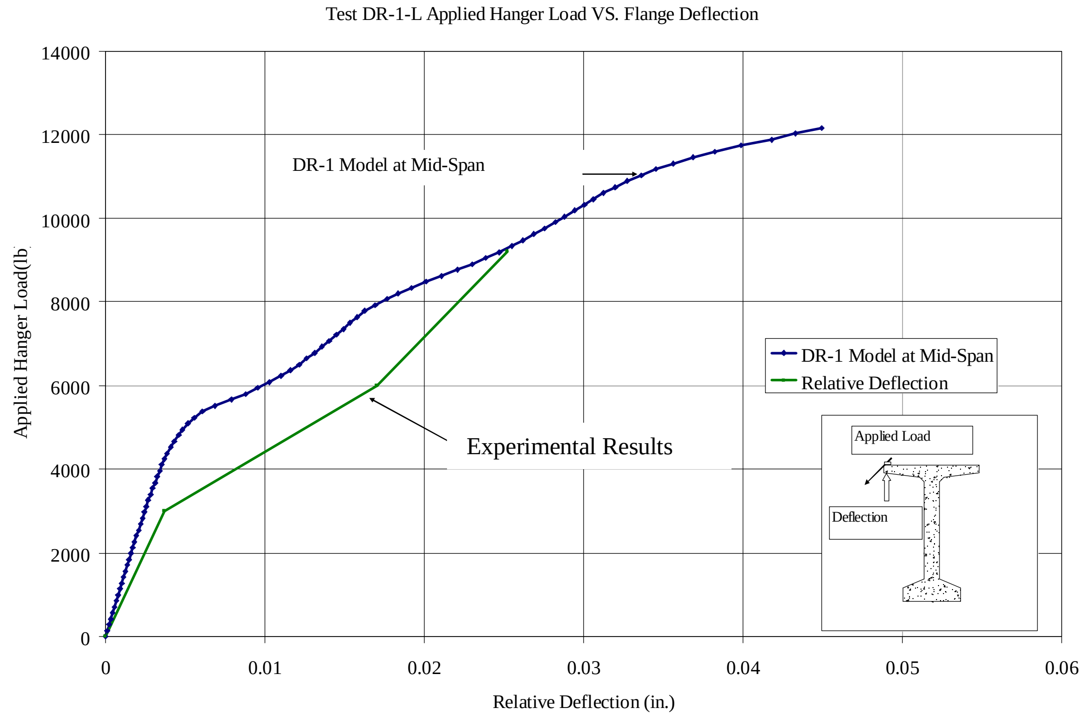

Figure 5.1 Experiment and Analytical results of test DR-1-L

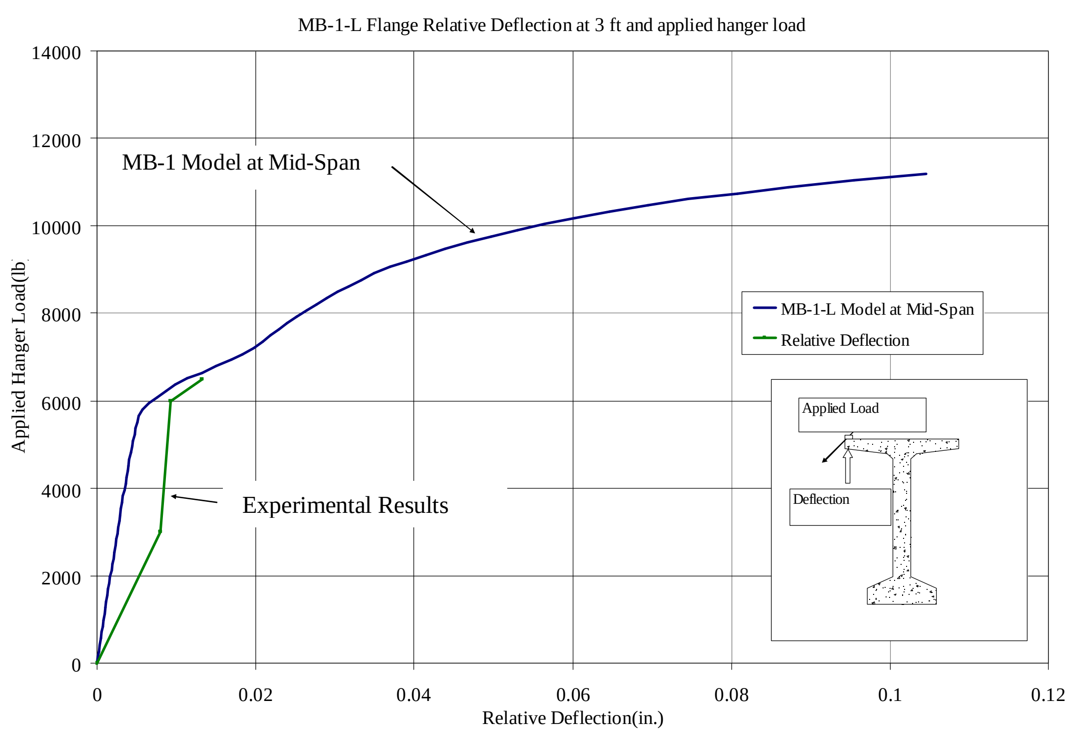

Figure 5.2 Experiment and Analytical results of test MB-1-L

As shown in Figure 5.1 and Figure 5.2, the finite element models predicted less initial deflection than the experimental testing results at the same applied load in both cases because the slope of the flange at the lateral support was not zero. The more ductile behavior was observed in the Meadow/Burke hangers. At 6,000 lb, the model predicted 40% and 30% less deflection than the experimental results for Dayton/Richmond and Meadow/Burke hangers, respectively. The predicted ultimate load of the Dayton/Richmond hanger model was 32% higher than the one from experimental result. For the Meadow/Burke hanger results, the finite element model predicted 46% more than the experimental result.

For the Dayton/Richmond hanger model, flexural failure was observed in the flange, while the experimental single Dayton/Richmond hanger test failed by crushing of concrete under the hanger head. The Meadow/Burke hanger model failed in a similar punching shear failure to that seen in the full scale tests.

5.5.2 Two hanger model

As shown in Figure 5.3, the experimental test centerline deflections were over predicted by the finite element model for the Dayton/Richmond hanger. Before the cracks were observed in the finite element model results, the initial stiffness of the curve was 70% higher than the experimental results. Figure 5.3 indicates that the yield points of both experimental and analytical tests are at the same location for a load of approximately 6,000 lbs. The predicted ultimate load of the model was 12,200 lbs., 20% higher than the experimental ultimate load. The mode of failure obtained from the finite element model was flexural and shear failure while the failure mode from the experimental testing was punching shear through the girder flange.

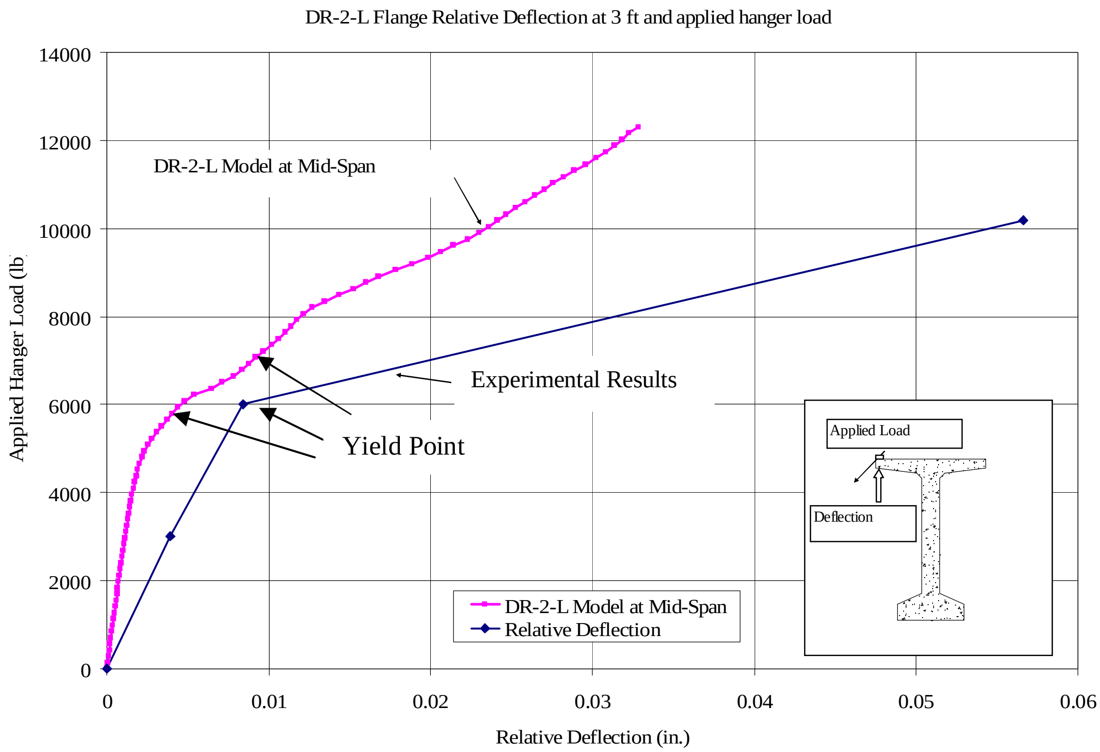

Figure 5.3 Experiment and Analytical of test DR-2-L

As shown in Figure 5.4, the experimental results for centerline deflection on the Meadow/Burke hanger were over predicted by the finite element model. Before the cracks were observed in the finite element model, the initial stiffness of the curve was approximately 76% higher than the experimental results. After the cracks were observed in the model, the stiffness of the model decreased. Figure 5.4 indicates that the yield points of both experimental and analytical are at the same locations approximately for a load of 6,000 lbs. The ultimate load of the finite element model is 10,600 lbs. which was approximately 56% higher than the experimental ultimate load. The Meadow/Burke model predicted a punching shear failure which was the same as the failure mode observed in the experimental testing.

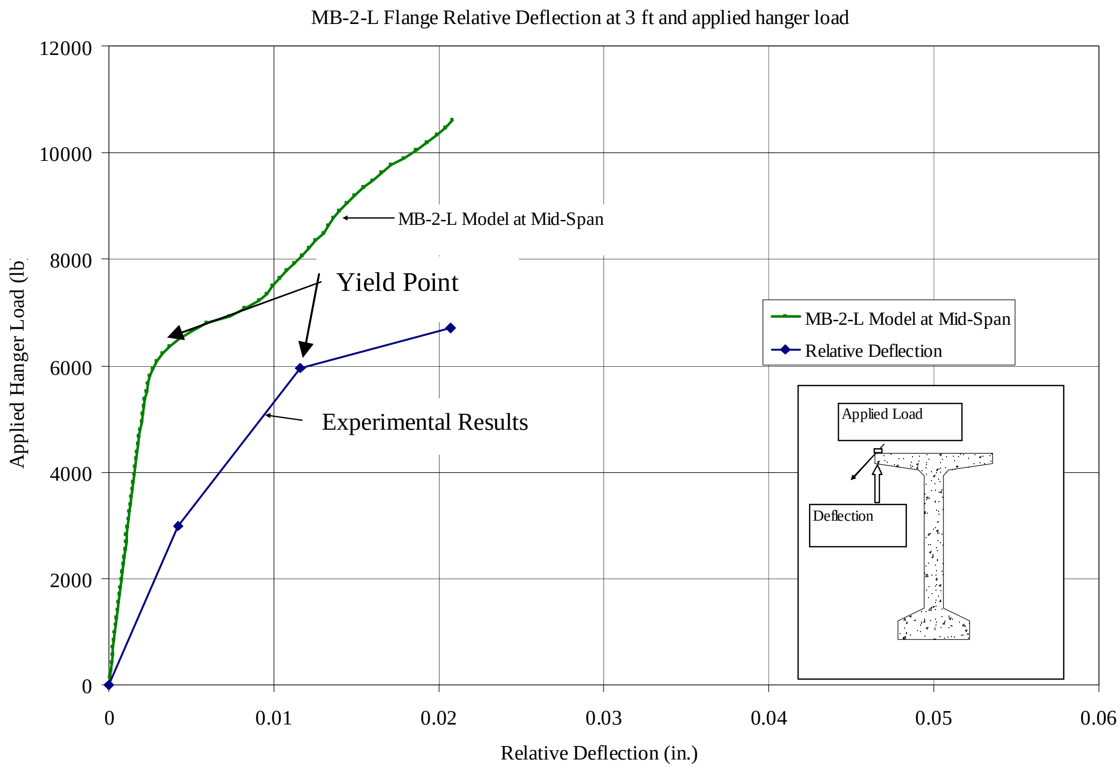

Figure 5.4 Experiment and Analytical of test MB-2-L

5.5.3 Four hanger model

The results from the four Meadow/Burke hanger finite element model were similar to the ones from the double Meadow/Burke hanger finite element model, see Figure 5.5. The initial stiffness of the curve was 86% higher than the experimental result. The predicted ultimate load was 10,600 lbs. and approximately 83 % higher than the experimental ultimate load. The predicted failure mode was punching shear failure which was the same as the first failure mode observed in the experimental testing.

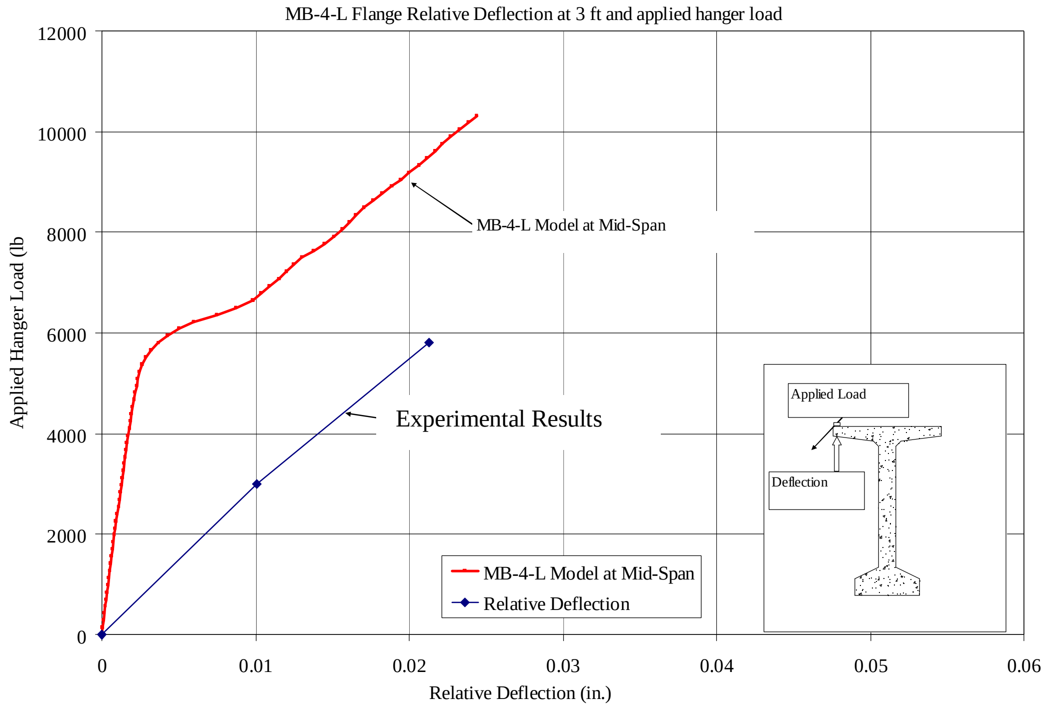

Figure 5.5 Experiment and Analytical of test MB-4-L

The finite element model accurately predicted the initial stiffness of the single hanger model but not for the multiple-hanger model because the slope of the experimental results is not zero at the lateral supports. The ultimate loads of the model were higher than the experimental results because the system failed locally before reaching the ultimate load controlled by the girder flange. The modifications of the models were made to accurately predict the behavior of the structure by refining the element size and using the small model discussed in Section 4. Model length was shortened from 40 in. to 12 in., and an element size was half the size of the original model.

5.5.4 Small finite element model

From the small finite element model results, the relationship of the applied hanger load and the deflection at the centerline of the model was observed. To compare the results to the modified finite element model, the difference between the deflection at the centerline and one foot away on ether side was used as the deflection. The results from the Dayton/Richmond and Meadow/Burke hanger were shown in Figure 5.6 and Figure 5.7.

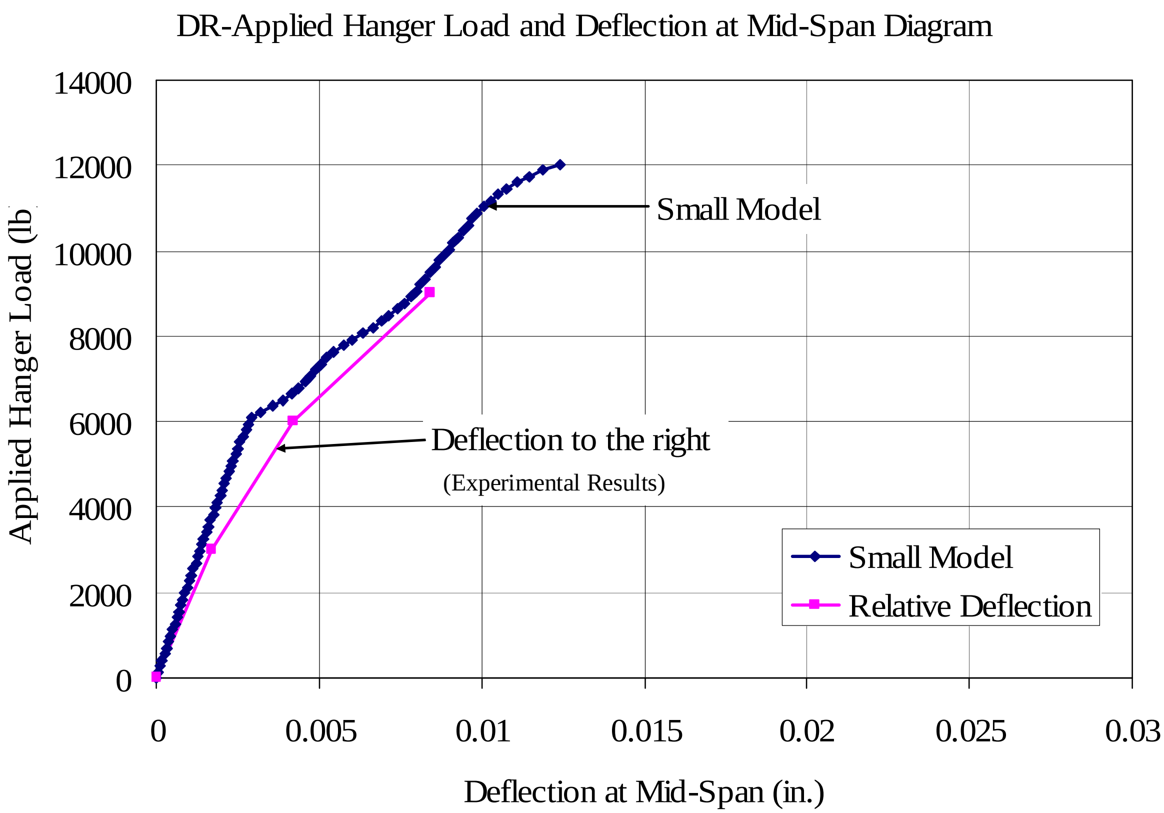

Figure 5.6 DR-Results from experiment and modified finite element model

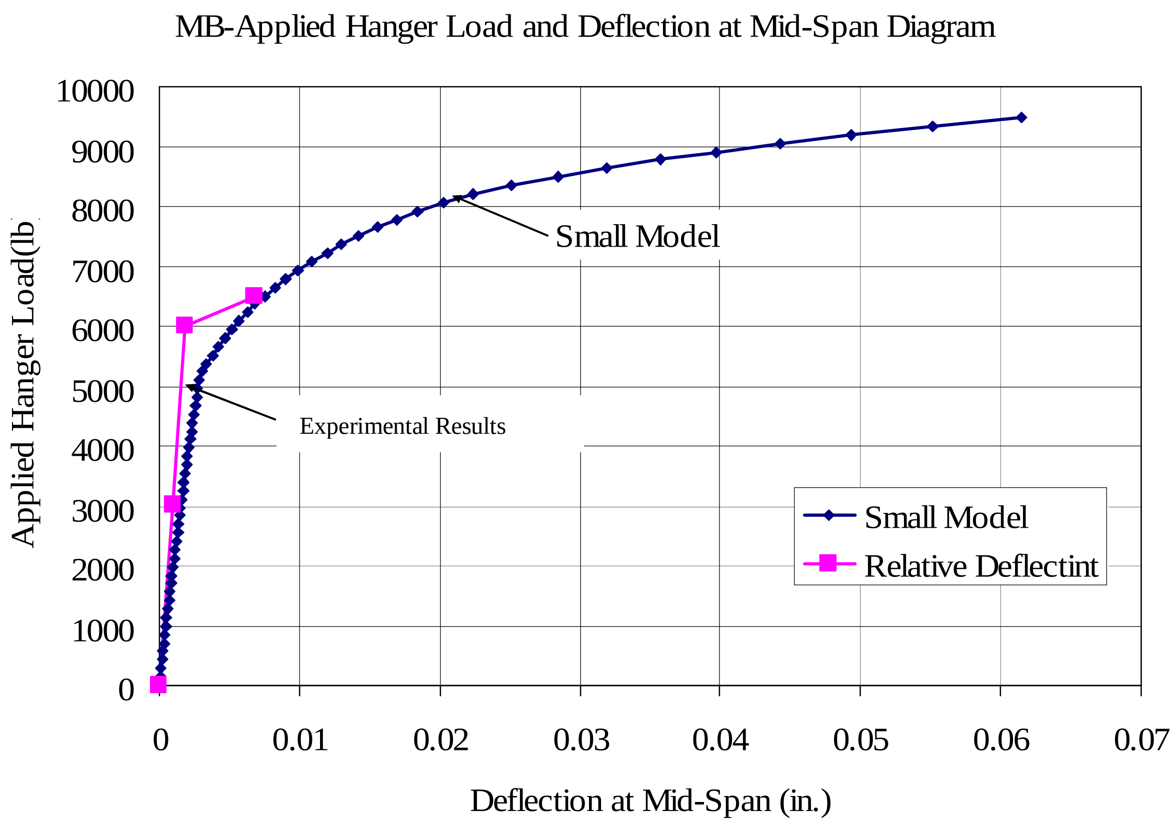

Figure 5.7 MB-Results form experiment and modified finite element model

The Dayton/Richmond hanger small model showed a better prediction than the original model. The deflection of the model was within the range of the deflection between the mid-span and one foot either sides of the experimental test results. The predicted ultimate load of the small finite model was 12,000 lbs. which was higher than the experimental results because the span length was shorter than the original model. The mode of failure of the modified model was a flexural failure which was different from the experimental results as would be expected.

The Meadow/Burke small model indicated an accurate deflection prediction from zero to 5000 lbs. After 5000 lb. the model predicted a ductile behavior which resulted in greater deflections compared to the experimental results, a brittle behavior. The mode of failure of the modified model was punching shear failure which correlated with the experimental test result.

The small model of the Dayton/Richmond and Meadow/Burke hangers predicted the behavior better than the original model, especially, at the beginning of the applied load. The predicted ultimate loads were higher than the experimental results because of the over restraints at the supports. However, only the Meadow/Burke small finite element model captured the failure mode from the experimental results.

5.5.5 Strain development

The strain developed under the girder flange as the load was applied. At the hanger location, high tensile strain was observed; see Figure 5.8 and 5.9 for the results from Dayton/Richmond and Meadow/Burke hanger models, respectively. From the experimental results, the tensile strain at 1.5 in. from the edge of the girder decreased to the compression strain at approximately 1 ft. from the hanger centerline. The result from the Dayton/Richmond models indicated a good prediction of the response from experimental results. For the Meadow/Burke model, the same pattern of response as the experimental result was observed. At the hanger centerline, there is an offset in value between the experimental and model result, however a good prediction of the strain was observed at 12 in. from hanger centerline.

The small finite element model indicates a high tensile strain at the centerline and decreased to the compressive stain at the fixed side supports. The results from the small models indicated the same pattern of response but with a different magnitude.

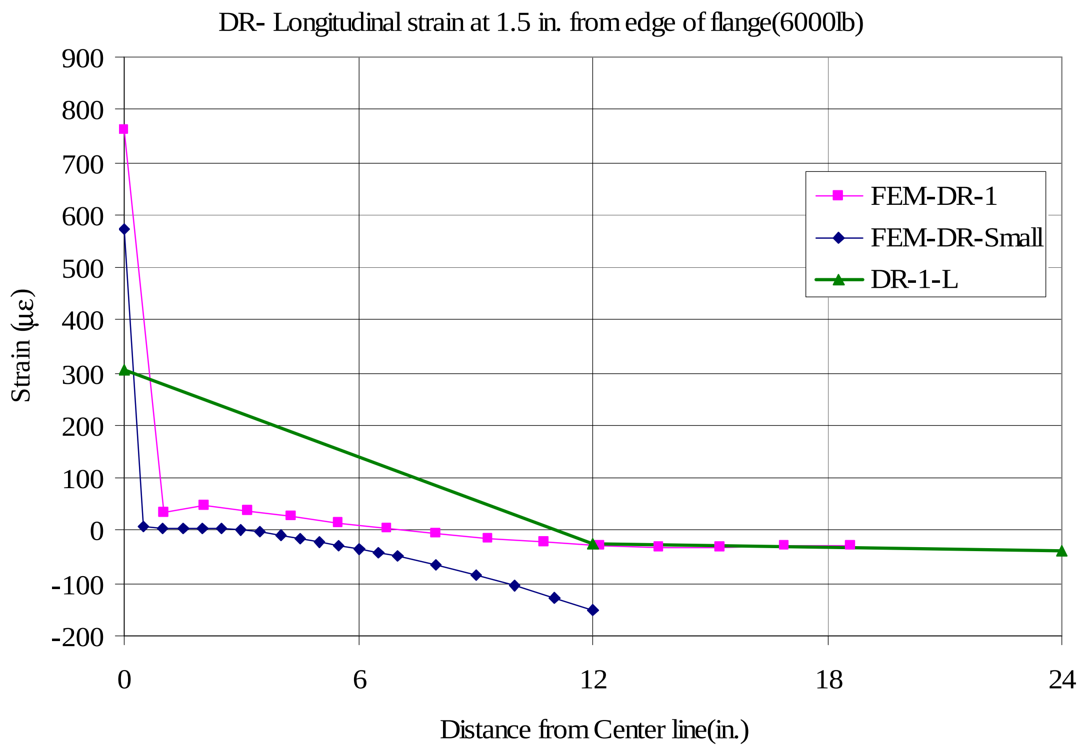

Figure 5.8 Longitudinal strains at 1.5 from edge of flange of test DR-1-L

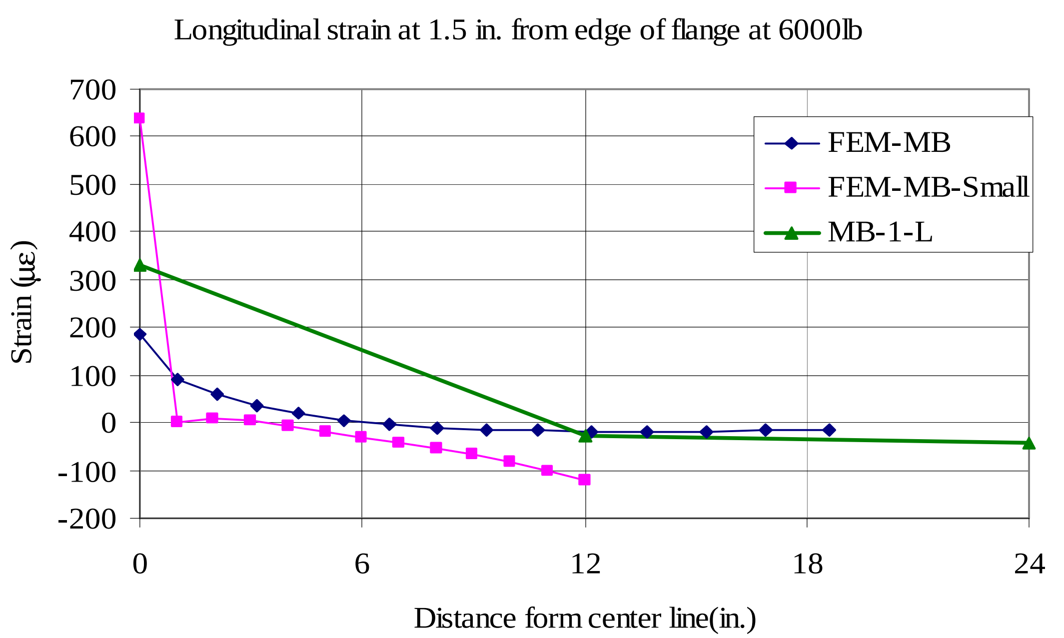

Figure 5.9 Longitudinal strain at 1.5 from edge of flange of test MB-1-L

A strain comparison between the small finite element model and the experimental results correlated well. However, the Dayton/Richmond and Meadow/Burke models predicted a significantly higher initial stiffness than the experimental results. The miss-prediction of the model occurred because the boundary conditions are different. The boundary conditions of the models are fix-end supports on three sides, while, in the experiments, the girder flange allowed vertical deflections at the lateral supports as illustrated in the flange deflections in Appendices B-H. Therefore, the finite element models predicted higher stiffness than the experimental results. For a better prediction, the deflection should use the difference between the deflection at the mid-span and at the lateral support, as does the deflection used in the small model.

5.5.6 Modified finite element model

A modification of the finite element model was applied to increase the ultimate load of the system. For Dayton/Richmond hanger model a larger loaded area under the hanger head was applied to simulate the use of a steel plate under the hanger head to prevent the bearing failure of the concrete. To increase the strength of the Meadow/Burke hanger model, the thicker flange was used to increase the punching shear strength. Comparisons of the small Dayton/Richmond and Meadow/Burke models are shown in the Figure 5.10 and Figure 5.11, respectively.

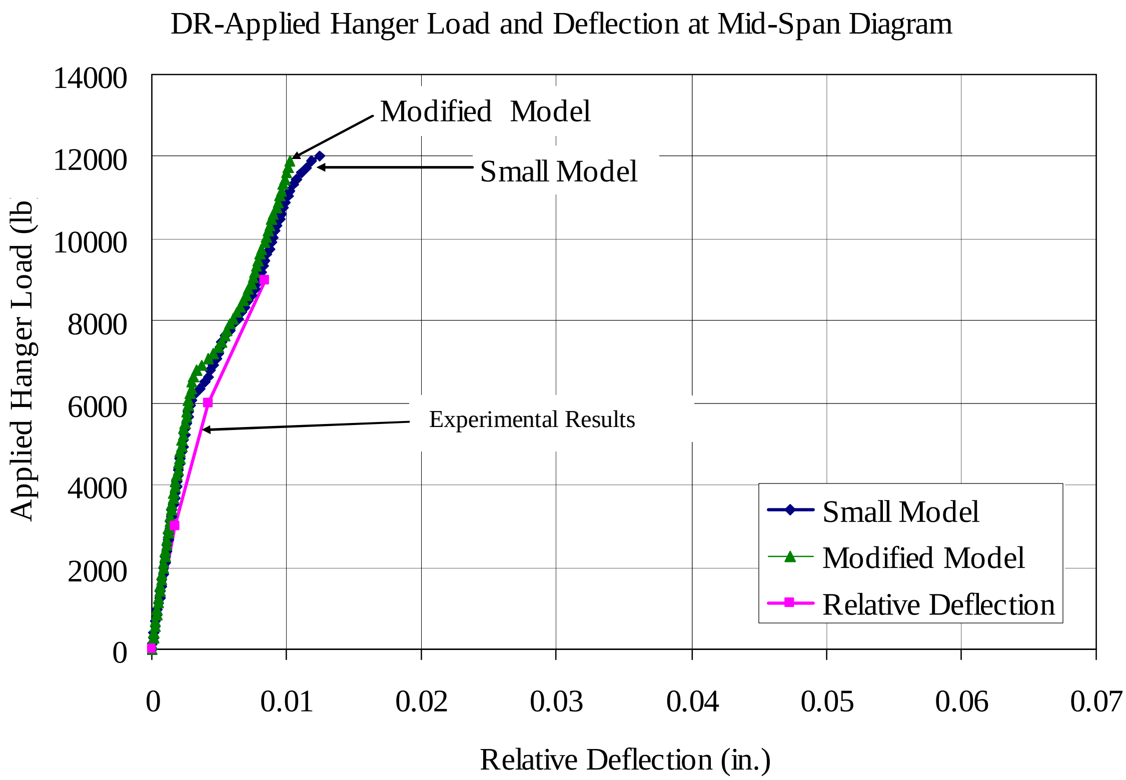

Figure 5.10 Dayton/Richmond Modified Small Model

To eliminate the localized failures such as the crushing of concrete under the hanger head, the steel plate may be used to distribute the load to a larger area of the flange. From the large loaded area model, the model failed in a flexural-shear failure. This indicated that if the crushing of concrete was prevented by the steel bearing plate, the hanger falsework system may reach the manufacturer specified ultimate load of 12,000 lbs.

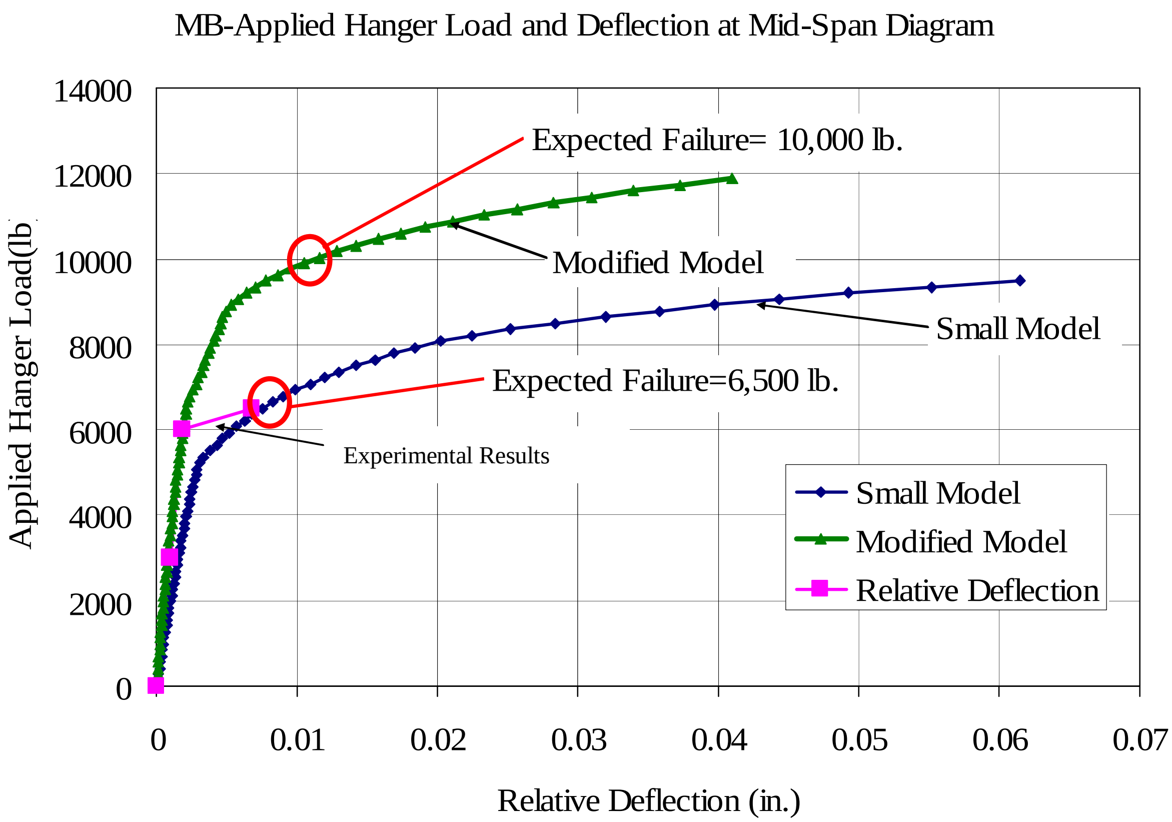

Figure 5.11 Meadow/Burke Modified Small Model

The Meadow/Burke hangers failed in punching shear. To increase the strength of the hanger flange system, a larger flange thickness would generate a greater punching shear capacity. From Figure 5.1, when the edge thickness increases from 3.5 in. to 5.5 in., the punching shear strengths were increased from 9,500 lb. to 11,900 lb.

To evaluate the thickness of concrete that can carry the 12,000 lb. applied hanger load, a strength per thickness ratio was applied. Based on the experimental result, the expected failure of the original model occurred at 6,500 lb. Therefore, the strength per thickness was 6,500 lb. / 3.5 in. which equals to 1857 lb./in. For the modified model the strength per thickness is 1818 lb./in. Based on these two models, the approximate strength per thickness was 1840 lb./in. To reach an applied ultimate load of 12,000 lb. the minimum thickness of the concrete flange is approximately 6.5 in.

5.6 ACI Code Analysis and Experimental Results Comparisons

As mentioned in section 4, the bearing strength of concrete under the hanger head was 5550 lbs. The experimental results of the Dayton/Richmond hangers showed the crushing of concrete started from 5000 lbs. and the large spalling of the concrete occurred around 7500 lbs. The crushing failure was not observed in the Meadow/Burke hanger test.

From The ACI318-02 specification provisions, the calculated punching shear strength was 19,100 lbs. while the Dayton/Richmond and Meadow/Burke hanger tests failed by punching shear failure at 10,200 lb. and 6,500 lb., respectively. The Dayton/Richmond and Meadow/Burke hanger punching shear strength was less than form ACI method by an approximate factor of 2 and 3, respectively

If the actual critical section was applied to calculate the punching shear strength, the punching shear strength is 11,300 lbs. The Dayton/Richmond and Meadow/Burke punching shear strengths were 10% and 51%, respectively, less than the punching shear strength calculated from the actual critical section.

The simple hand calculation of the bearing and punching shear stress predicted the behavior accurately for the bearing strength. The punching shear behavior seen in the system was more complex than the ACI methodology takes into account. An important variable, the horizontal force from the front hanger leg of the Meadow/Burke hanger, was not taken into account for the calculation of the punching shear strength. However, if the punching shear strength is calculated by the actual critical section, a better prediction of the

Dayton/Richmond is observed. Therefore, the ACI approach inaccurately predicted punching shear if the actual critical section was or was not applied.

5.7 Summary

The three major parameters affected the behavior of the overhang falsework hanger system in the terms of ultimate strength and the stiffness: the girder shear reinforcement level, effect of adjacent loaded hanger, and the type of hanger. To fully understand the behavior, the finite element modeling method and ACI approach was applied to capture the results from each experimental test.

Based on the discussions and comparisons mentioned in this section, the observations, recommendations, and a summary of this research are presented in the next section. The observation from the experimental and analytical investigations leads to the recommendation for field applications and future research, and the conclusions of this research are made.

6.0 RECOMMENDATIONS AND CONCLUSIONS

This section discusses several observations from the experimental and analytical investigations and recommendations for the field application and future research. The conclusions of the experimental test program and analytical results are discussed herein.

6.1 Observations

6.1.1 Experimental observations

From the relationship of applied hanger load and mid-span deflection, the mid-span deflection of the test performed in the high shear reinforcement region was less than the one of that tested in the light shear reinforcement region. The shear reinforcement not only stiffened the overall behavior but also limited the shape of the crack pattern. From the Meadow/Burke hanger testing results, it was observed that the cracks propagated wider in the light shear reinforcement region test than in the one with high shear reinforcement.

When two or four hangers were loaded at the same time, the deflection at mid-span was larger than when a single hanger was loaded. The crack patterns for the multiple hanger loaded test were similar to the single hanger loaded test for the same type of hanger. The cracks at each of the tested hangers did not intersect. For the Meadow/Burke hanger test, a reduction in the ultimate load was not observed between the one and two hanger test results. However, for the four-hanger test, a reduction of 11% was observed in comparison to the single hanger test.

While the only major geometric difference between the Dayton/Richmond and Meadow/Burke hangers was the front leg which embedded into the concrete flange right behind the hanger head, many different behavior types were observed. First of all, at ultimate load, a large amount of rotation of the hanger head was observed in the Dayton/Richmond hanger test, while a small amount of rotation of the hanger head was observed for the Meadow/Burke hanger test. In terms of failure mode, there were two different types, punching shear and local concrete bearing underneath the hanger head. The punching shear failure was consistently observed for all of the Meadow/Burke hanger tests, and local concrete bearing was observed for the Dayton/Richmond hangers. Finally, the observed ultimate loads of Dayton/Richmond hanger tests were higher than the one of Meadow/Burke hanger test by approximately 42%.

The maximum torque applied to the MBT girder during the test program (four hanger test) was approximately 25% of the cracking torque as calculated in accordance with ACI specification. This is notable because the current NCDOT practice often requires additional measures to improve the torsional resistance of the MBT girders.

6.1.2 Analytical observations

For the large finite element models, it was observed that the initial stiffness of the applied hanger load and the relative deflection of the model were close to the single hanger experimental results but higher than the results from the multiple hanger test. The finite element models predicted higher ultimate loads than those observed in the experimental results. The finite element models predicted flexural and punching shear failure for the Dayton/Richmond and Meadow/Burke model, respectively. When multiple hanger loading was considered, the ultimate loads predicted by the models decreased for the Meadow/Burke model.

From the small finite element models, a more accurate prediction of the specimen stiffness was observed. However, after formation of cracks in the concrete, the flange model predicted more mid-span deflection than observed in the experimental tests. At the ultimate load, the Dayton/Richmond model predicted flexural failure of the girder flange and the Meadow/Burke model predicted punching shear failure underneath the hanger head.

6.2 Recommendations

Based on the experimental test results, it is recommended that the safe working load of the Dayton/Richmond and Meadow/Burke 45 degree overhang hangers be reduced. For the thin flange MBT girders, the use of different type of overhang hanger system such as through flange hanger appears to be necessary to support the 12,000 lb. ultimate load required for a 6,000 lb. safe working load utilizing a factor of safety of 2 to1.

To improve the strength of the girder-hanger system, the following recommendations are suggested. From the modified Dayton/Richmond hanger model mentioned in Section 5, using a bearing plate under the hanger head to distribute the load may increase the load carrying capacity, see Figure 6.1. For the Meadow/Burke hanger, a modification of the front leg by extending it further back into the girder to an area of reinforced concrete may increase the load carrying capacity, see Figure 6.2. In terms of the girder, the addition of another reinforcing bar along the edge of the girder flange may increase the strength of the girder flange.

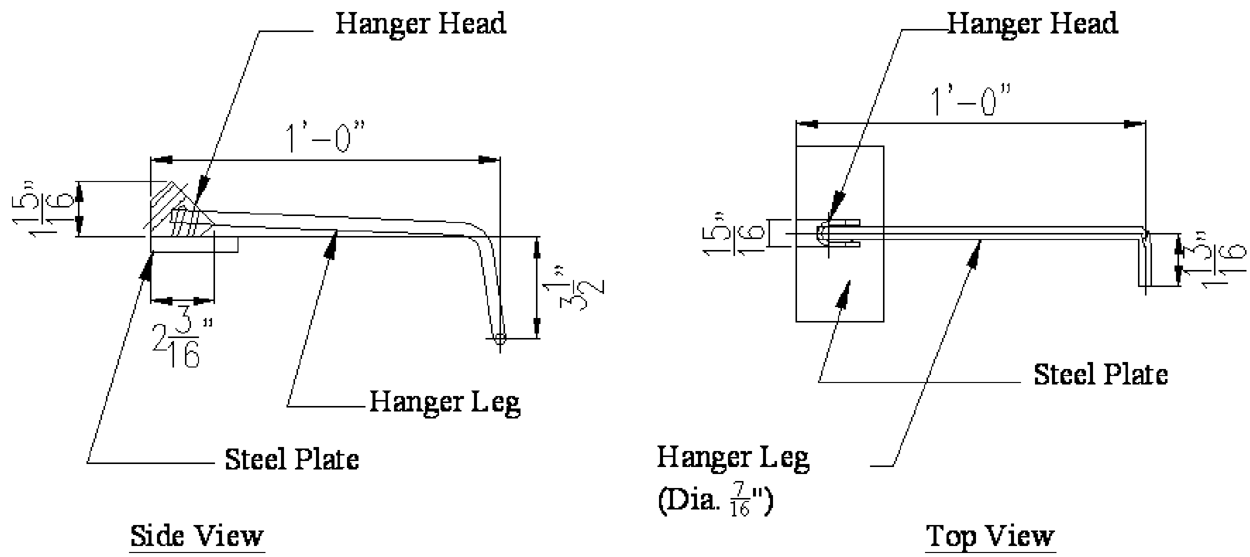

Figure 6.1 Potential Modification of the Dayton/Richmond hanger

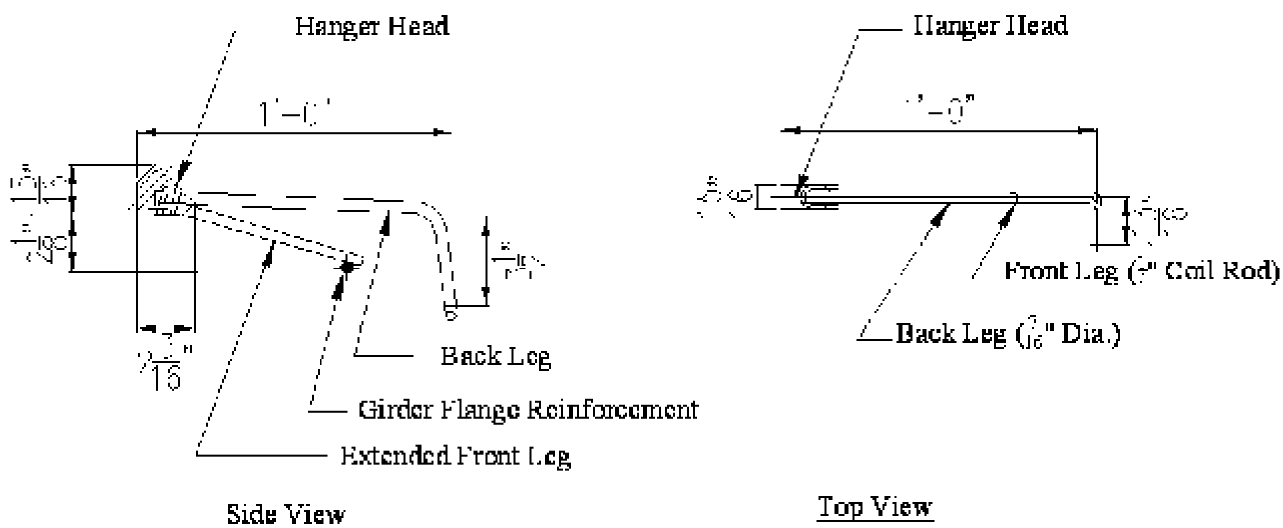

Figure 6.2 Potential Modification of the Meadow/burke hanger

6.3 Conclusions

From the experimental, analytical investigation and the observation mentioned above, the conclusions of the falsework hanger system are summarized herein:

- The girder shear reinforcement affects the ultimate strength and behavior of the falsework hanger system.

- The front leg on the Meadow/Burke hanger reduces the rotation of the hanger head. However, it induces the punching shear failure to the girder flange.
- The observed ultimate loads of the Dayton/Richmond hanger tests are higher than the loads observed in the Meadow/Burke hanger tests. However, the observed ultimate loads were all less than the manufacturer's specified ultimate load of 12,000 lbs.
- The failure of hanger head for Dayton/Richmond hanger occurs because the rotation of hanger head. The bearing failure of Dayton/Richmond hanger test causes the excessive rotation of hanger head.
- The small finite element models predict the behavior of Dayton/Richmond hanger behavior more accurately than that of the large finite element model.
- The finite element models were unable to capture the crushing of concrete of the Dayton/Richmond hanger
- The punching shear failure of Meadow/Burke hanger test can be captured by using the large or small model.

6.4 Summary

The main purposes of this research are to verify the strength of the 45-degree overhang falsework hanger on the NCDOT modified bulb tee (MBT) girder and create a finite element model to predict the behavior of the falsework hanger system. The experimental program was created to find the strength of the hanger while simulating the field conditions. The finite element models were used to predict the experimental testing results in the terms of the response and limit states.

It is recommended that the safe working load of the Dayton/Richmond and Meadow/Burke falsework hanger embedded on the NCDOT modified bulb tee (MBT) girder be reduced. The large finite element models did not accurately capture the response of the system. On the other hand, the small finite element model used in this research did capture the response as observed in the experimental investigation.

7.0 References

ACI (1995), *"Form work for concrete," ACI committee* 347, American concrete Institute, Michigan.

ACI (2002), *"Building Code Requirements for Structural Concrete and Commentary" ACI committee* 318, American concrete Institute, Michigan.

AISC (2003), *Manual of Steel Construction; Load and resistance Factor Design 3rd Edition,* American Institute of Steel Construction, Chicago, IL.

ANACAP user's manual (2004), ANATECH Corp.

Bortolotti, L. (2003). "Strength of Concrete Subjected to Pullout Load," *Journal* of *Materials in Civil Engineering,* ASCE, September/October, 491-495.

Chu, K.H., Johnson, RB. (1974). "Torsion in Beams with Open Sections," *Journal* of *Structural Engineering,* ASCE, 100(7), 1397-1419.

Dayton Superior (2004), "Concrete Prestressing Products Hand Book,"

Evick, D.R, Heins, C.P. (1972). "Torsion of Nonprismatic Beams of Open Section," *Journal* of *Structural Engineering,* ASCE, 98(12), 2769-2784.

Hasnat, A, Akhtaruzzaman, Wafa, F.F. (1993). "Prestressed Beams with Openings and No Stirrups under Torsion and Bending," *Journal* of *Structural Engineering,* ASCE, 119(10),1280-1286.

Henry, RL., Zia, P. (1974). "Prestressed Beams in Torsion, Bending, and Shear," *Journal* of *Structural Engineerin*g,, ASCE, 99(11), 2229-2244.

MacGregor, J.G. (1992). *"Reinforced concrete' mechanics and design,", 3rd ed.,* Prentice Hall Inc., New Jersey.

Magdi, M., Farhood, N. (2003). "Exact Finite Element for Nonuniform Torsion of Open Sections," *Journal* of *Structure Engineering,* ASCE, 123(2), 215-223.

Martin, L.H., Wainwright, P.J. (1973). "Torsion and Bending of Prestressed Concrete Beams," *Journal* of *Structural Engineering g,* ASCE, 100(5), 933-952.

Loo, Y.C., Guan, H. (1997). "Cracking and Punching Shear Failure Analysis of RC Flat Plates," *Journal* of *Structural Engineering,* ASCE, 123(10), 1321-1330.

Nawy, E.G. (2003). *"Prestressed Concrete* :a *Fundamental Approach-4th ed.,"* Prentice Hall Inc., New Jersey.

Shehab, M. (1997). "Resistance Factors for Blind Bolts in Direct Tension," *Journal* of *Structure Engineering,* Elsevier Science Ltd., 19(12),995-1000.

Tarek, E., John, B.K. (1996). "Punching Strength of Deck Slabs in Skew Composite Bridges," *Journal* of *Bridge Engineering,* ASCE, 1 (5),59-65.

Wafa, F.F., Shihata, S.A, Ashour, S.A, Akhtaruzzaman, AA (1995). "Prestressed High-Strength concrete Beams under Torsion," *Journal of Structural Engineering,* ASCE, 121(9), 1280-1286.

Warwaruk, J., Mukherjee, P.R. (1971), "Torsion, Bending, and Shear in Prestressed Concrete," *Journal of Structural Engineering,* ASCE, 97(4),1063-1079.

Woodhead, HR., McMullen AE. (1974). "Torsional Strength of Prestressed Concrete Beams," *Journal Structural Engineering,* ASCE, 100(5),881-900.

Appendix A-Test Setup Details

<u>Girder Details</u>

Girder Information:

Area	814 in^2
Neutral Axis	30.8 in. from bottom flange

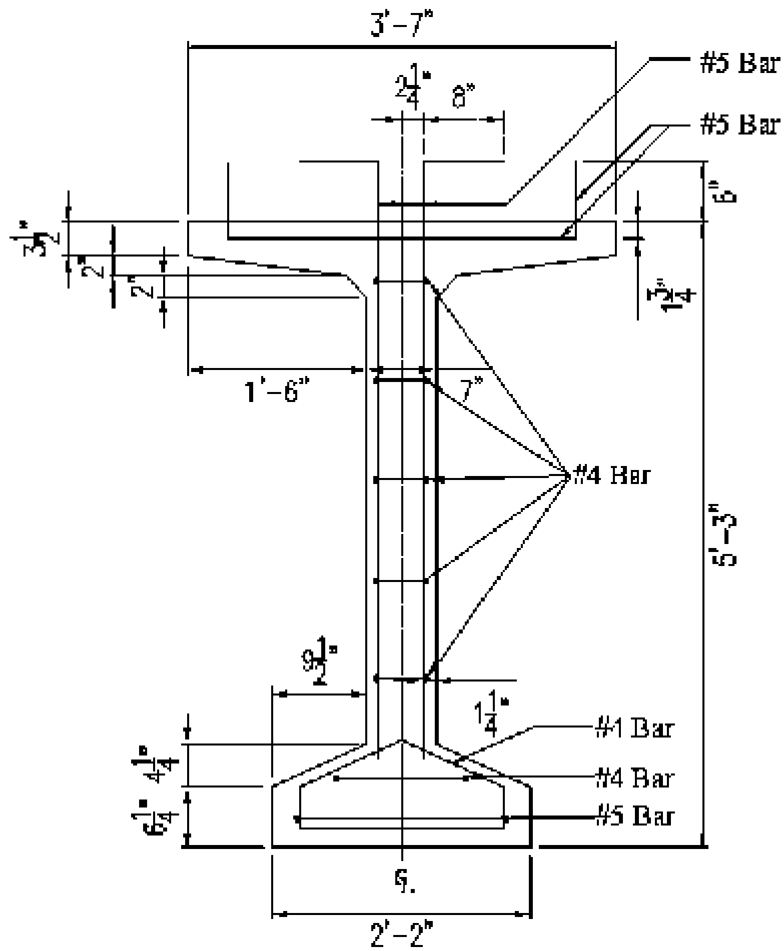

NCDOT Modified Bulb Tee Girder cross-section

Strand details

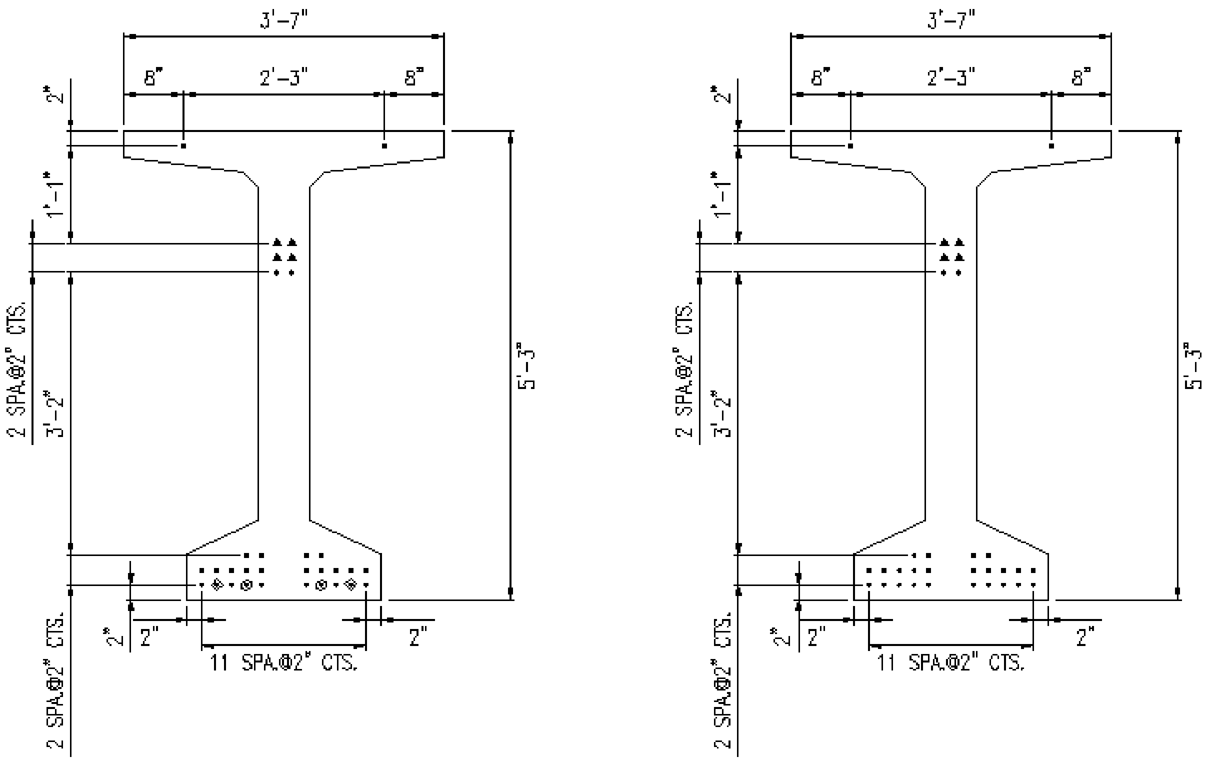

Debonding Legend

- Strands Bebonded For 4'-0" From End of Girder
- Strands Bebonded For 12'-0" From End of Girder
- Strands Bebonded For 22'-0" From End of Girder
- Fully Bonded Strands

HSS-Frame

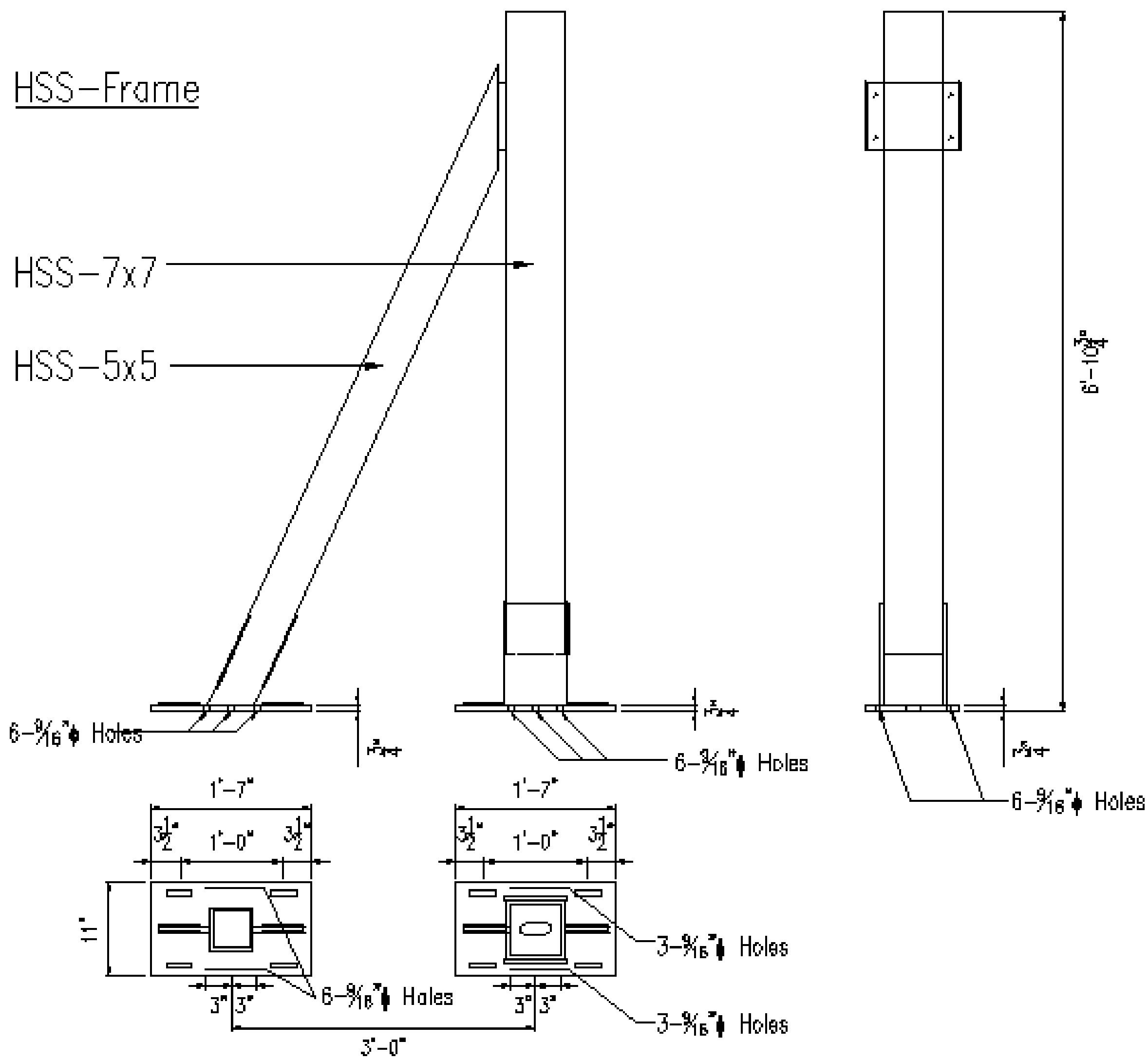
HSS–Frame
HSS–7x7
HSS–5x5
6–9/16"ϕ Holes
6–9/16"ϕ Holes
6–9/16"ϕ Holes
6'–10 3/4"
1'–7"
1'–7"
3 1/2"
1'–0"
3 1/2"
3 1/2"
1'–0"
3 1/2"
11"
3"
3"
6–9/16"ϕ Holes
3"
3"
3–9/16"ϕ Holes
3–9/16"ϕ Holes
3'–0"

Jack Mounting Bracket

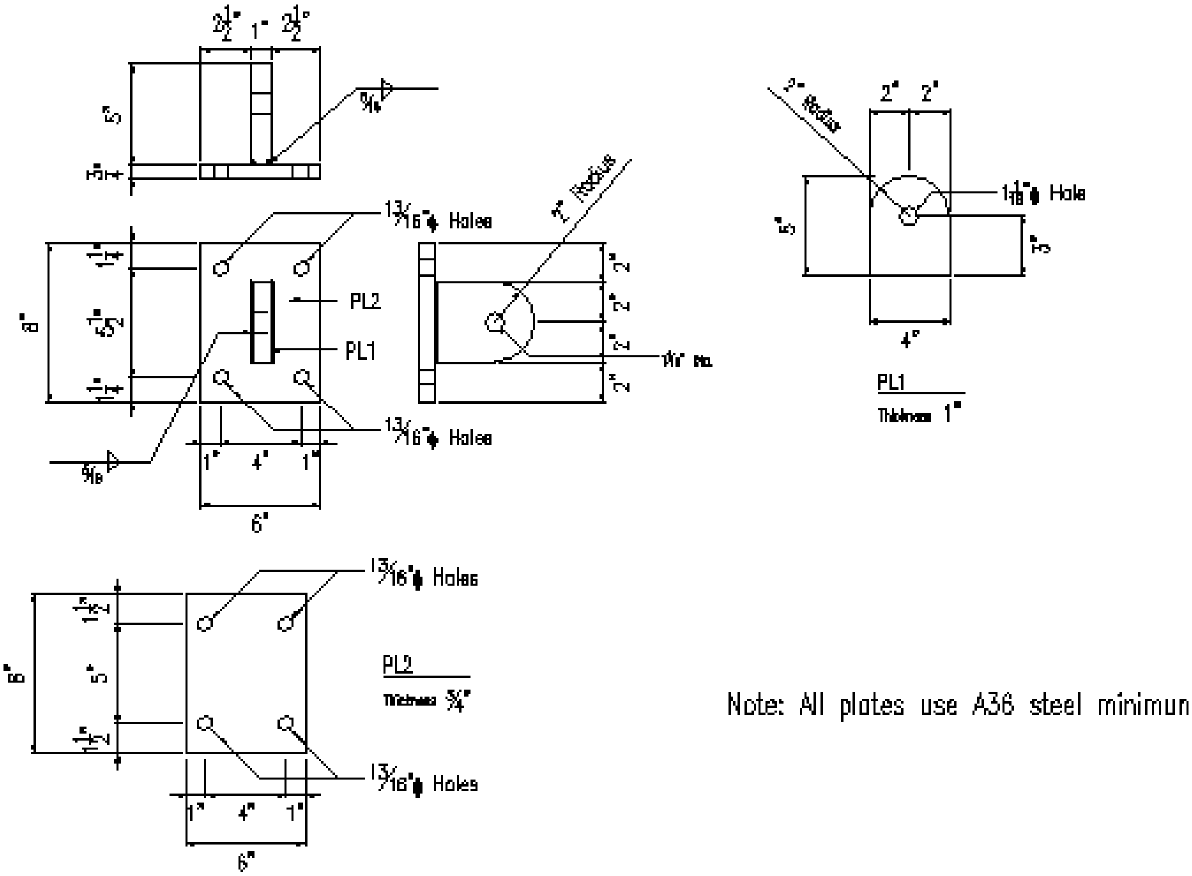

JACK MOUNTING BRACKET

Loading Beam

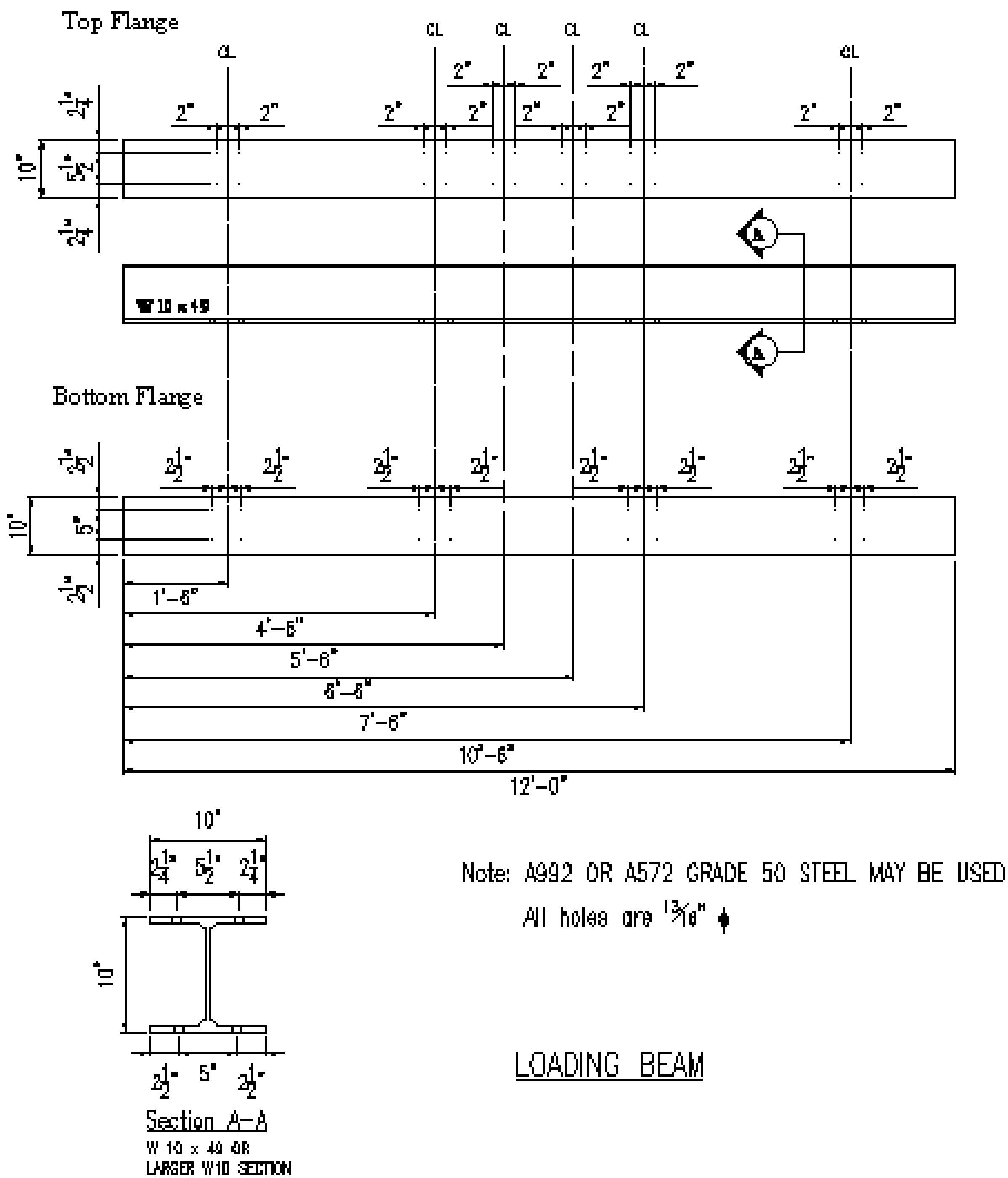

Beam Mounting Bracket

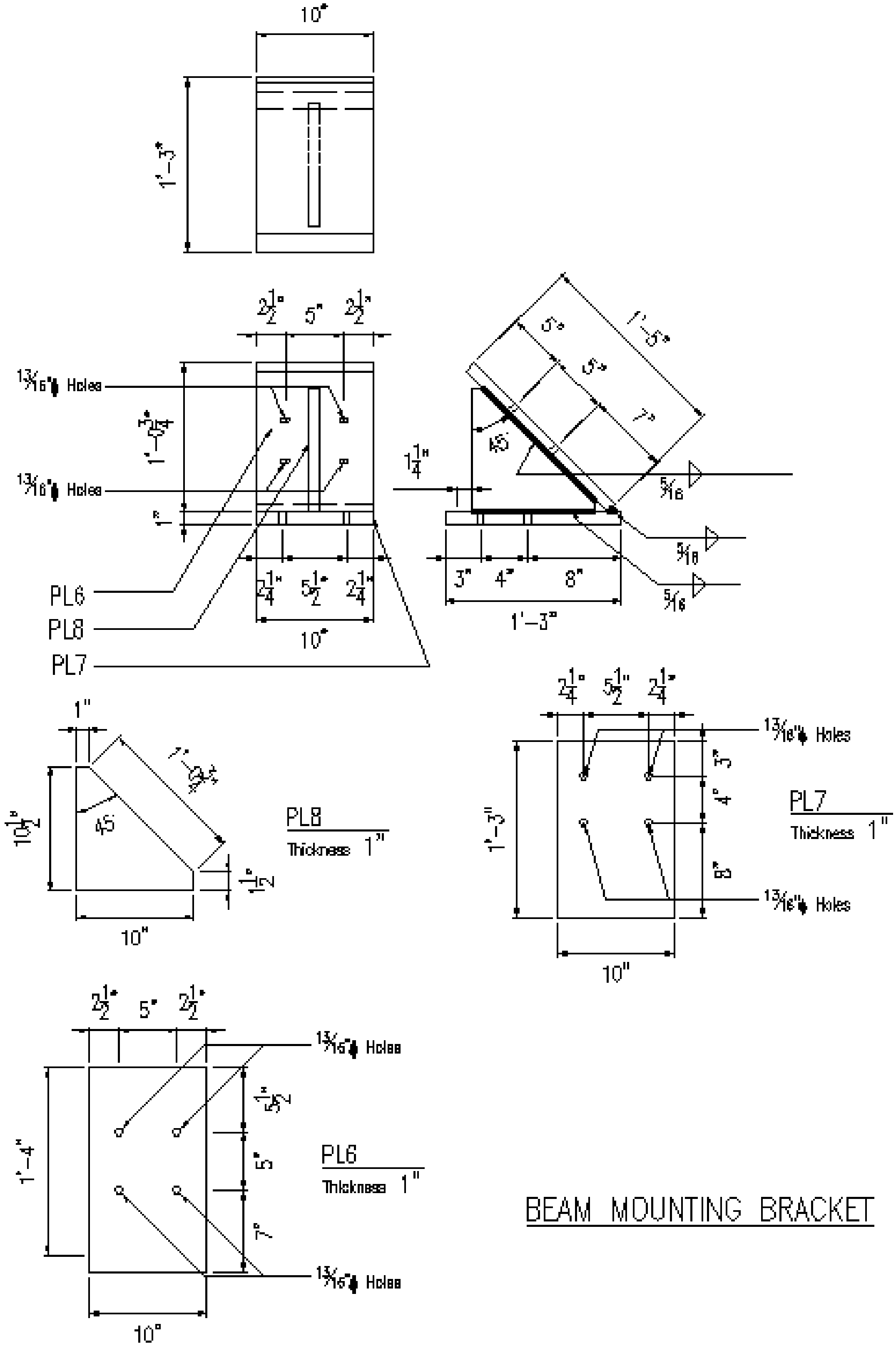

Appendix B Hanger Test Summary Sheet

Test ID:	DR-1-H (Dayton Hanger, Single Pull, High Reinforcement)
Test Date:	September 19, 2005
Sponsor:	NCDOT
Tested By:	Emmett Sumner, Ph. D., P.E. and Donlawit Ariyasajjakorn, E.I.
Test Location:	Constructed Facilities Laboratory (CFL), NC State University

Test Description

Dayton/Richmond hanger, Single hanger pulled by 45 degree angle at the end of girder (high shear reinforcement).

Hanger: Dayton/Richmond hanger C-24-4-APR

Coil Rod: ½ in. Meadow/Burke Coil Rod, 9000 lb. Safe Working Load

Girder: NCDOT Modified Bulb Tee 63 in.
Concrete Cylinder Strength = 7500 psi

Experimental Results

Maximum Applied Load	= 9200 lb
Maximum Flange Vertical Displacement at Center Line of Test Set Up	= 0.0732 in.
Maximum Flange Vertical Deflection at Hanger	= 0.0259 in.
Maximum Girder Rotation at Center Line of Test Set Up	= 0.0031 rad
Maximum Girder Vertical Displacement at Center Line of Test Set Up	= 0.0133 in.

Test observations:

At 3600 lb,	first crack was observed at the concrete back of hanger head.
At 5000 lb,	crack propagated form back side of hanger to the edge of flange
At 6000 lb,	crack propagated around hanger area.
At 6500 lb,	large amount of hanger rotation was observed.
At 7500 lb,	spalling of concrete occurred at the edge of flange under hanger. This result is allowed the hanger to rotate.
At 9200 lb,	Failure occurred when hanger rotated and embedded in top flange of girder. The rotation caused hanger leg rupture by producing high bending stress in hanger leg.

Test#1 DR-1-H

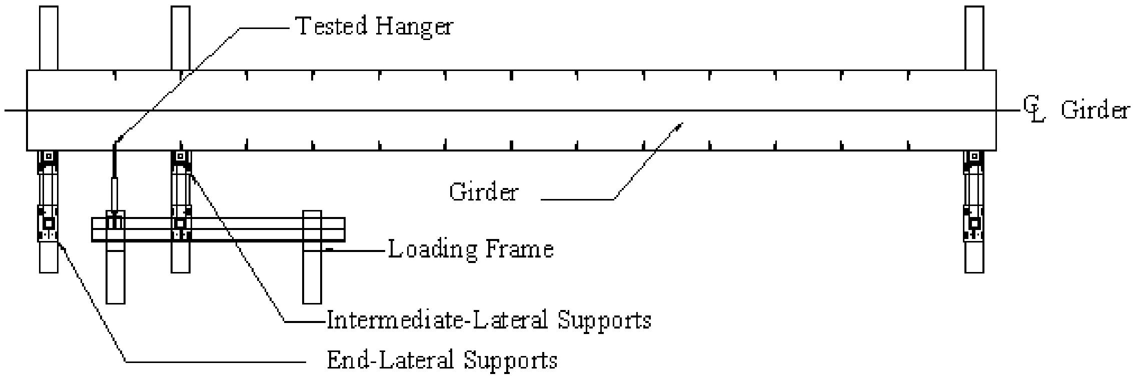

Plan View of Tested Hanger Position

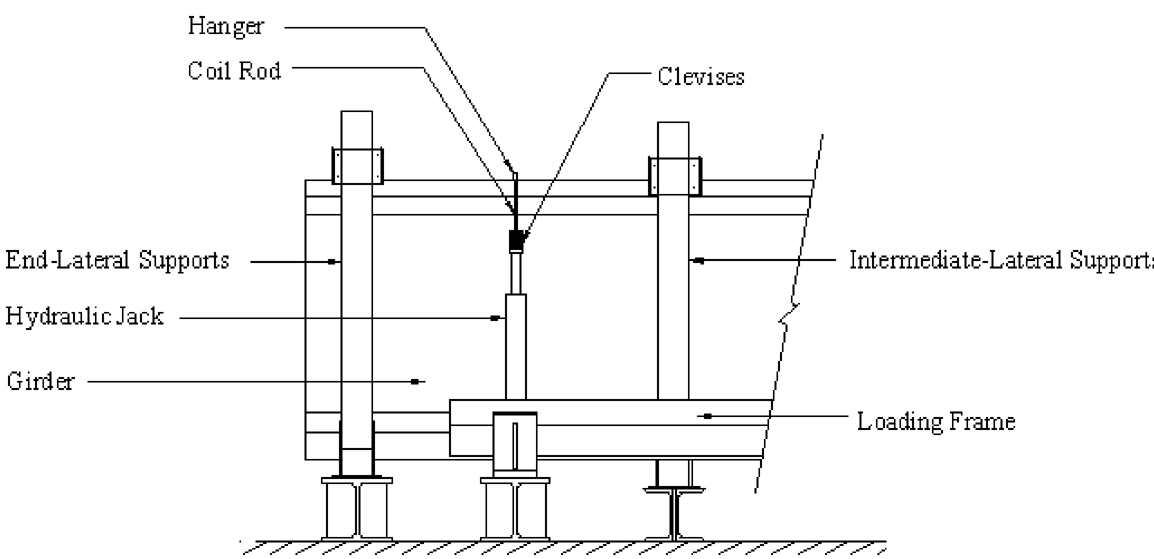

DR-1-H   Elevation of Test Set Up

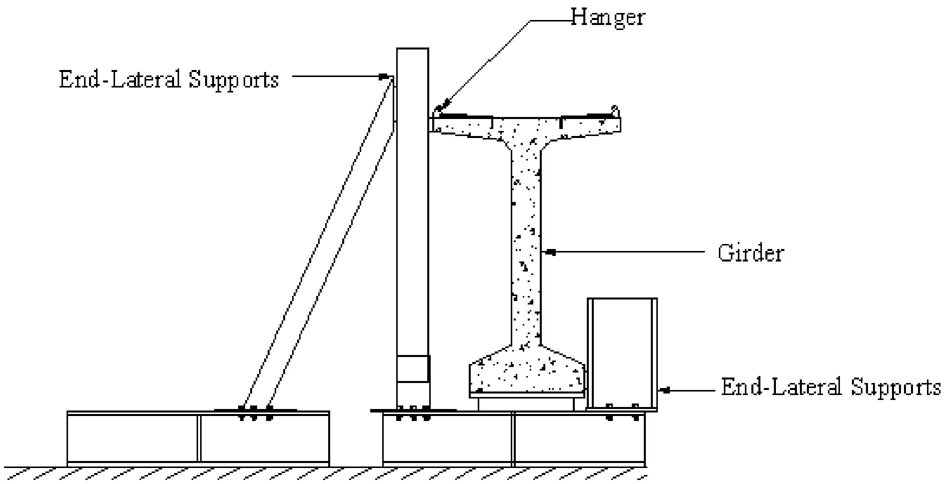

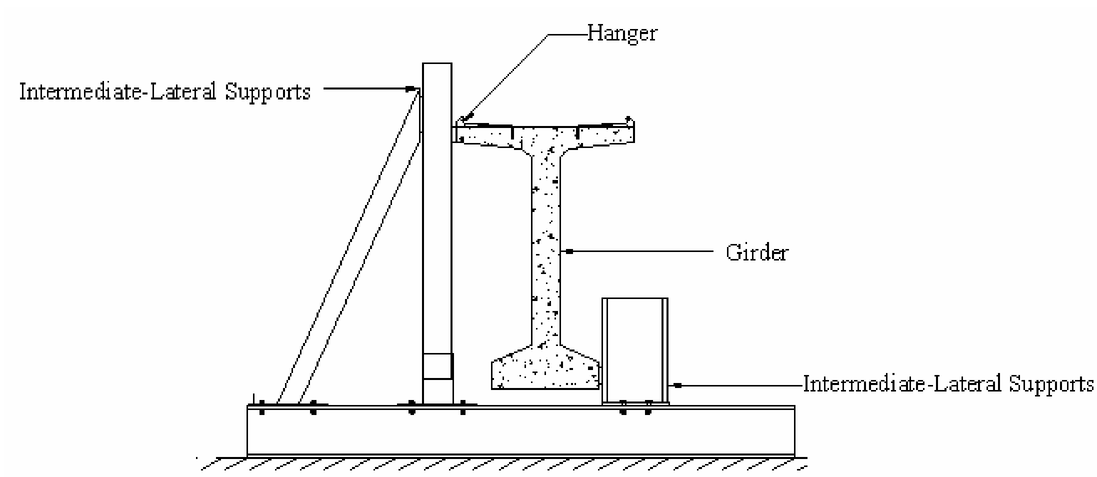

DR-1-H Cross Section at End-Support

DR-1-H Cross Section at Intermediate-Lateral Support

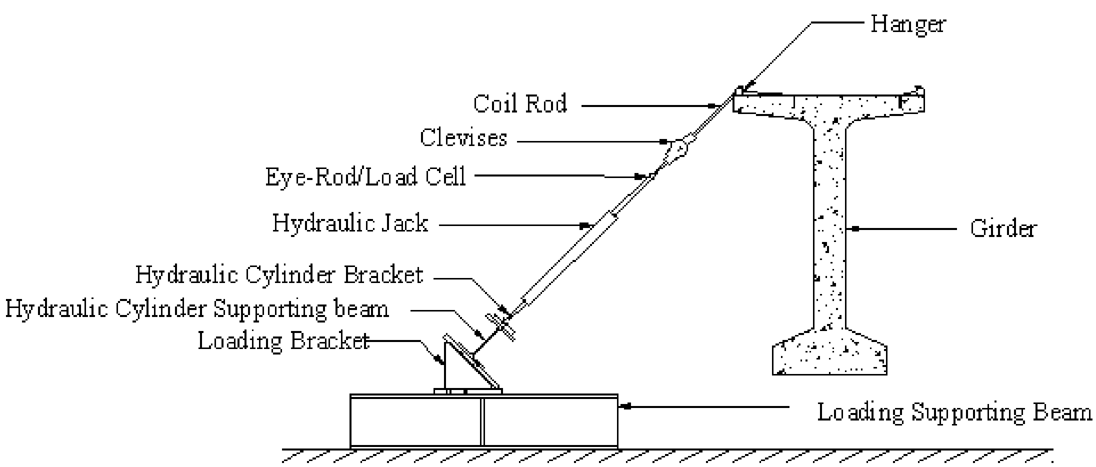

DR-1-H Cross Section at Loading Frame

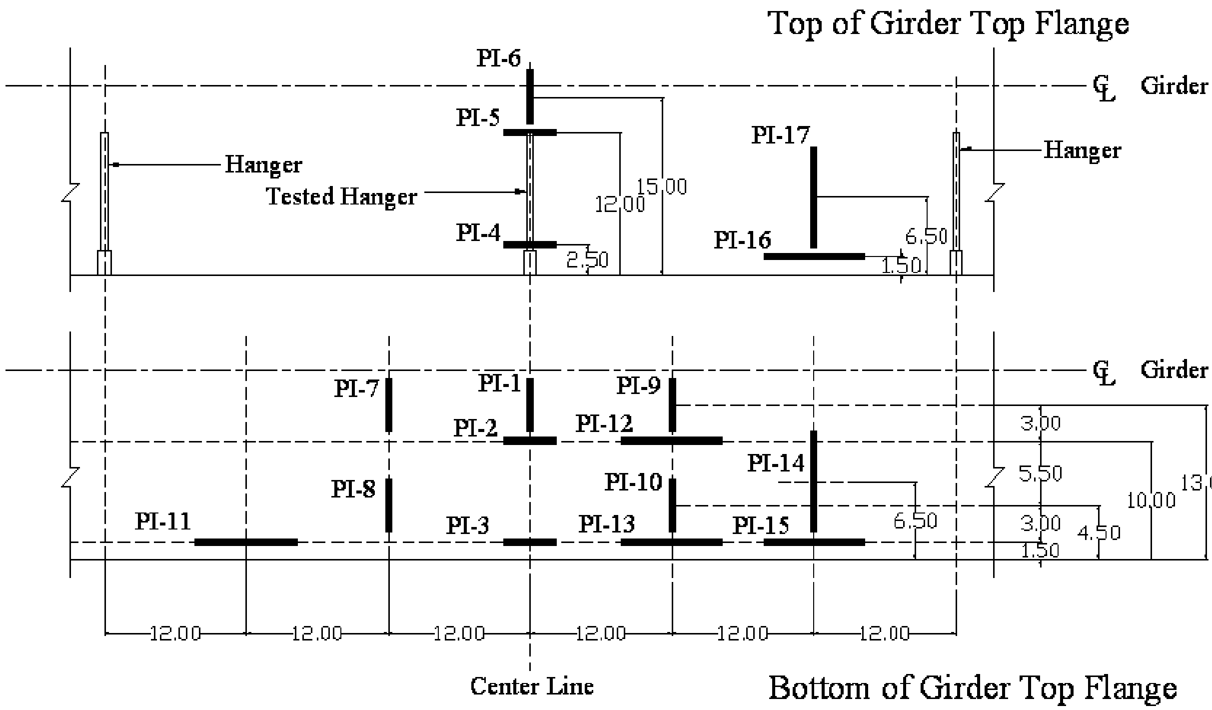

DR-1-H Instrumentation – PI-Gauge Assignment

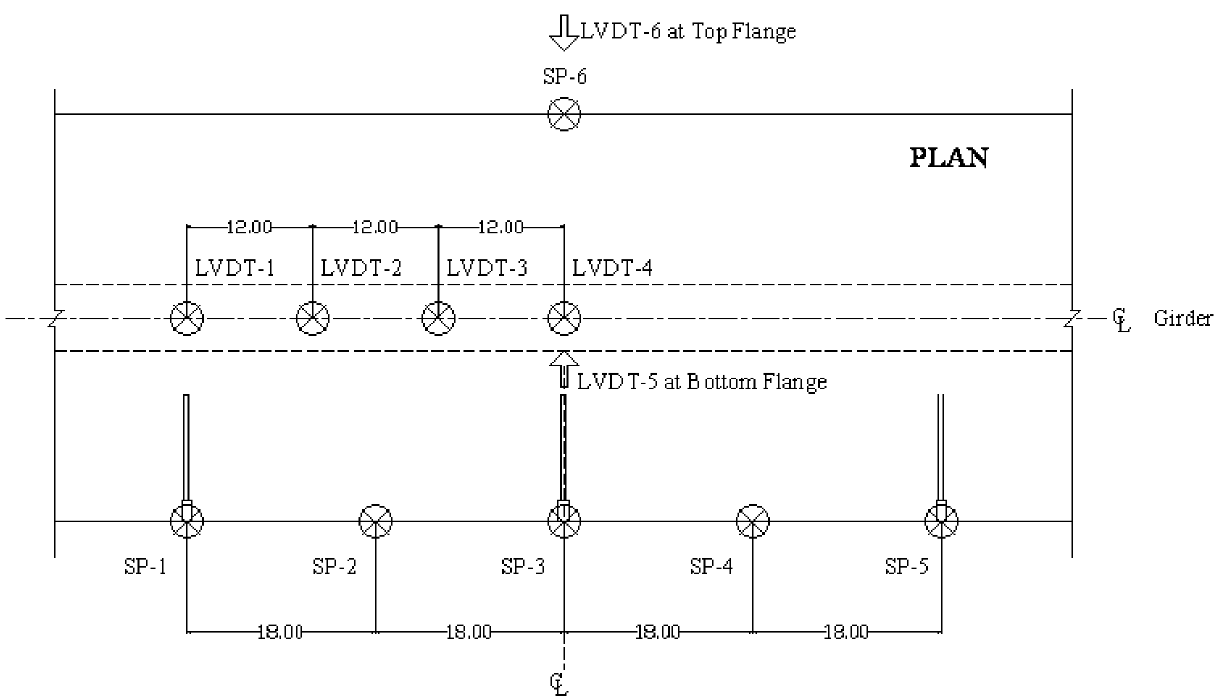

DR-1-H Instrumentation – Linear and String Pot Assignment

DR-1-H Overall Test Set Up

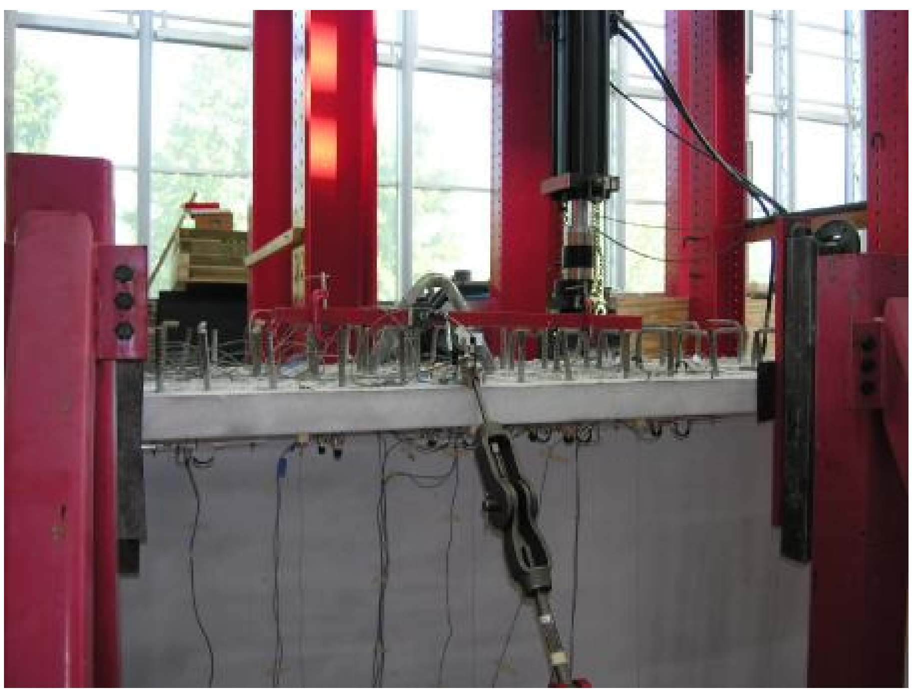

DR-1-H Overall Test Set Up

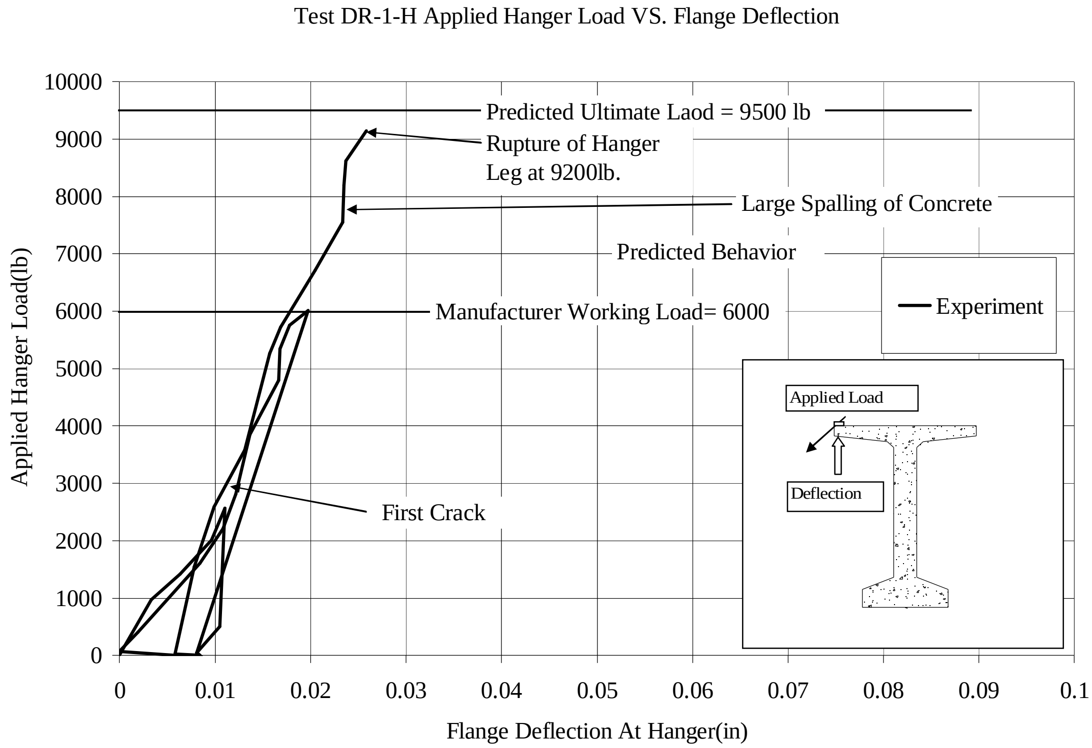

DR-1-H Deflection at Center Line

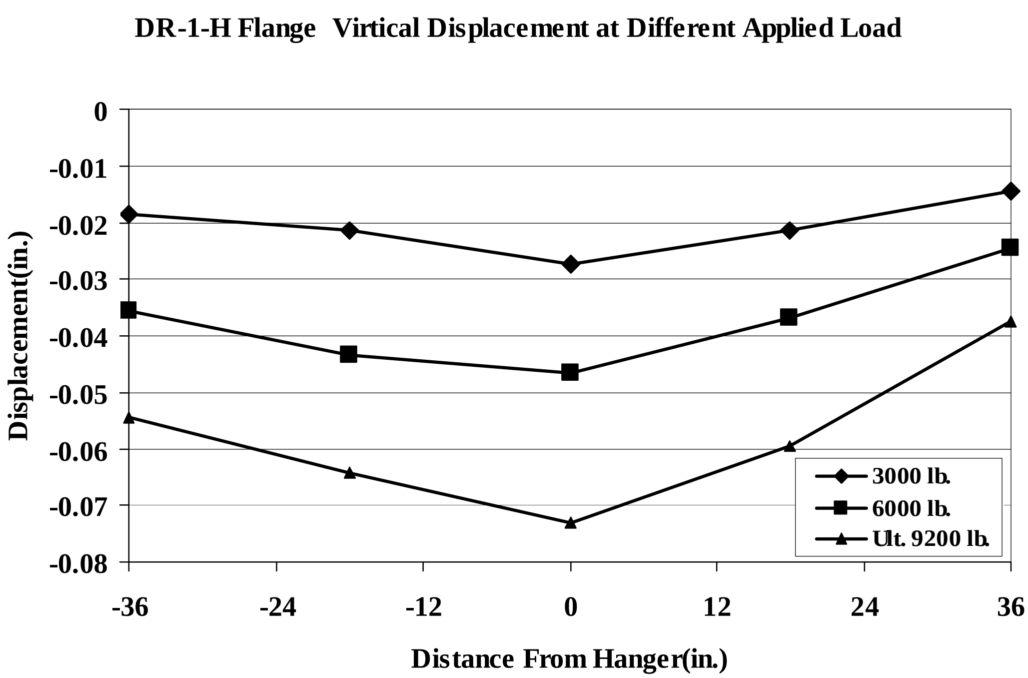

DR-1-H Vertical Displacement at Different Applied Load

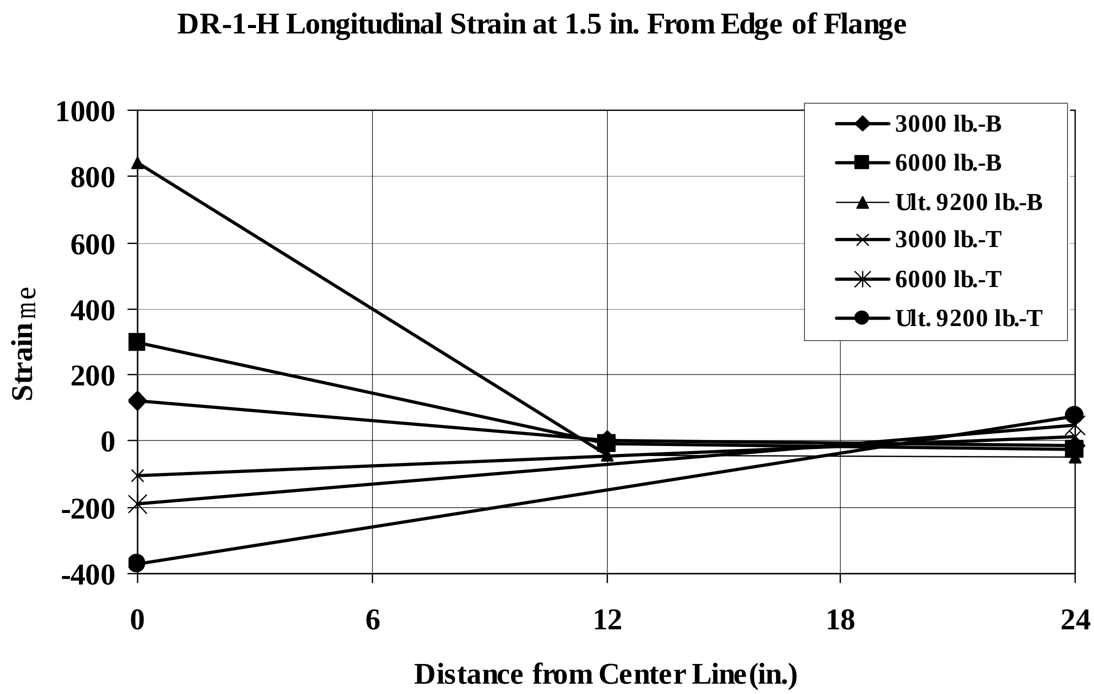

DR-1-H Longitudinal Strain from Top and Bottom along Edge of Flange

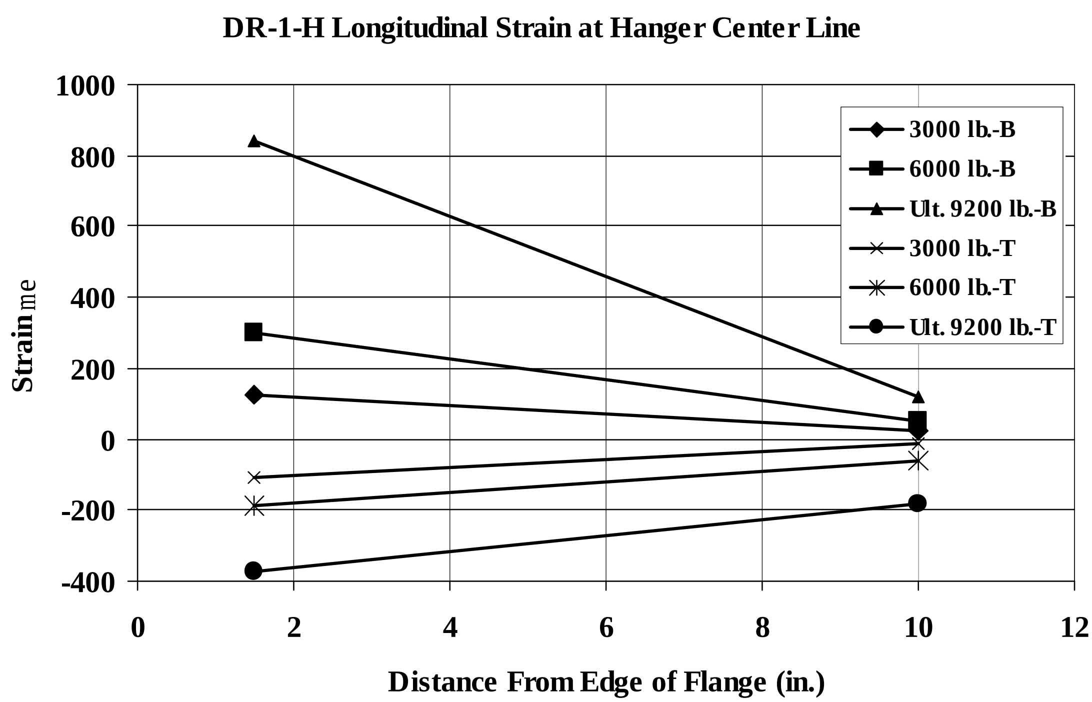

DR-1-H Longitudinal Strain from Top and Bottom at Center Line

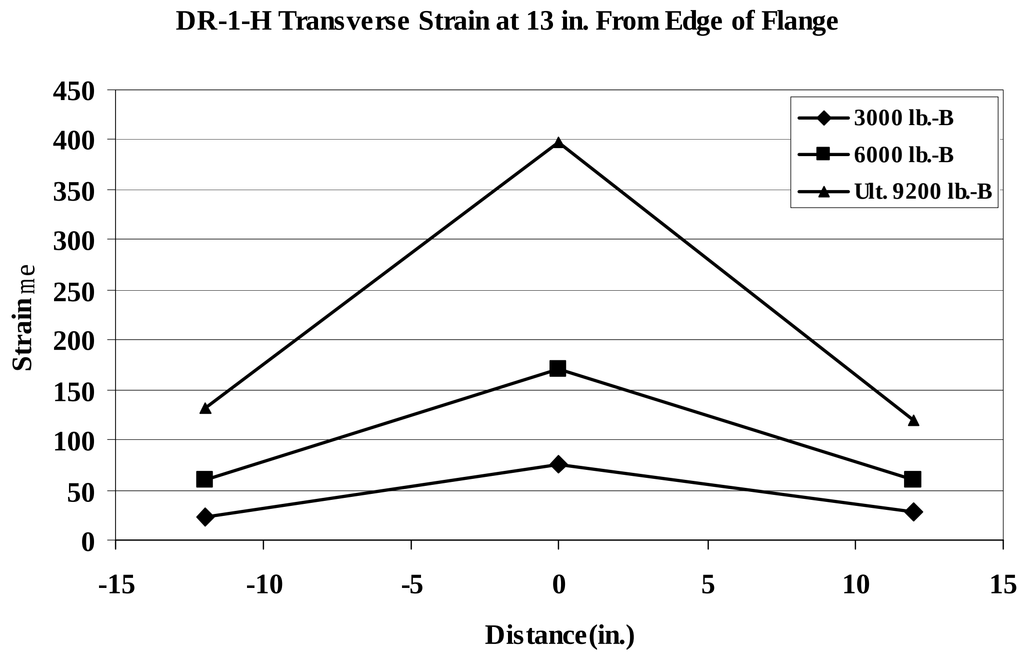

DR-1-H Longitudinal Strain at 13 in. from Edge of Flange

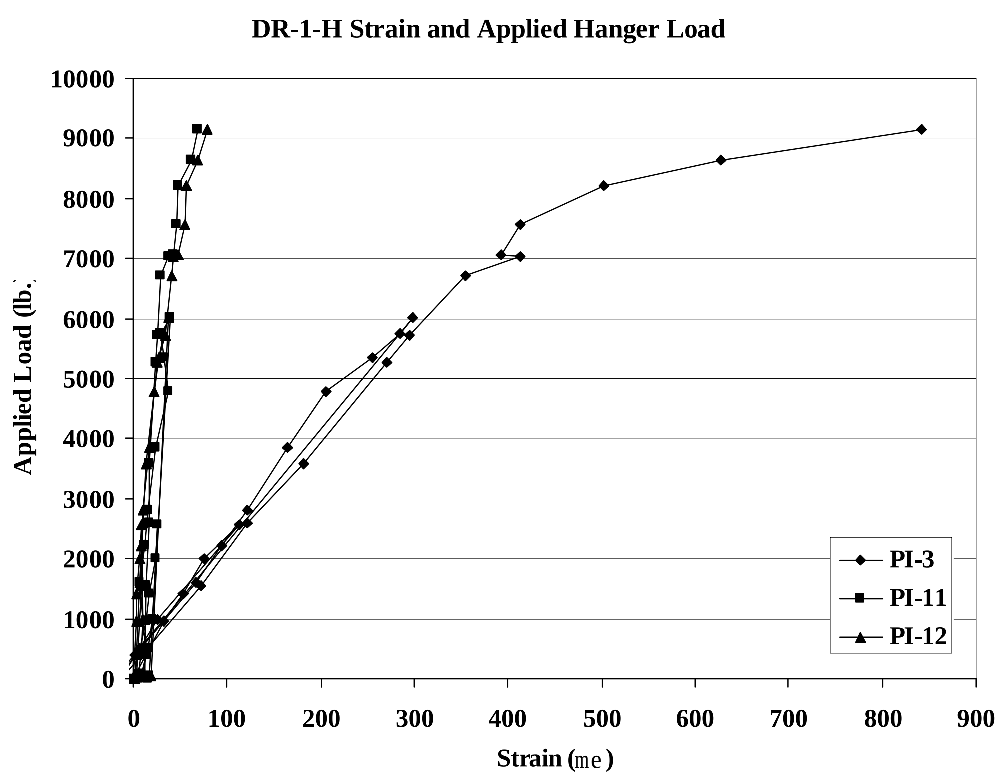

DR-1-H Longitudinal Strain at 1.5 in. from Edge of Flange

DR-1-H Failure-Rotation of Hanger Head

DR-1-H Bar Rupture Failure at Hanger Leg

Appendix C Hanger Test Summary Sheet

Test ID: DR-1-L (Dayton Hanger, Single Pull, Light Reinforcement)
Test Date: September 22, 2005
Sponsor: NCDOT
Tested By : Emmett Sumner, Ph. D., P.E. and Donlawit Ariyasajjakorn, E.I.
Test Location: Constructed Facilities Laboratory (CFL), NC State University

Test Description

Dayton/Richmond hanger, Single hanger pulled by 45 degree angle at the middle of girder (Light shear reinforcement).

Hanger: Dayton/Richmond hanger C-24-4-APR

Coil Rod: ½ in. Meadow/Burke Coil Rod, 9000 lb. Safe Working Load

Girder: NCDOT Modified Bulb Tee 63 in.
Concrete Cylinder Strength = 7500 psi

Experimental Results

Maximum Applied Load	= 9200 lb
Maximum Flange Vertical Displacement at Center Line of Test Set Up	= 0.0726 in.
Maximum Flange Vertical Deflection at hanger	= 0.0474 in.
Maximum Girder Rotation at Center Line of Test Set Up	= 0.0029 rad
Maximum Girder Vertical Displacement at Center Line of Test Set Up	= 0.0180 in.

Test observations:

At 3000 lb,	back side of hanger started lifting up
At 3700 lb,	first crack be found both sides of hanger
At 4500 lb,	crack propagated form back side of hanger to the edge of flange.
At 6100 lb,	large amount of hanger rotation found.
At 7000 lb,	spalling of concrete occurred at the edge of flange under hanger. This result is allowed the hanger to rotate.
At 9200 lb,	Failure occurred when hanger rotated and embedded in top flange of girder. This caused weld between hanger leg and head rupture.

Test#2 DR-1-L

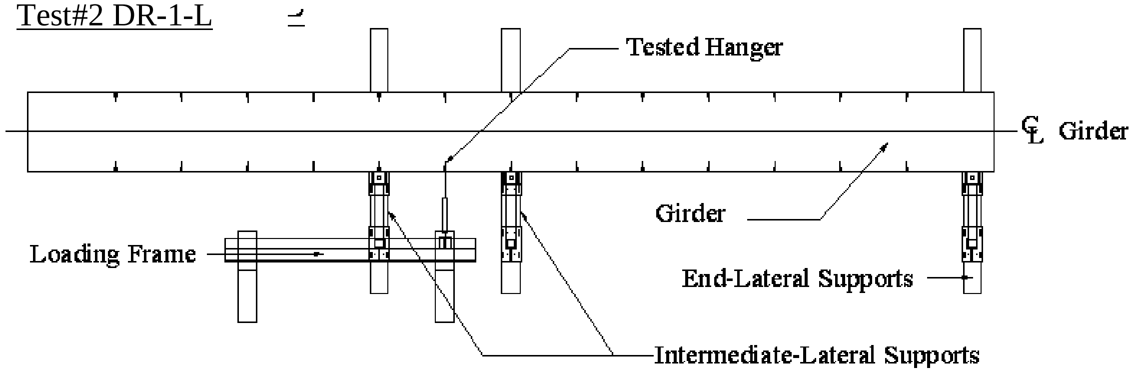

Plan View of Tested Hanger Position

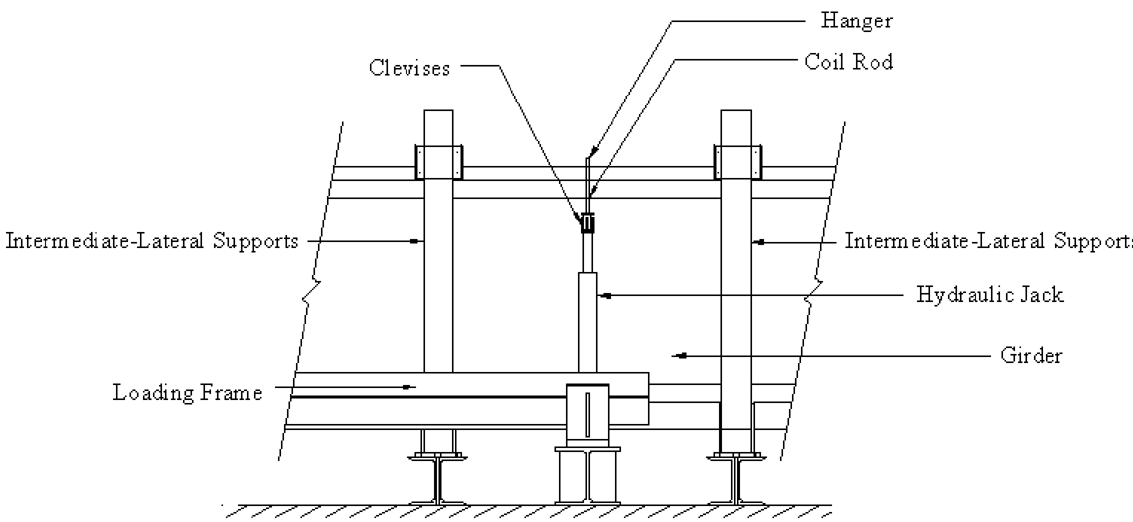

DR-1-L Test Set Up Elevation

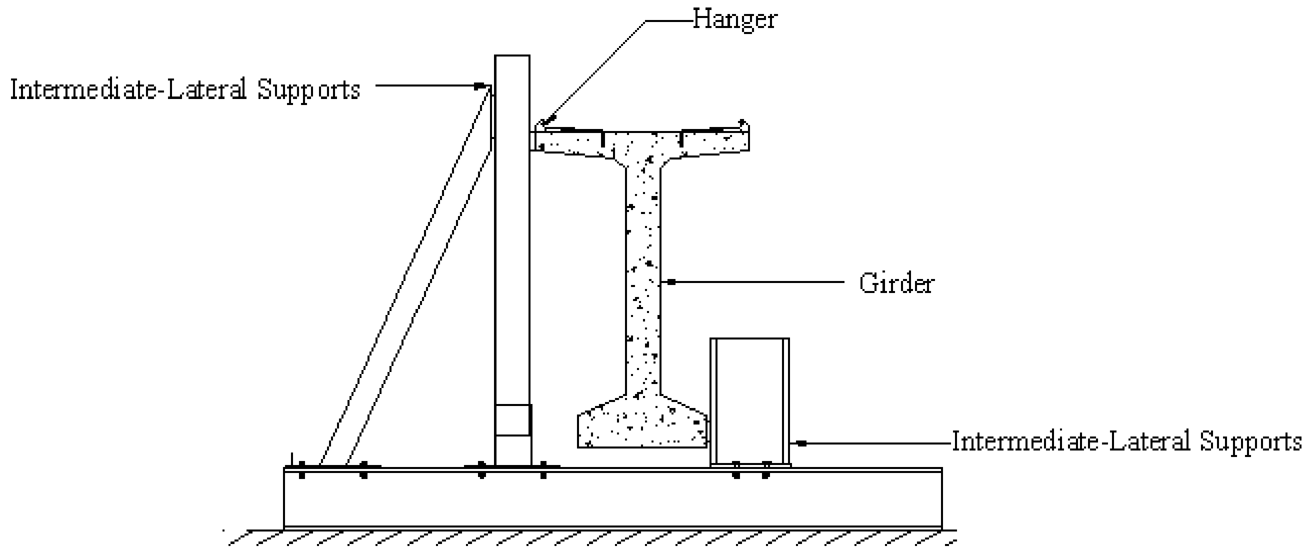

DR-1-L Cross Section at Intermediate-Lateral Support

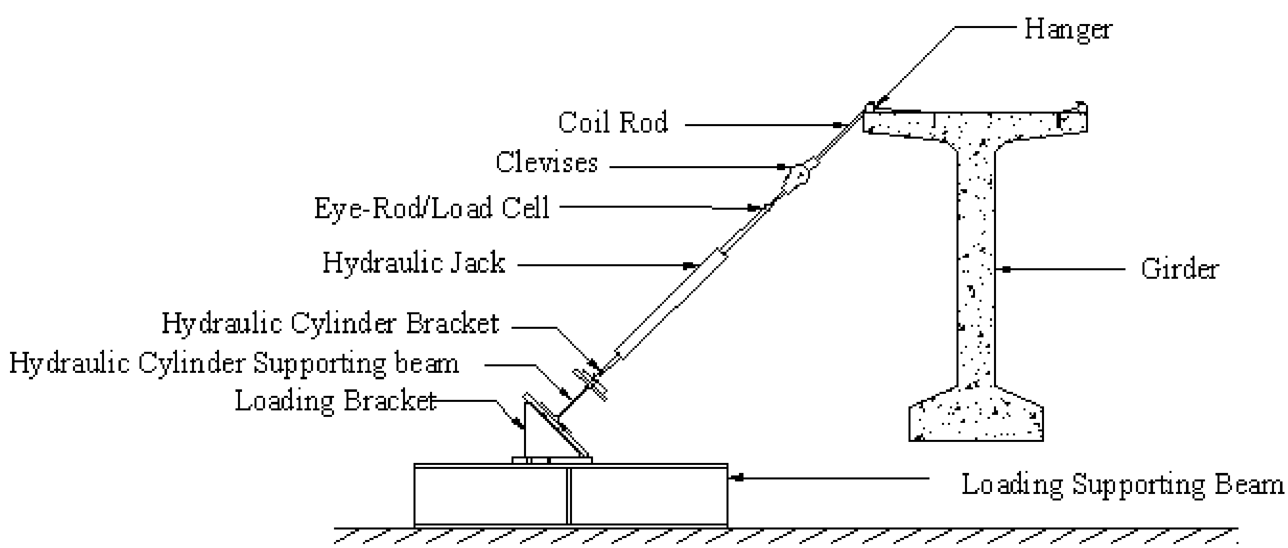

DR-1-L   Cross Section at Loading Frame

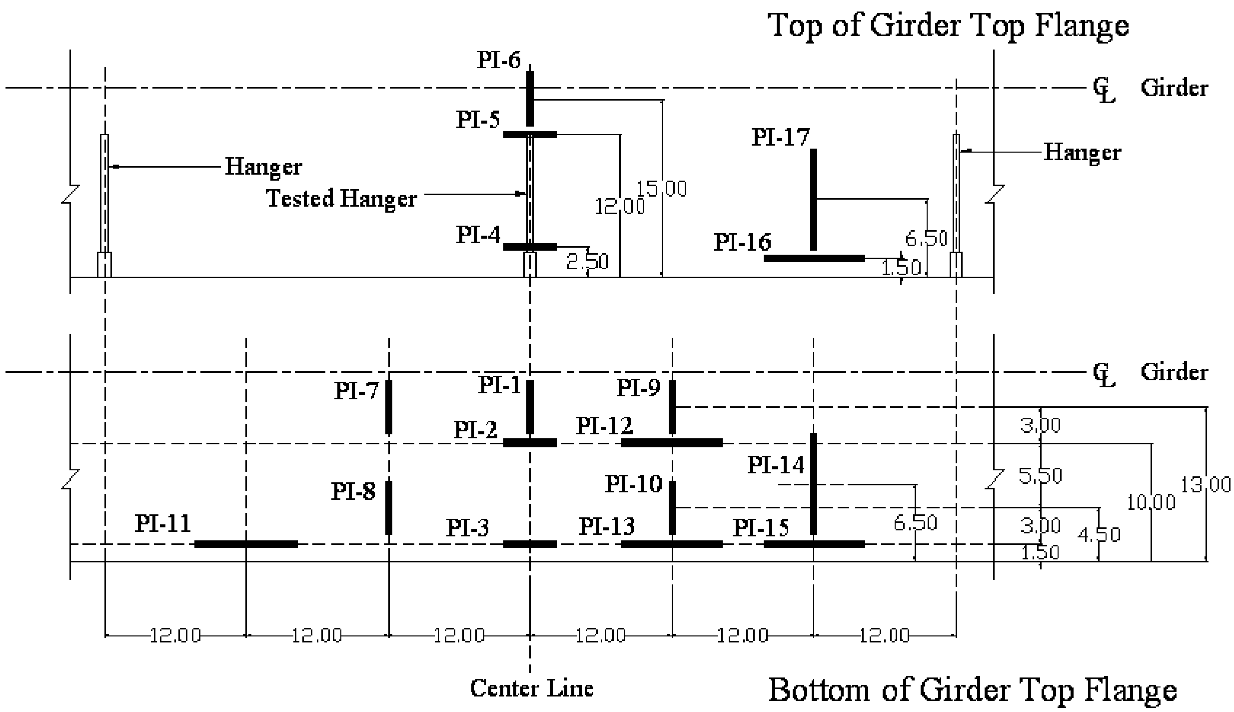

DR-1-L Instrumentation – PI-Gauge Assignment

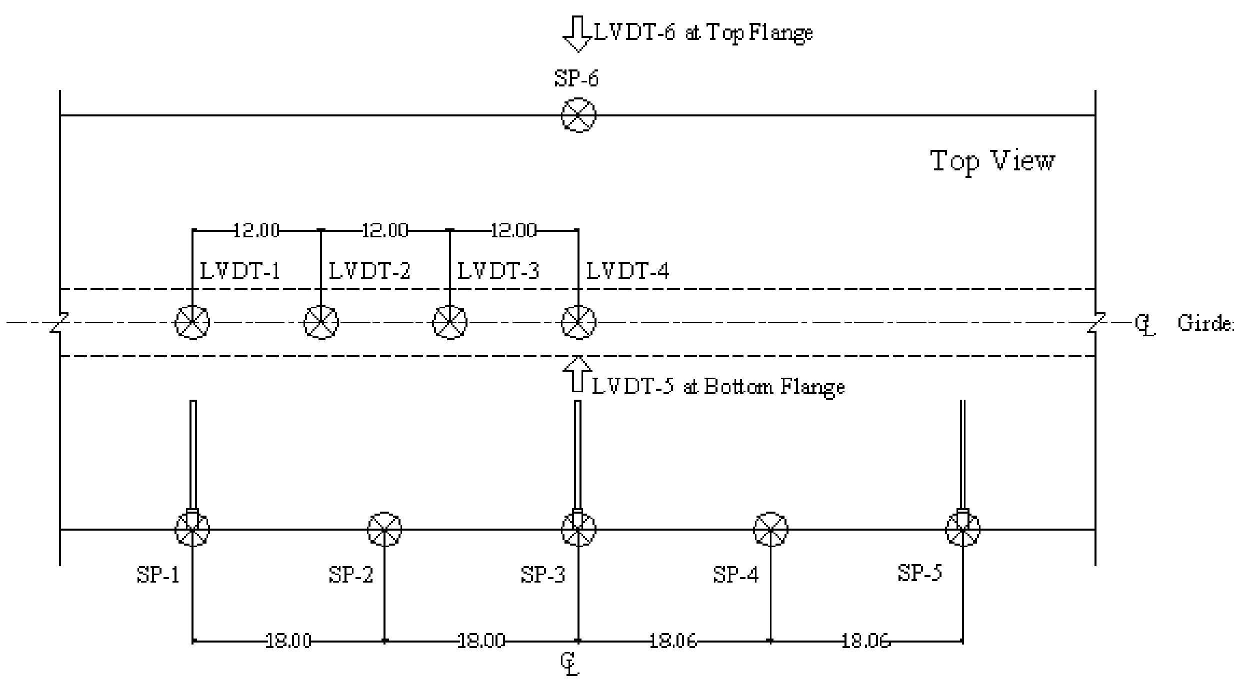

DR-1-L Instrumentation – Linear and String Pot Assignment

DR-1-L Overall Test Set Up

DR-1-L Installment of PI-Gauge

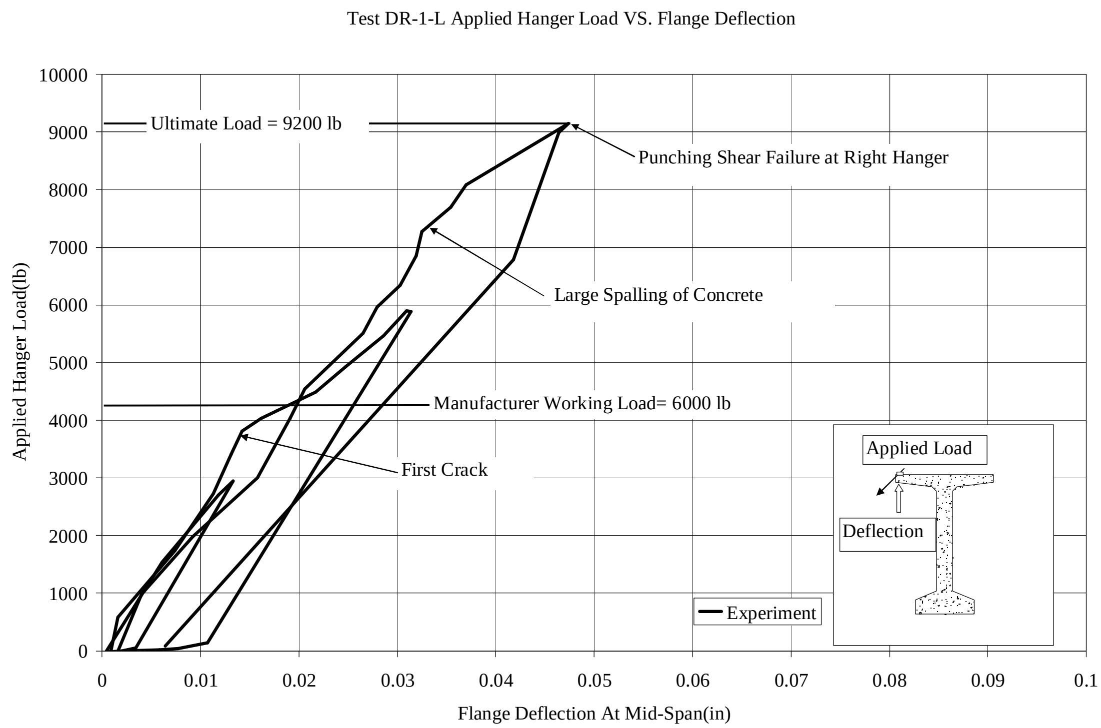

DR-1-L Deflection at Center Line

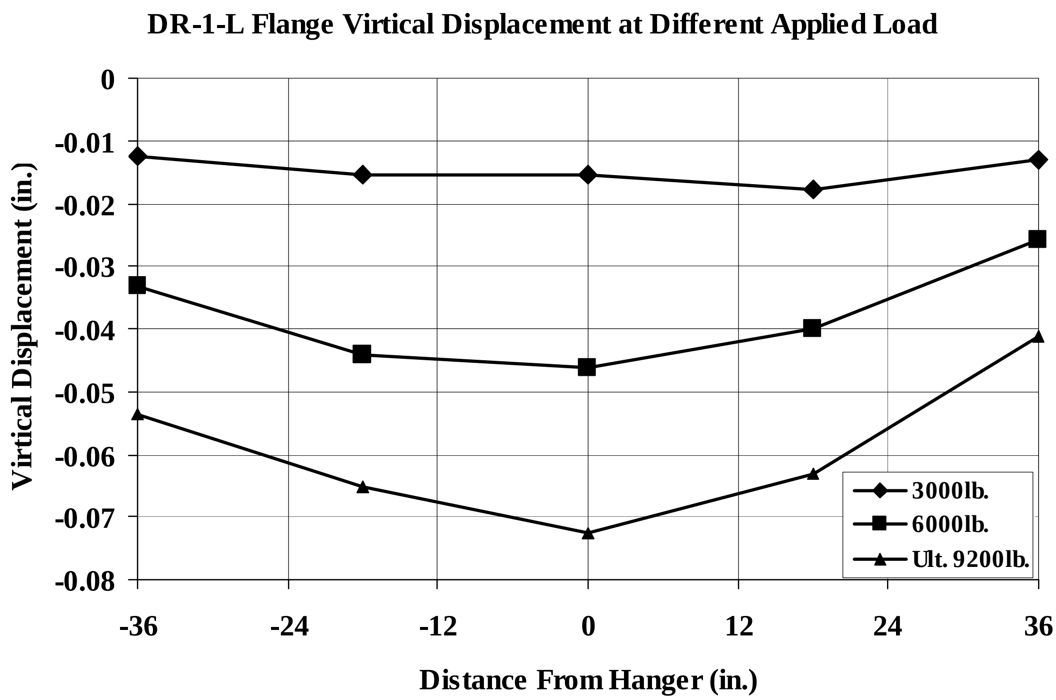

DR-1-L Vertical Displacement at Different Applied Load

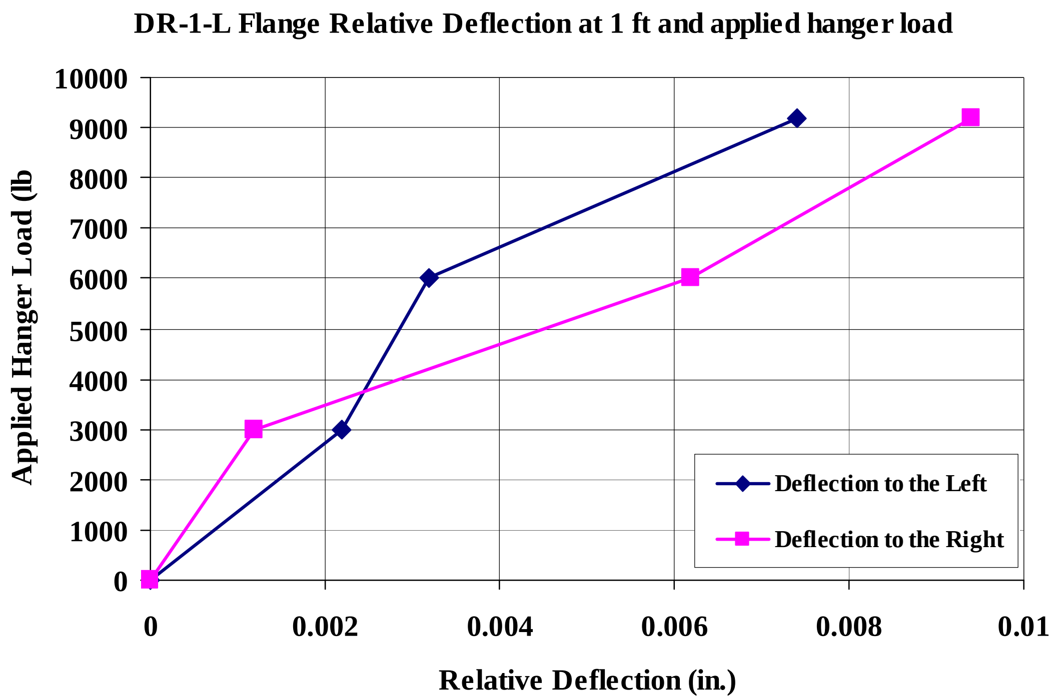

DR-1-L Relative Deflection Between 1ft from the Mid-Span and Mid-Span

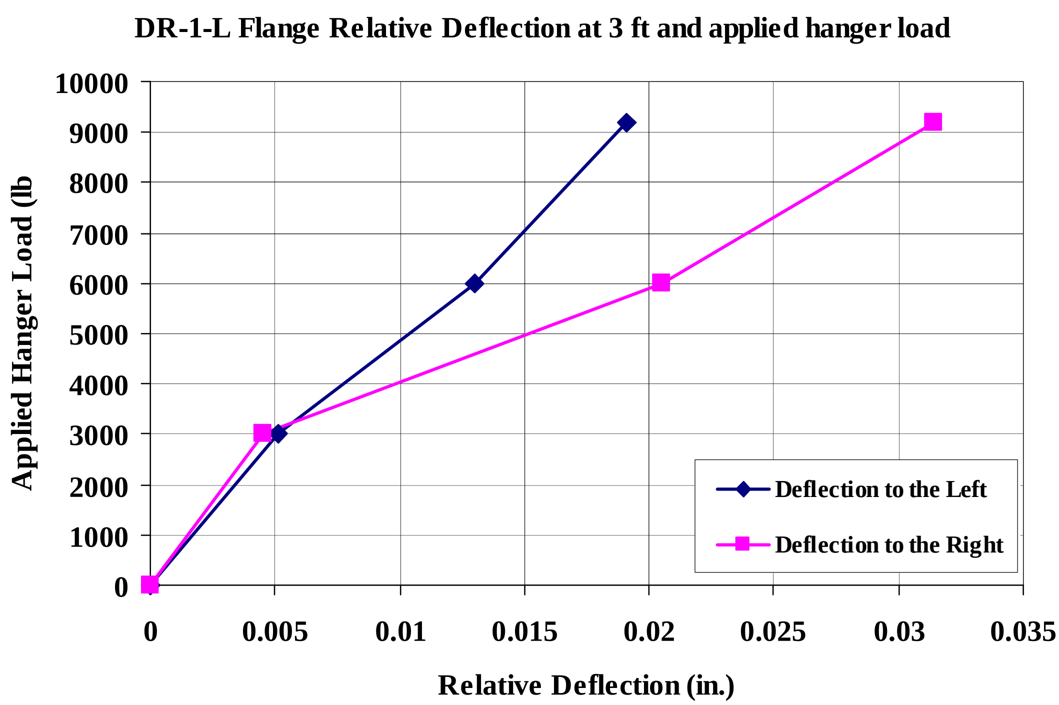

DR-1-L Relative Deflection Between 3ft from the Mid-Span and Mid-Span

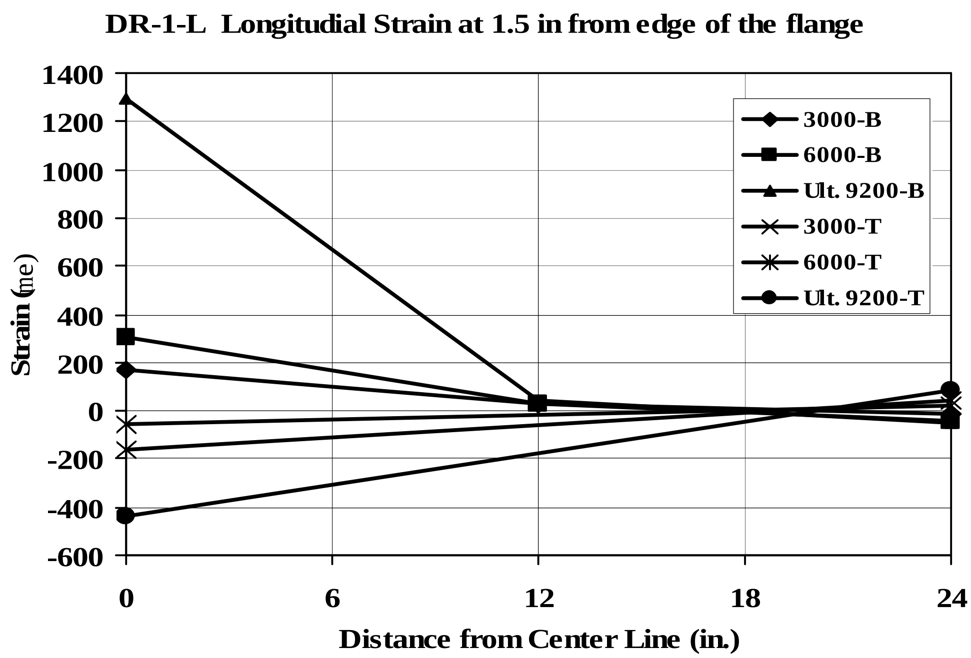

DR-1-L Longitudinal Strain from Top and Bottom along Edge of Flange

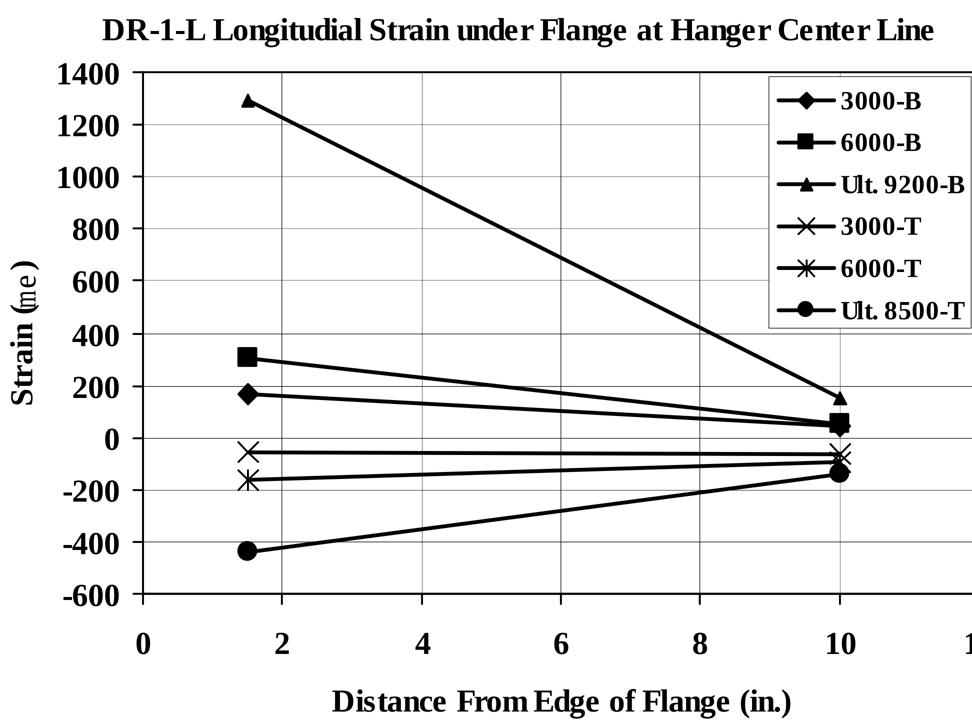

DR-1-L Longitudinal Strain from Top and Bottom at Center Line

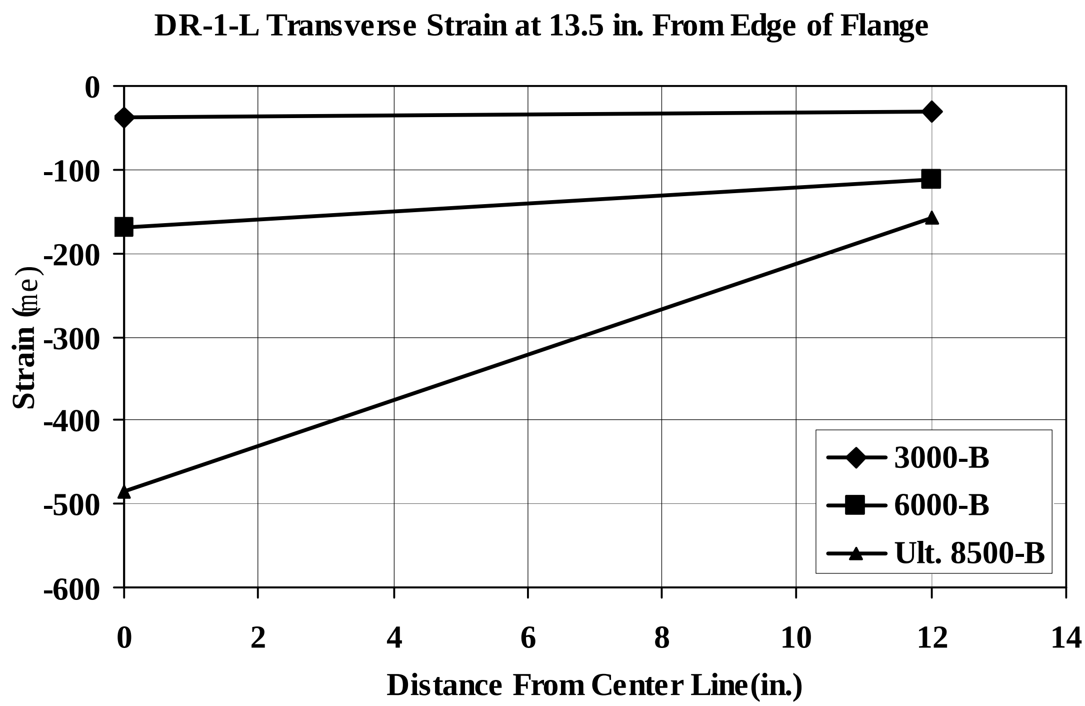

DR-1-L Longitudinal Strain at 13.5 in. from Edge of Flange

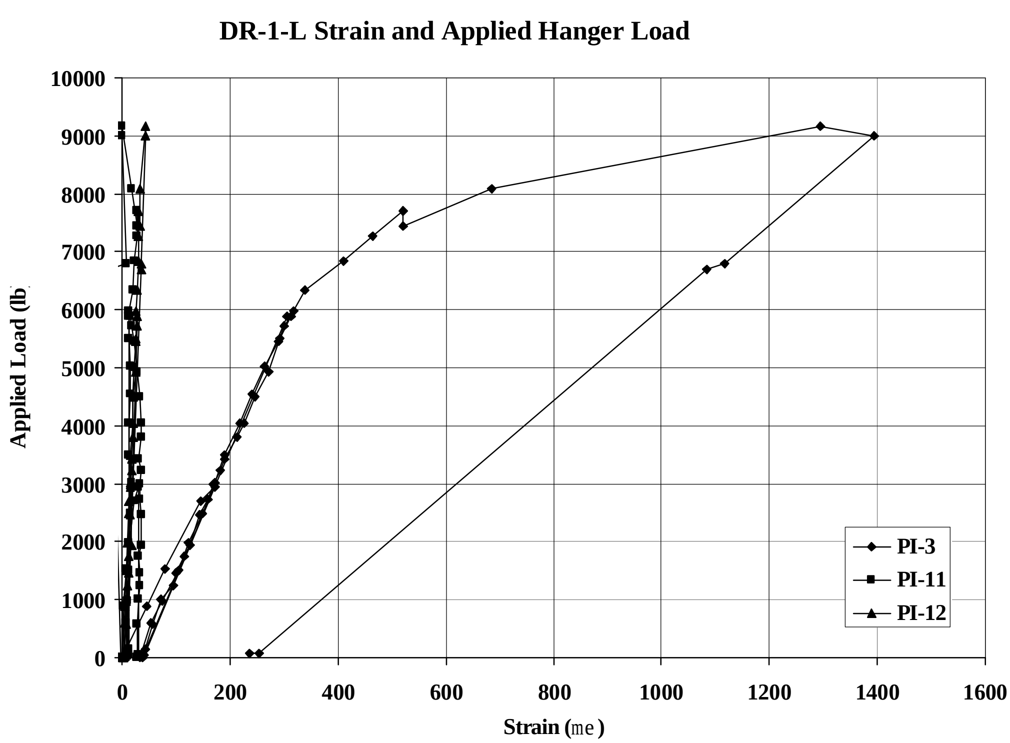

DR-1-L Longitudinal Strain at 1.5 in. from Edge of Flange

DR-1-L Spalling of Concrete Under Hanger

DR-1-L Weld Rupture of Hanger leg

Appendix D Hanger Test Summary Sheet

Test ID: DR-2-L (Dayton Hanger, Double Pull, Light Reinforcement)
Test Date: September 26, 2005
Sponsor: NCDOT
Tested By : Emmett Sumner, Ph. D., P.E. and Donlawit Ariyasajjakorn, E.I.
Test Location: Constructed Facilities Laboratory (CFL), NC State University

Test Description

Dayton/Richmond hanger, Double hanger pulled by 45 degree angle at the middle of girder (Light shear reinforcement).

Hanger: Dayton/Richmond hanger C-24-4-APR

Coil Rod: ½ in. Meadow/Burke Coil Rod, 9000 lb. Safe Working Load

Girder: NCDOT Modified Bulb Tee 63 in.
Concrete Cylinder Strength = 7500 psi

Experimental Results

Maximum Applied Load	= 10200 lb
Maximum Flange Vertical Displacement at Center Line of Test Set Up	= 0.1544 in.
Maximum Flange Vertical Displacement at Hanger	= 0.1602 in.
Maximum Flange Vertical Deflection at Hanger	= 0.0645 in.
Maximum Girder Rotation at Center Line of Test Set Up	= 0.0047 rad
Maximum Girder Vertical Displacement at Center Line of Test Set Up	= 0.0201 in.

Test observations:

At 3000 lb,	back side of hanger started lifting up at left hanger
At 3500 lb,	first crack was found both sides of hanger at left hanger
At 4500 lb,	crack propagated form back side of hanger to the edge of flange at left hanger. Small crack was found at right hanger
At 6100 lb,	large amount of hanger rotation was found at left hanger. Crack propagate to the edge at right hanger
At 8000 lb,	Large spalling of concrete occurred at the edge of flange under left hanger. This result is allowed the hanger to rotate and dig into girder's flange.
At 10200 lb,	Failure occurred at right hanger, punching shear failure. Severe hanger rotation was found at left hanger.

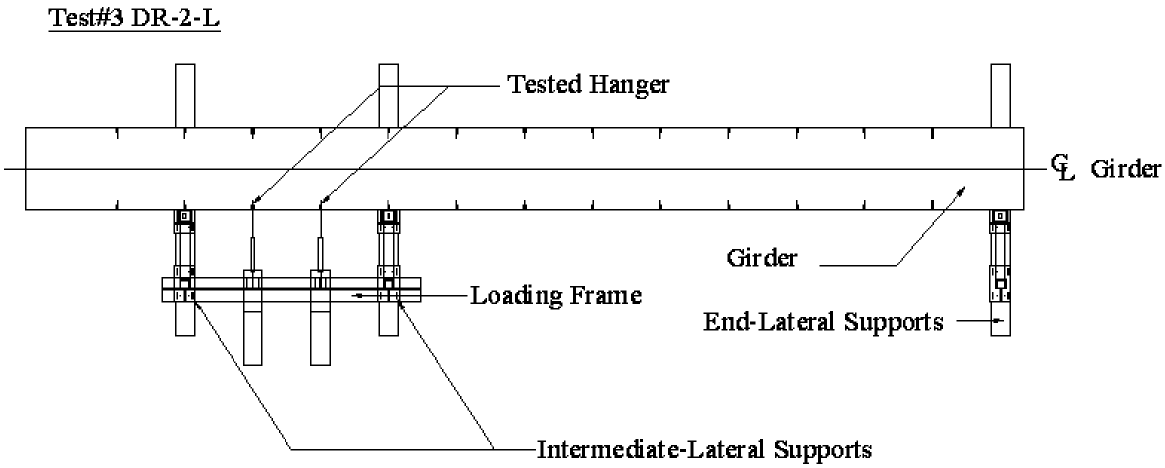

Plan View of Tested Hanger Position

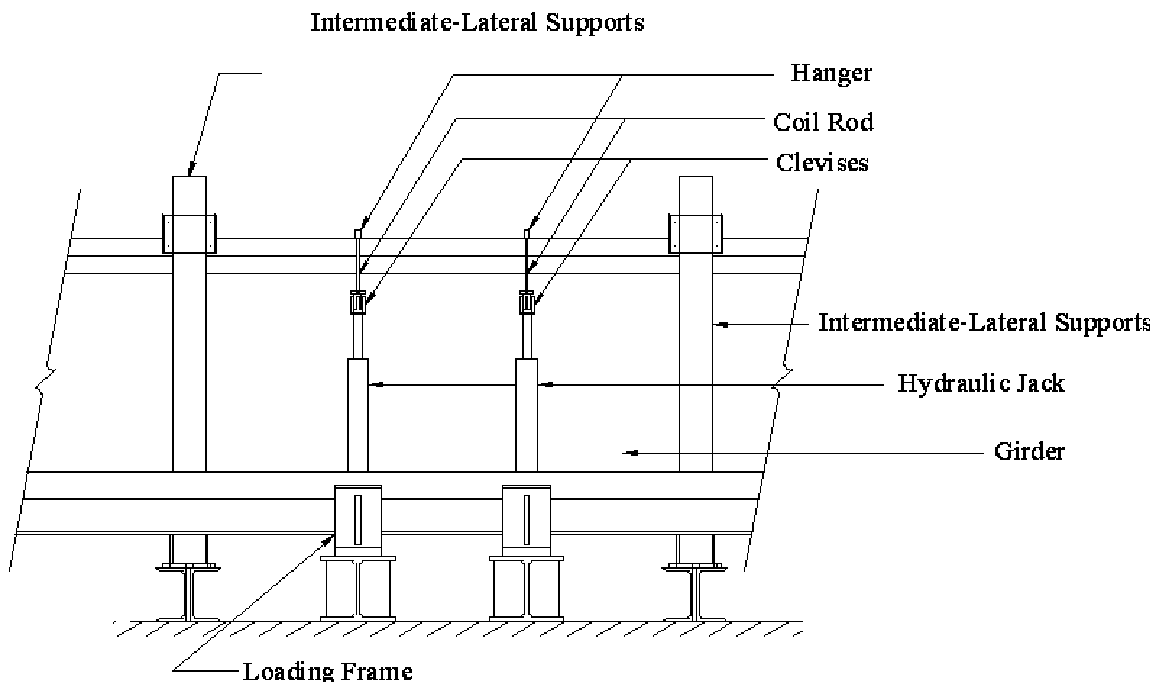

DR-2-L Test Set Up - Elevation

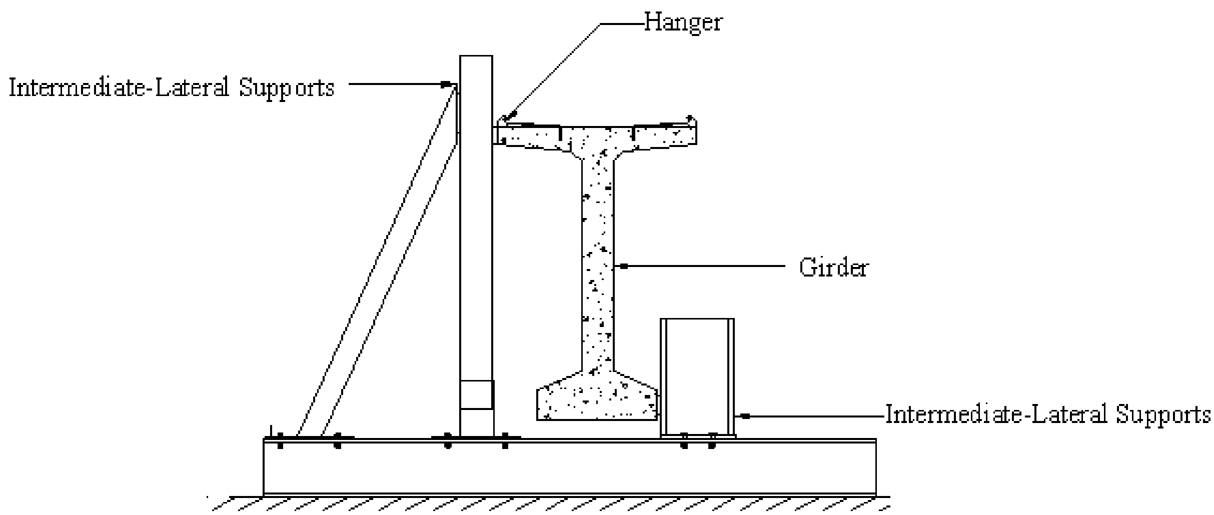

DR-2-L Cross Section at Intermediate-Lateral Support

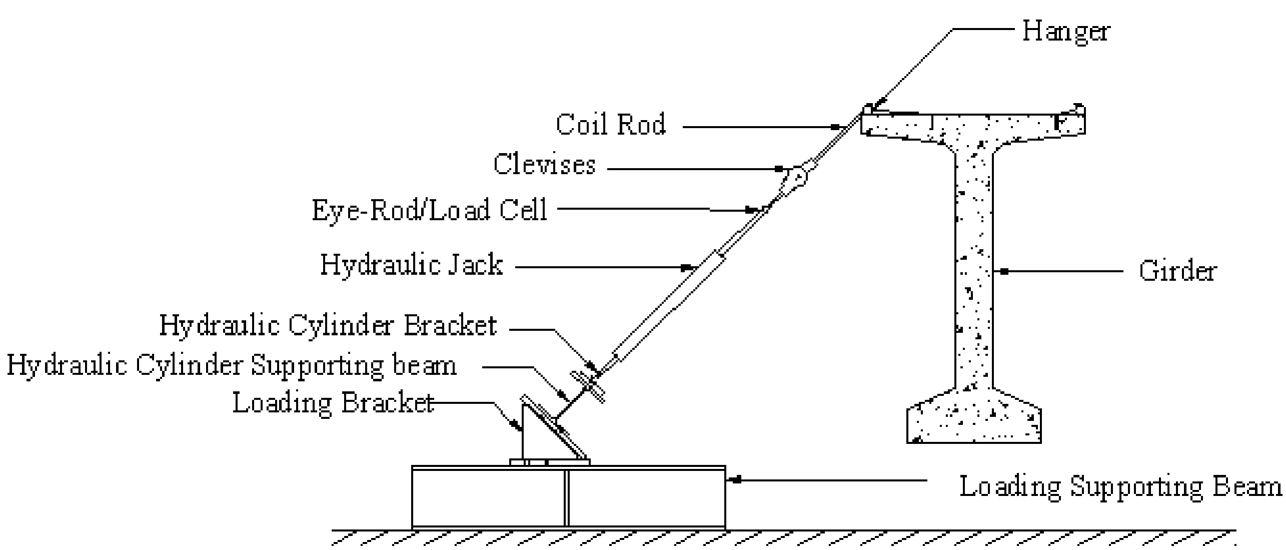

DR-2-L Cross Section at Loading Frame

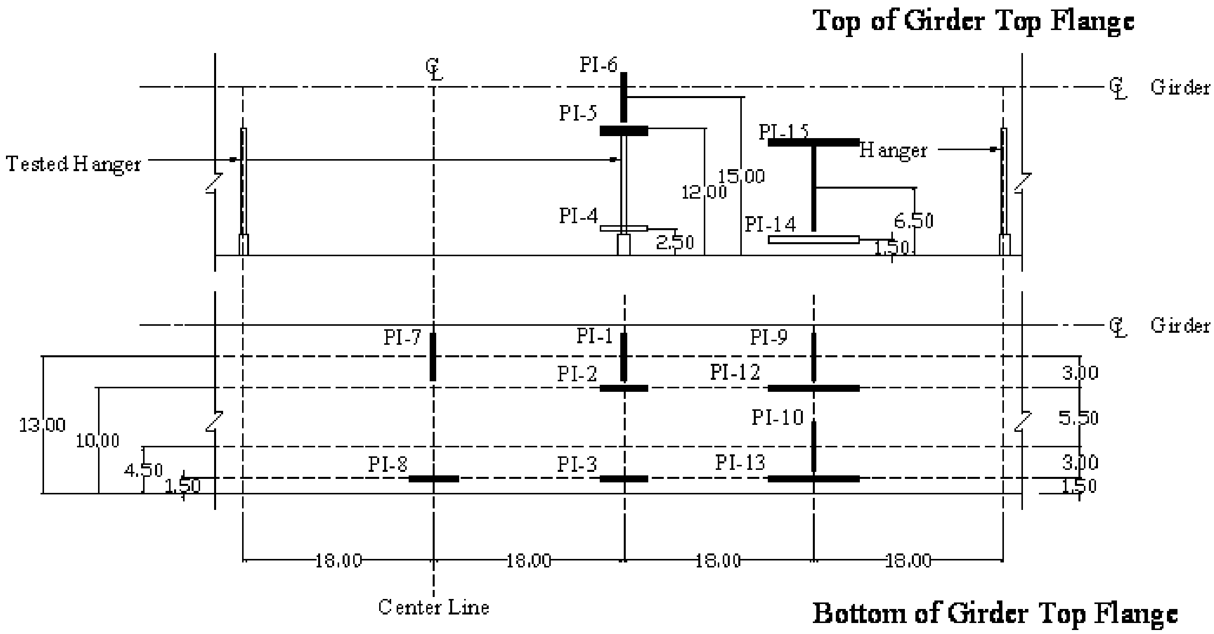

DR-2-L Instrumentation – PI-Gauge Assignment

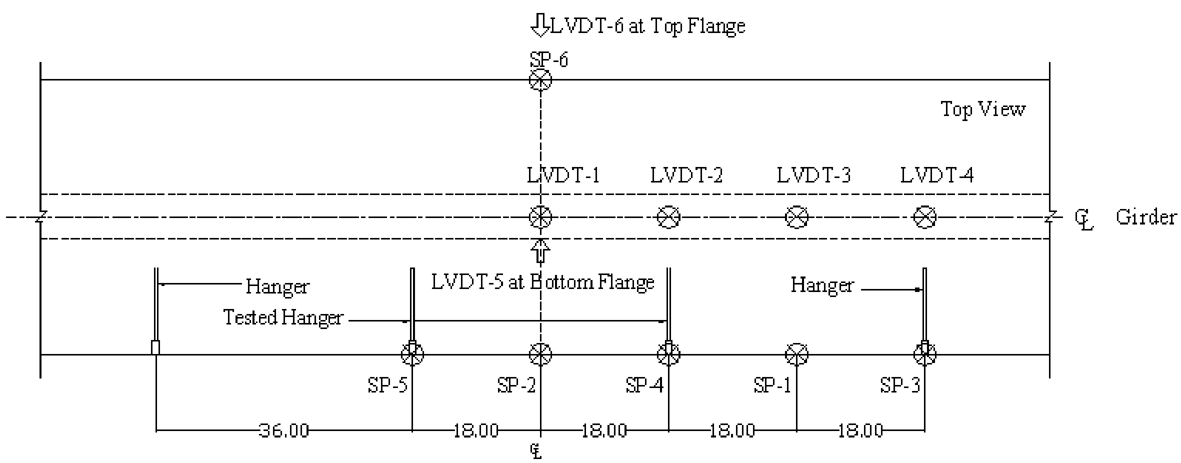

DR-2-L Instrumentation – Linear and String Pot Assignment

DR-2-L Overall Test Set Up

DR-2-L Installment of PI-Gauge

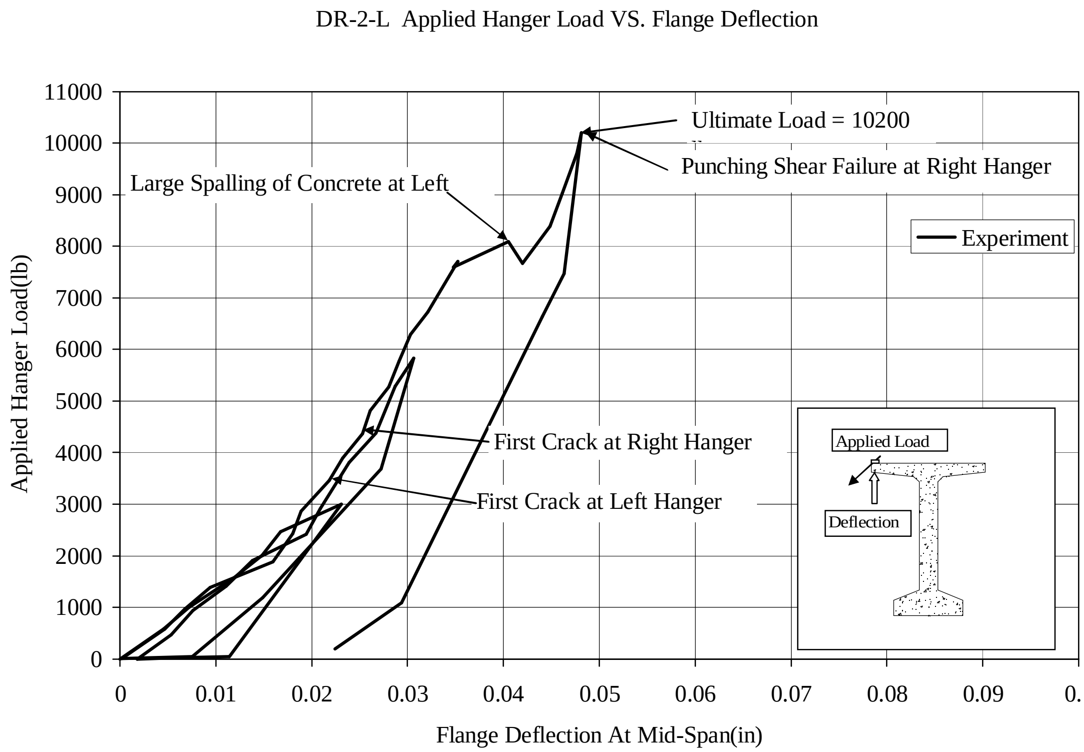

DR-2-L Deflection at Center Line

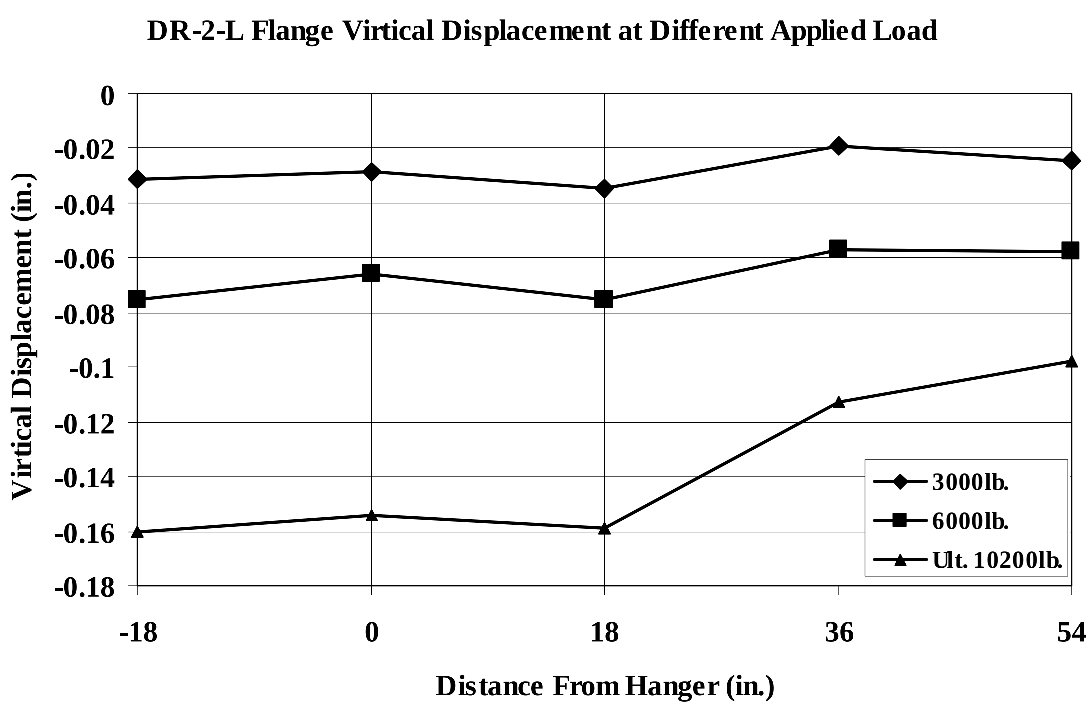

DR-2-L Vertical Displacement at Different Applied Load

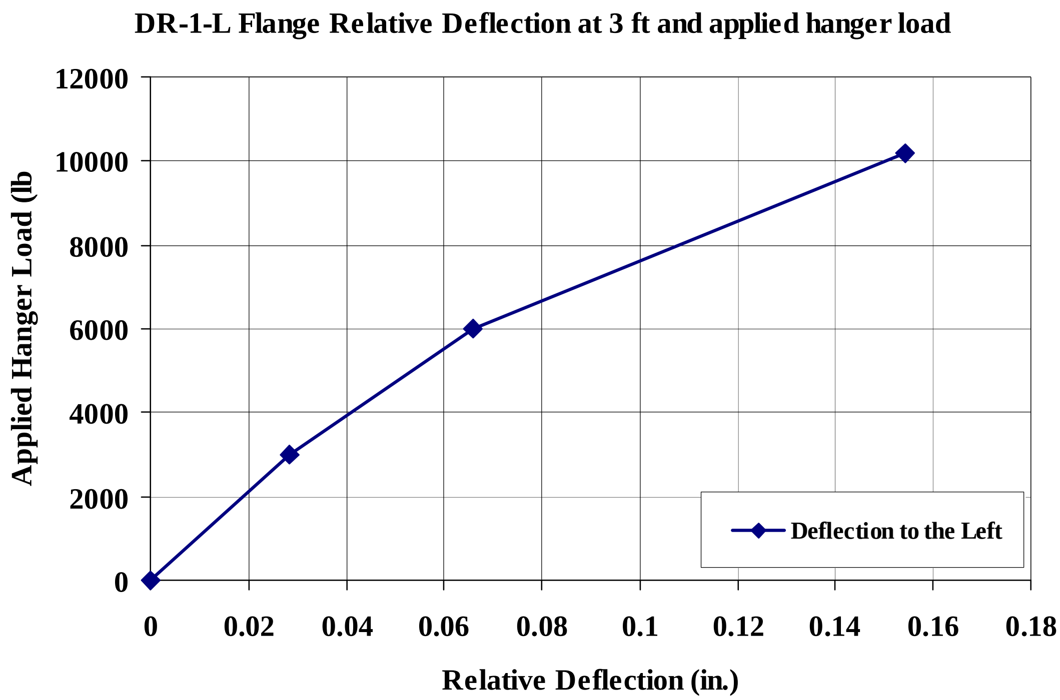

DR-2-L Relative Deflection Between 3ft from the Mid-Span and Mid-Span

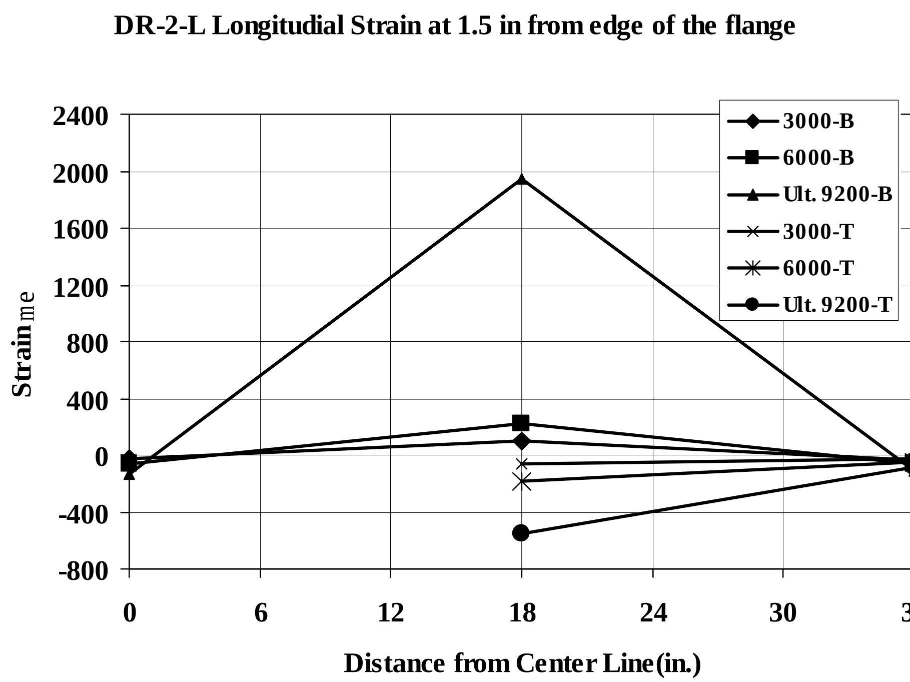

DR-2-L Longitudinal Strain from Top and Bottom along Edge of Flange

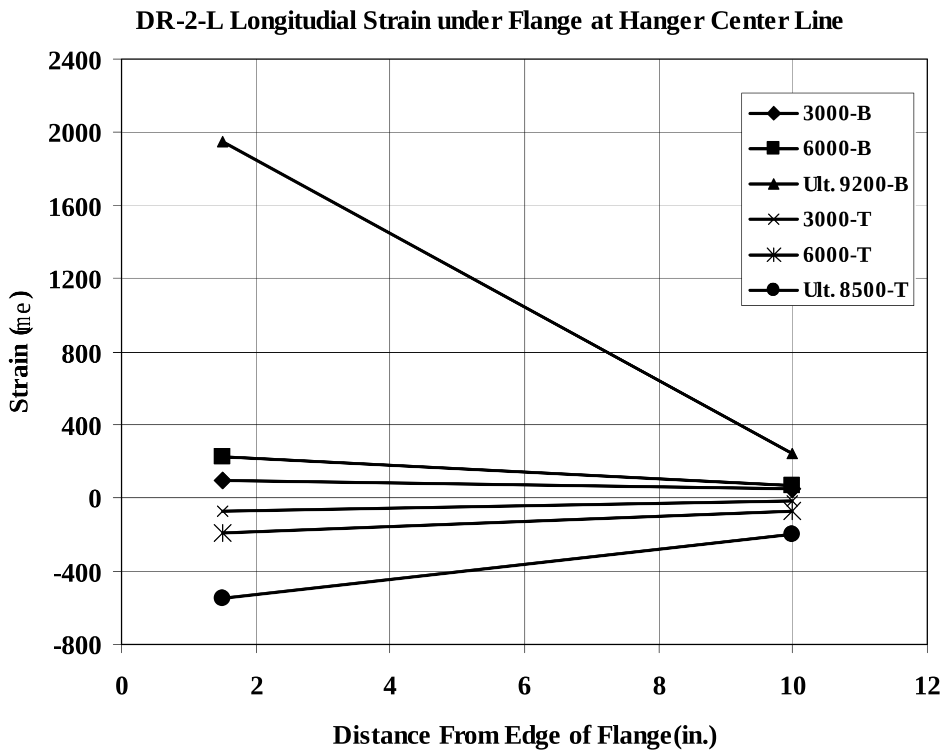

DR-2-L Longitudinal Strain from Top and Bottom at Center Line

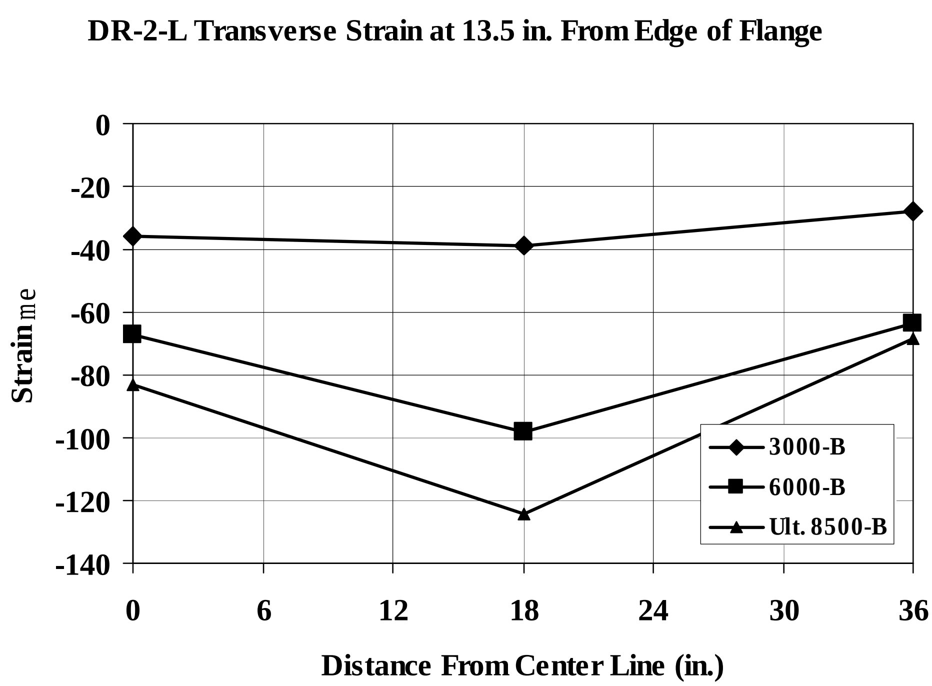

DR-2-L Longitudinal Strain at 13 in. from Edge of Flange

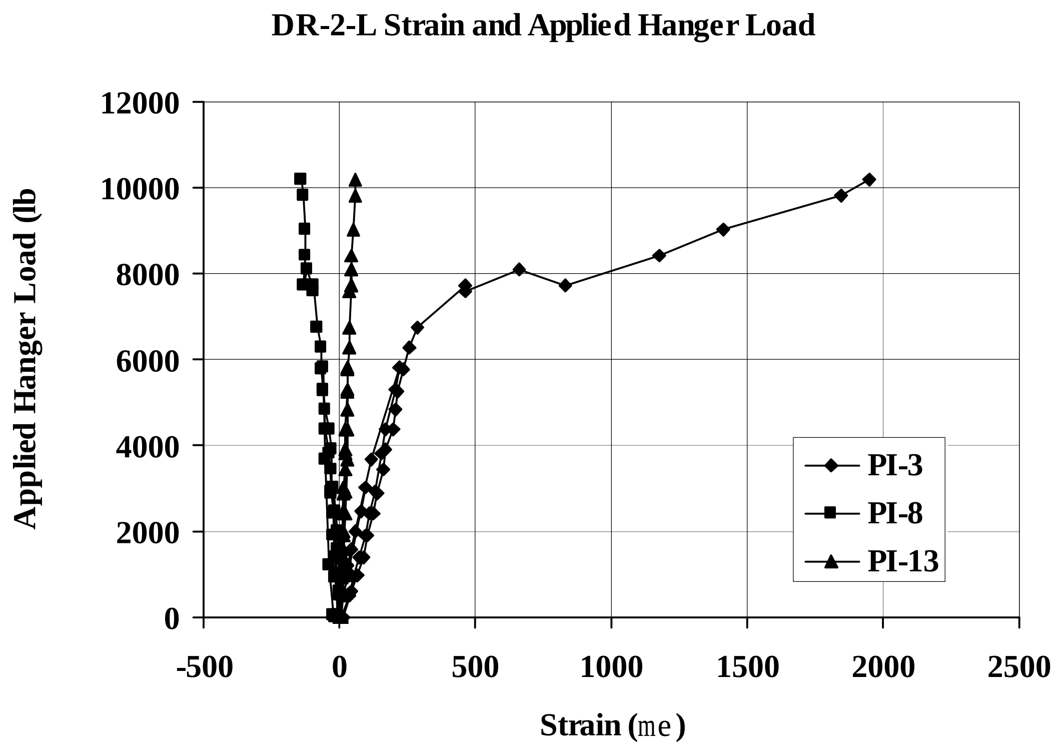

DR-2-L Longitudinal Strain at 1.5 in. from Edge of Flange

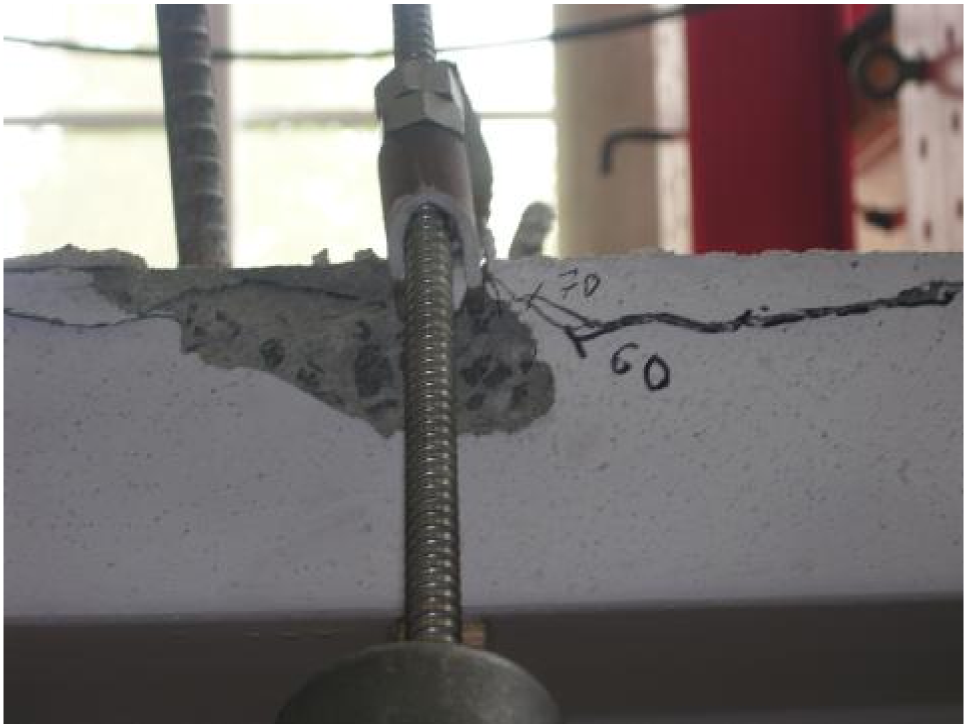

DR-2-L Spalling of Concrete Under Left Hanger

DR-2-L Punching Shear Failure of Right Hanger

Appendix E Hanger Test Summary Sheet

Test ID:	MB-1-H (Meadow/Burke Hanger, 1 Pull, High Reinforcement)
Test Date:	September 29, 2005
Sponsor:	NCDOT
Tested By :	Emmett Sumner, Ph. D., P.E. and Donlawit Ariyasajjakorn, E.I.
Test Location:	Constructed Facilities Laboratory (CFL), NC State University

Test Description

Meadow/Burke hanger, Single hanger pulled by 45 degree angle at the end of girder (High shear reinforcement).

Hanger: Meadow/Burke hanger HF-43 (Two Legs)

Coil Rod: ½ in. Meadow/Burke Coil Rod, 9000 lb. Safe Working Load

Girder: NCDOT Modified Bulb Tee 63 in.
Concrete Cylinder Strength = 7500 psi

Experimental Results

Maximum Applied Load	= 8500 lb
Maximum Flange Vertical Displacement at Center Line of Test Set Up	= 0.0608 in.
Maximum Flange Vertical Displacement at Hanger	= 0.0608 in.
Maximum Flange Vertical Deflection at Hanger	= 0.0200 in.
Maximum Girder Rotation at Center Line of Test Set Up	= 0.0017 rad
Maximum Girder Vertical Displacement at Center Line of Test Set Up	= 0.0051 in.

Test observations:

At 3000 lb,	nothing was noted at this applied load
At 6000 lb,	nothing was noted at this applied load. No bending in coil rod was found
At 8000 lb,	first was found and propagate slowly to the edge
At 8500 lb,	crack propagated and developed shear cone around the hanger. Crack width increased while sustain applied load
At 8500 lb,	Punching Shear Failure occurred after about 5 min of sustain load

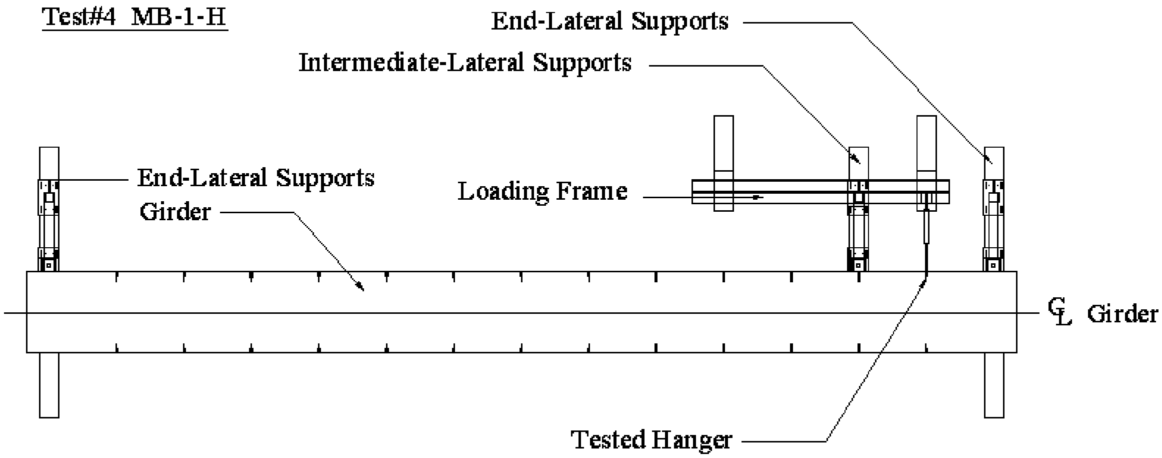

Plan View of Tested Hanger Position

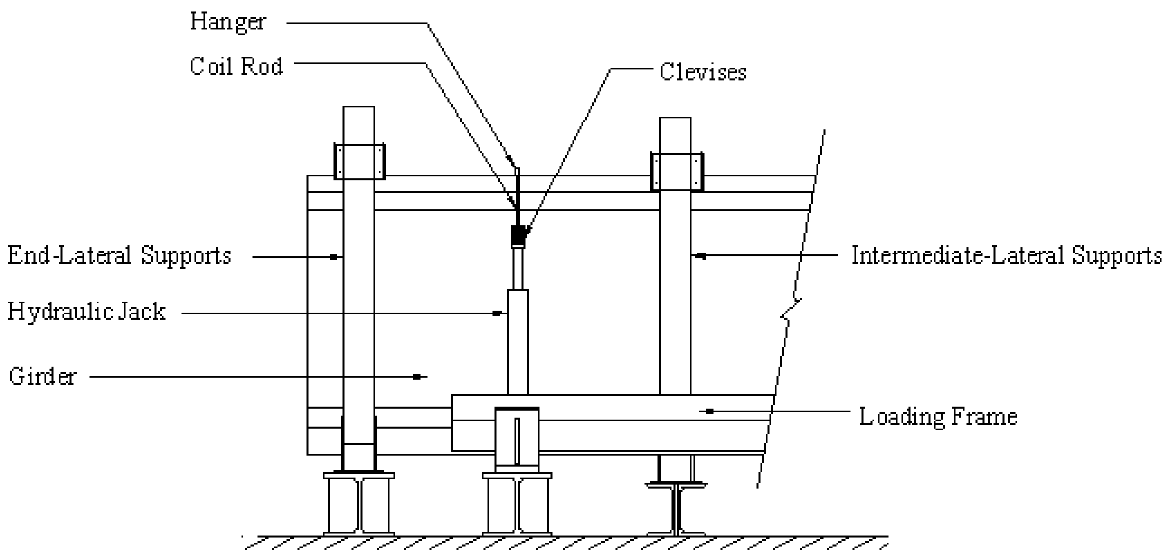

MB-1-H Elevation

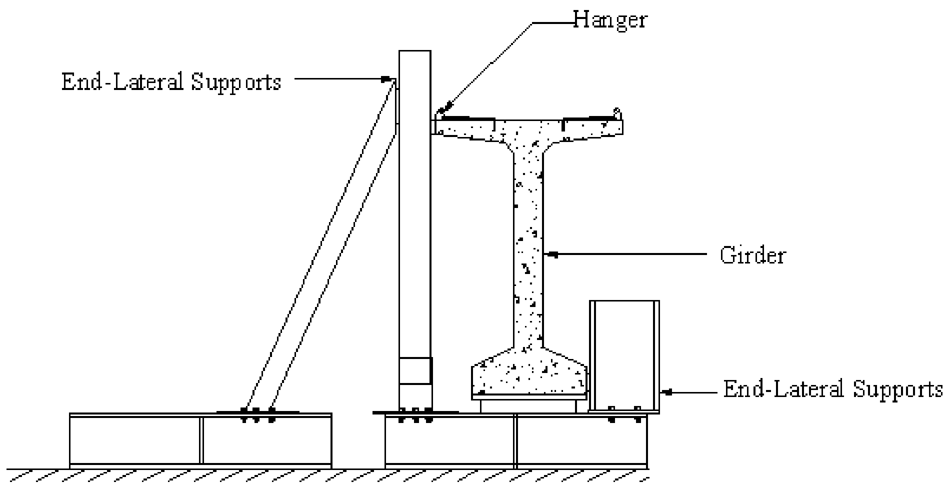

MB-1-H Cross Section at End-Support

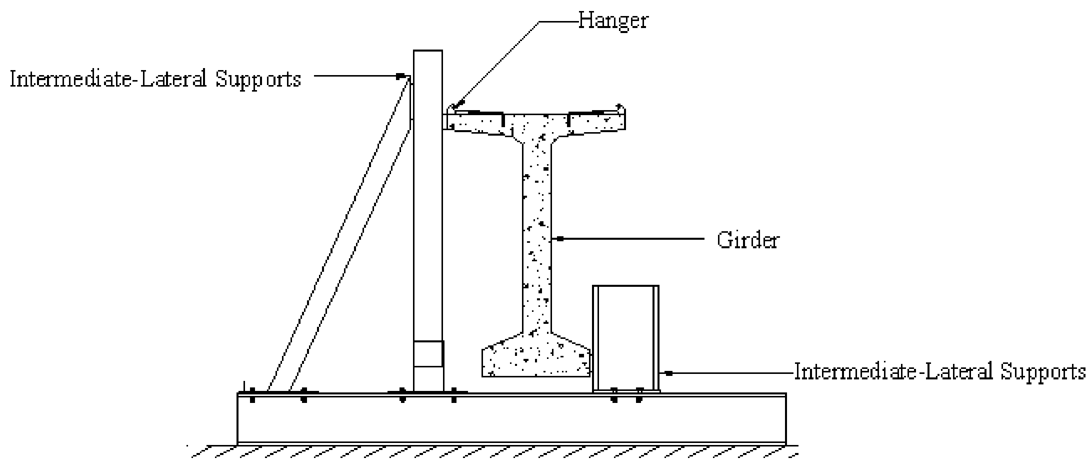

MB-1-H Cross Section at Intermediate-Lateral Support

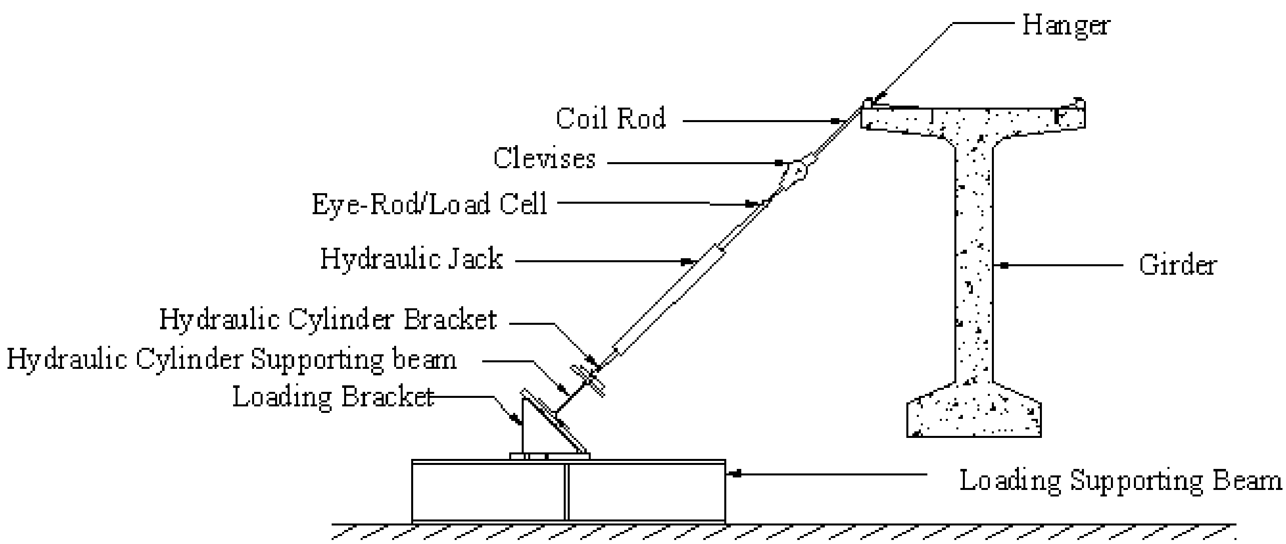

MB-1-H Cross Section at Loading Frame

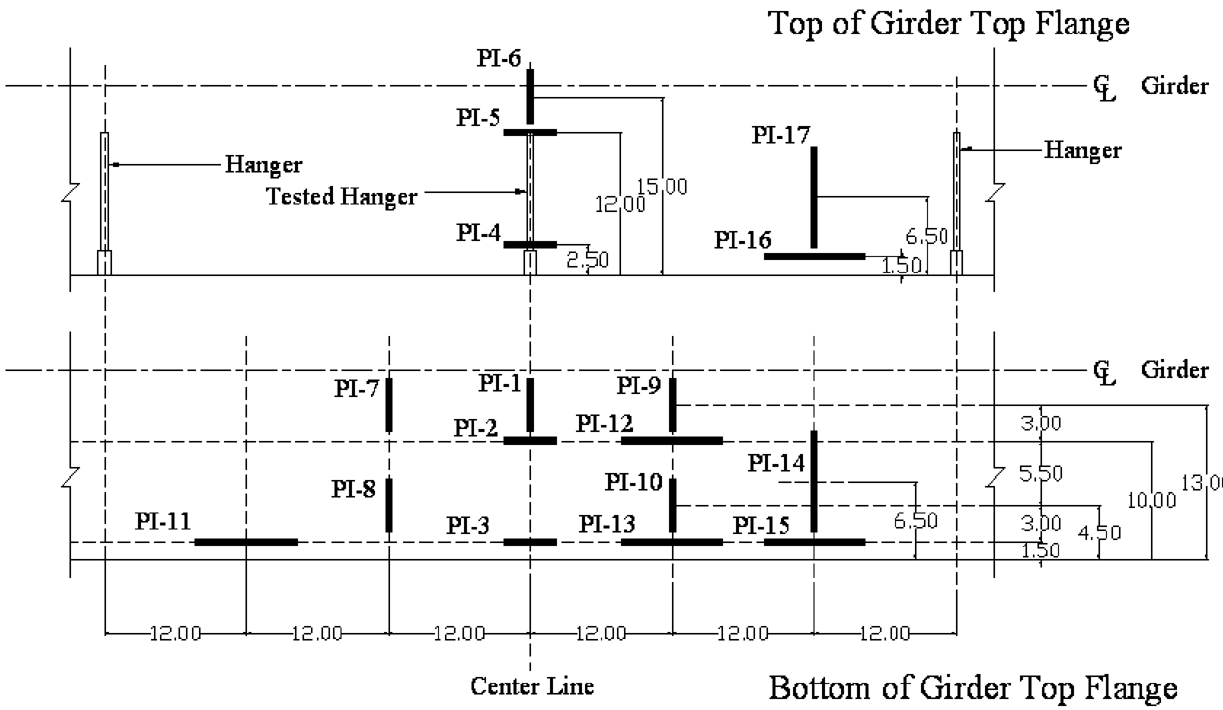

MB-1-H Instrumentation – PI-Gauge Assignment

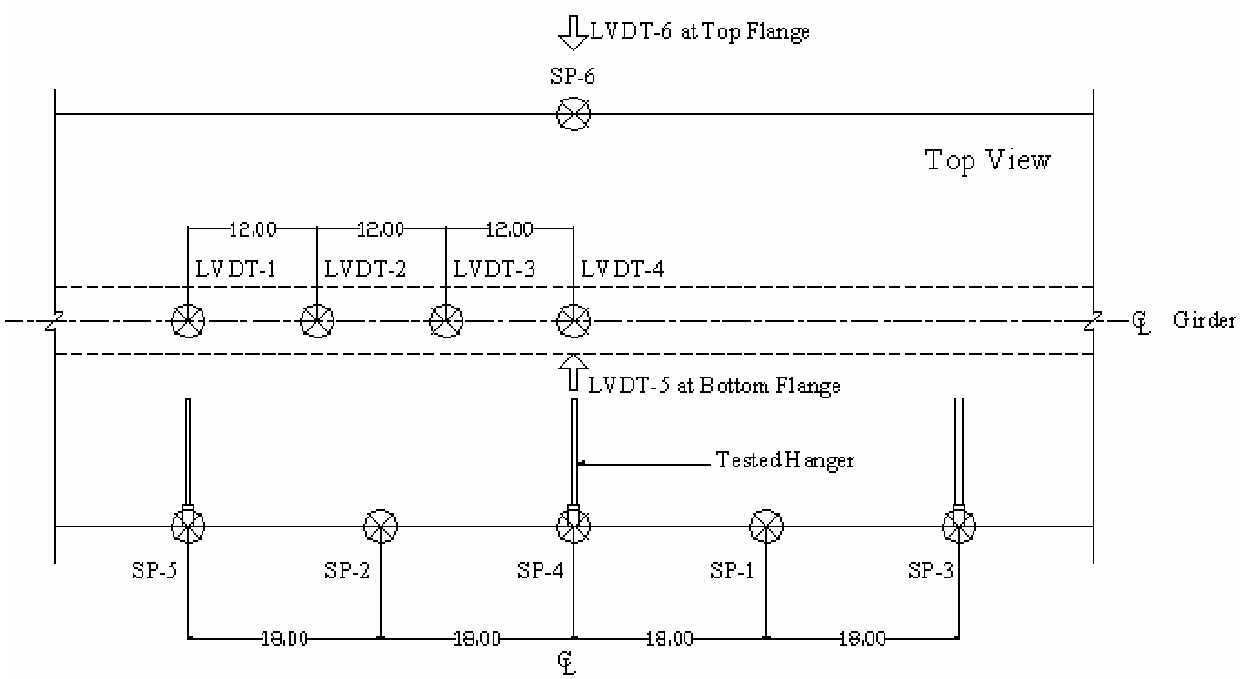

MB-1-H Instrumentation – Linear and String Pot Assignment

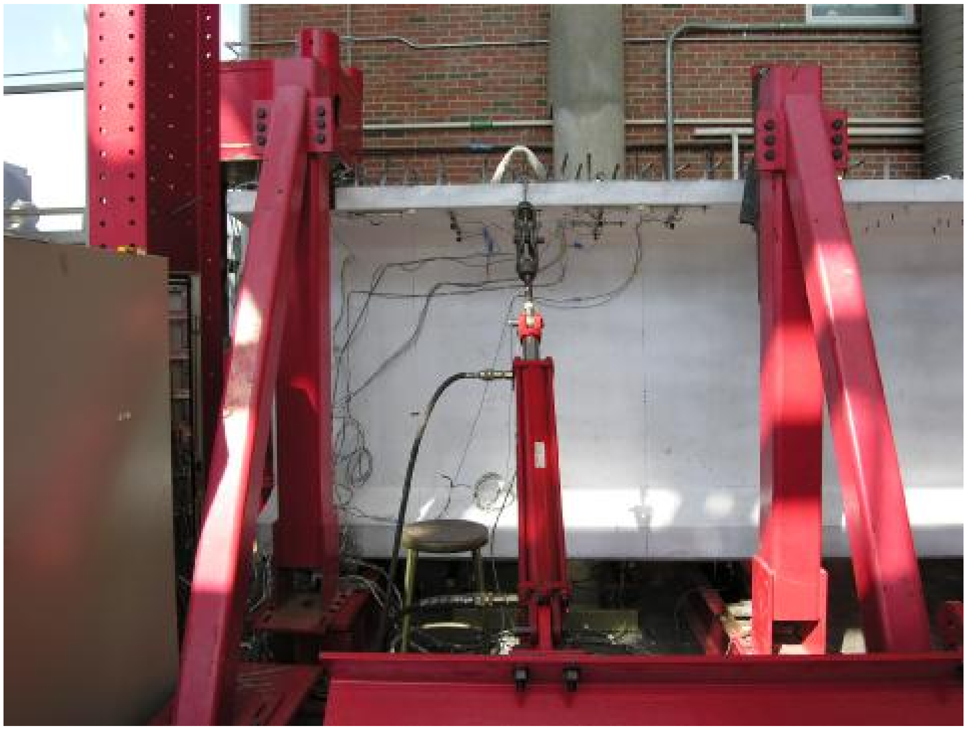

MB-1-H Overall Test Set Up

MB-1-H Installment of PI-Gauge

MB-1-H Applied Hanger Load VS. Flange Deflection (MB)

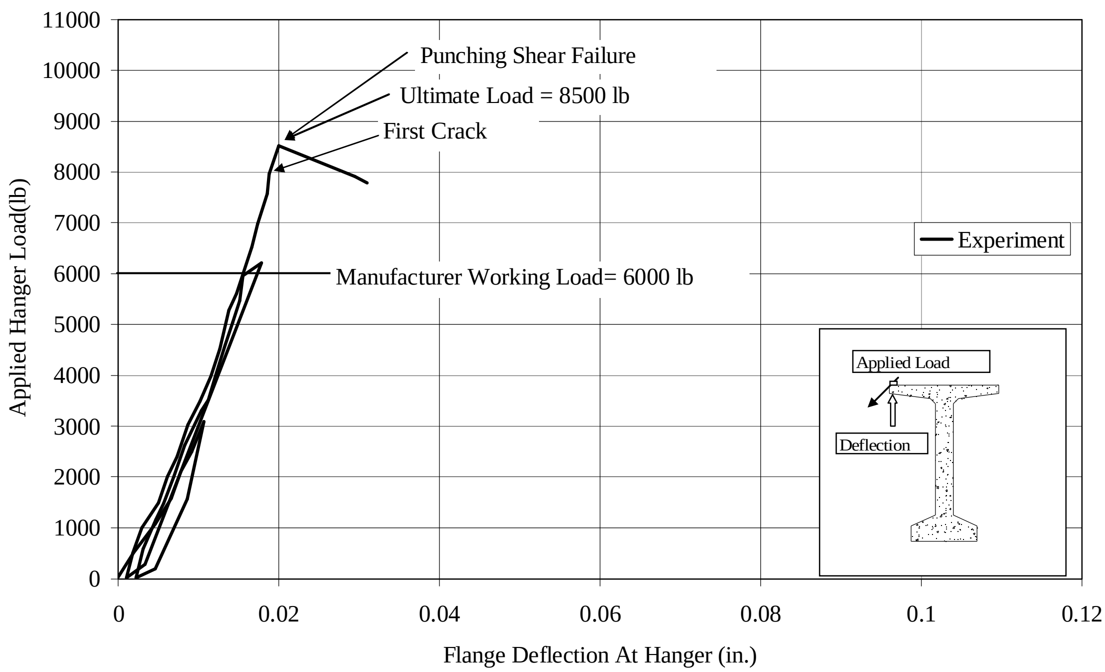

MB-1-H Flange Deflection at Hanger

MB-1-H Flange Virtical Displacement at Different Applied Load

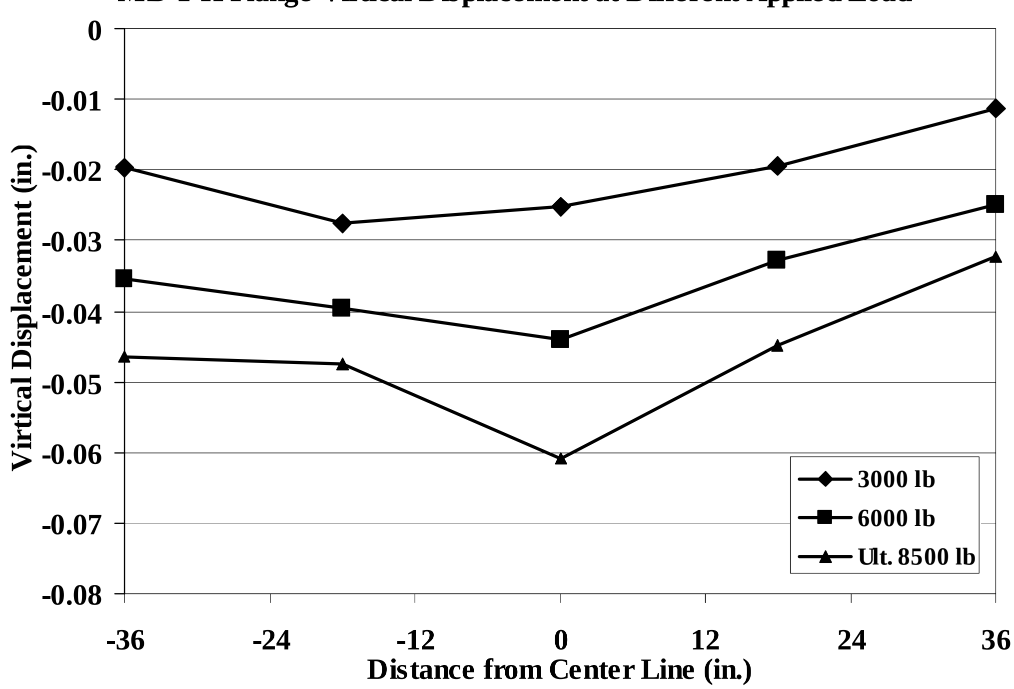

MB-1-H Vertical Displacement at Different Applied Load

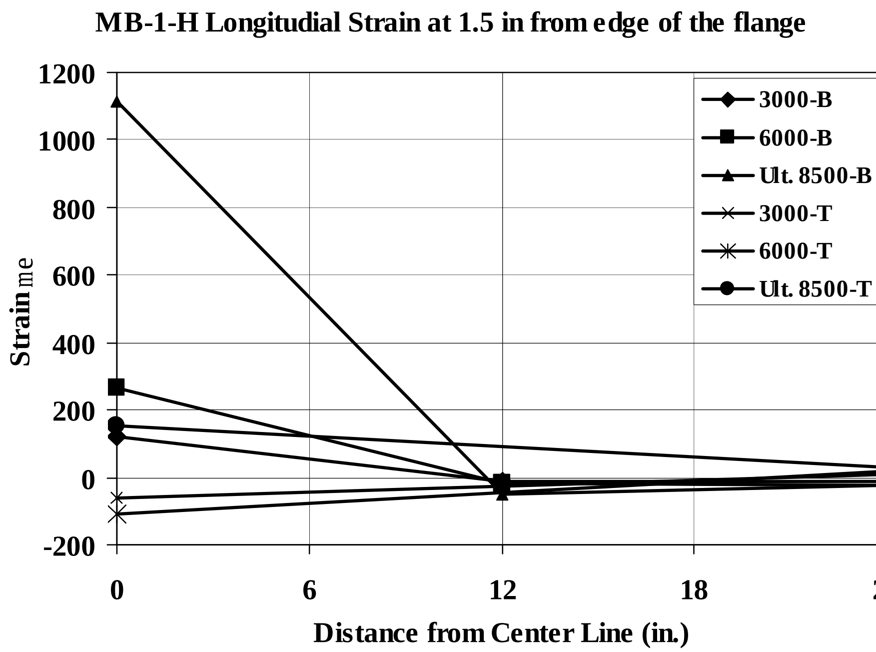

MB-1-H Longitudinal Strain from Top and Bottom along Edge of Flange

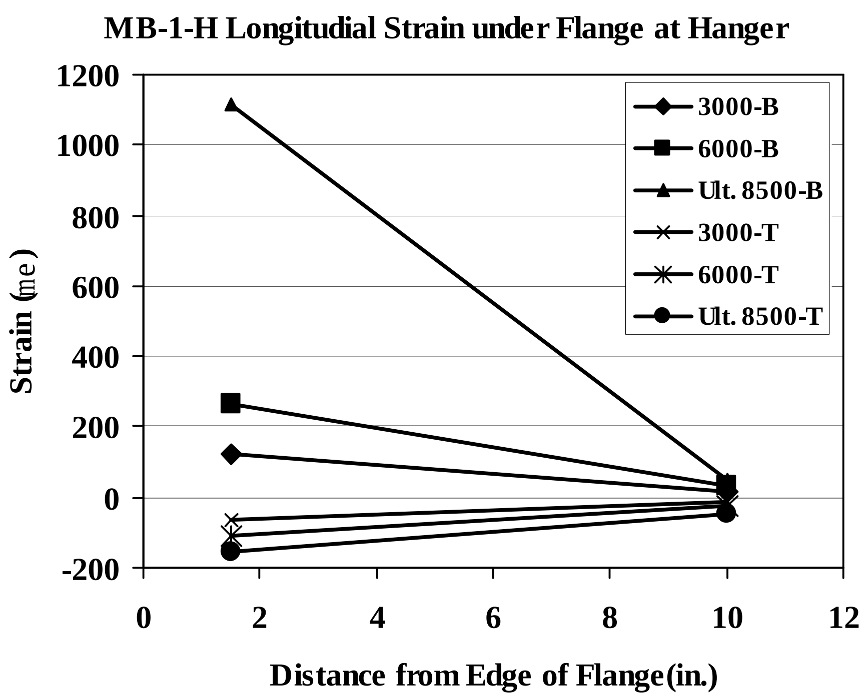

MB-1-H Longitudinal Strain from Top and Bottom at Center Line

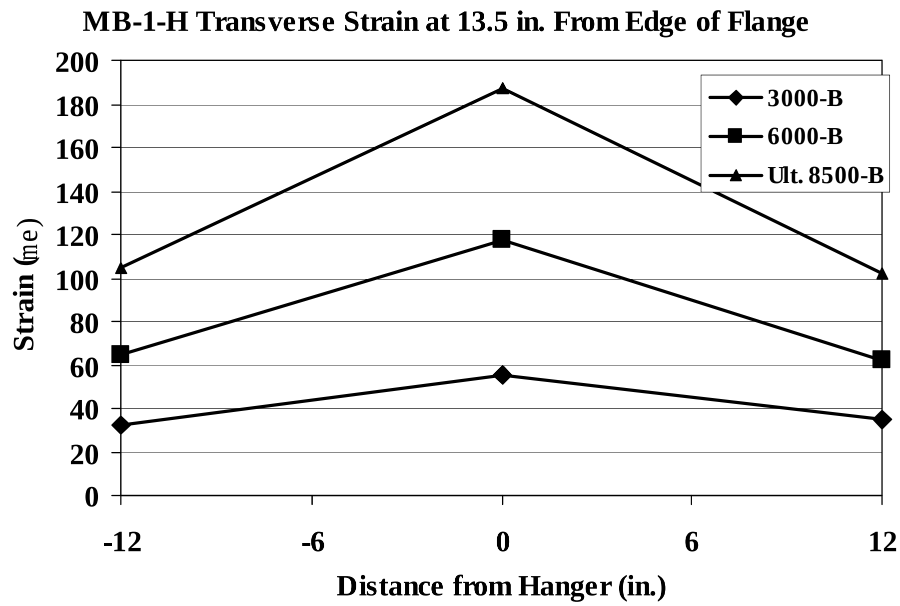

MB-1-H Longitudinal Strain at 13 in. from Edge of Flange

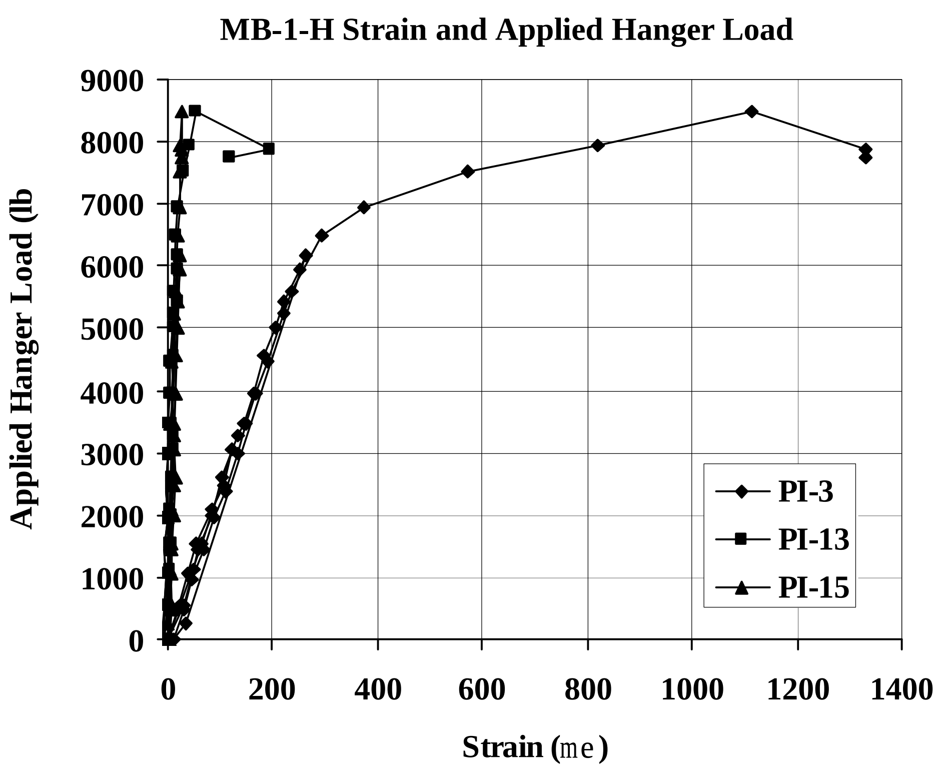

MB-1-H Longitudinal Strain at 1.5 in. from Edge of Flange

MB-1-H Punching Shear Failure

MB-1-H Punching Shear Failure

Appendix F Hanger Test Summary Sheet

Test ID:	MB-1-L (Meadow/Burke Hanger, 1 Pull, Light Reinforcement)
Test Date:	September 29, 2005
Sponsor:	NCDOT
Tested By :	Emmett Sumner, Ph. D., P.E. and Donlawit Ariyasajjakorn, E.I.
Test Location:	Constructed Facilities Laboratory (CFL), NC State University

Test Description

Meadow/Burke hanger, Single hanger pulled by 45 degree angle at middle of girder (Light shear reinforcement).

Hanger: Meadow/Burke hanger HF-43 (Two Legs)

Coil Rod: ½ in. diameter Meadow/Burke Coil Rod, 9000 lb. Safe Working Load

Girder: NCDOT Modified Bulb Tee 63 in.
Concrete Cylinder Strength = 7500 psi

Experimental Results

Maximum Applied Load	= 6500 lb
Maximum Flange Vertical Displacement at Center Line of Test Set Up	= 0.0429 in.
Maximum Flange Vertical Displacement at Hanger	= 0.0429 in.
Maximum Flange Vertical Deflection at Hanger	= 0.0296 in.
Maximum Girder Rotation at Center Line of Test Set Up	= 0.0031 rad
Maximum Girder Vertical Displacement at Center Line of Test Set Up	= 0.0057 in.

Test observations:

At 3000 lb,	nothing was noted at this applied load
At 6000 lb,	first was found and propagate slowly to the edge
At 6500 lb,	crack propagated and developed shear cone around the hanger. Crack width increased while sustain applied load
At 6500 lb,	Punching Shear Failure occurred after about 5 min of sustain load

Test#5 MB-1-L

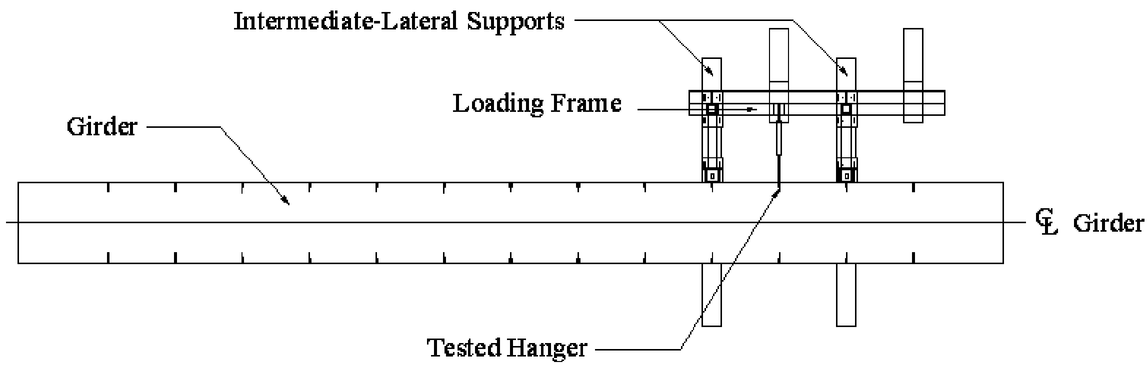

Plan View of Tested Hanger Position

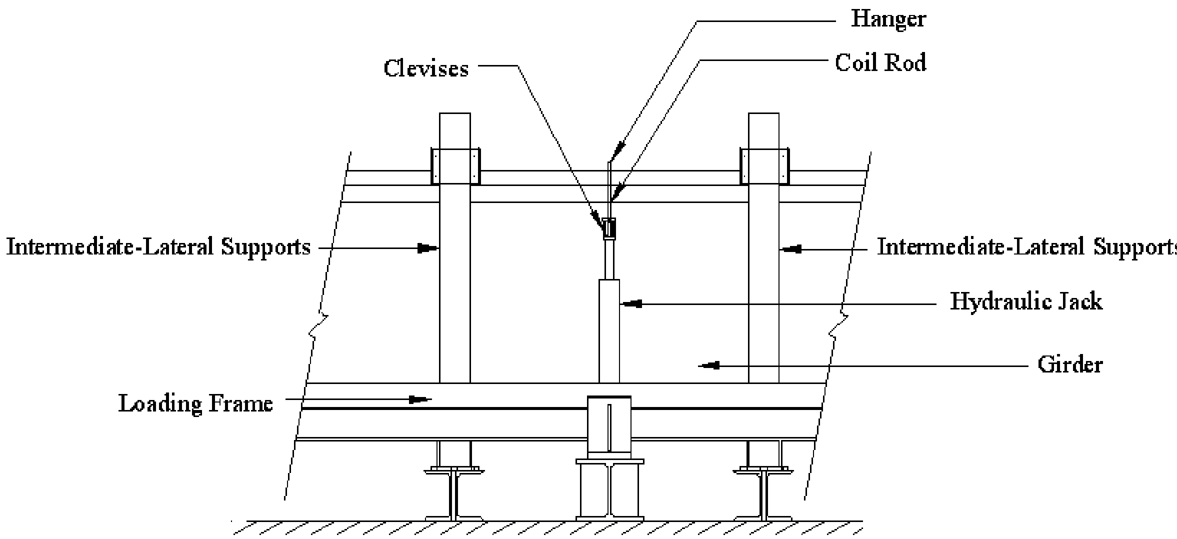

MB-1-L Elevation

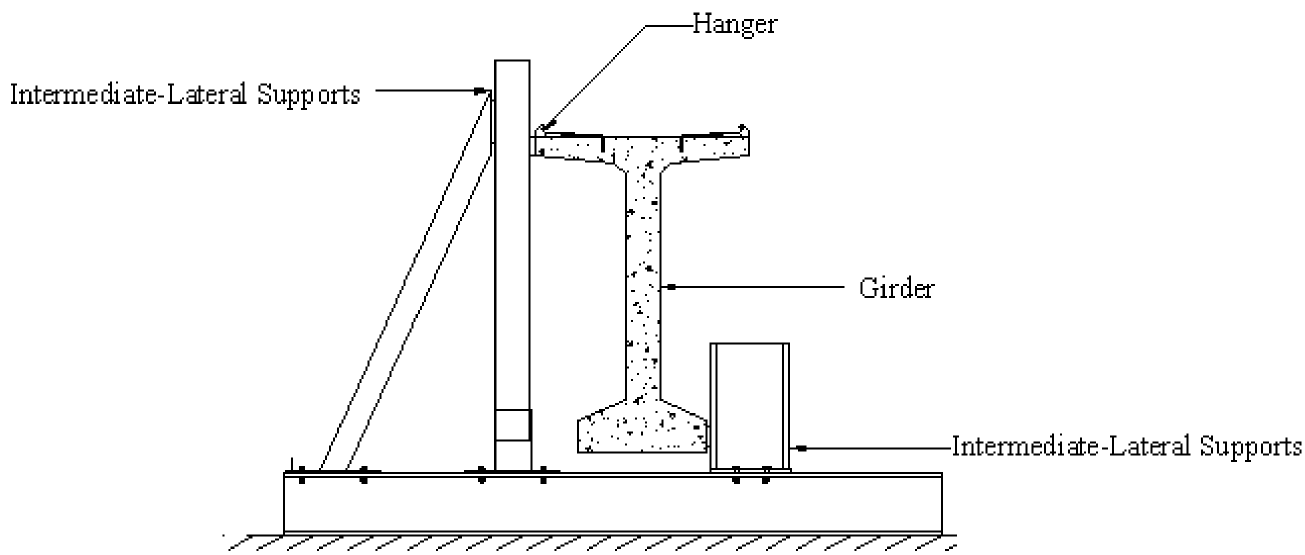

MB-1-L Cross Section at Intermediate-Lateral Support

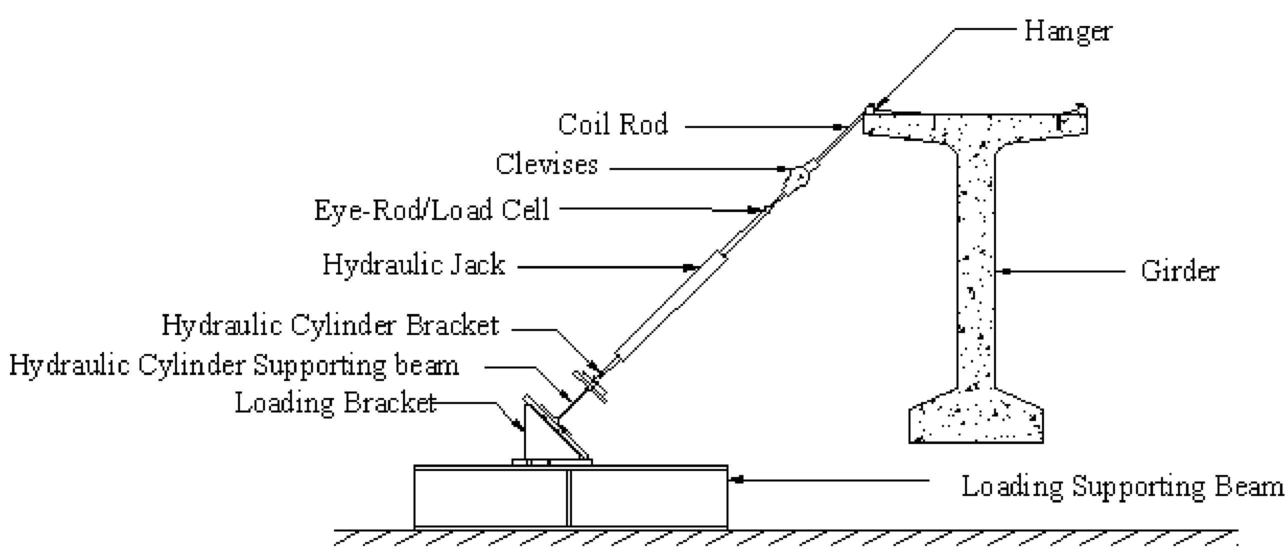

MB-1-L Cross Section at Loading Frame

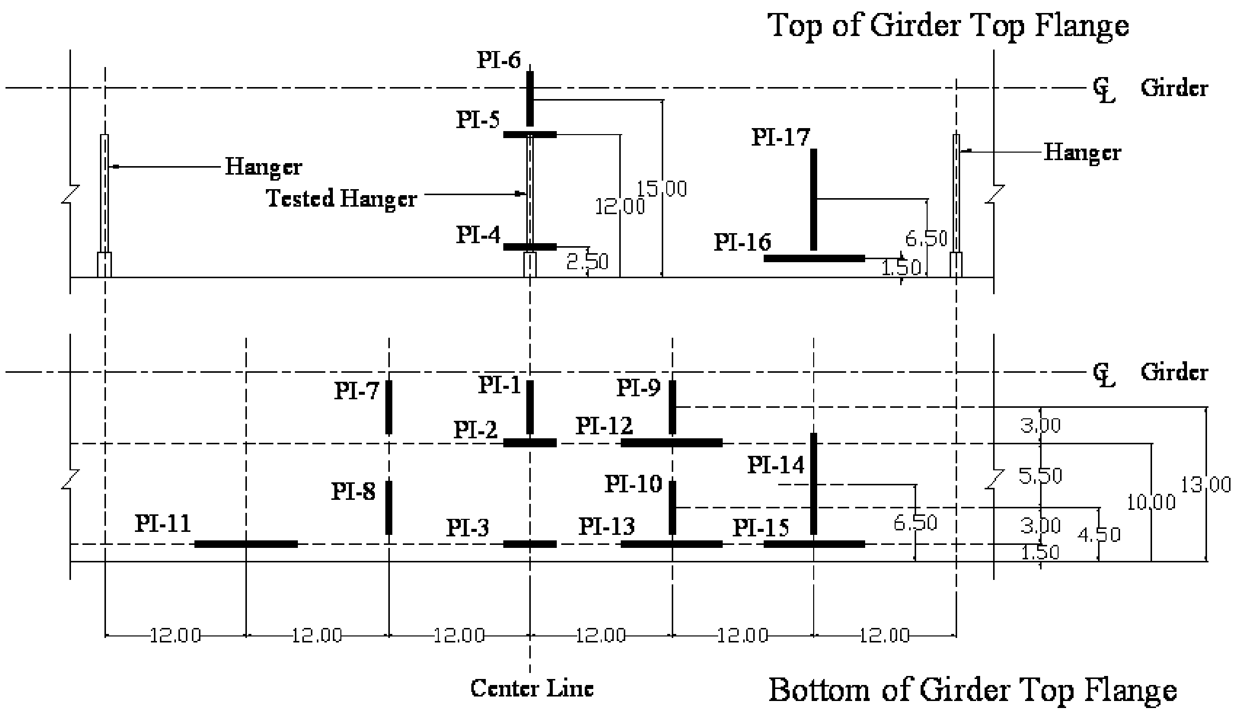

Test MB-1-L Instrumentation – PI-Gauge Assignment

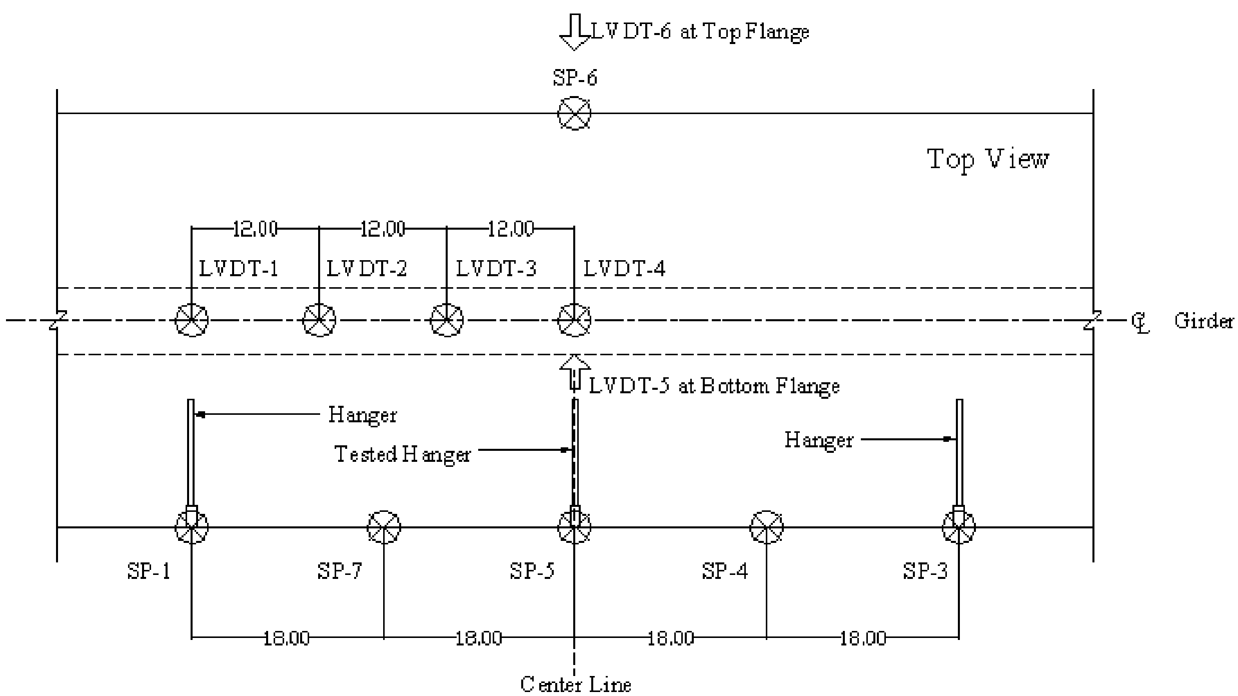

MB-1-L Instrumentation – Linear and String Pot Assignment

MB-1-L Overall Test Set Up

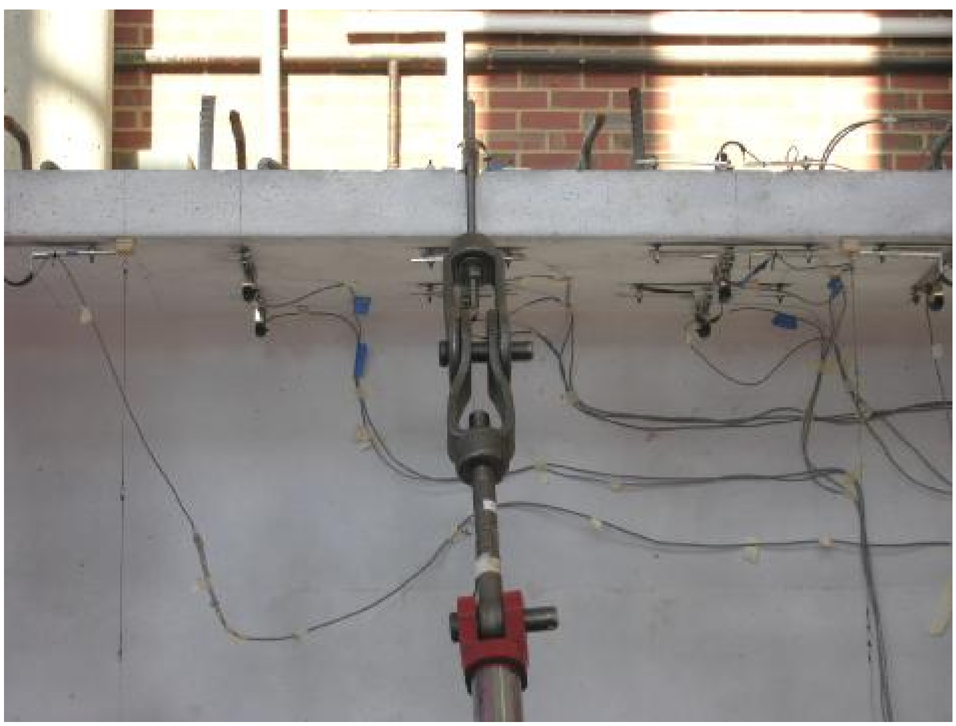

MB-1-L Installment of PI-Gauge

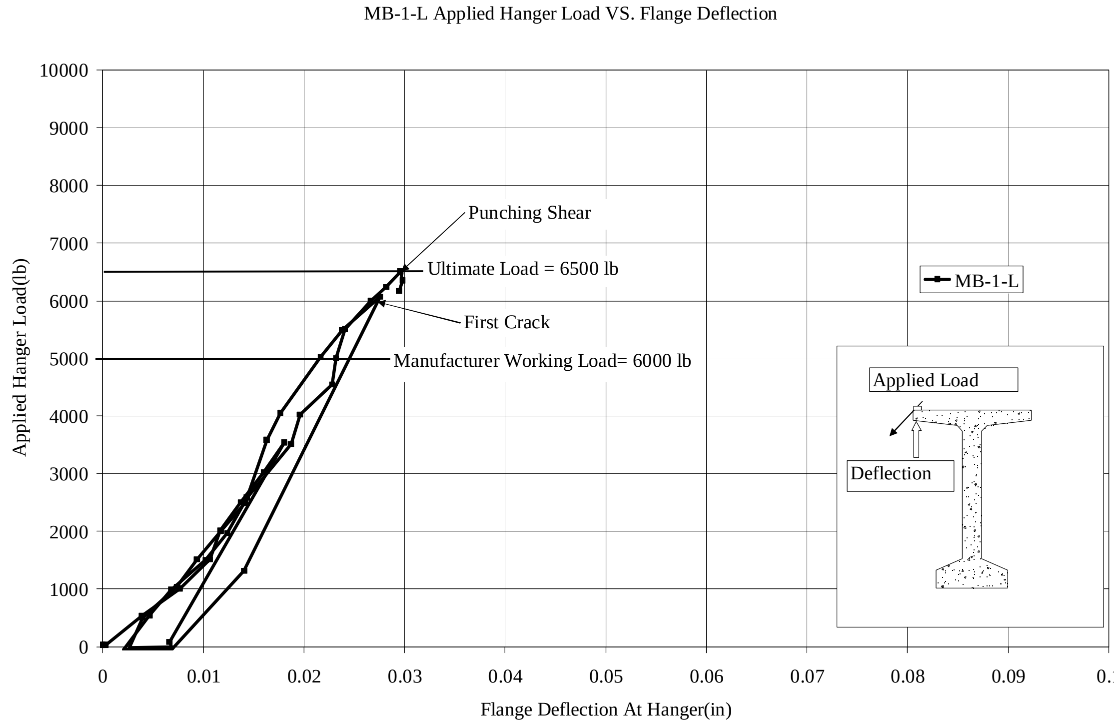

MB-1-L Flange Deflection at Middle of Edge of Flange

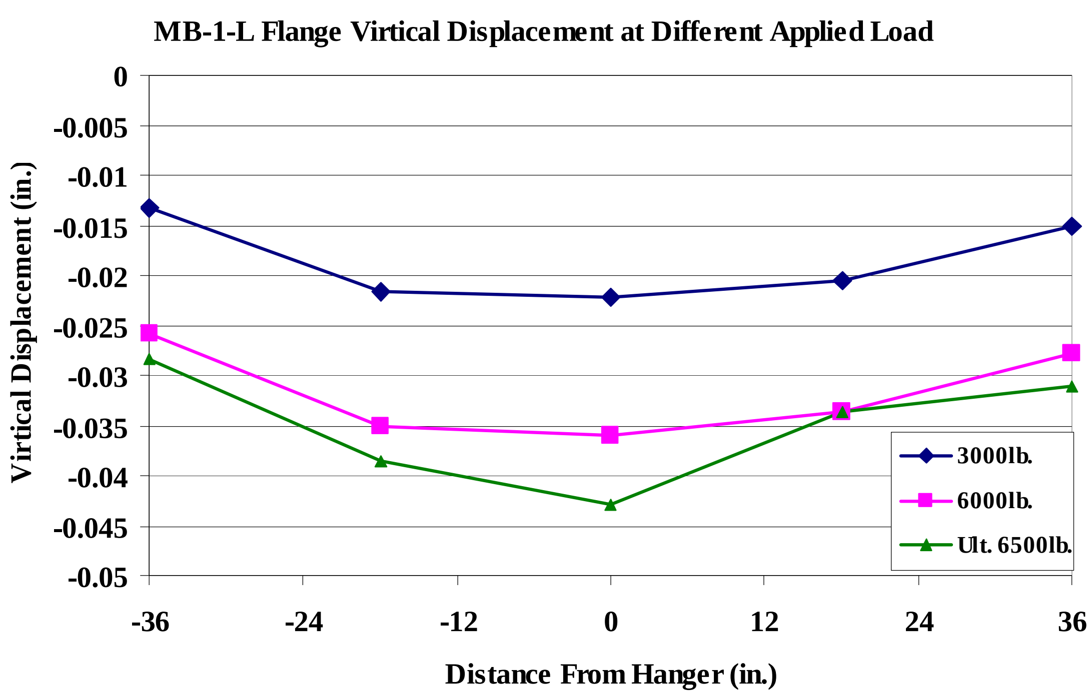

MB-1-L Vertical Displacement at Different Applied Load

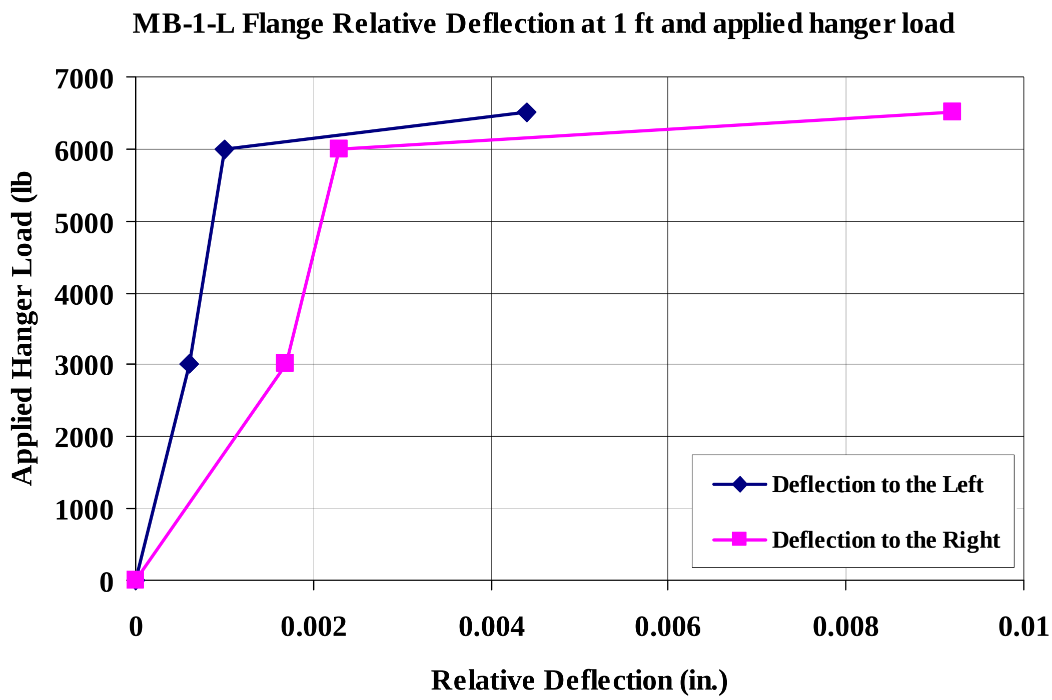

MB-1-L Relative Deflection Between 3ft from the Mid-Span and Mid-Span

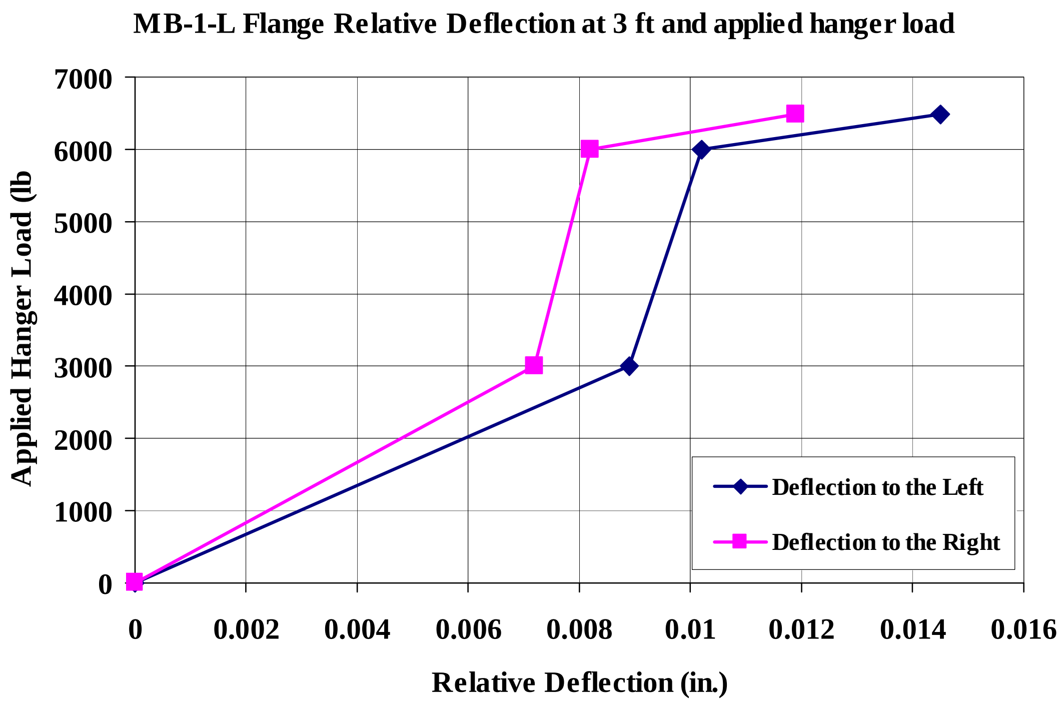

MB-1-L Relative Deflection Between 3ft from the Mid-Span and Mid-Span

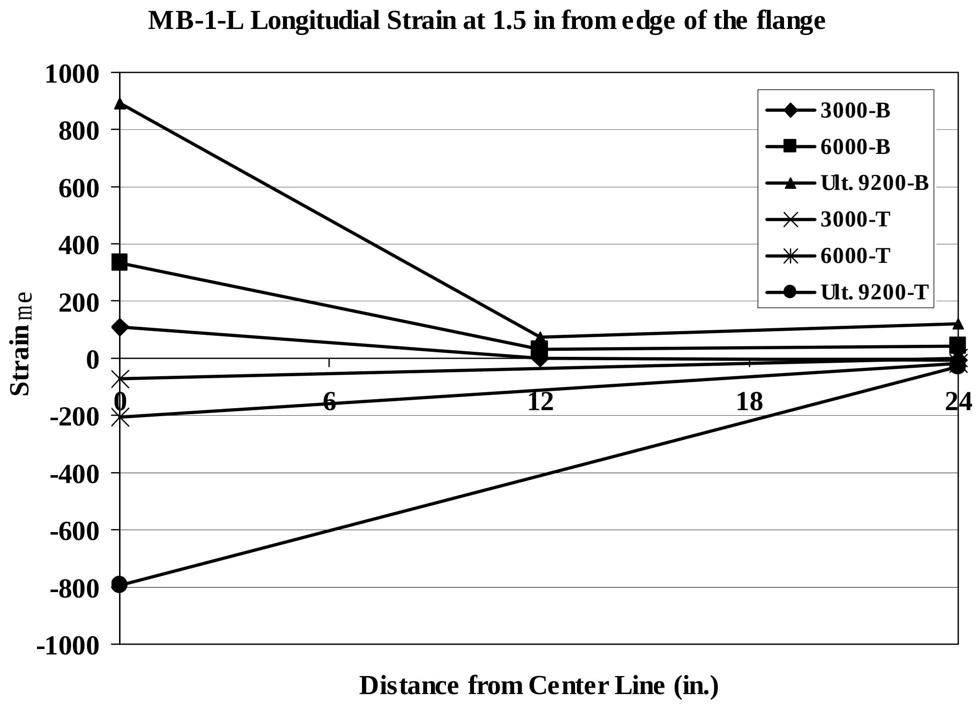

MB-1-L Longitudinal Strain from Top and Bottom along Edge of Flange

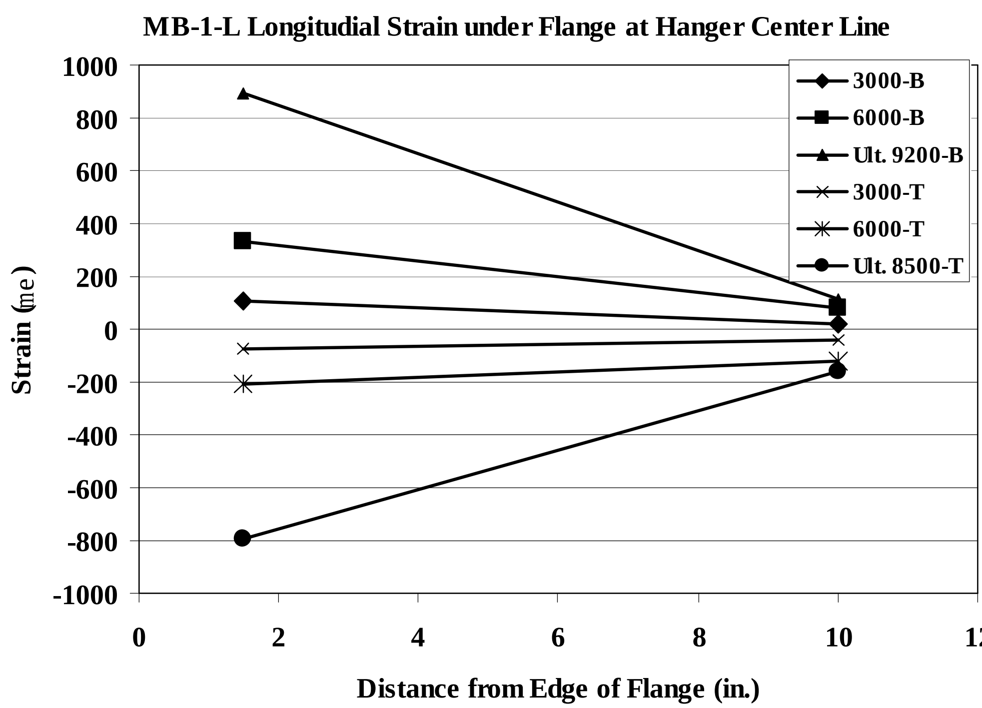

MB-1-L Longitudinal Strain from Top and Bottom at Center Line

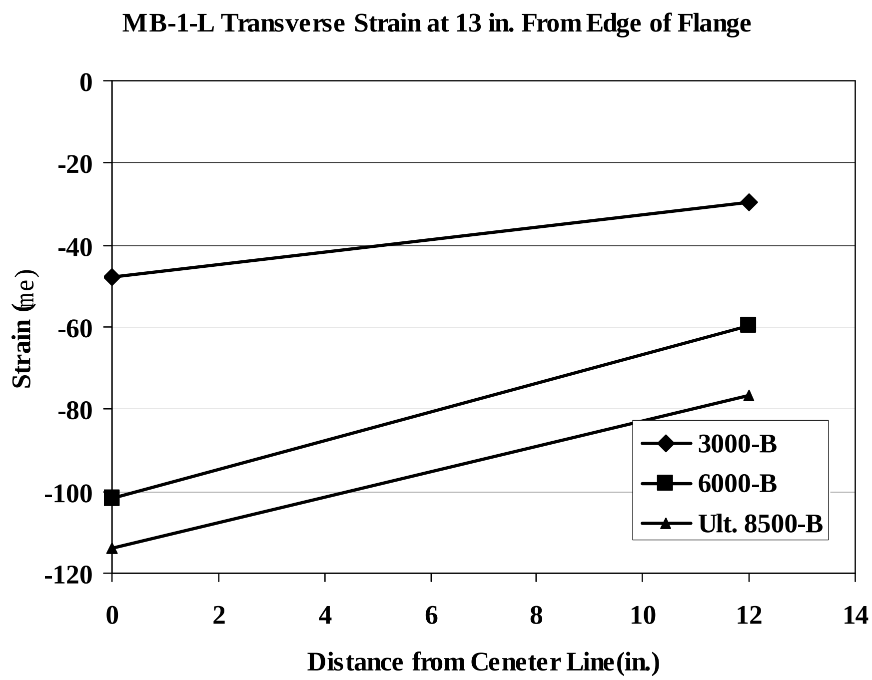

MB-1-L Longitudinal Strain at 13 in. from Edge of Flange

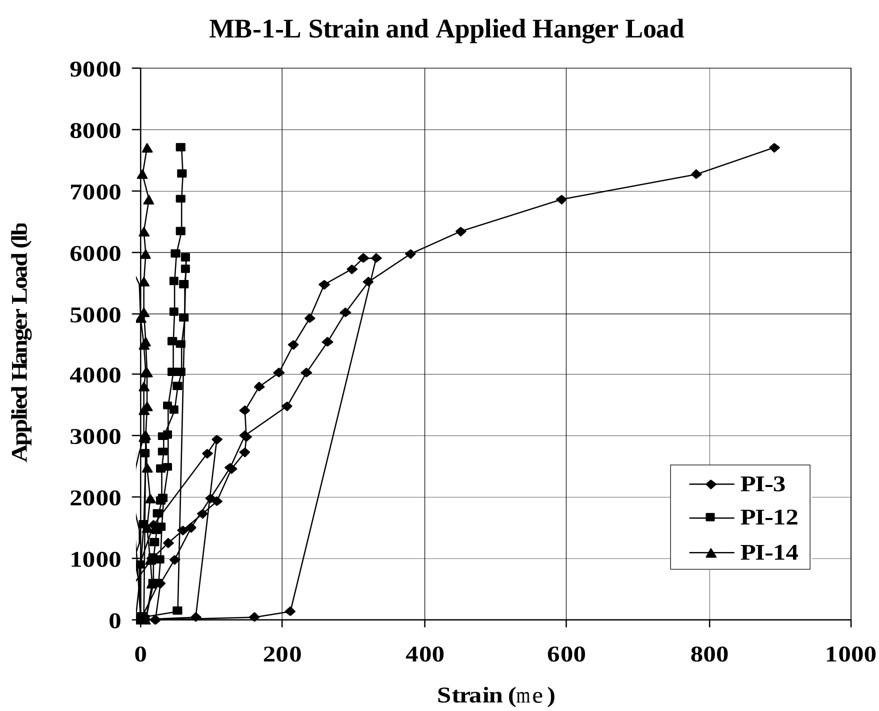

MB-1-L Longitudinal Strain at 1.5 in. from Edge of Flange

MB-1-L Punching Shear Failure

MB-1-L Punching Shear Failure

Appendix G Hanger Test Summary Sheet

Test ID:	MB-2-L (Meadow/Burke Hanger, 2 Pull, Light Reinforcement)
Test Date:	October 1, 2005
Sponsor:	NCDOT
Tested By :	Emmett Sumner, Ph. D., P.E. and Donlawit Ariyasajjakorn, E.I.
Test Location:	Constructed Facilities Laboratory (CFL), NC State University

Test Description

Meadow/Burke hanger, Double hanger pulled by 45 degree angle at middle of girder (Light shear reinforcement).

Hanger: Meadow/Burke hanger HF-43 (Two Legs)

Coil Rod: ½ in. diameter Meadow/Burke Coil Rod, 9000 lb. Safe Working Load

Girder: NCDOT Modified Bulb Tee 63 in.
Concrete Cylinder Strength = 7500 psi

Experimental Results

Maximum Applied Load	= 6500 lb
Maximum Flange Vertical Displacement at Center Line of Test Set Up	= 0.0429 in.
Maximum Flange Vertical Displacement at Hanger	= 0.0429 in.
Maximum Flange Vertical Deflection at Hanger	= 0.0333 in.
Maximum Girder Rotation at Center Line of Test Set Up	= 0.0031 rad
Maximum Girder Vertical Displacement at Center Line of Test Set Up	= 0.0057 in.

Test observations:

At 3000 lb,	nothing was noted at this applied load
At 6000 lb,	first was found at left hanger and propagate slowly to the edge
At 6800 lb,	crack propagated and developed shear cone around the left hanger. Crack width increased while sustain applied load
At 6800 lb,	Punching Shear Failure occurred at left hanger. Small crack was found at the right hanger
At 7700 lb,	Punching Shear Failure occurred at the right hanger

Test#6 MB-2-L

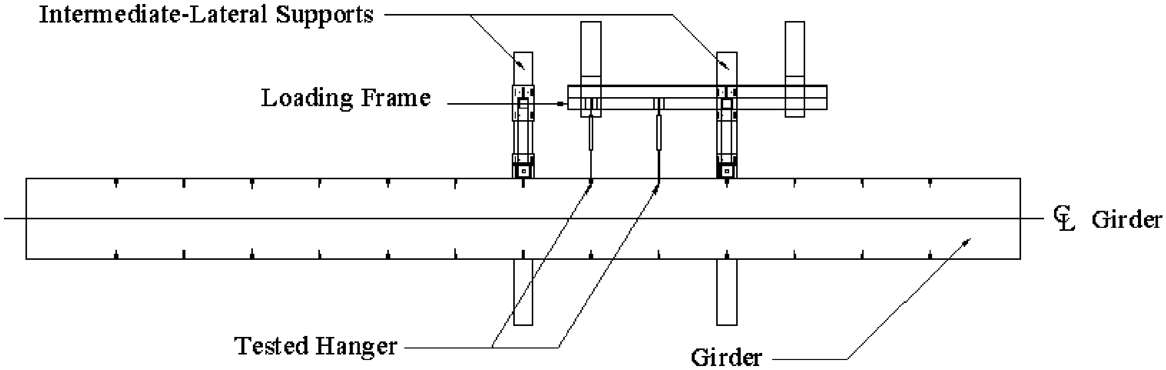

Plan View of Tested Hanger Position

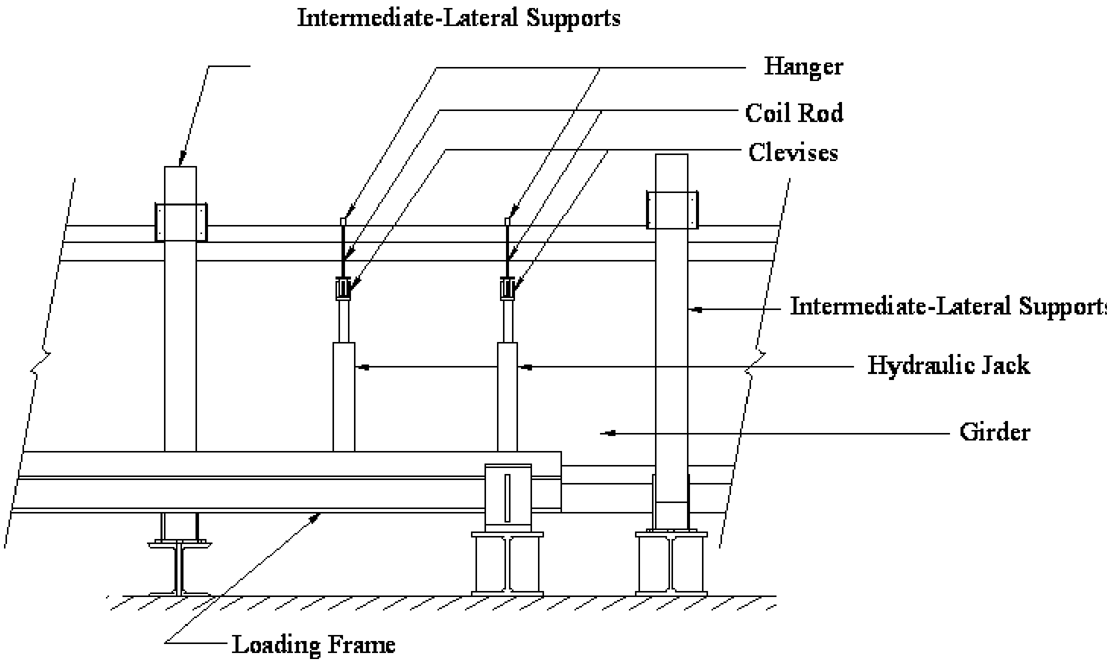

MB-2-L Test Set Up - Elevation

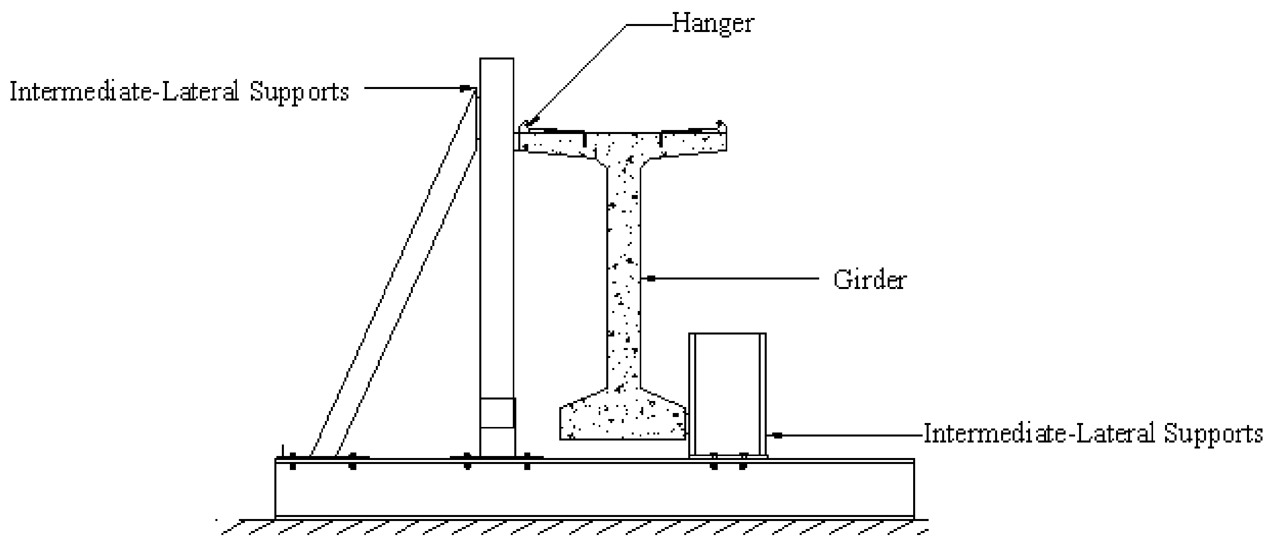

MB-2-L Cross Section at Intermediate-Lateral Support

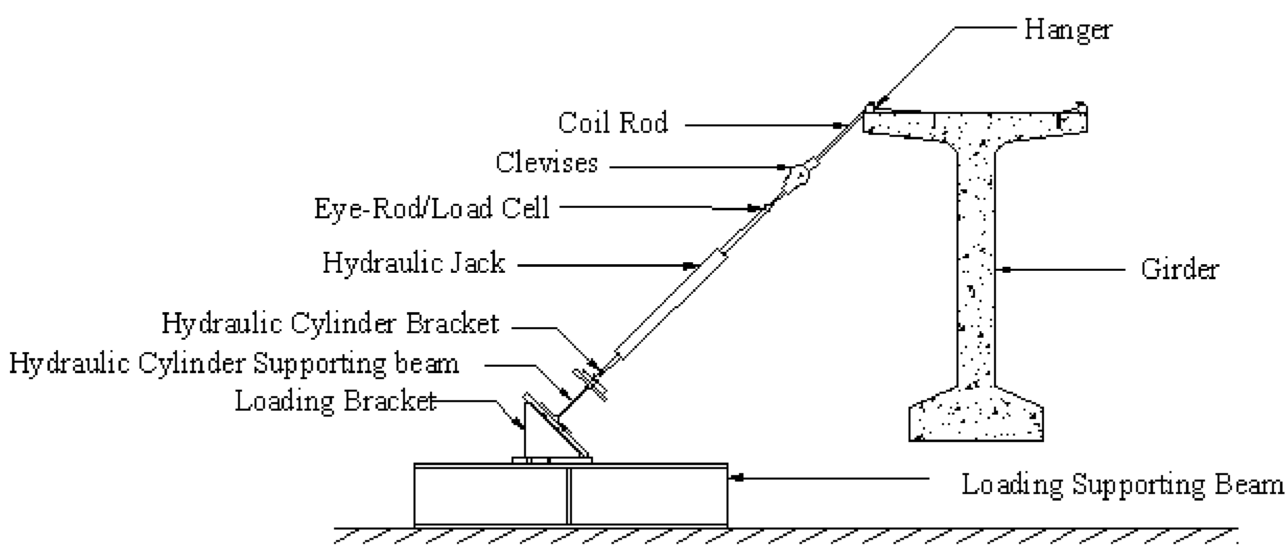

MB-2-L Cross Section at Loading Frame

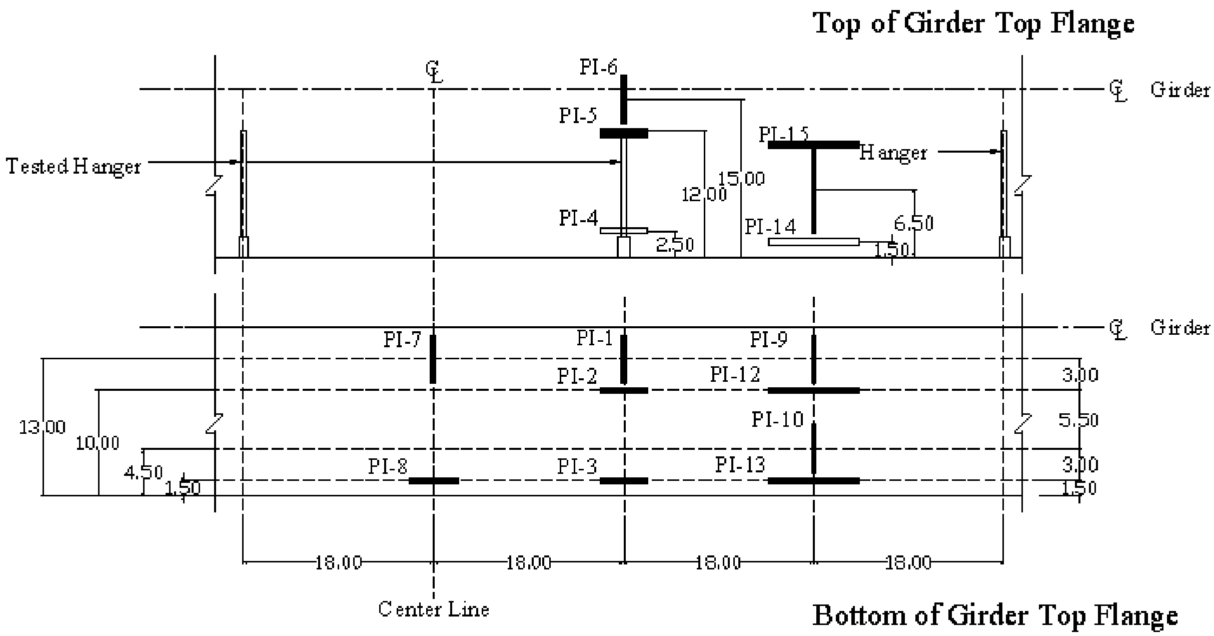

Test MB-2-L Instrumentation – PI-Gauge Layout

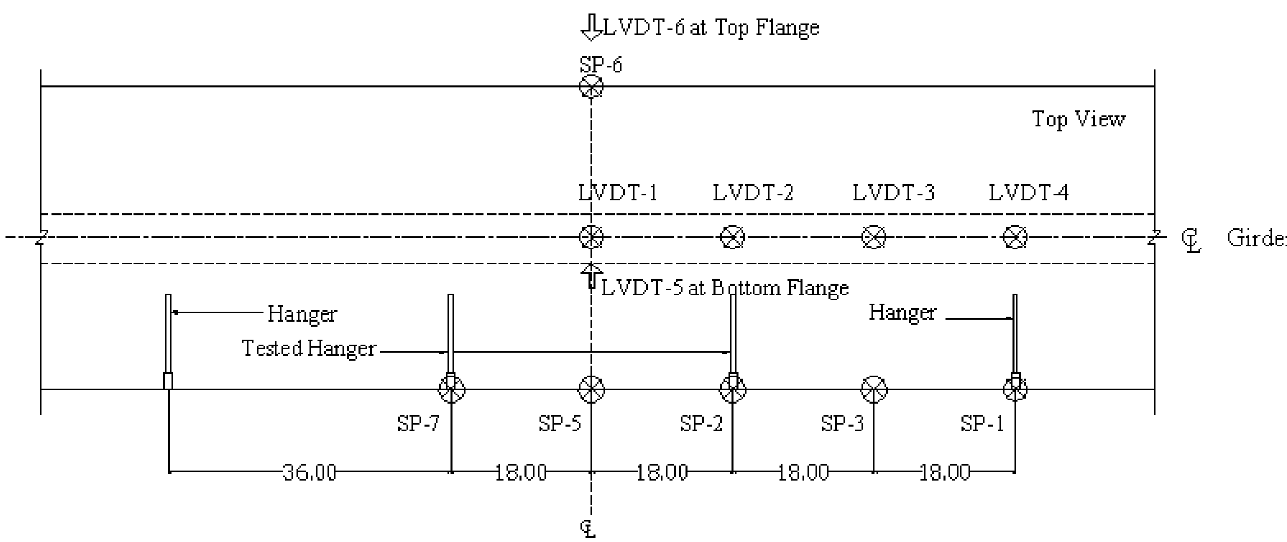

MB-2-L Instrumentation – Linear and String Pot Layout

MB-2-L Overall Test Set Up

MB-2-L Installment of PI-Gauge

MB-2-L Applied Hanger Load VS. Flange Deflection (MB)

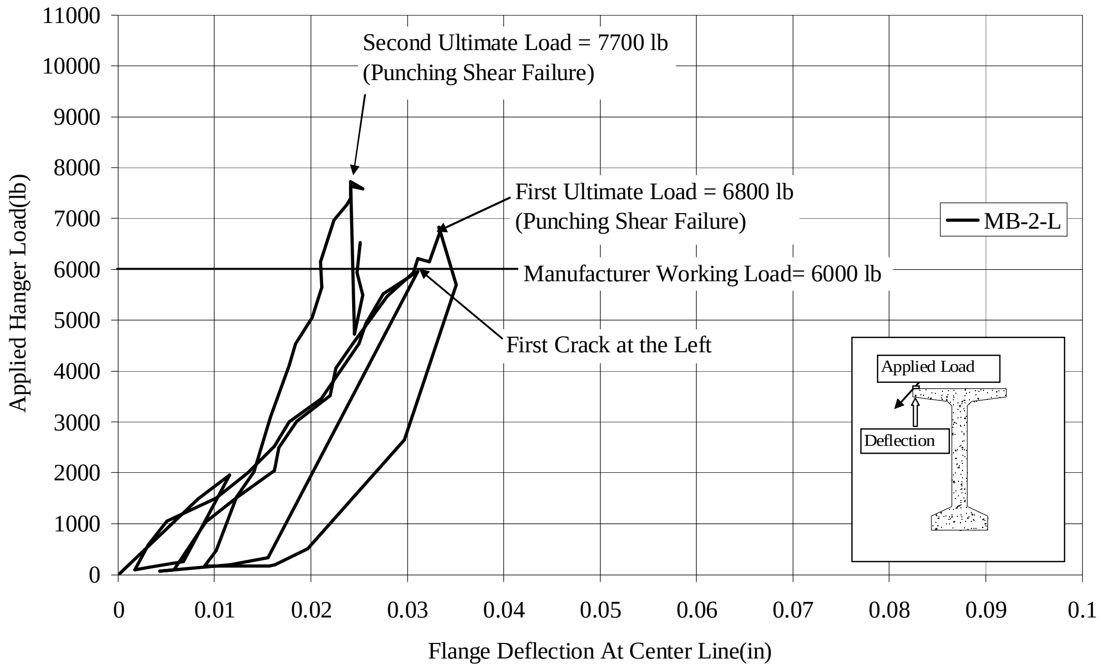

MB-2-L Flange Deflection at Middle of Edge of Flange

MB-2-L Vertical Edge Deflection For Different Applied Hanger Load

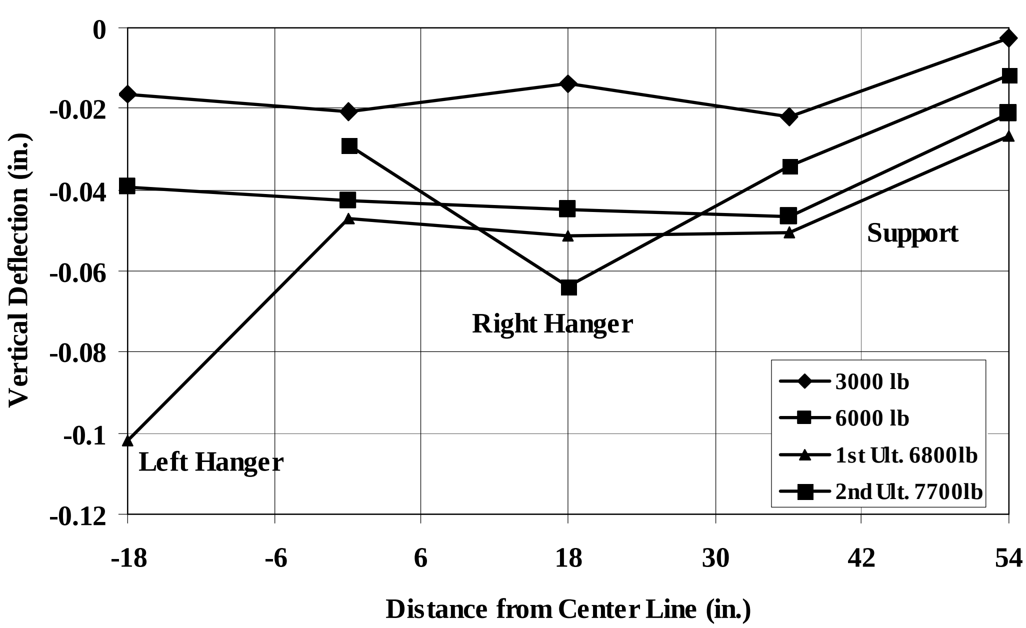

MB-2-L Vertical Displacement at Different Applied Load

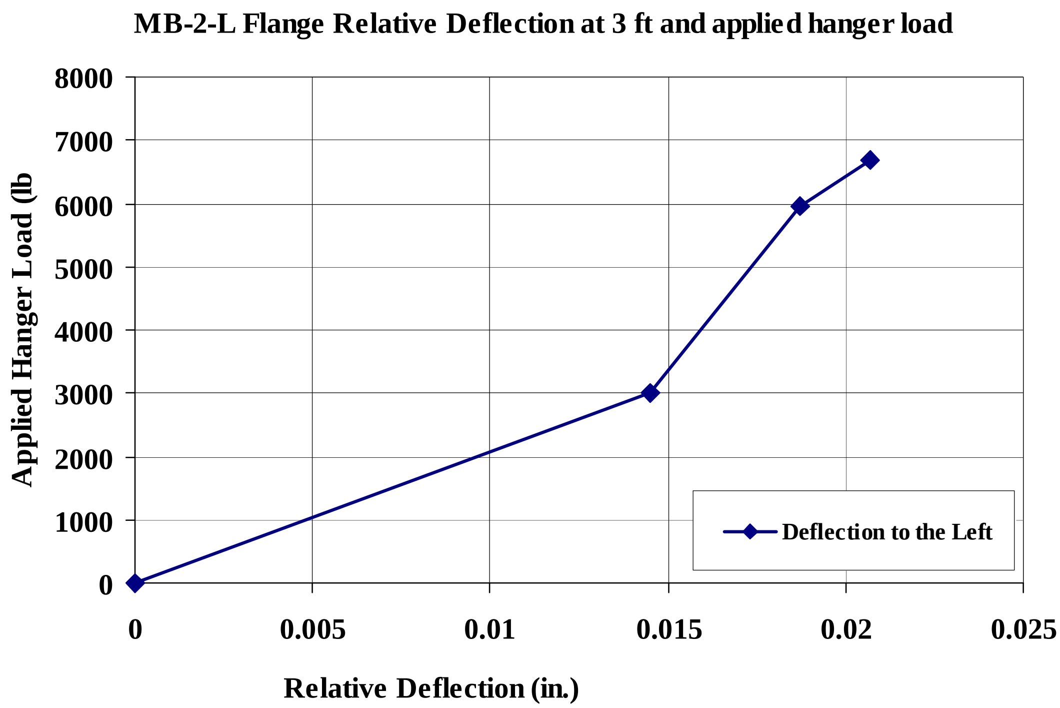

MB-2-L Relative Deflection Between 3ft from the Mid-Span and Mid-Span

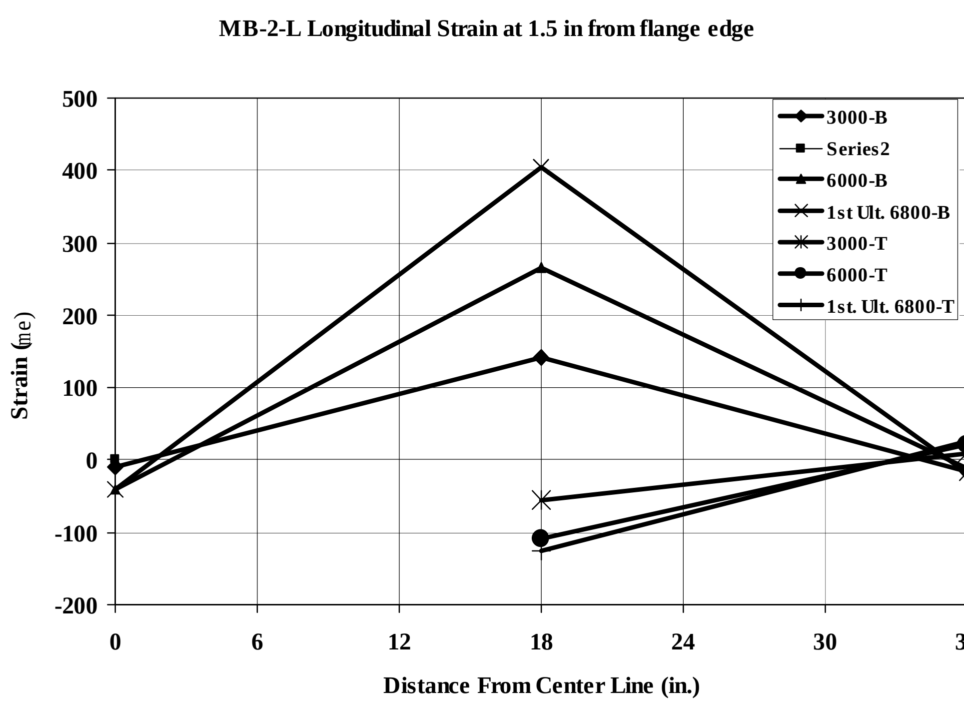

MB-2-L Longitudinal Strain from Top and Bottom along Edge of Flange

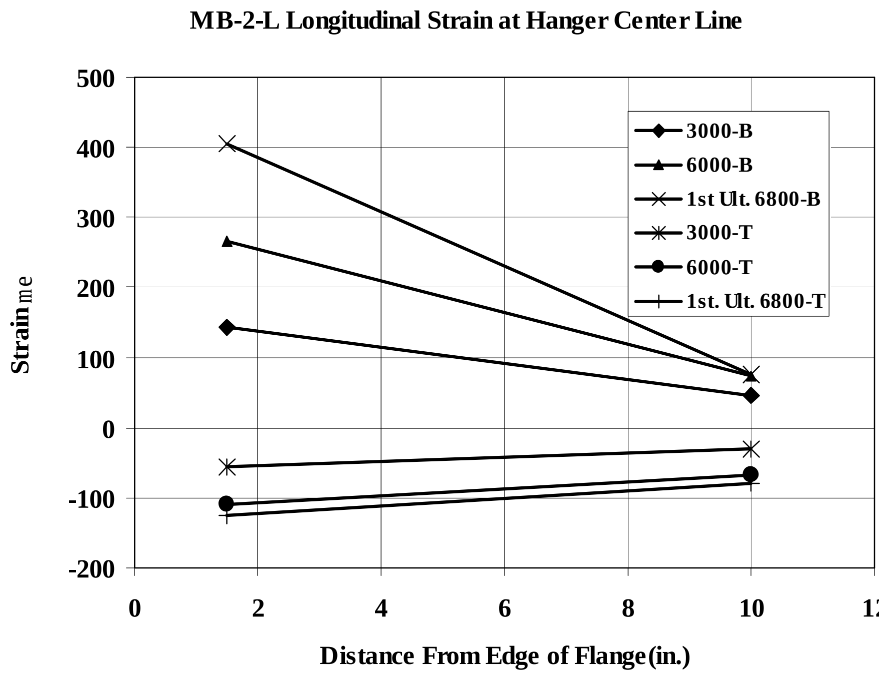

MB-2-L Longitudinal Strain from Top and Bottom at Center Line

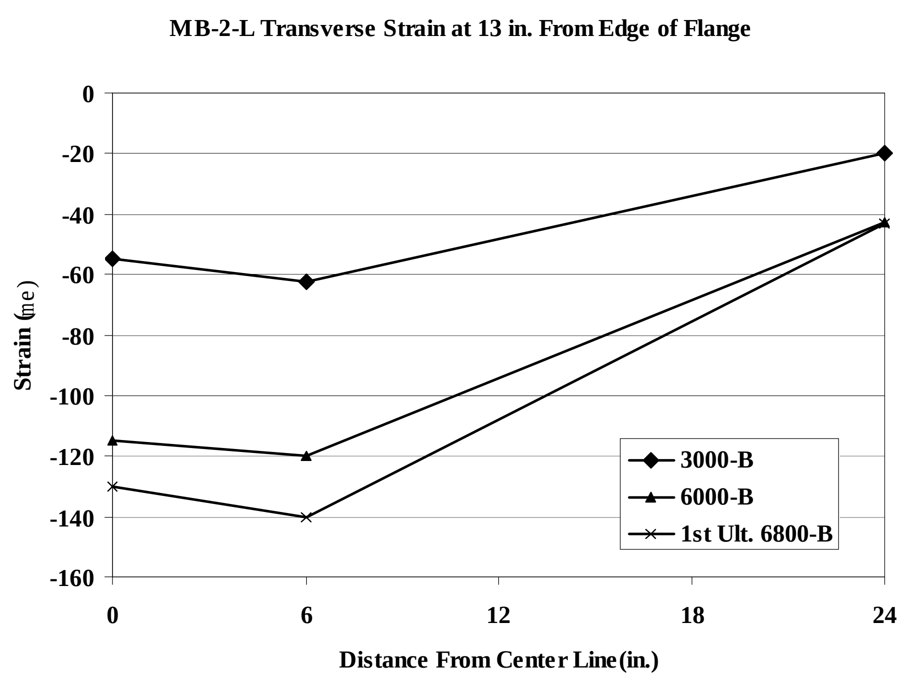

MB-2-L Longitudinal Strain at 13 in. from Edge of Flange

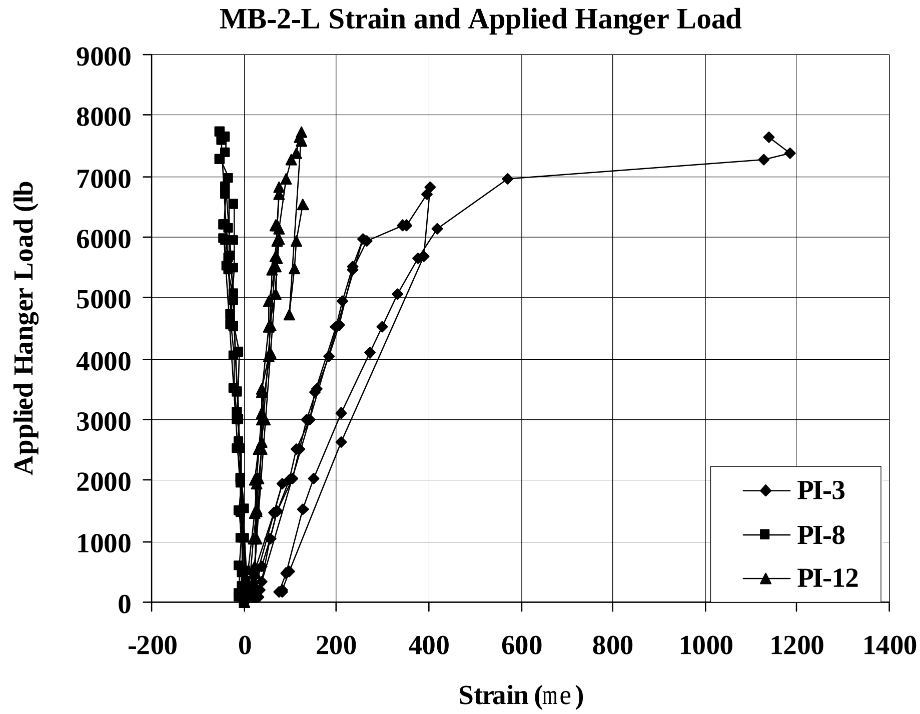

MB-2-L Longitudinal Strain at 1.5 in. from Edge of Flange

MB-2-L Punching Shear Failure at Left Hanger

MB-2-L Punching Shear Failure at Right Hanger

Appendix H Hanger Test Summary Sheet

Test ID: MB-4-L (Meadow/Burke Hanger, Pull, Light Reinforcement)
Test Date: October 4, 2005
Sponsor: NCDOT
Tested By : Emmett Sumner, Ph. D., P.E. and Donlawit Ariyasajjakorn, E.I.
Test Location: Constructed Facilities Laboratory (CFL), NC State University

Test Description

Meadow/Burke hanger, 4 hangers pulled by 45 degree angle at middle of girder (Light shear reinforcement).

Hanger: Meadow/Burke hanger HF-43 (Two Legs)

Coil Rod: ½ in. diameter Meadow/Burke Coil Rod, 9000 lb. Safe Working Load

Girder: NCDOT Modified Bulb Tee 63 in.
Concrete Cylinder Strength = 7500 psi

Experimental Results (First Ultimate)

Maximum Applied Load	= 5800 lb
Maximum Flange Vertical Displacement at Center Line of Test Set Up	= 0.0541 in.
Maximum Flange Vertical Displacement at Hanger	= 0.2062 in.
Maximum Flange Vertical Deflection at Hanger	= 0.0477 in.
Maximum Girder Rotation at Center Line of Test Set Up	= 0.0037 rad
Maximum Girder Vertical Displacement at Center Line of Test Set Up	= 0.0078 in.

Test observations:

At 5000 lb,	first crack was found at Second and Third Hanger and propagate to edge slowly
At 5500 lb,	crack was found at bottom at third hanger. First crack was found at the fourth hanger
At 5800 lb,	Punching Shear Failure occurred at the third hanger
At 6000 lb,	Punching Shear Failure occurred at second hanger. First crack was found at the first hanger
At 6100 lb,	Punching Shear Failure occurred at the fourth hanger
At 6800 lb,	Punching Shear Failure occurred at the first hanger

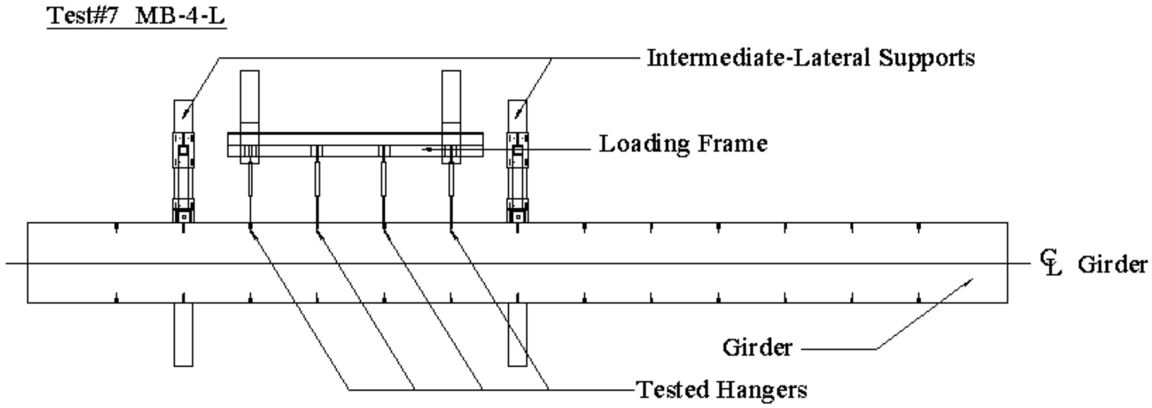

Plan View of Tested Hanger Position

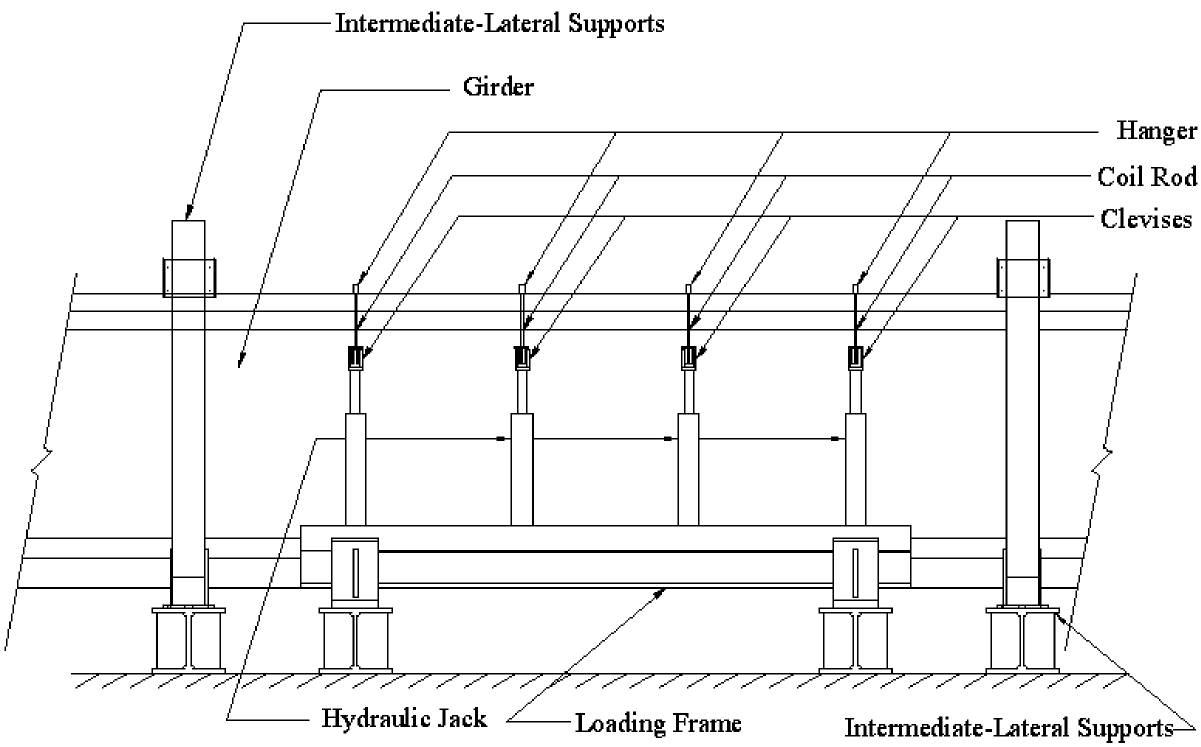

MB-4-L Test Set Up - Elevation

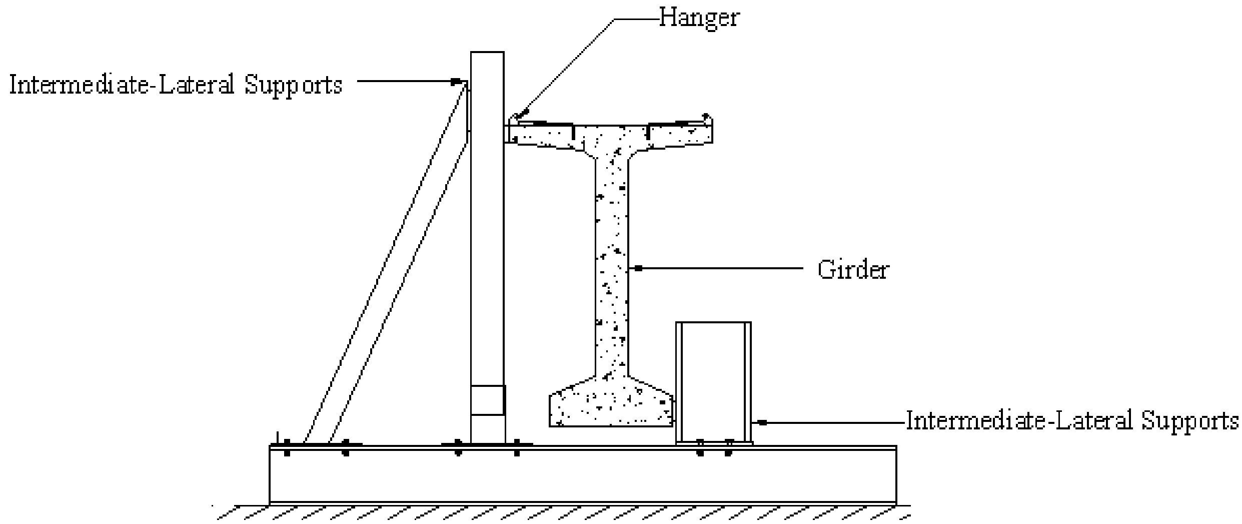

MB-4-L Cross Section at Intermediate-Lateral Support

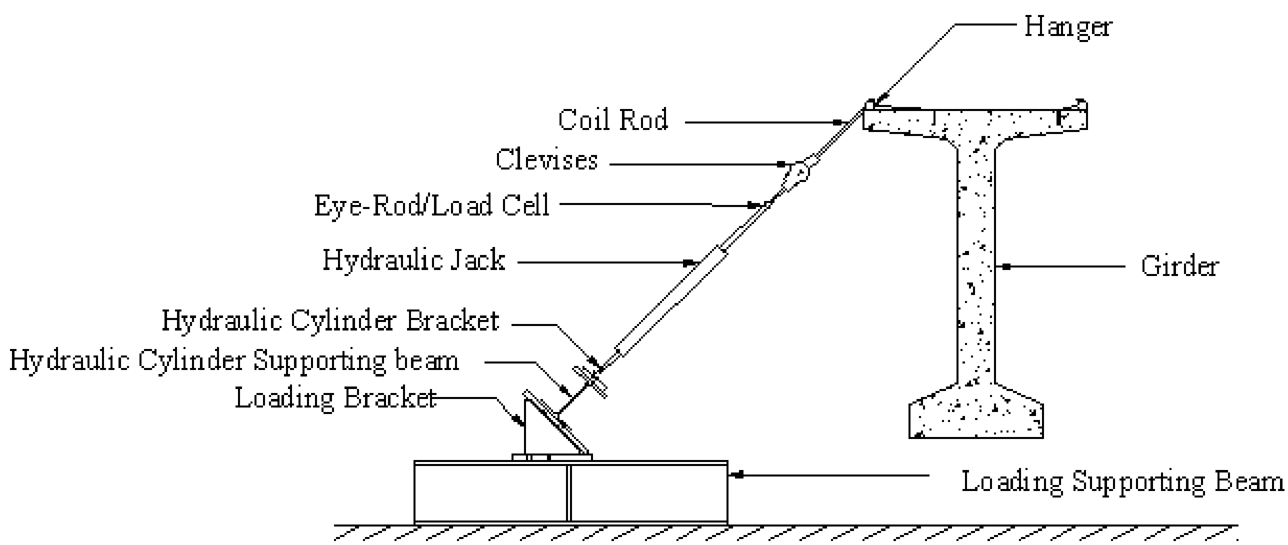

MB-4-L Cross Section at Loading Frame

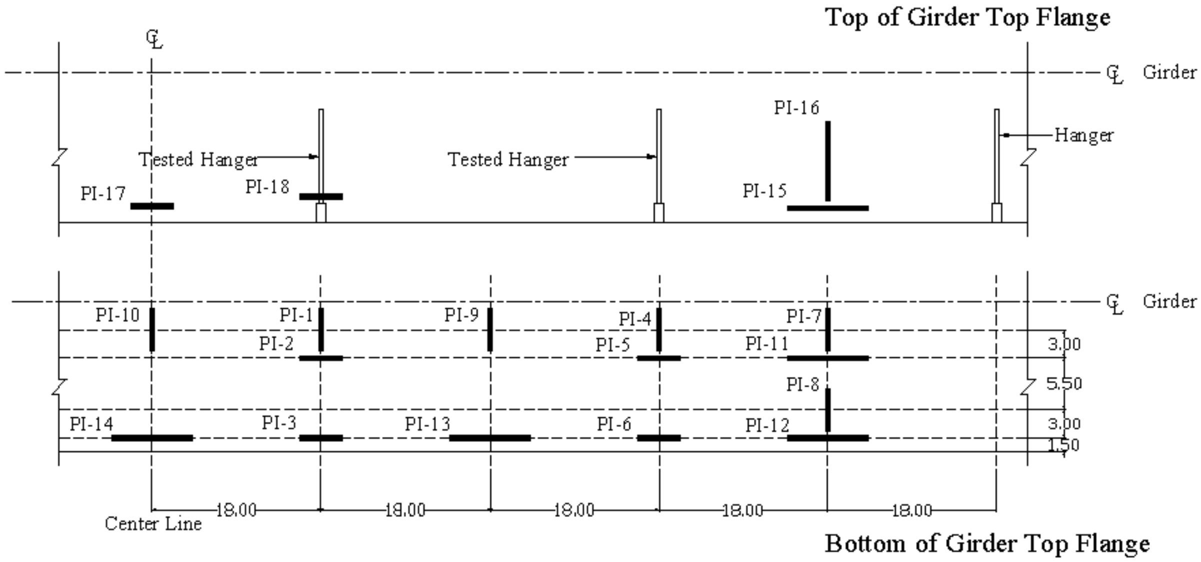

MB-4-L Instrumentation – PI-Gauge Layout

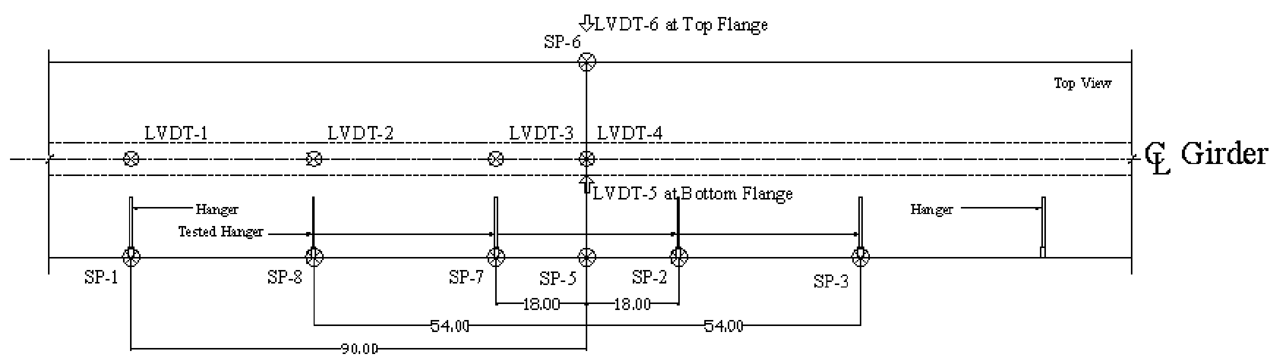

MB-4-L Instrumentation – Linear and String Pot Layout

MB-4-L Overall Test Set Up

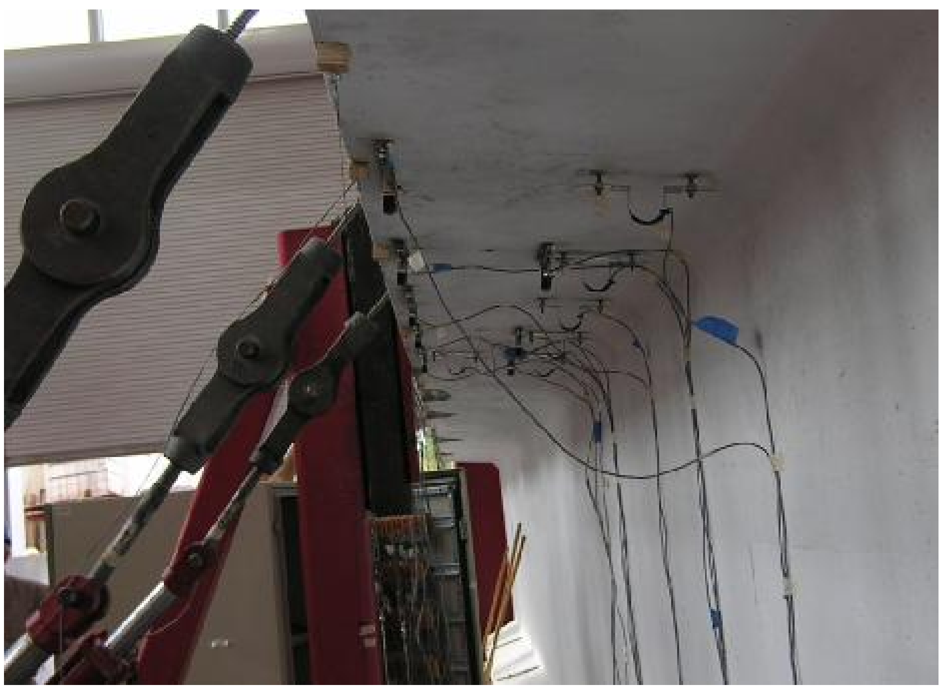

MB-4-L Installment of PI-Gauge

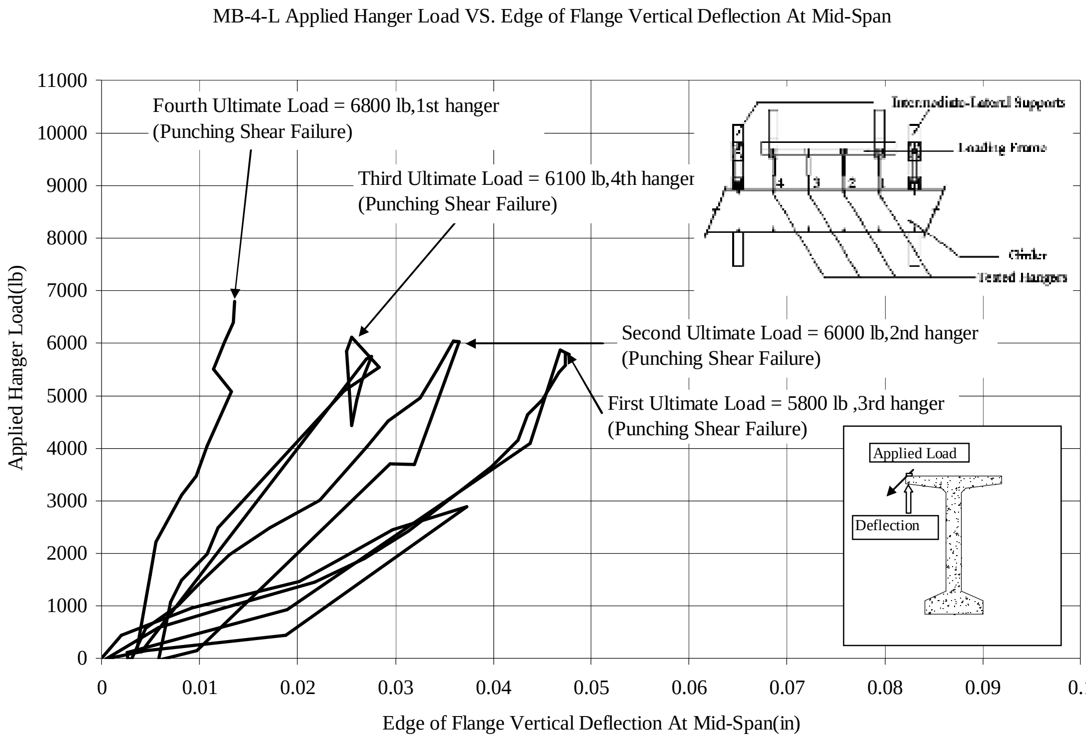

MB-4-L Flange Deflection at Middle of Edge of Flange

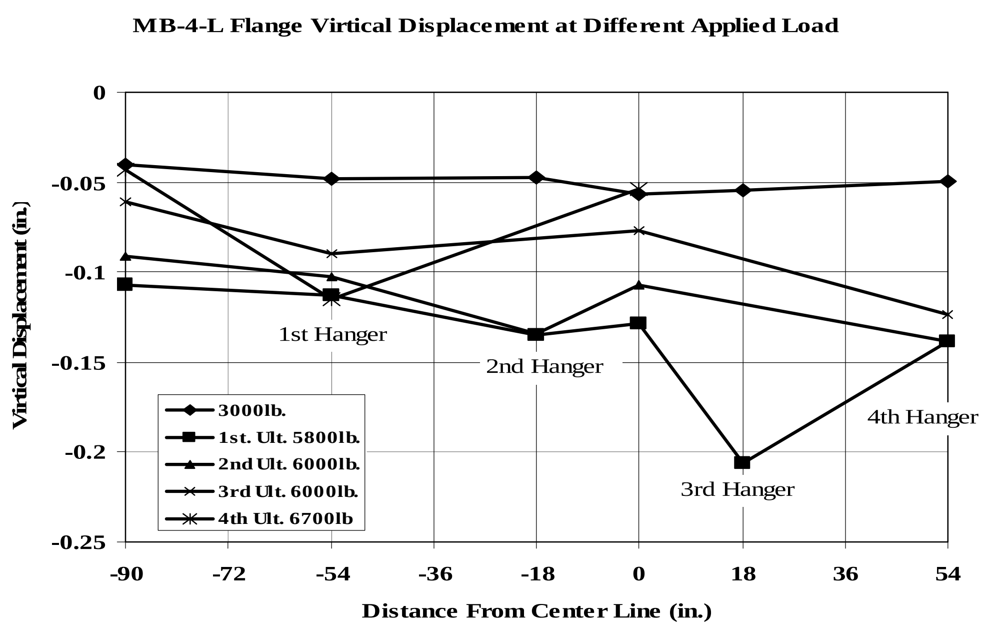

MB-4-L Vertical Displacement at Different Applied Load

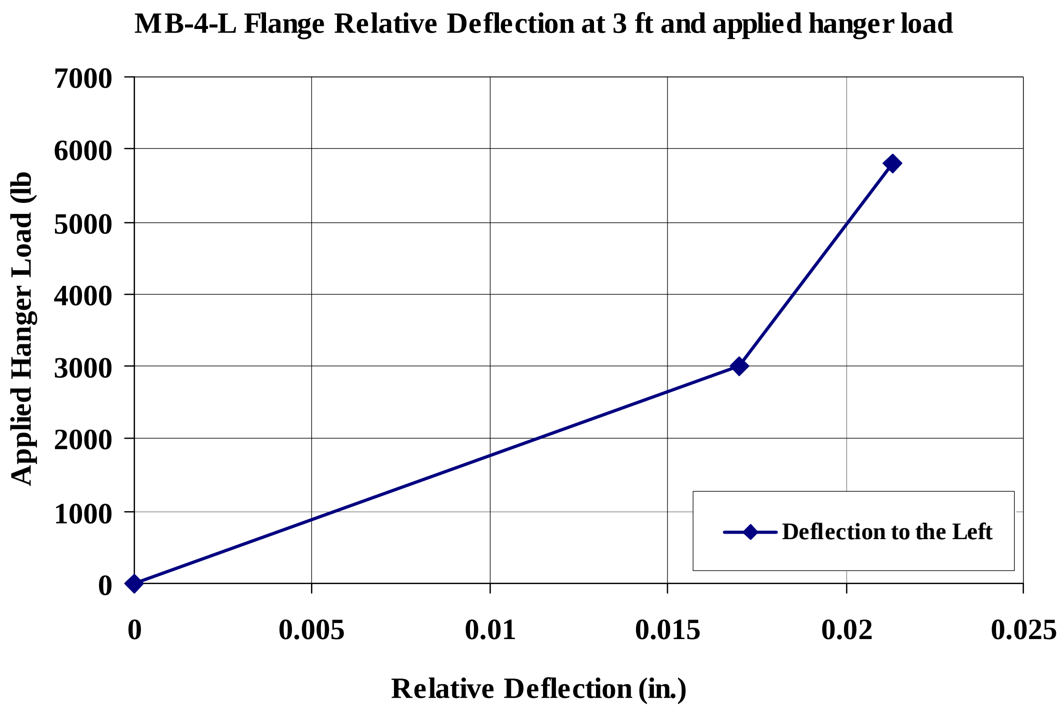

MB-4-L Relative Deflection Between 3ft from the Mid-Span and Mid-Span

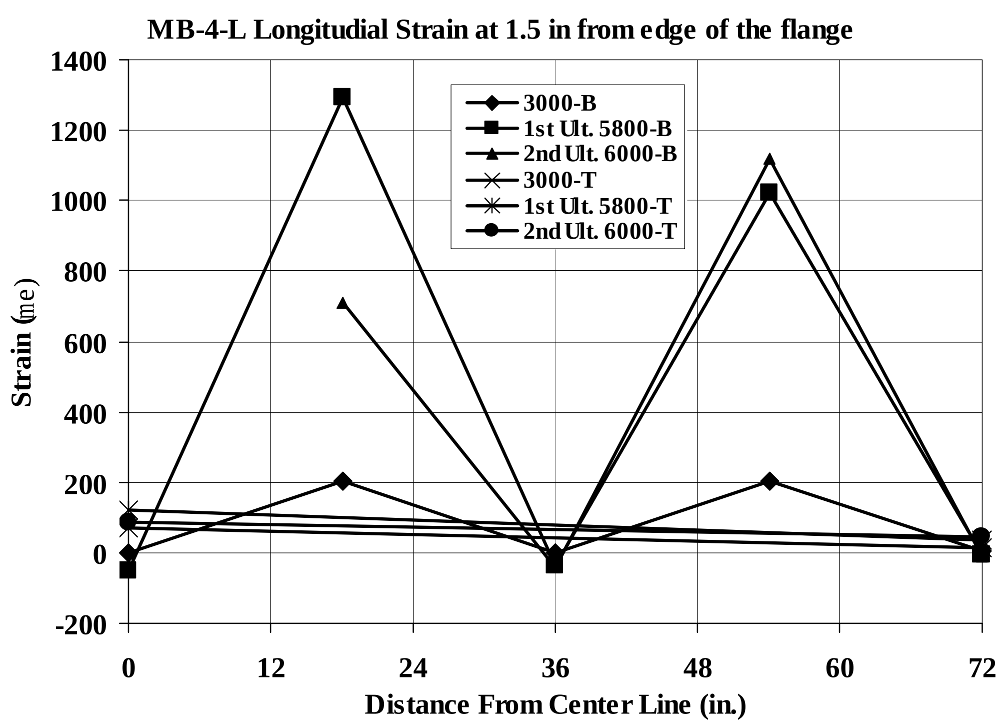

MB-4-L Longitudinal Strain from Top and Bottom along Edge of Flange

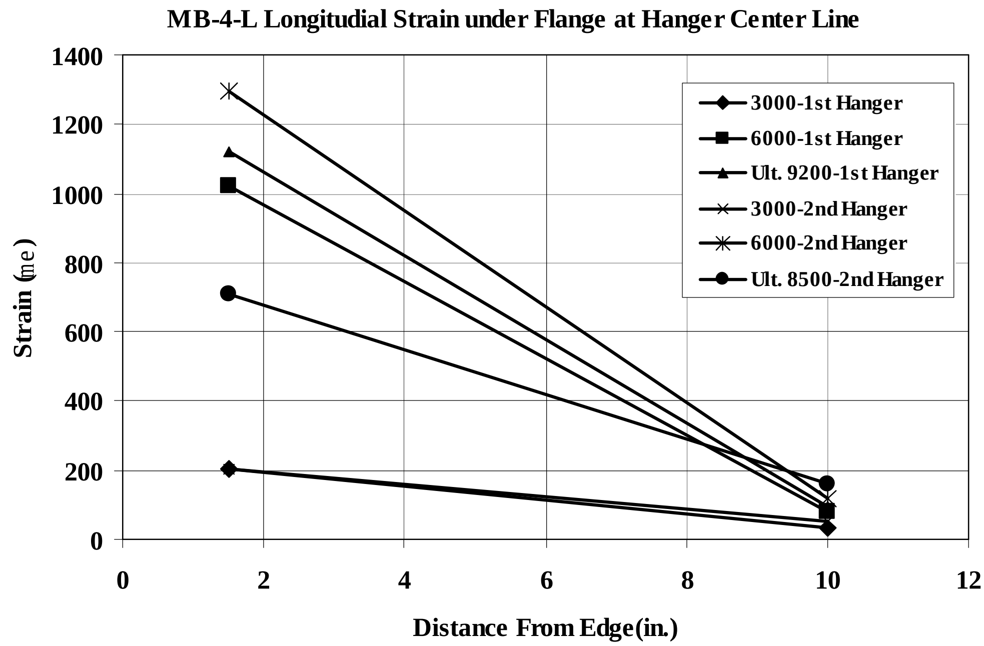

MB-4-L Longitudinal Strain from Top and Bottom at Center Line

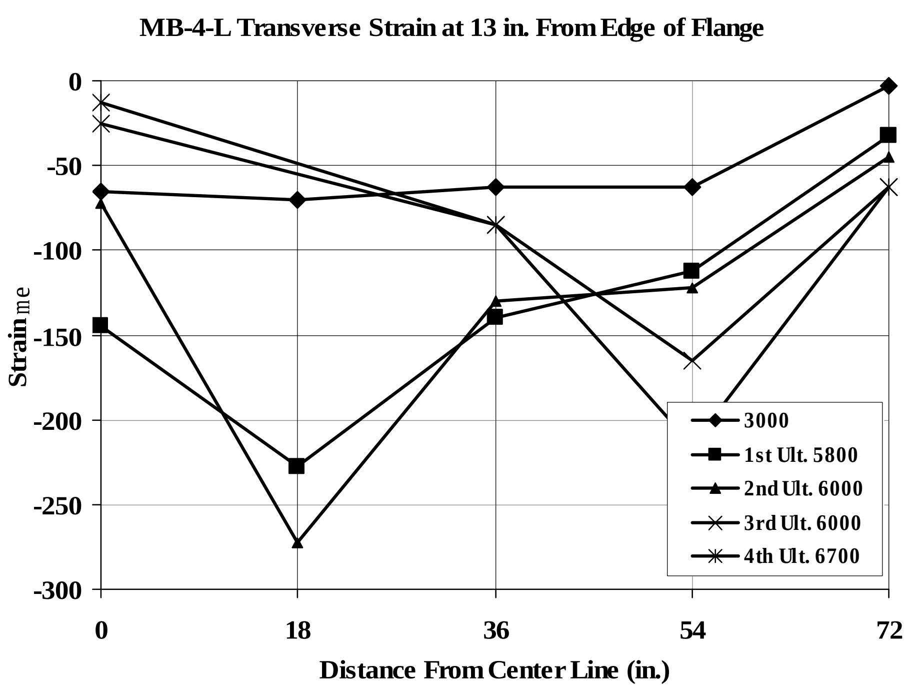

MB-4-L Longitudinal Strain at 13 in. from Edge of Flange

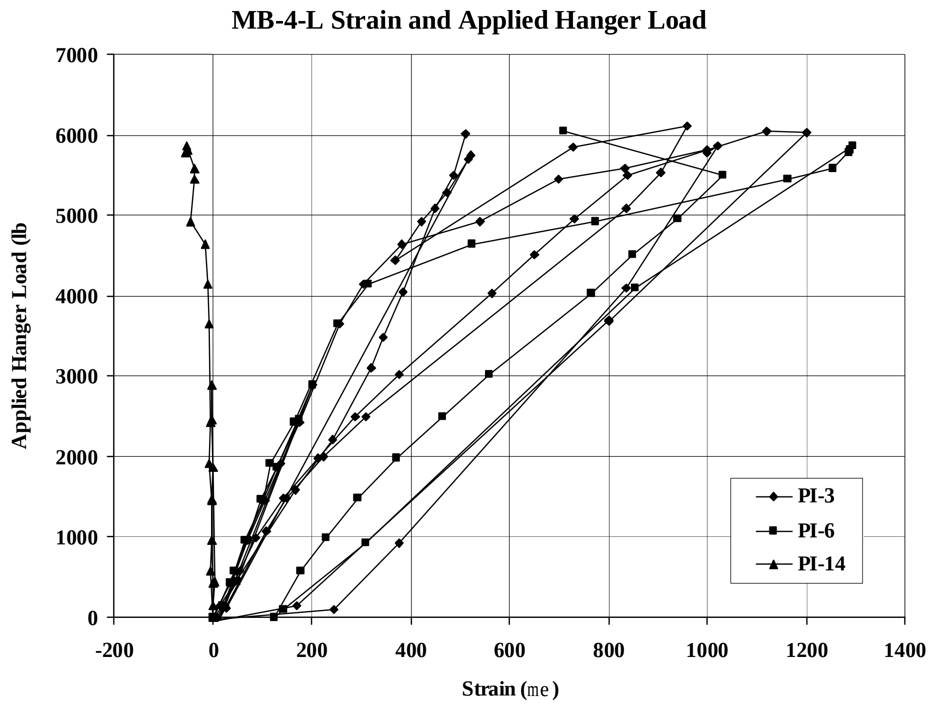

MB-4-H Longitudinal Strain at 1.5 in. from Edge of Flange

MB-4-L Punching Shear Failure at Third Hanger(First Failure)

MB-4-L Second Hanger before Failure (Second Failure)

MB-4-L Punching Shear Failure at the Forth Hanger(Third Failure)

MB-4-L Punching Shear Failure at The First Hanger(Fourth Failure)

Appendix I Finite Element Method Summary Sheet

Test ID:	DR-1 (Dayton Hanger, Single Pull)
Test Date:	September 19, 2005
Sponsor:	NCDOT
Tested By:	Emmett Sumner, Ph. D., P.E. and Donlawit Ariyasajjakorn, E.I.
Program:	ANACAP

Model Description

Dayton/Richmond hanger model, 40 inches Symmetry flange model

Element Type: B8-3D

Material properties

Concrete		Concrete strength	=	7,500	psi
		Young's modulus	=	5,250,000	psi
		Mass Density	=	0.0868	pcf
		Poisson's ratio	=	0.167	
Rebar and Anchor (RT1, RT2, RT3 and Anchor)					
		Yield Strength	=	60,000	psi
		Young's modulus	=	29,000,000	psi
		Poisson's ratio	=	0.3	
Note:	RT1	Area	=	0.622	in^2
	RT2	Area	=	0.311	in^2
	RT3	Area	=	0.151	in^2
Prestressing Strand					
		Grade	=	270	
		Young's modulus	=	28,500,000	psi
		Yield strength	=	100,000	psi
		Ultimate strength	=	118,000	psi
		Area	=	0.153	in^2

Load Type: Static

Experimental Results

Maximum Applied Load	= 11,200	lb
Maximum Flange Vertical Displacement at Center Line	= 0.0449	in.

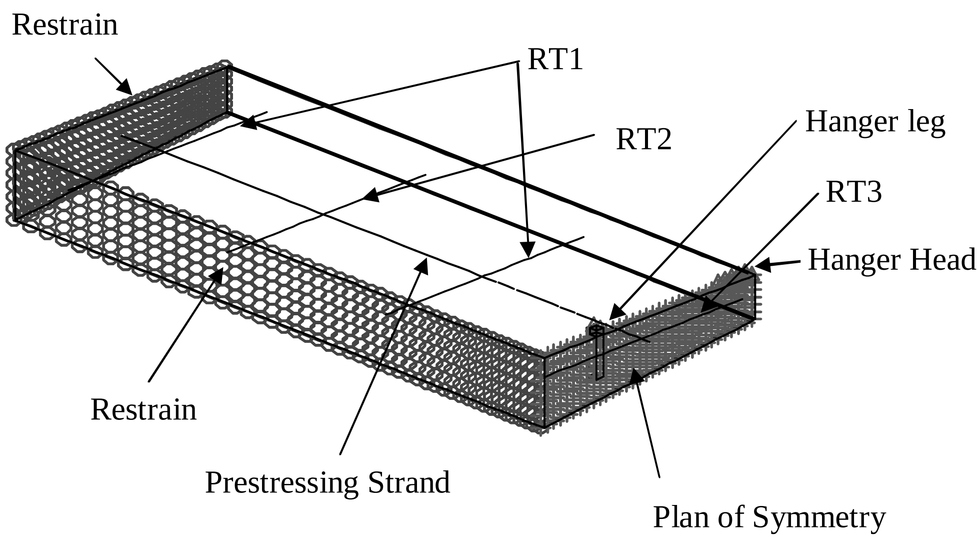

DR-1 Finite element model

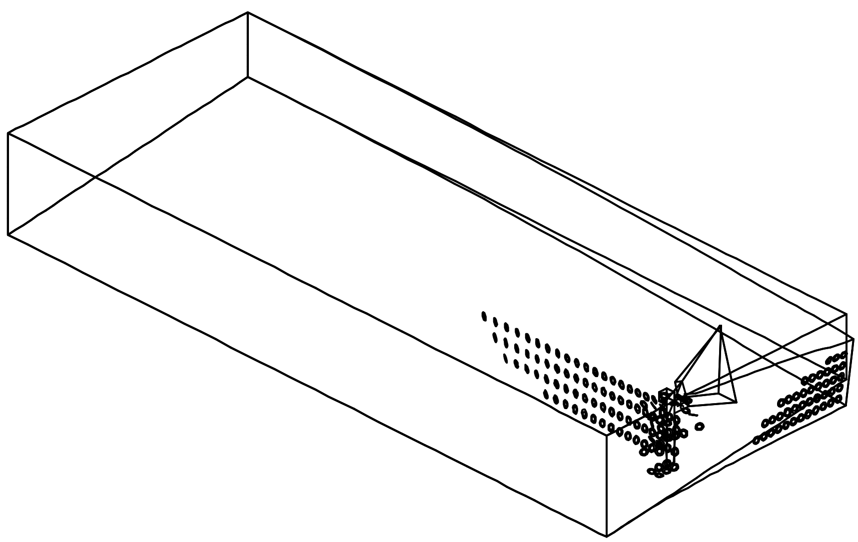

DR-1 Crack pattern at 5,600 lb. applied hanger load

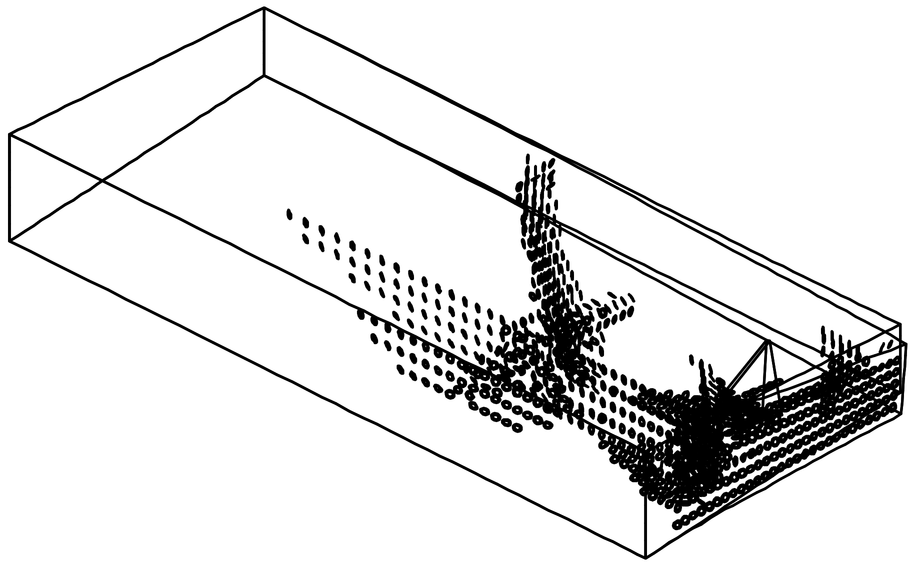

DR-1 Crack Pattern at 11,300 lb. applied hanger load

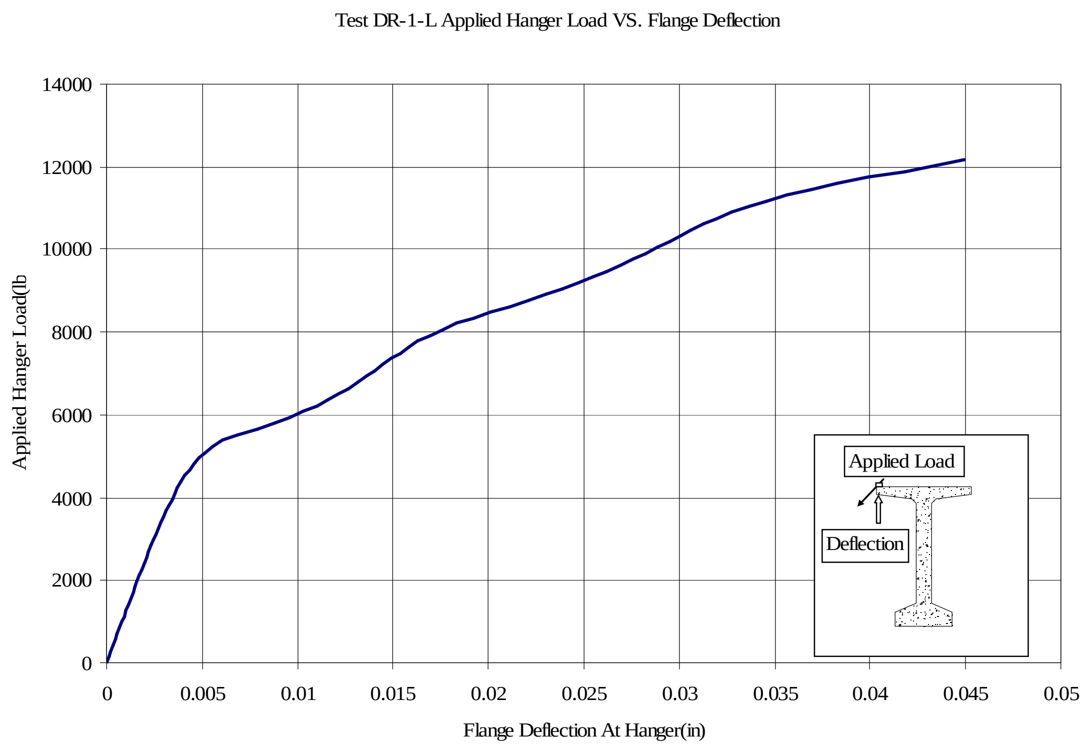

DR-1 Mid-span deflection

Finite Element Method Summary Sheet

Test ID:	DR-2 (Dayton Hanger, Double Pull)
Test Date:	September 19, 2005
Sponsor:	NCDOT
Tested By:	Emmett Sumner, Ph. D., P.E. and Donlawit Ariyasajjakorn, E.I.
Program:	ANACAP

Model Description

Dayton/Richmond hanger model, 58 inches Symmetry flange model

Element Type: B8-3D

Material properties

<u>Concrete</u>		Concrete strength	=	7,500	psi
		Young's modulus	=	5,250,000	psi
		Mass Density	=	0.0868	pcf
		Poisson's ratio	=	0.167	
<u>Rebar and Anchor</u> (RT1, RT2 and Anchor)					
		Yield Strength	=	60,000	psi
		Young's modulus	=	29,000,000	psi
		Poisson's ratio	=	0.3	
Note:	RT1	Area	=	0.622	in^2
	RT2	Area	=	0.311	in^2
<u>Prestressing Strand</u>					
		Grade	=	270	
		Young's modulus	=	28,500,000	psi
		Yield strength	=	100,000	psi
		Ultimate strength	=	118,000	psi
		Area	=	0.153	in^2

Load Type: Static

Experimental Results

Maximum Applied Load	= 12,300	lb
Maximum Flange Vertical Displacement at Center Line	= 0.0328	in.
Maximum Flange Vertical Displacement	= 0.0480	in.

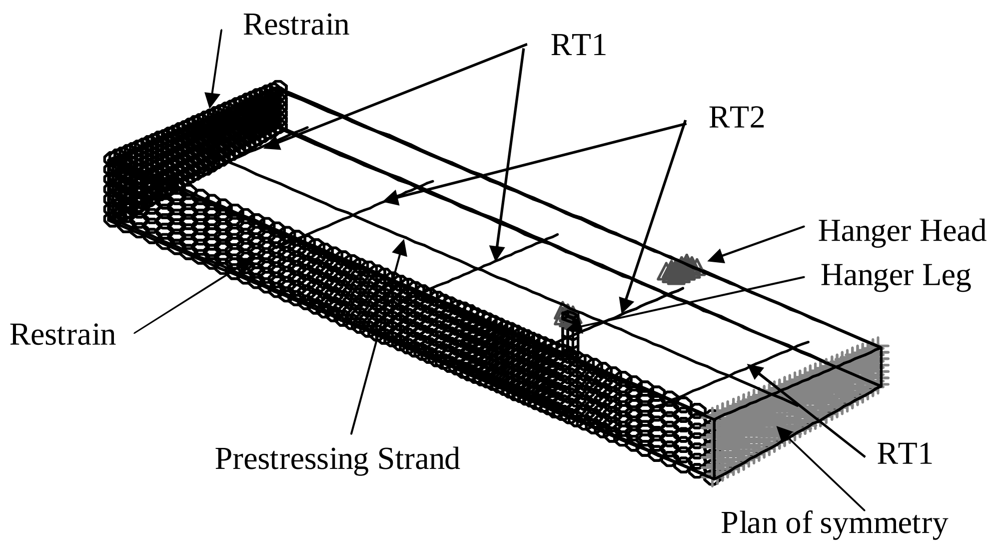

DR-2 Finite Element Model

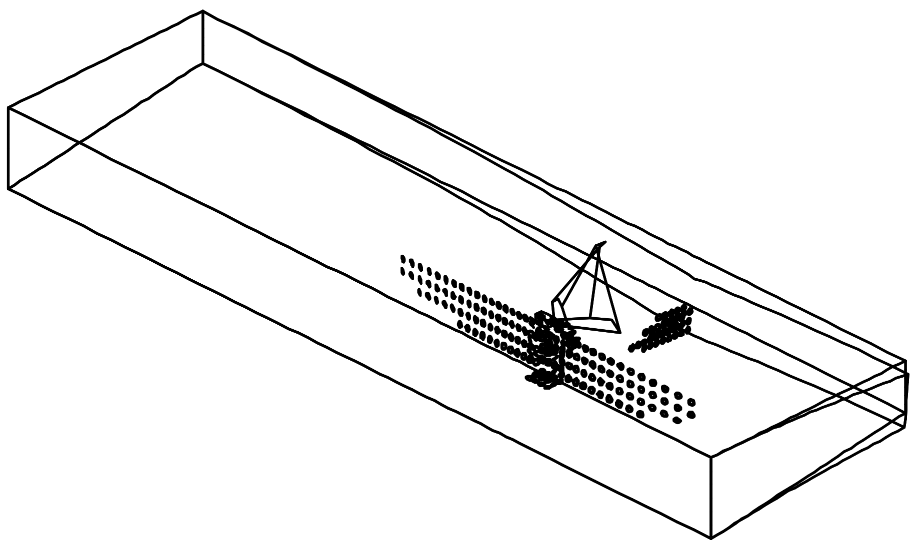

DR-2 Crack pattern at 5,600 lb. applied hanger load

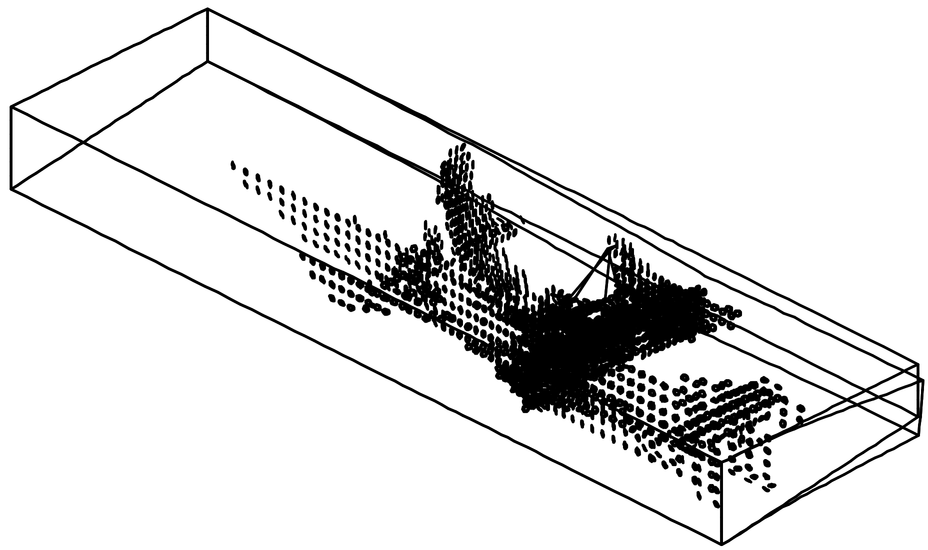

DR-2 Crack Pattern at 11,300 lb. applied hanger load

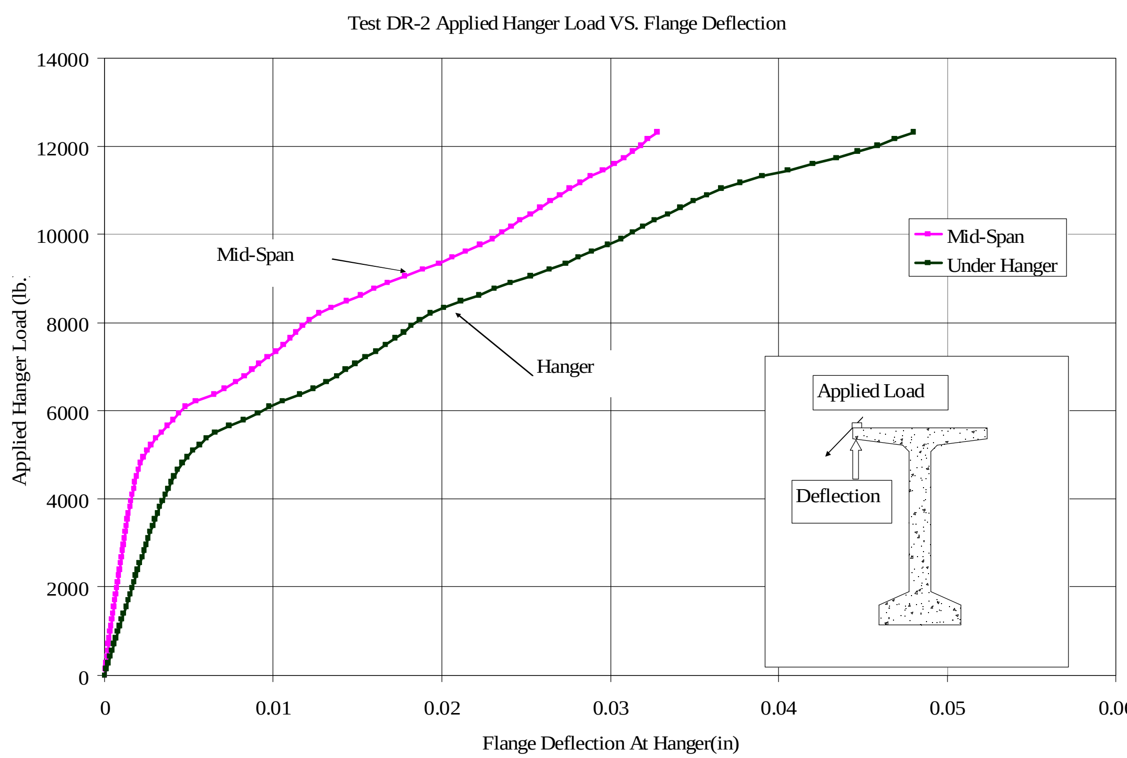

DR-2 Mid-Span and Hanger Flange Deflection

Finite Element Method Summary Sheet

Test ID:	MB-1 (Meadow/Burke Hanger, Single Pull)
Test Date:	September 19, 2005
Sponsor:	NCDOT
Tested By:	Emmett Sumner, Ph. D., P.E. and Donlawit Ariyasajjakorn, E.I.
Program:	ANACAP

Model Description

Dayton/Richmond hanger model, 40 inches Symmetry flange model

Element Type: B8-3D

Material properties

Concrete		Concrete strength	=	7,500	psi
		Young's modulus	=	5,250,000	psi
		Mass Density	=	0.0868	pcf
		Poisson's ratio	=	0.167	
Rebar and Anchor (RT1, RT2, RT3 and Anchor)					
		Yield Strength	=	60,000	psi
		Young's modulus	=	29,000,000	psi
		Poisson's ratio	=	0.3	
Note:	RT1	Area	=	0.622	in^2
	RT2	Area	=	0.311	in^2
	RT2	Area	=	0.151	in^2
Prestressing Strand					
		Grade	=	270	
		Young's modulus	=	28,500,000	psi
		Yield strength	=	100,000	psi
		Ultimate strength	=	118,000	psi
		Area	=	0.153	in^2

Load Type: Static

Experimental Results

Maximum Applied Load	= 11,200 lb
Maximum Flange Vertical Displacement at Center Line	= 0.1045 in.

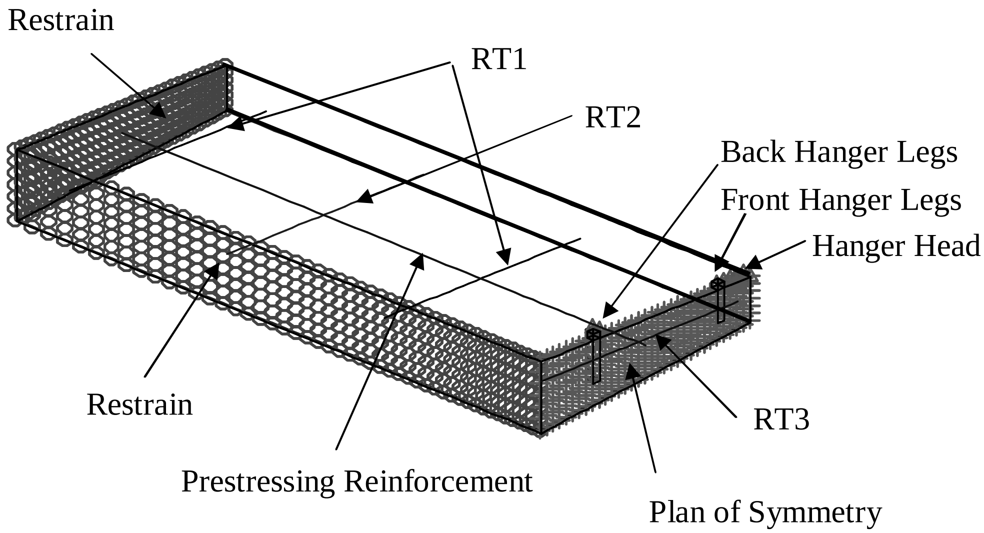

MB-1 Finite Element Model

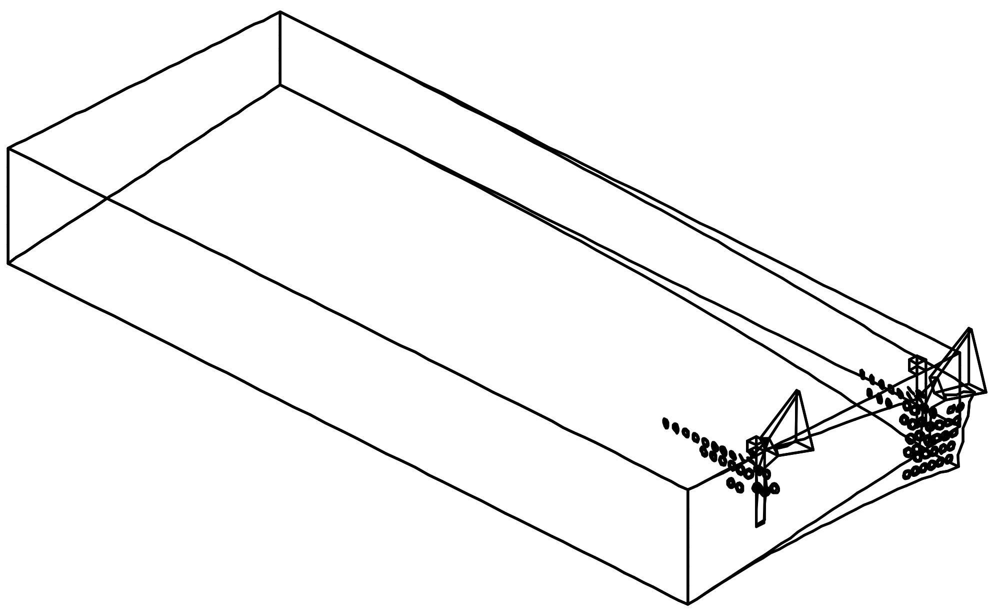

MB-1 Crack pattern at 5,600 lb. applied hanger load

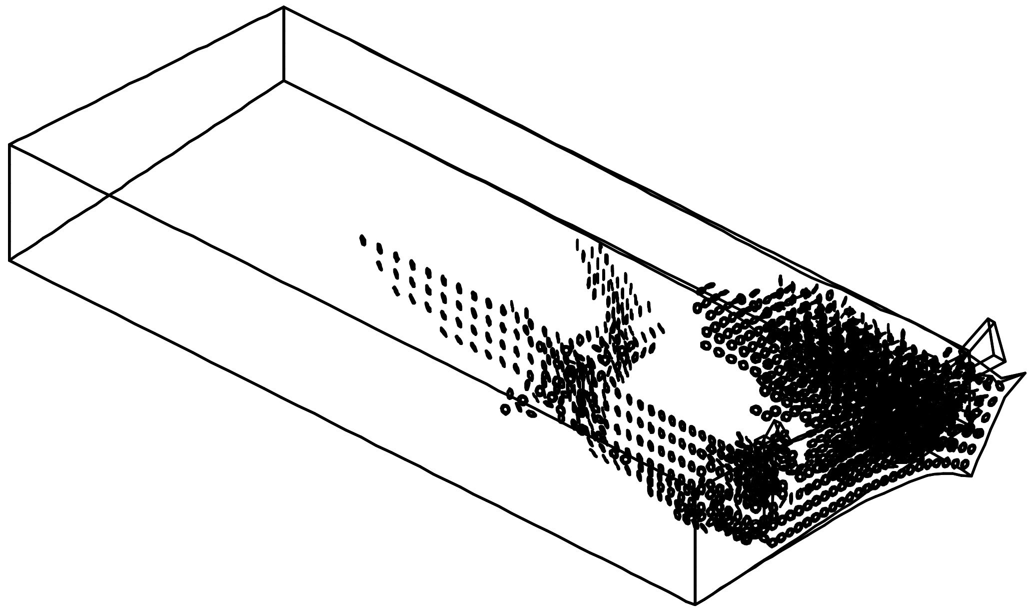

MB-1 Crack pattern at 11,300 lb. applied hanger load

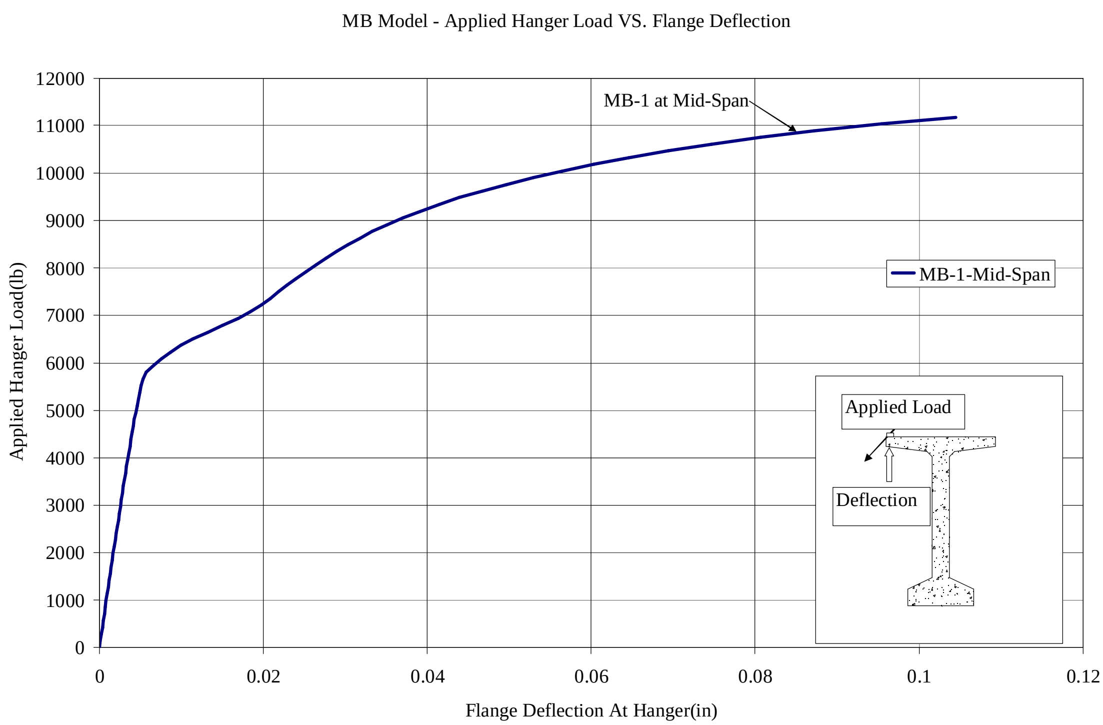

MB-1 Result

Finite Element Method Summary Sheet

Test ID:	MB-2 (Meadow/Burke Hanger, Double Pull)
Test Date:	September 19, 2005
Sponsor:	NCDOT
Tested By:	Emmett Sumner, Ph. D., P.E. and Donlawit Ariyasajjakorn, E.I.
Program:	ANACAP

Model Description

Dayton/Richmond hanger model, 58 inches Symmetry flange model

Element Type: B8-3D

Material properties

<u>Concrete</u>		Concrete strength	=	7,500	psi
		Young's modulus	=	5,250,000	psi
		Mass Density	=	0.0868	pcf
		Poisson's ratio	=	0.167	
<u>Rebar and Anchor</u> (RT1, RT2 and Anchor)					
		Yield Strength	=	60,000	psi
		Young's modulus	=	29,000,000	psi
		Poisson's ratio	=	0.3	
Note:	RT1	Area	=	0.622	in^2
	RT2	Area	=	0.311	in^2
<u>Prestressing Strand</u>					
		Grade	=	270	
		Young's modulus	=	28,500,000	psi
		Yield strength	=	100,000	psi
		Ultimate strength	=	118,000	psi
		Area	=	0.153	in^2

Load Type: Static

Experimental Results

Maximum Applied Load	= 10,600	lb
Maximum Flange Vertical Displacement at Center Line	= 0.0976	in.
Maximum Flange Vertical Displacement	= 0.0208	in.

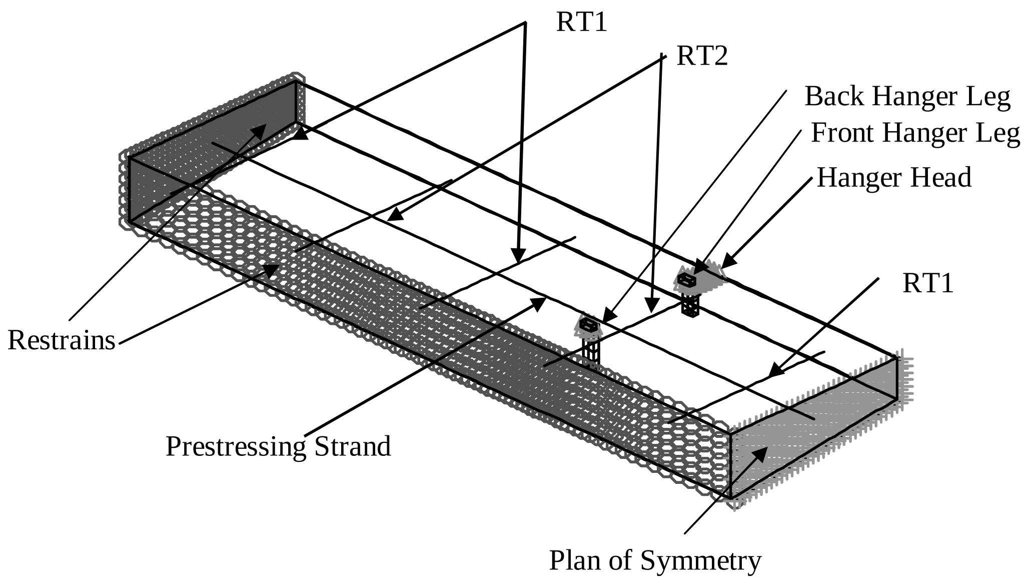

MB-2 Finite Element Model

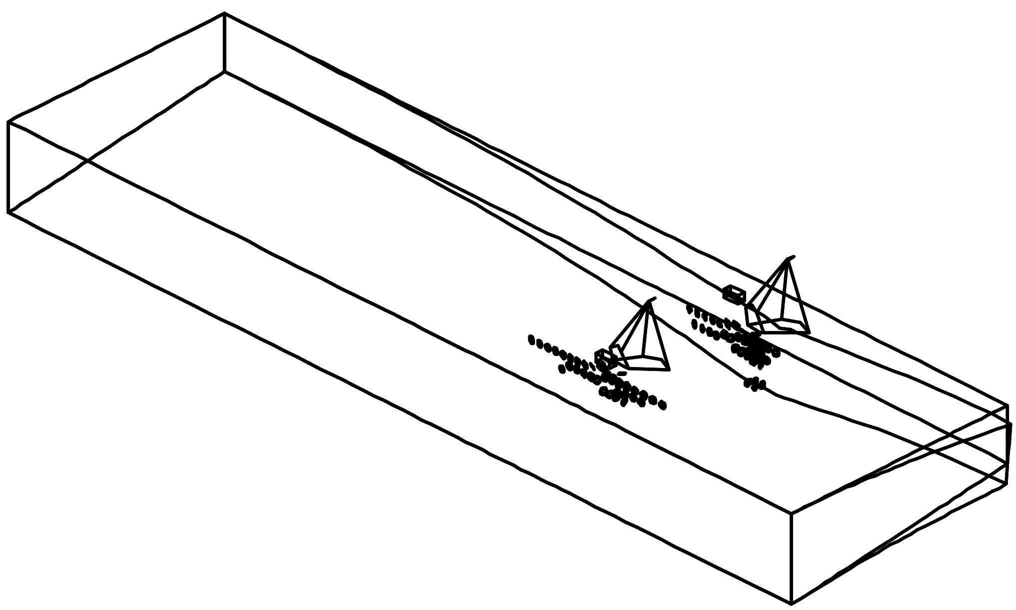

MB-2 Crack pattern at 5,600 lb. applied hanger load

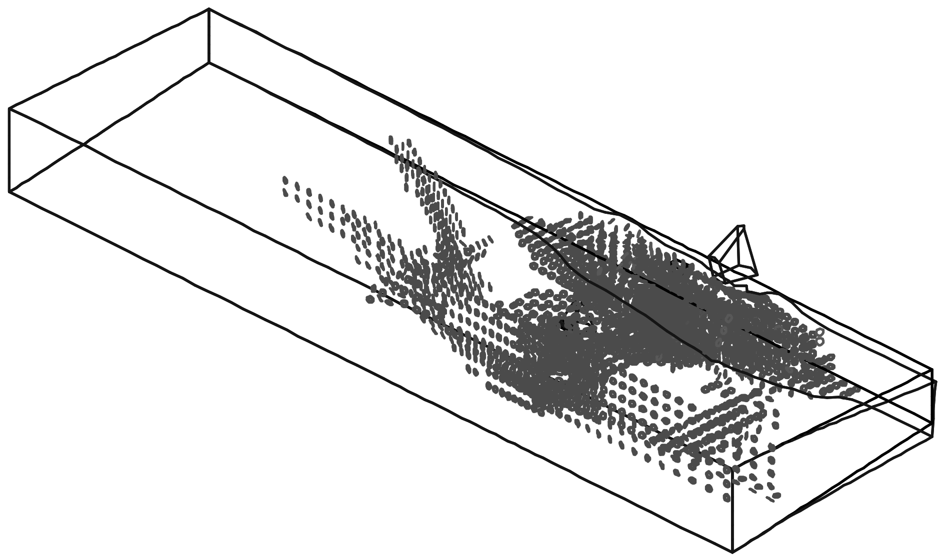

MB-2 Crack pattern at 10,600 lb. applied hanger load

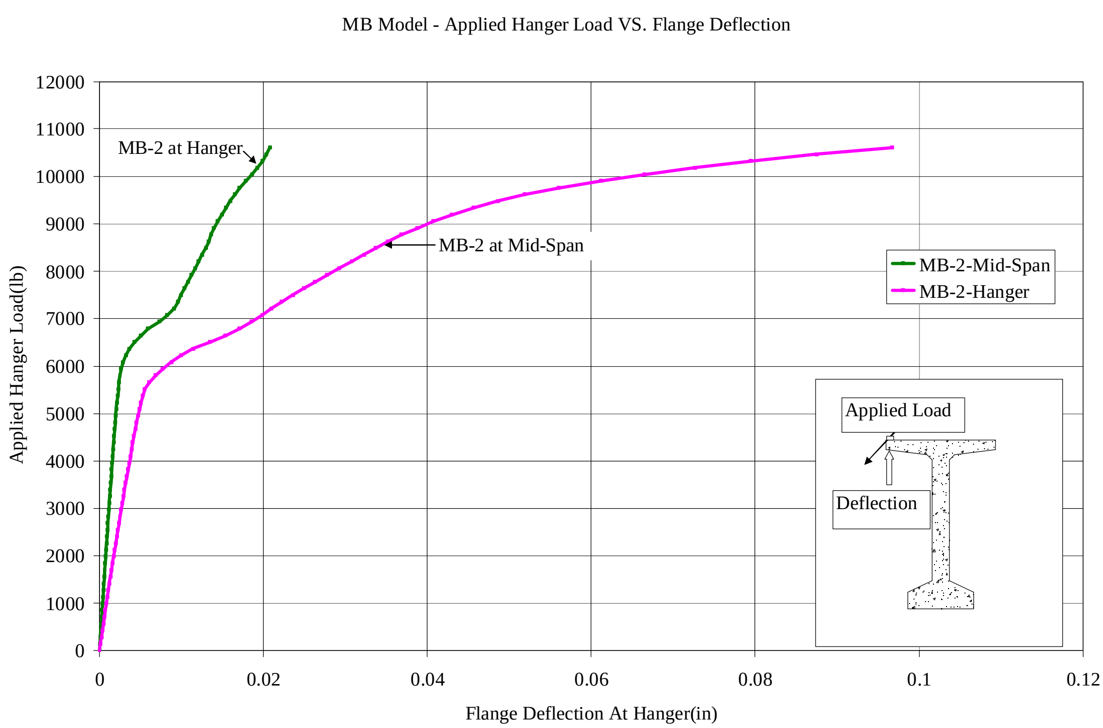

MB-2 Result

Finite Element Method Summary Sheet

Test ID:	MB-4 (Meadow/Burke Hanger, Single Pull)
Test Date:	September 19, 2005
Sponsor:	NCDOT
Tested By:	Emmett Sumner, Ph. D., P.E. and Donlawit Ariyasajjakorn, E.I.
Program:	ANACAP

Model Description

Dayton/Richmond hanger model, 94 inches Symmetry flange model

Element Type: B8-3D

Material properties

<u>Concrete</u>		Concrete strength	=	7,500	psi
		Young's modulus	=	5,250,000	psi
		Mass Density	=	0.0868	pcf
		Poisson's ratio	=	0.167	
<u>Rebar and Anchor</u> (RT1, RT2 and Anchor)					
		Yield Strength	=	60,000	psi
		Young's modulus	=	29,000,000	psi
		Poisson's ratio	=	0.3	
Note:	RT1	Area	=	0.622	in^2
	RT2	Area	=	0.311	in^2
<u>Prestressing Strand</u>					
		Grade	=	270	
		Young's modulus	=	28,500,000	psi
		Yield strength	=	100,000	psi
		Ultimate strength	=	118,000	psi
		Area	=	0.153	in^2

Load Type: Static

Experimental Results

Maximum Applied Load	= 10,300	lb
Maximum Flange Vertical Displacement at Center Line	= 0.0952	in.
Maximum Flange Vertical Displacement	= 0.0244	in.

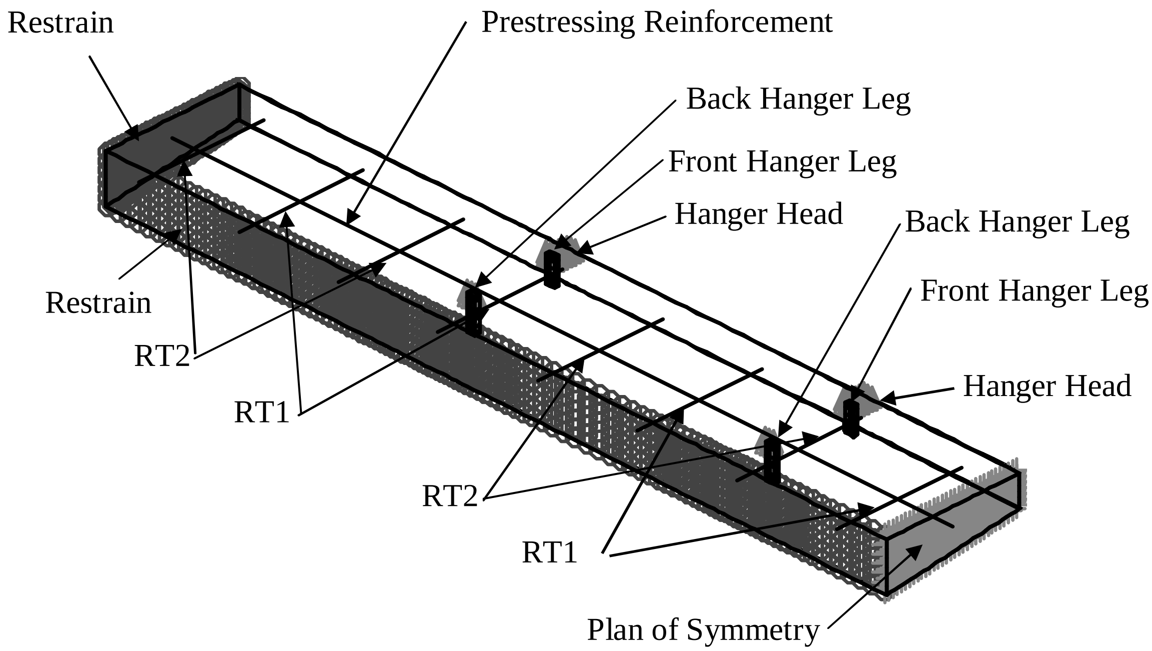

MB-4 Finite Element Model

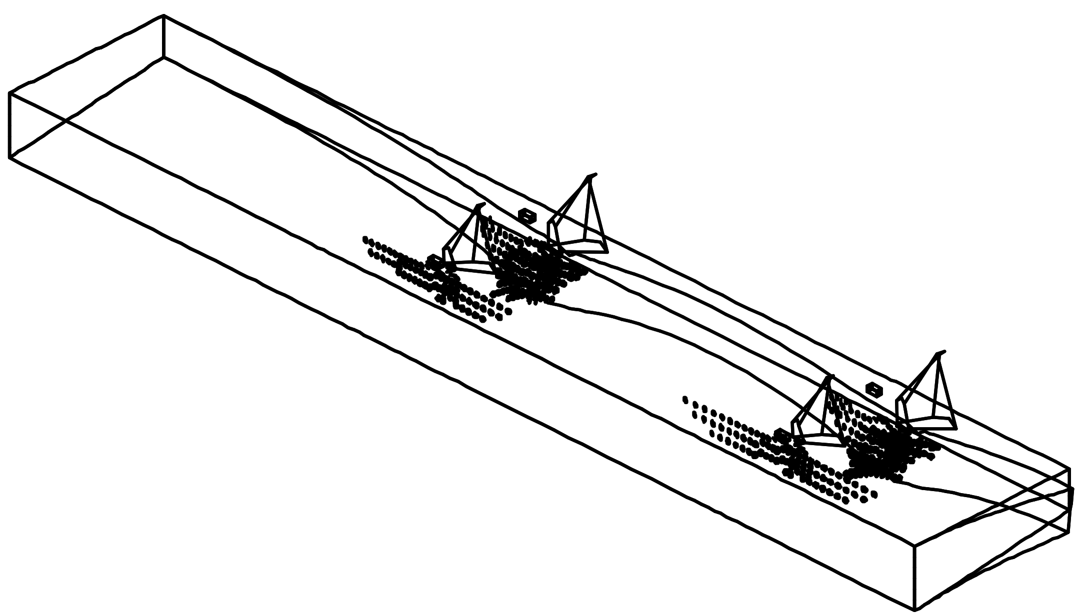

MB-4 Crack Pattern at 5,600 lb. applied hanger load

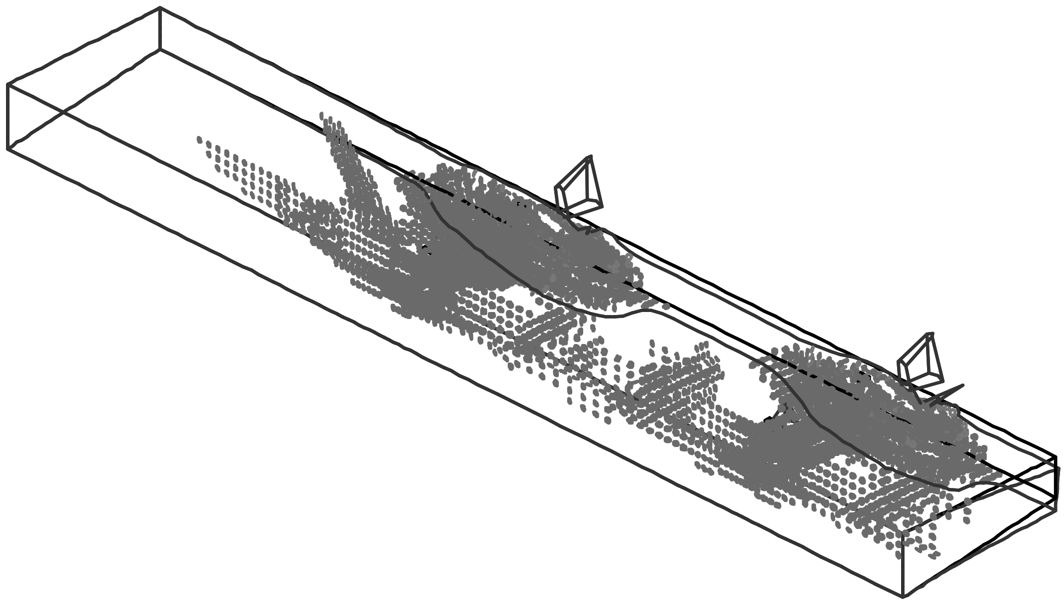

MB-4 Crack Pattern at 9,900 lb. applied hanger load

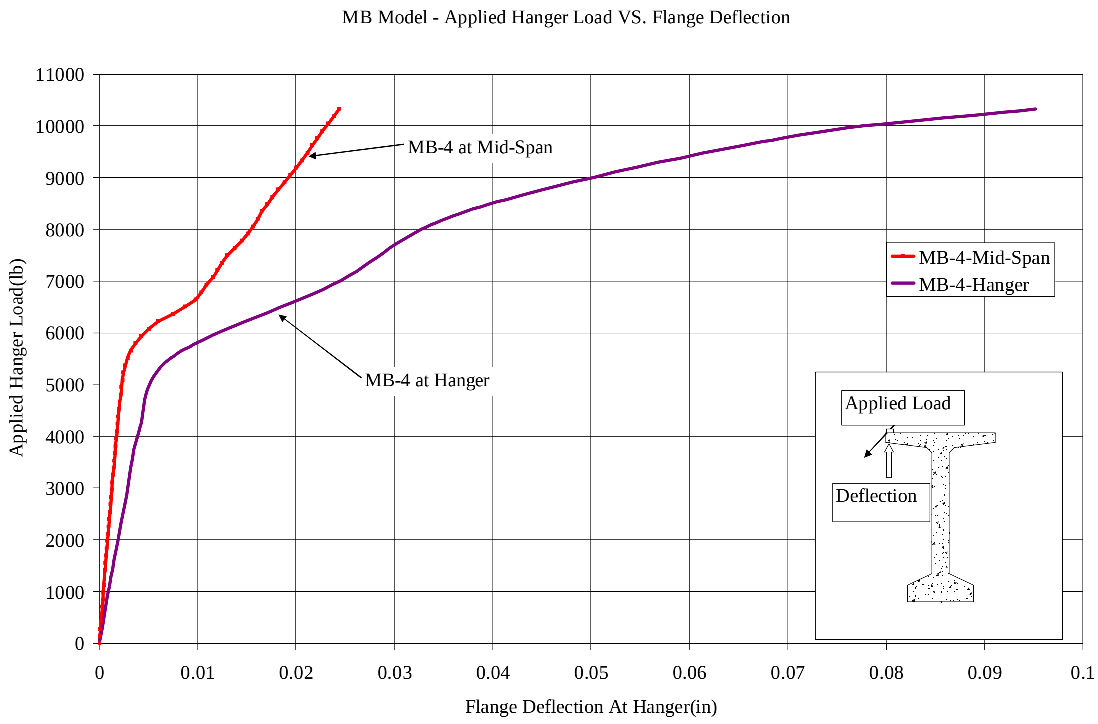

MB-4 Result

Finite Element Method Summary Sheet

Test ID:	DR-Small (Dayton/Richmond Hanger, Single Pull, Small Model)
Test Date:	September 19, 2005
Sponsor:	NCDOT
Tested By:	Emmett Sumner, Ph. D., P.E. and Donlawit Ariyasajjakorn, E.I.
Program:	ANACAP

Model Description

Dayton/Richmond hanger model, 12 inches Symmetry flange model

Element Type: B8-3D

Material properties

Concrete	Concrete strength	=	7,500	psi
	Young's modulus	=	5,250,000	psi
	Mass Density	=	0.0868	pcf
	Poisson's ratio	=	0.167	
Rebar and Anchor (RT3 and Anchor)				
	Yield Strength	=	60,000	psi
	Young's modulus	=	29,000,000	psi
	Poisson's ratio	=	0.3	
Note: RT3	Area	=	0.151	in^2
Prestressing Strand				
	Grade	=	270	
	Young's modulus	=	28,500,000	psi
	Yield strength	=	100,000	psi
	Ultimate strength	=	118,000	psi
	Area	=	0.153	in^2

Load Type: Static

Experimental Results

Maximum Applied Load	= 12,000	lb
Maximum Flange Vertical Displacement at Center Line	= 0.0124	in.

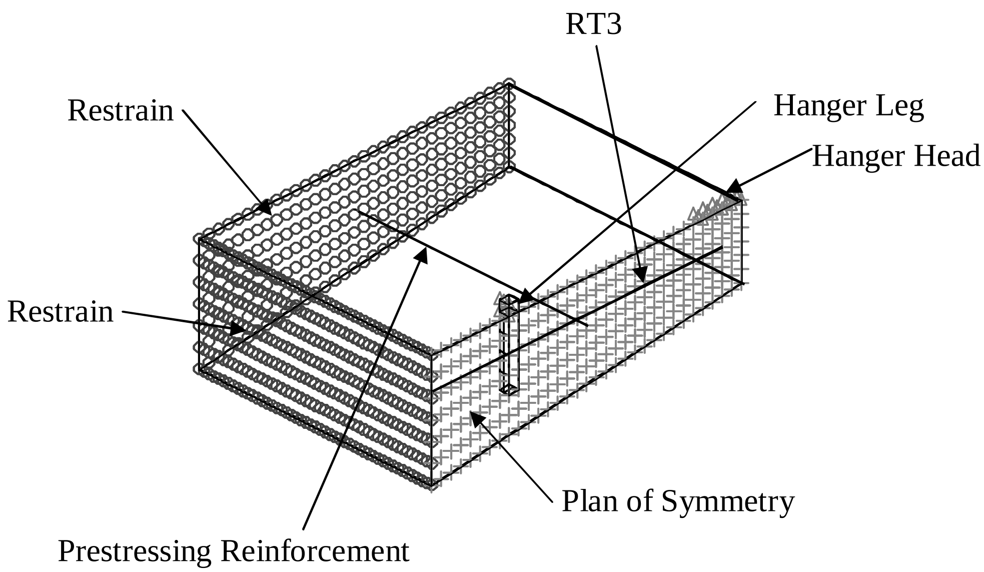

DR-Small Finite element model

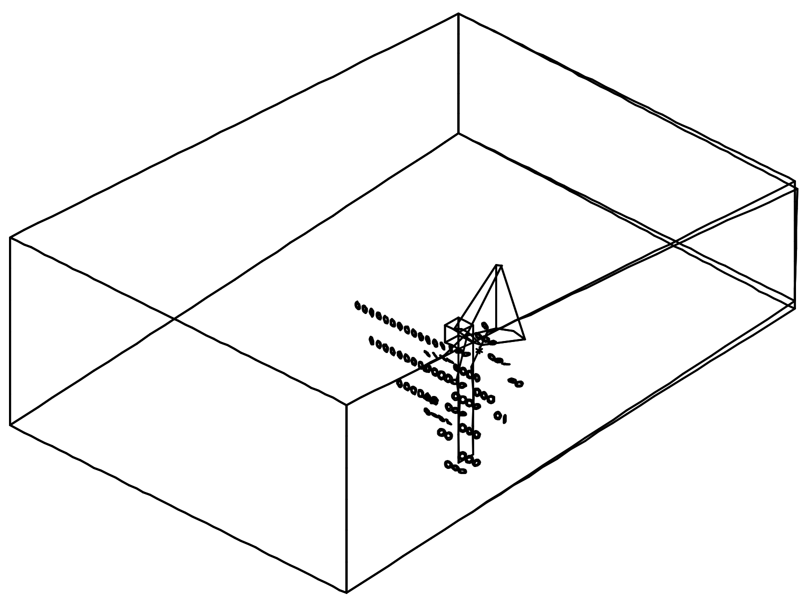

DR-Small Crack pattern at 5,600 lb. applied hanger load

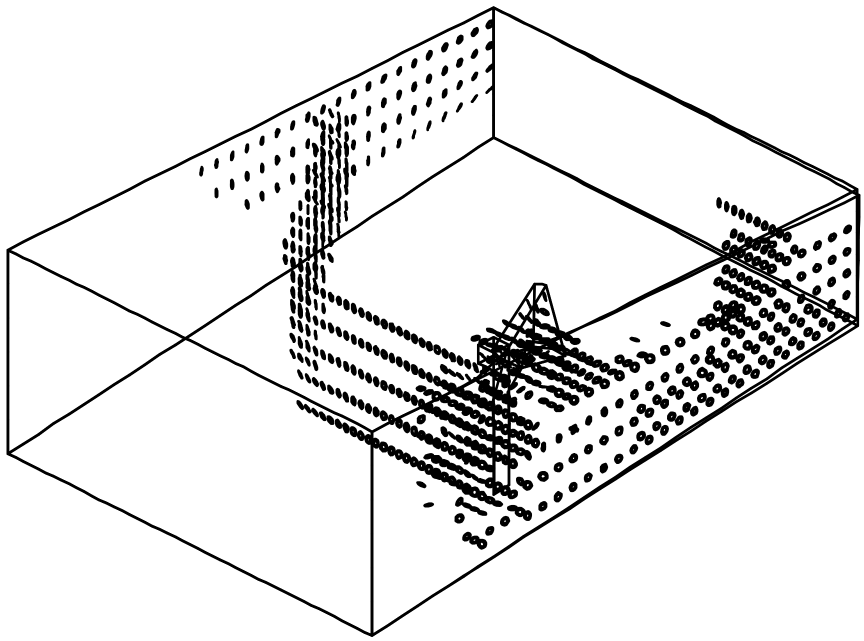

DR-Small Crack pattern at 11,300 lb. applied hanger load

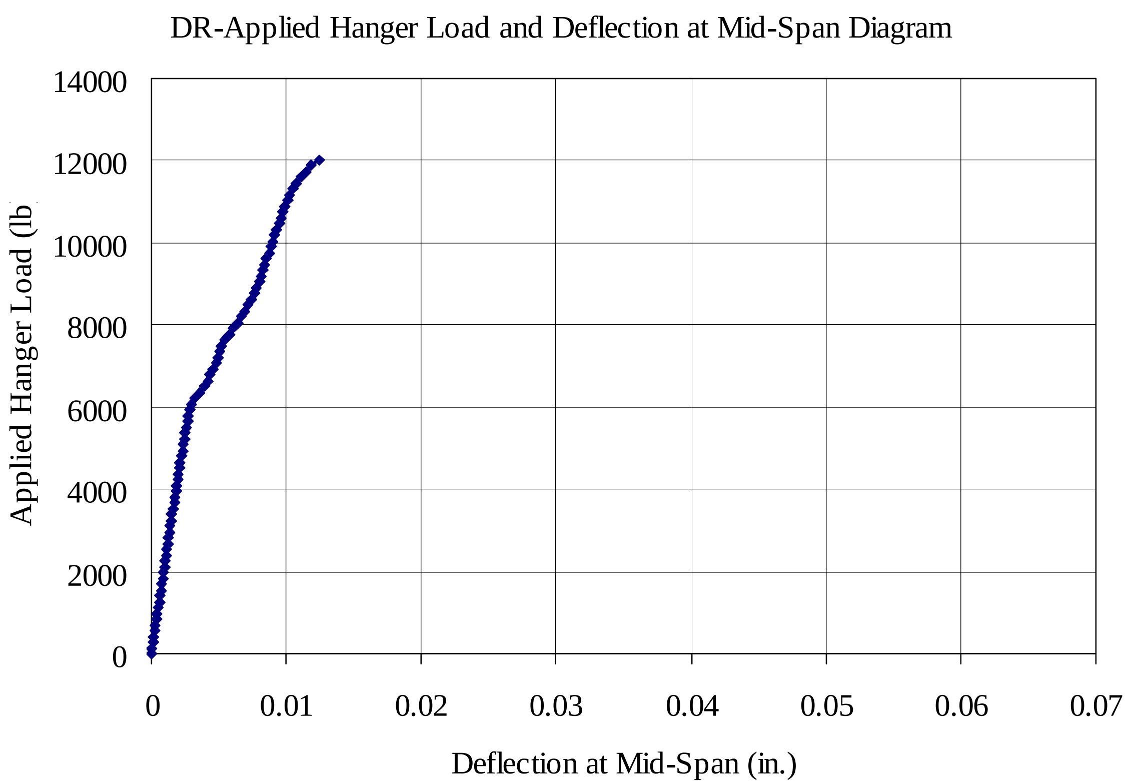

DR-Small Mid-span deflection

Finite Element Method Summary Sheet

Test ID:	MB-Small (Meadow/Burke Hanger, Single Pull, Small Model)
Test Date:	September 19, 2005
Sponsor:	NCDOT
Tested By:	Emmett Sumner, Ph. D., P.E. and Donlawit Ariyasajjakorn, E.I.
Program:	ANACAP

Model Description

Dayton/Richmond hanger model, 12 inches Symmetry flange model

Element Type: B8-3D

Material properties

<u>Concrete</u>	Concrete strength	=	7,500	psi
	Young's modulus	=	5,250,000	psi
	Mass Density	=	0.0868	pcf
	Poisson's ratio	=	0.167	
<u>Rebar and Anchor</u> (RT3 and Anchor)				
	Yield Strength	=	60,000	psi
	Young's modulus	=	29,000,000	psi
	Poisson's ratio	=	0.3	
Note: RT3	Area	=	0.151	in^2
<u>Prestressing Strand</u>				
	Grade	=	270	
	Young's modulus	=	28,500,000	psi
	Yield strength	=	100,000	psi
	Ultimate strength	=	118,000	psi
	Area	=	0.153	in^2

Load Type: Static

Experimental Results

Maximum Applied Load	= 9,500 lb
Maximum Flange Vertical Displacement at Center Line	= 0.0614 in.

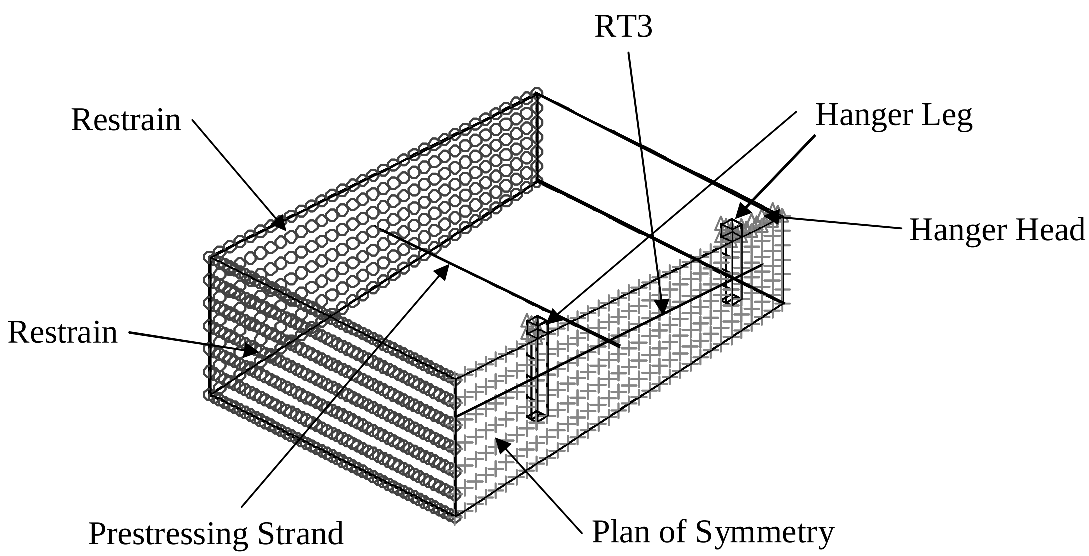

MB-Small Finite element model

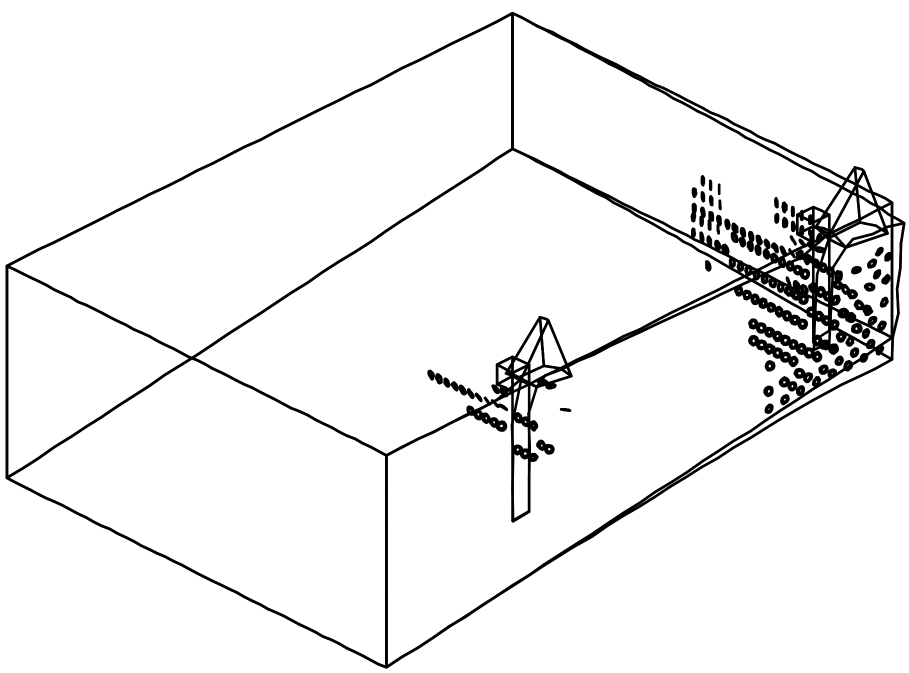

MB-Small Crack pattern at 5,600 lb. applied hanger load

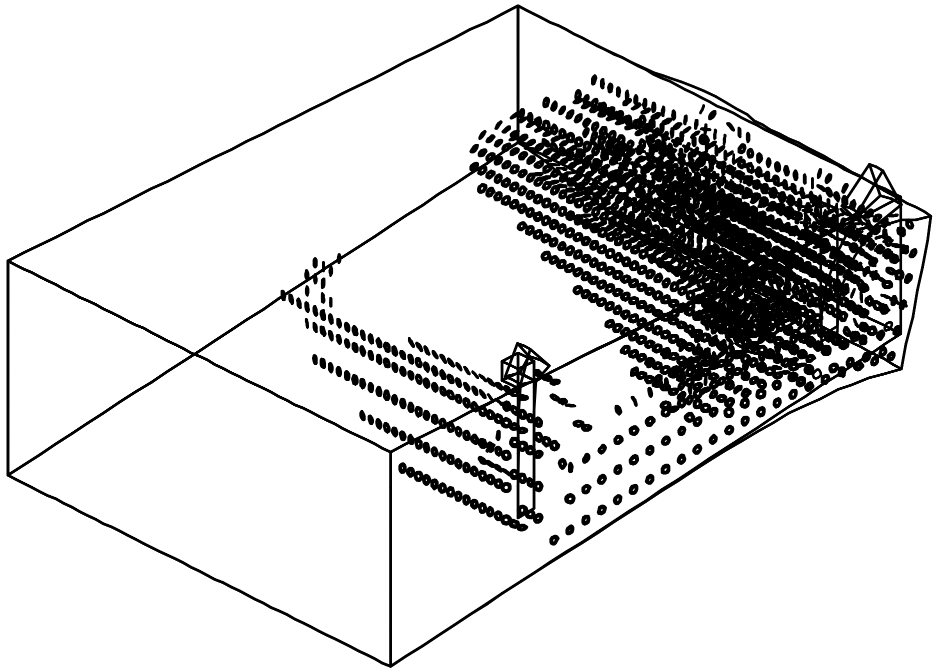

MB-Small Crack pattern at 9,200 lb. applied hanger load

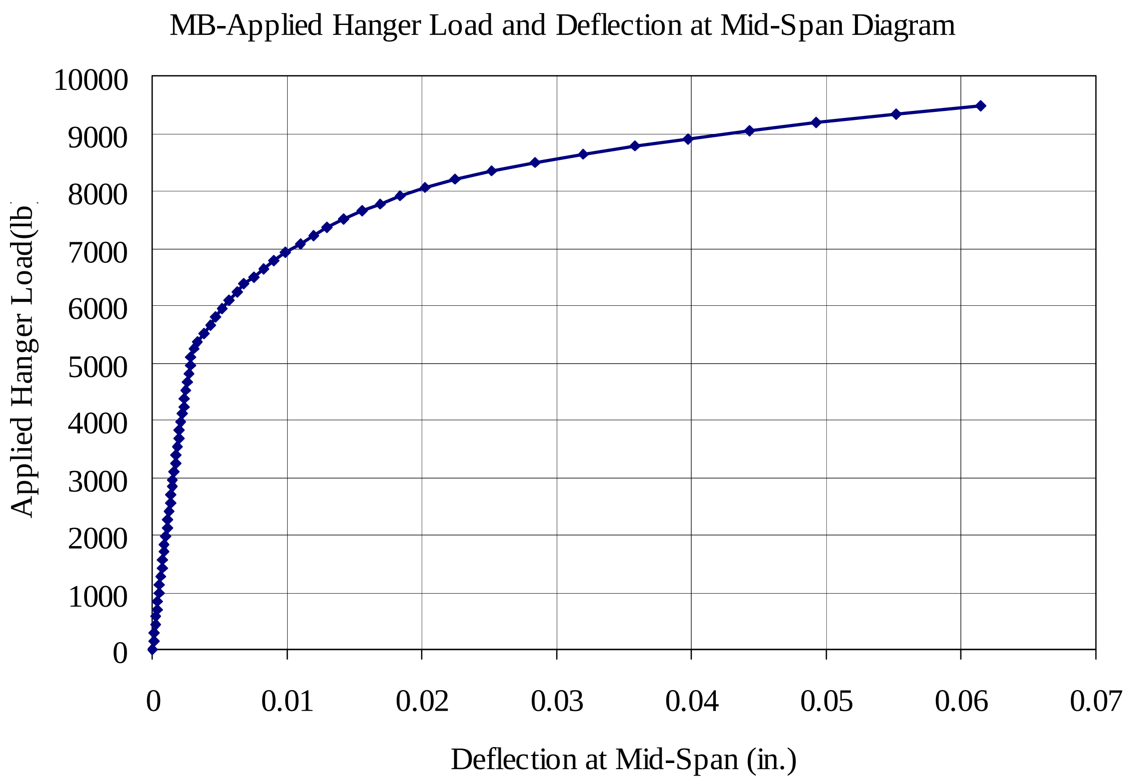

MB-Small Mid-span deflection

Finite Element Method Summary Sheet

Test ID: Modified DR-Small(Dayton/Richmond Hanger, Single Pull, Small Model)
Test Date: January 06, 2005
Sponsor: NCDOT
Tested By: Emmett Sumner, Ph. D., P.E. and Donlawit Ariyasajjakorn, E.I.
Program: ANACAP

Model Description

Dayton/Richmond hanger model, 12 inches Symmetry flange model. 2 by 4 in. loaded area.

Element Type: B8-3D

Material properties

Concrete	Concrete strength	=	7,500	psi
	Young's modulus	=	5,250,000	psi
	Mass Density	=	0.0868	pcf
	Poisson's ratio	=	0.167	
Rebar and Anchor (RT3 and Anchor)				
	Yield Strength	=	60,000	psi
	Young's modulus	=	29,000,000	psi
	Poisson's ratio	=	0.3	
Note: RT3	Area	=	0.151	in^2
Prestressing Strand				
	Grade	=	270	
	Young's modulus	=	28,500,000	psi
	Yield strength	=	100,000	psi
	Ultimate strength	=	118,000	psi
	Area	=	0.153	in^2

Load Type: Static

Experimental Results

Maximum Applied Load	= 12,000	lb
Maximum Flange Vertical Displacement at Center Line	= 0.0104	in.

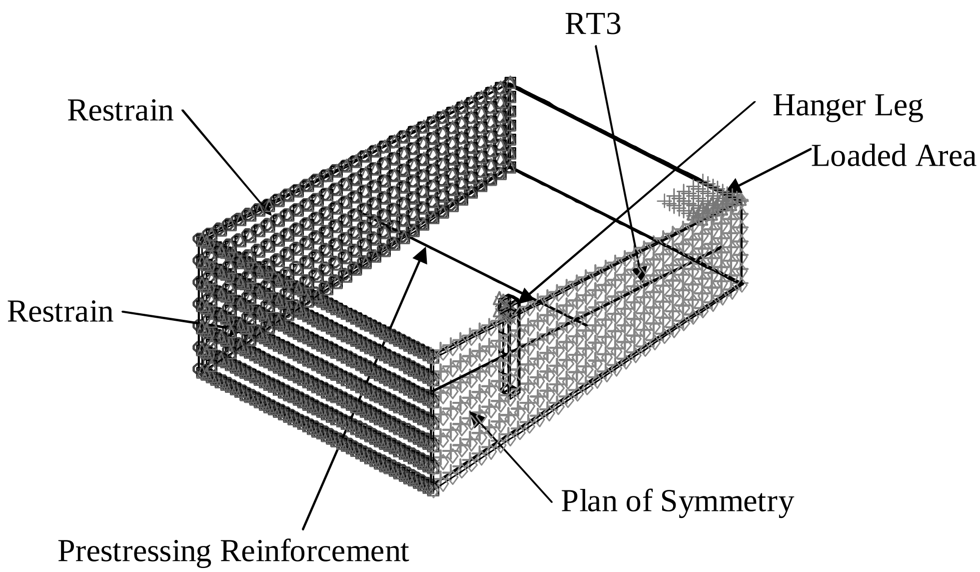

Modified DR-Small Finite element model

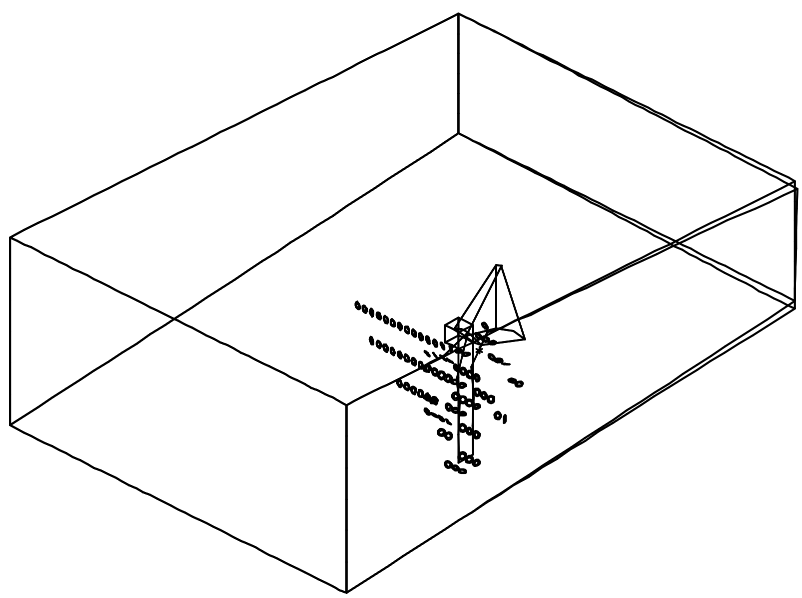

Modified DR-Small Crack pattern at 5,600 lb. applied hanger load

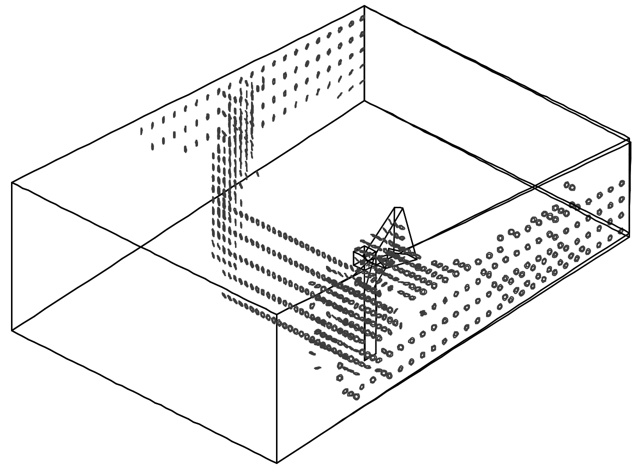

Modified DR-Small Crack pattern at 11,300 lb. applied hanger load

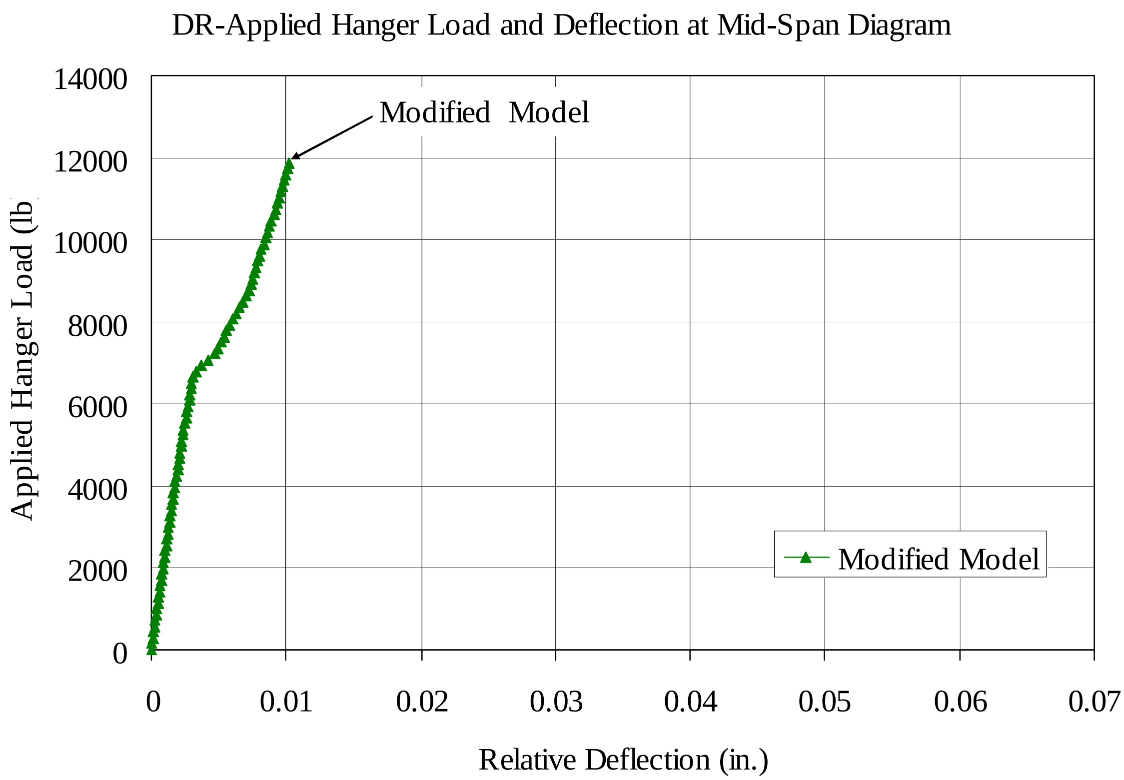

Modified DR-Small Mid-span deflection

Finite Element Method Summary Sheet

Test ID: 5.5 in. MB-Small (Meadow/Burke Hanger, Single Pull, Small Model)
Test Date: January 07, 2005
Sponsor: NCDOT
Tested By: Emmett Sumner, Ph. D., P.E. and Donlawit Ariyasajjakorn, E.I.
Program: ANACAP

Model Description

Dayton/Richmond hanger model, 12 inches Symmetry flange model. 5.5 inches thickness.

Element Type: B8-3D

Material properties

Concrete	Concrete strength	=	7,500	psi
	Young's modulus	=	5,250,000	psi
	Mass Density	=	0.0868	pcf
	Poisson's ratio	=	0.167	
Rebar and Anchor (RT3 and Anchor)				
	Yield Strength	=	60,000	psi
	Young's modulus	=	29,000,000	psi
	Poisson's ratio	=	0.3	
Note: RT3	Area	=	0.151	in^2
Prestressing Strand				
	Grade	=	270	
	Young's modulus	=	28,500,000	psi
	Yield strength	=	100,000	psi
	Ultimate strength	=	118,000	psi
	Area	=	0.153	in^2

Load Type: Static

Experimental Results

Maximum Applied Load = 11900 lb
Maximum Flange Vertical Displacement at Center Line = 0.0410 in.

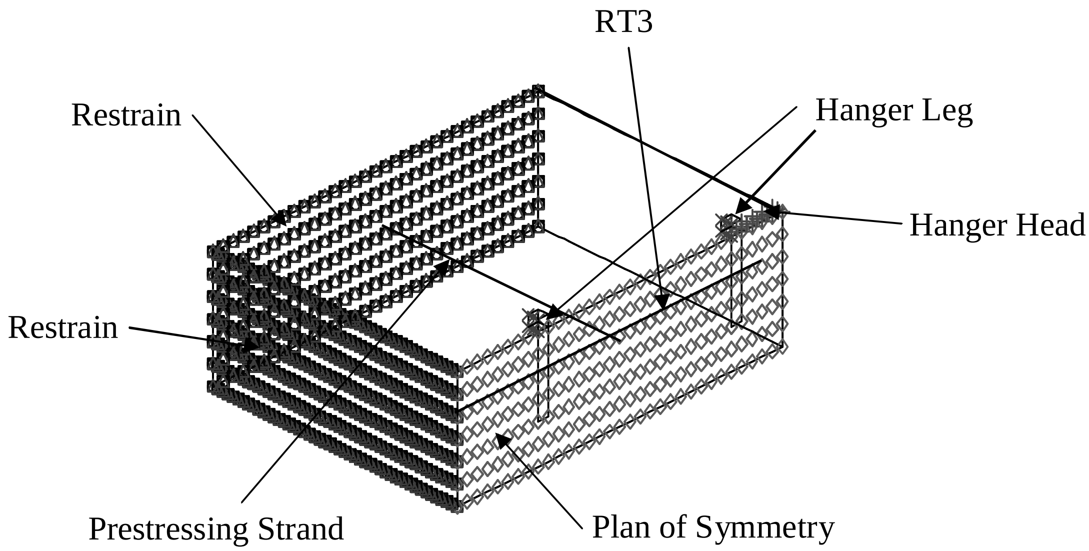

5.5 in. MB-Small Finite element model

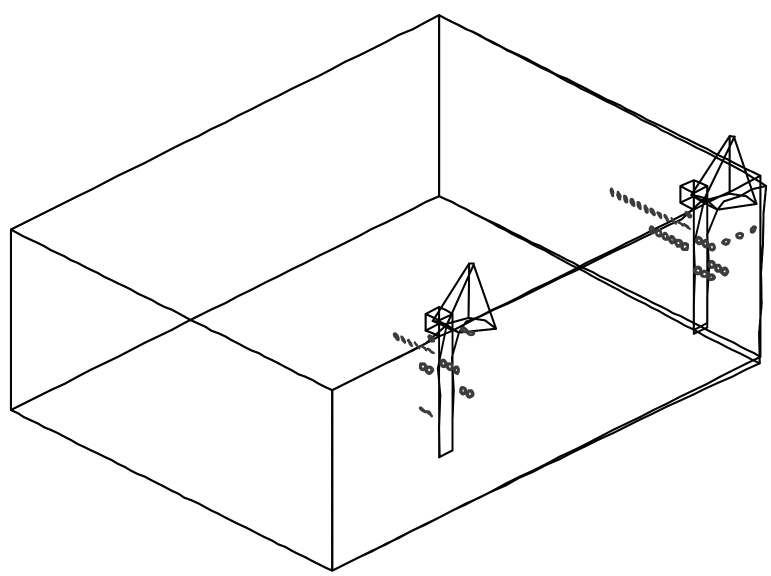

5.5 in. MB-Small Crack pattern at 5,600 lb. applied hanger load

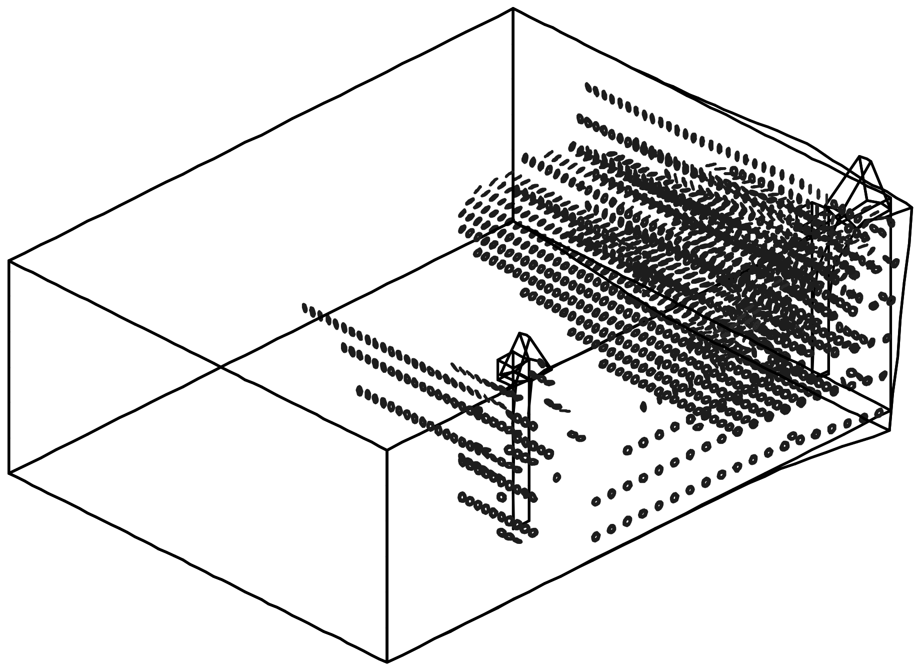

5.5 in. MB-Small Crack pattern at 11,200 lb. applied hanger load

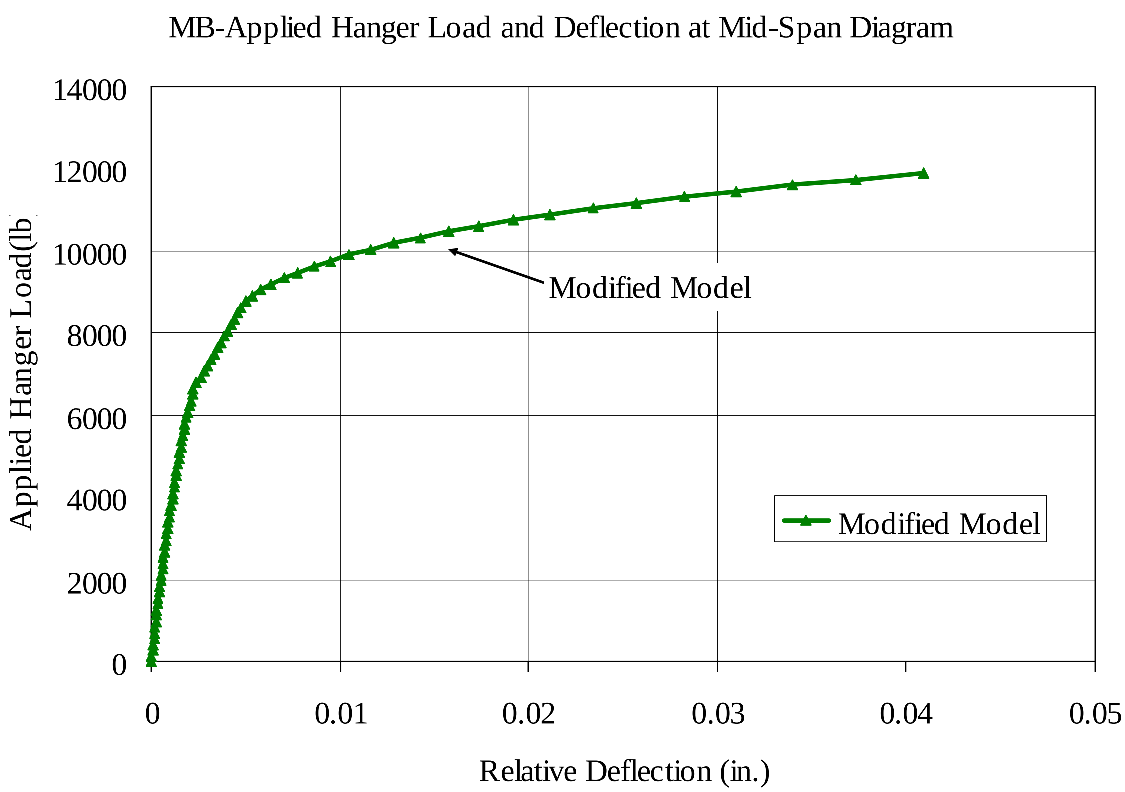

5.5 in. MB-Small Mid-span deflection

Finite Element Method Summary Sheet

Test ID: 6.5 in. MB-Small (Meadow/Burke Hanger, Single Pull, Small Model)
Test Date: January 07, 2005
Sponsor: NCDOT
Tested By: Emmett Sumner, Ph. D., P.E. and Donlawit Ariyasajjakorn, E.I.
Program: ANACAP

Model Description

Dayton/Richmond hanger model, 12 inches Symmetry flange model. 6.5 inches thickness.

Element Type: B8-3D

Material properties

Concrete	Concrete strength	=	7,500	psi
	Young's modulus	=	5,250,000	psi
	Mass Density	=	0.0868	pcf
	Poisson's ratio	=	0.167	
Rebar and Anchor (RT3 and Anchor)				
	Yield Strength	=	60,000	psi
	Young's modulus	=	29,000,000	psi
	Poisson's ratio	=	0.3	
Note: RT3	Area	=	0.151	in^2
Prestressing Strand				
	Grade	=	270	
	Young's modulus	=	28,500,000	psi
	Yield strength	=	100,000	psi
	Ultimate strength	=	118,000	psi
	Area	=	0.153	in^2

Load Type: Static

Experimental Results

Maximum Applied Load	= 13500	lb
Maximum Flange Vertical Displacement at Center Line	= 0.0335	in.

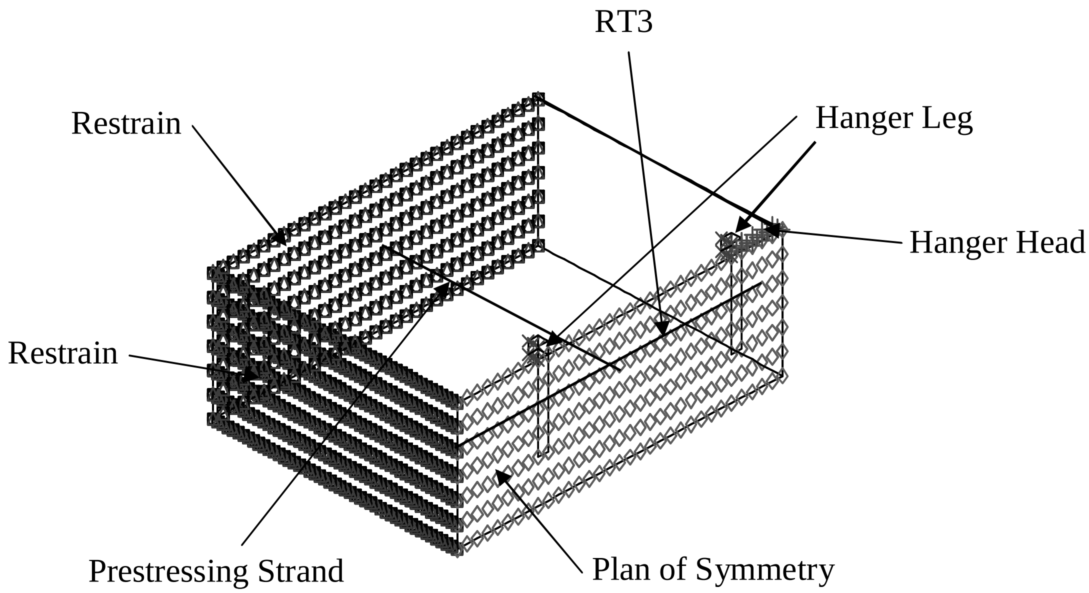

6.5 in. MB-Small Finite element model

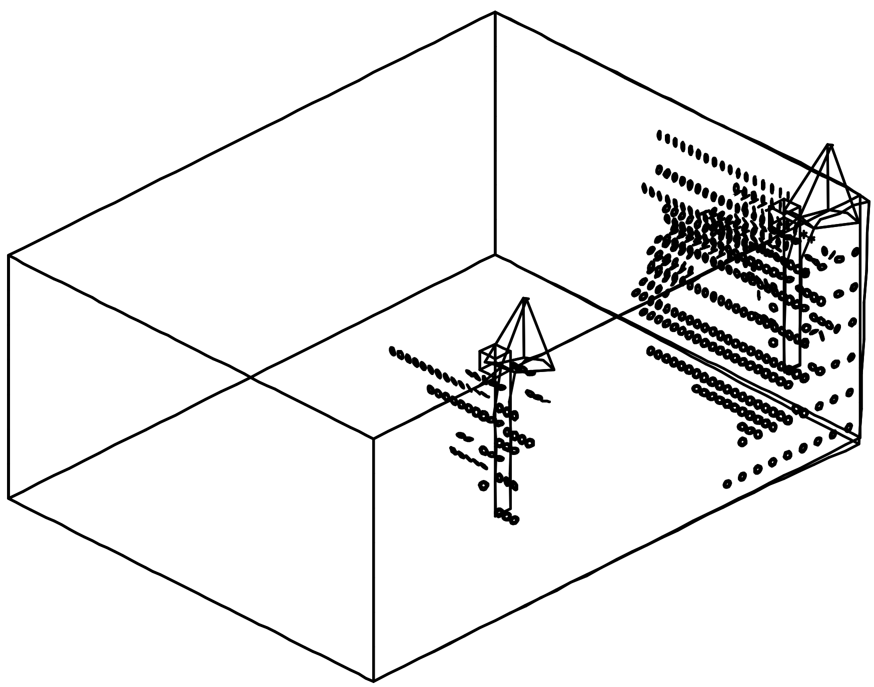

6.5 in. MB-Small Crack pattern at 5,600 lb. applied hanger load

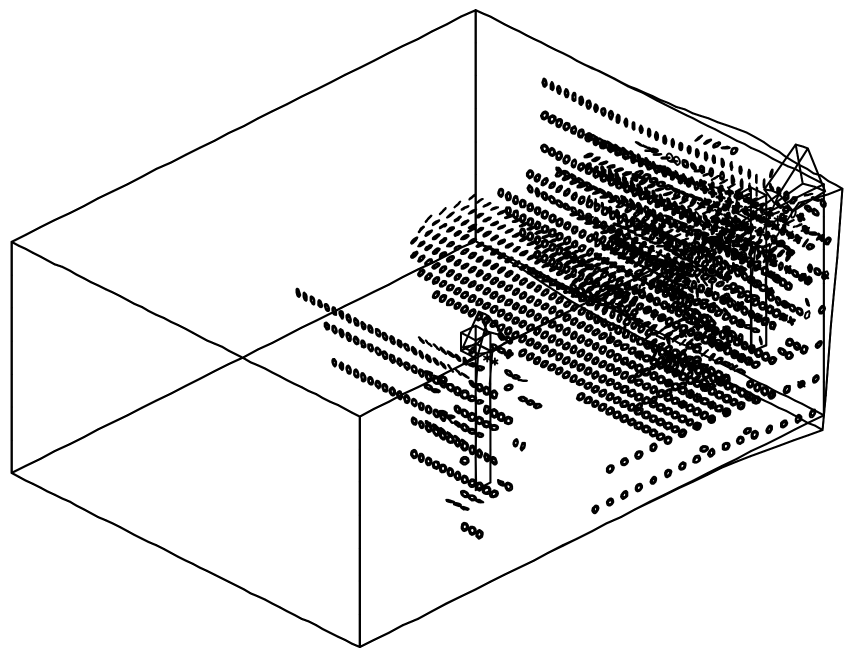

6.5 in. MB-Small Crack pattern at 13,200 lb. applied hanger load

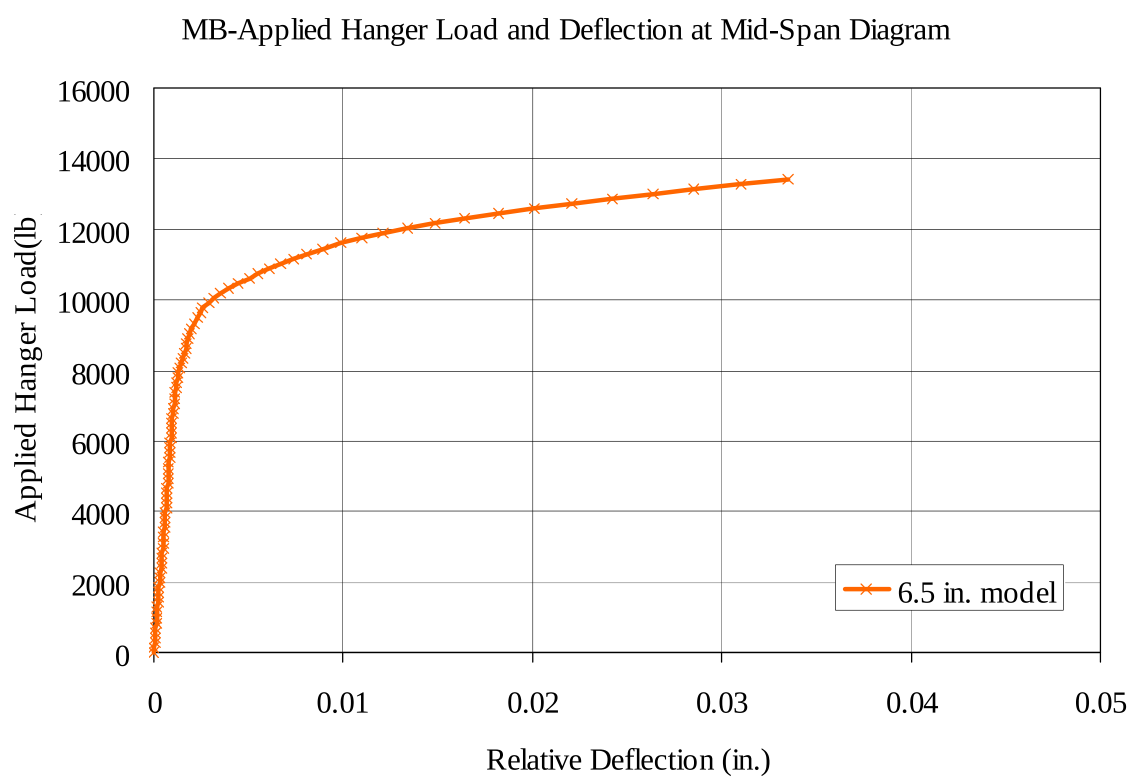

6.5 in. MB-Small Mid-span deflection

Appendix J Sample Calculations According to ACI Specification Provisions

Bearing Strength Calculation

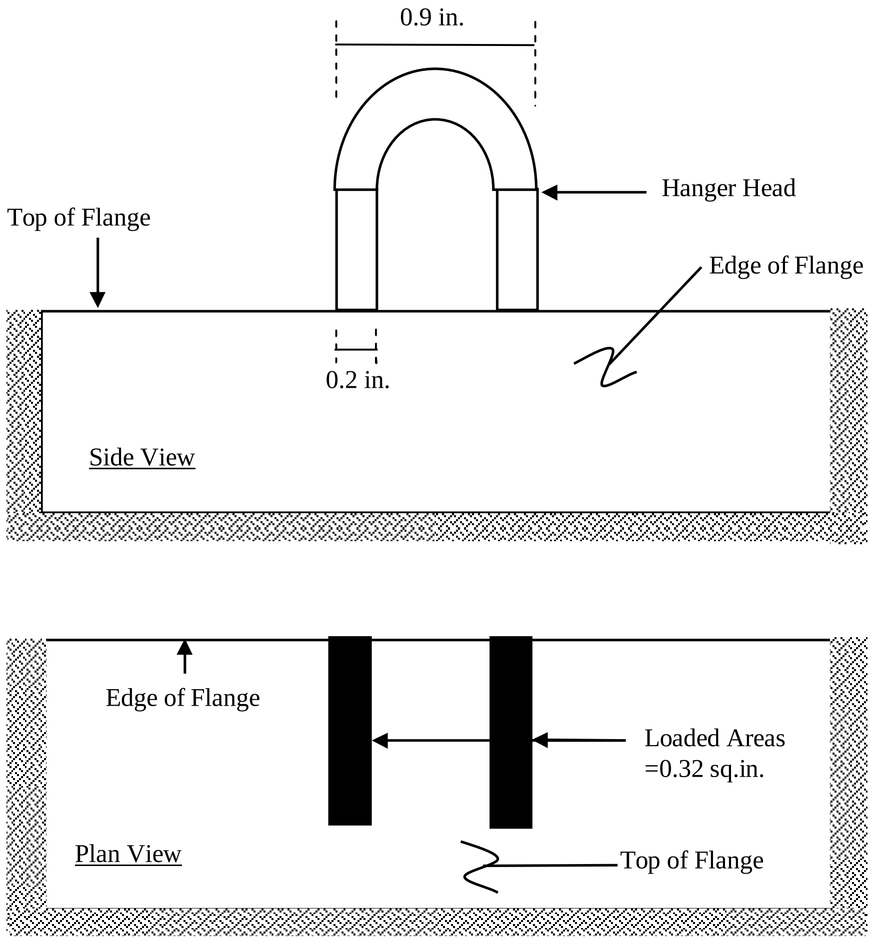

Actual loaded area of hanger head

The bearing strength equation was

$$F_{br} = 0.85 f_c^{'} A = 0.85(7500)(0.32 \times 2) = 4080 \text{ lb.}$$

Where F_{br} = Bearing strength, lb.

$f_c^{'}$ = specified compressive strength of concrete, psi

A = loaded area, in^2

Modified the result to the applied hanger load

$$F_{br} = 4080/0.707 = 5770 \text{ lb.}$$

Punching shear strength calculation

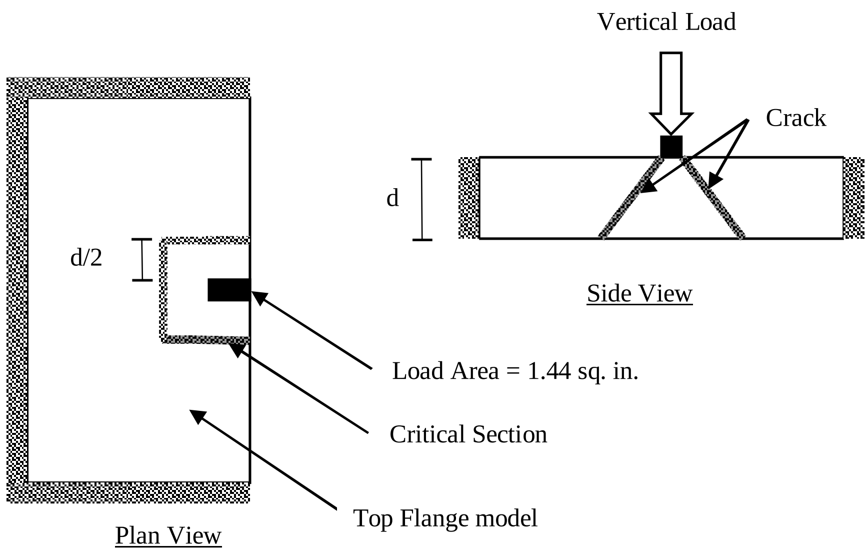

Critical section of punching shear failure

The Punching Shear Strength was the smallest of the following equations.

$$V_c = \left(2 + \frac{4}{b_c}\right)\sqrt{f_c^{'}}\, b_0 d = \left(2 + \frac{4}{1.78}\right)\sqrt{7500}(11.1)(3.5) \quad =15,000 \text{ lb.}$$

$$V_c = \left(\frac{a_s d}{b_0} + 2\right)\sqrt{f_c^{'}}\, b_0 d = \left(\frac{30(3.5)}{11.1} + 2\right)\sqrt{7500}(11.1)(3.5) =38560 \text{ lb.}$$

$$V_c = 4\sqrt{f_c^{'}}\, b_0 d \quad = 4\sqrt{7500}(11.1)(3.5) \quad = 13500 \text{ lb.}$$

Where: V_c = nominal shear strength provided by concrete, lb

$f_c^{'}$ = specified compressive strength of concrete = 7500 psi

b_0 = perimeter of critical section for slabs = 11.1 in.

d = thickness of slab = 3.5 in.

a_s = constant used to compute V_c for edge column = 30

b_c = ratio of long side to short side of concentrated load = 1.77

The punching shear strength was 13,500 lb. which equal to the 13,500/0.707 = 19,100 lb. applied hanger load.

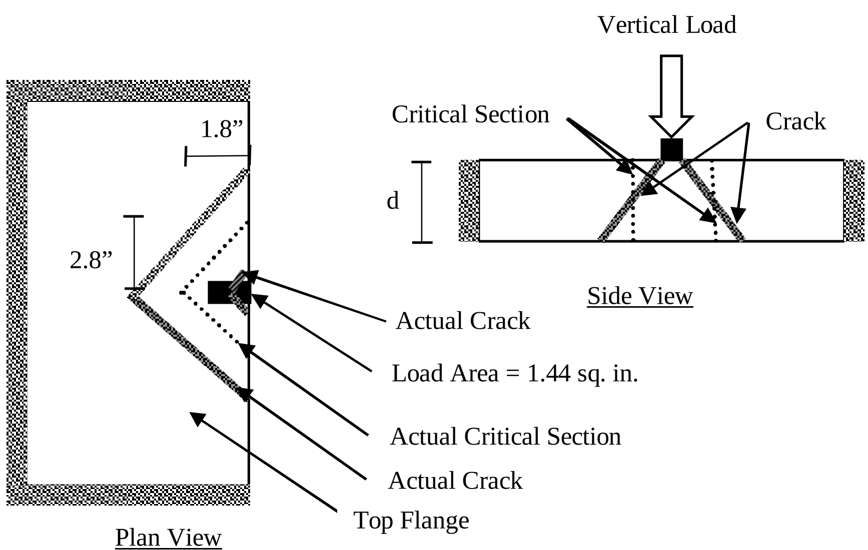

Critical section of punching shear failure

If the punching shear strength was calculated from the actual critical section, the strength was 11,300 lb. applied hanger load.

Torsional strength calculation

$$T_{cr} = 4\sqrt{f_c^{'}}\left(\frac{A_{cp}^2}{P_{cp}}\right)\sqrt{1+\frac{f_{pc}}{4\sqrt{f_c^{'}}}} = 4\sqrt{7500}\left(\frac{814^2}{227}\right)\sqrt{1+\frac{937.5}{4\sqrt{7500}}}$$

= 1,946,000 lb.

Where: T_{cr} = Cracking Torque, lb-in.

$f_c^{'}$ = Specified compressive strength of concrete = 7500 psi

A_{cp} = Area enclosed by outside perimeter of concrete cross section

= 814 in.^{2}

P_{cp} = Outside perimeter of the concrete cross-section = 227 in.

f_{pc} = Compressive stress in concrete at centroid of cross section resisting externally applied loads = 12.5% of $f_c^{'}$ = 937.5 psi